UC San Diego

UC San Diego Electronic Theses and Dissertations

Title

Structure-Guided Design and Synthesis of Small Molecules Targeting Hepatitis C Virus Internal Ribosome Entry Site RNA

Permalink

https://escholarship.org/uc/item/1wg444hw

Author

Ding, Kejia

Publication Date

2014

Peer reviewed|Thesis/dissertation

UNIVERSITY OF CALIFORNIA, SAN DIEGO

Structure-Guided Design and Synthesis of Small Molecules Targeting Hepatitis C Virus
Internal Ribosome Entry Site RNA

A dissertation submitted in partial satisfaction of the requirements for the degree

Doctor of Philosophy

in

Chemistry

by

Kejia Ding

Committee in charge:

  Professor Thomas Hermann, Chair
  Professor Nathan Gianneschi
  Professor Uli Müller
  Professor Joseph O'Connor
  Professor Nicholas Spitzer

2014

The Dissertation of Kejia Ding is approved, and it is acceptable in quality and for publication on microfilm and electronically:

_____

_____

_____

_____

_____

Chair

University of California, San Diego

2014

TABLE OF CONTENTS

LIST OF FIGURES

LIST OF TABLES

LIST OF SCHEMES

LIST OF SPECTRA

ACKNOWLEDGMENTS

VITA

2008   Bachelor of Science, San Jose State University, Chemistry

2011   Master of Science, University of California, San Diego, Chemistry

2014   Doctor of Philosophy, University of California, San Diego, Chemistry

PUBLICATIONS

1. Ding, K.; Wang, A.; Boerneke, M.A.; Dibrov, S.M.; Hermann, T. Aryl-Substituted Aminobenzimidazoles Targeting the Hepatitis C Virus Internal Ribosome Entry Site. *Bioorg. Med. Chem. Lett.* **2014**, accepted.

2. Dibrov, S.M.; Parsons, J.; Carnevali, M.; Zhou, S; Rynearson, K.D.; Ding, K.; Garcia Sega, E.; Brunn, N.D.; Boerneke, M.A.; Castaldi, M.P.; Hermann, T. Hepatitis C Virus Translation Inhibitors Targeting the Internal Ribosome Entry Site. *J. Med. Chem*. **2013**, 57, 1694-1707.

3. Ding, K.; Dibrov, S.M.; Hermann, T. Synthesis and Crystal Structure of a Phenazine N-oxide *J. Chem.Cryst.* **2013**, *43*, 550-553.

4. Zhou, S.; Rynearson K.D.; Ding, K.; Brunn, N.D.; Hermann, T. Screening for Inhibitors of the Hepatitis C Virus Internal Ribosome Entry Site RNA. *Bioorg. Med. Chem*. **2013**, *21*, 6139-6144.

5. Dibrov S.M.; Ding K.; Brunn, N.D.; Parker, M.A.; Bergdahl, B.M.; Wyles, D.L.; Hermann, T. Structure of a Hepatitis C Virus RNA Domain in Complex with a Translation Inhibitor Reveals a Binding Mode Reminiscent of Riboswitches. *Proc. Natl. Acad. Sci. USA.* **2012**, *109*, 5223-5228.

6. Luchetti, G.; Ding, K.; Kornienko, A.; d'Alarcao, M. Synthesis of Differentially Protected *myo-* and *chiro-* Inositols from D-Xylose: Stereoselectivity in Intramolecular SmI$_2$-Promoted Pinacol Reactions. *Synthesis* **2008**, *19*, 3142-3147.

7. Luchetti, G.; Ding, K.; d'Alarcao, M.; Kornienko, A. Enantio- and Diastereodivergent Synthetic Route to Multifarious Cyclitols from D-Xylose via Ring-Closing Metathesis. *Synthesis* **2008**, *19*, 3148-3154.

ABSTRACT OF THE DISSERTATION

Structure-Guided Design and Synthesis of Small Molecules Targeting Hepatitis C Virus
Internal Ribosome Entry Site RNA

by

Kejia Ding

Doctor of Philosophy in Chemistry

University of California, San Diego, 2014

Professor Thomas Hermann, Chair

This study focuses on the structure-guided design and synthesis of small

molecules that target hepatitis C virus internal ribosome entry site subdomain IIa RNA -

a structural element that plays a key role in the viral protein translation initiation

process. A series of aryl-substituted benzimidazole molecules was designed using

guidance from a shape-similarity screening that utilized the structure of a known

subdomain IIa RNA-binding benzimidazole translation inhibitor as the query molecule.

The syntheses of the designed aryl-substituted benzimidazole molecules were

described. Their binding affinities towards the target RNA were assessed by a FRET

xxx

assay. The structure-binding relationship of these molecules was analyzed. The second part of the study explores the design and synthetic development of 2-aminoquinazolin-4-one and 2-amino-lin-benzoguanine molecules, whose design were guided by the ligand-bound subdomain IIa RNA crystal structure.

Chapter 1. RNA as Drug Target

Central dogma of molecular biology

The central dogma is a description used to explain the genetic information flow within a biological system[1]. For the majority of living organisms, their genetic information is carried in their deoxyribonucleic acid (DNA) sequence. This information can either be copied into a new sequence of DNA by DNA replication or be passed onto a sequence of messenger RNA (mRNA) in a process known as transcription. mRNA is, in this particular case, a passive carrier of the genetic information. It eventually needs to work with the ribosome in order to translate its RNA sequence into a protein. Proteins then carry out many important functions inside living organisms. For a retrovirus such as human immunodeficiency virus (HIV) or hepatitis C virus (HCV), RNA is the carrier of the genetic information. In order for the virus to replicate, RNA must first be reverse-transcribed into DNA[2].

$$DNA \rightleftharpoons RNA \longrightarrow Protein$$

RNA types and functions

Since the description of the central dogma, various forms of RNAs are found to be responsible for many important biological functions, extending the role of RNA as a passive carrier of genetic information between DNA and protein[3]. For example,

ribosomal RNA (rRNA) accounts for about 65% of the ribosome and are essential for

protein synthesis[4-10]. Transfer RNAs (tRNA) carry amino acids to ribosomes for use in

protein synthesis[11,12]. Small nuclear RNAs (snRNA) form stable complex with specific

proteins and mediate the splicing of eukaryotic gene transcripts into mRNA [13-16]. Small

noncoding RNAs, such as small interfering RNAs (siRNA), micro RNAs (miRNA) and small

nucleolar RNAs (snoRNA), serve a number of novel biological functions ranging from

disrupting gene expression, controlling developmental timing, to catalyzing chemical

modifications[17-24]. More recently, riboswitches have been discovered as regulatory

elements of the mRNAs that can specifically bind to target small molecules and control

the expression of downstream mRNAs[25-28]. And internal ribosome entry site (IRES) RNAs

found in certain viruses allow viral protein translation initiation to bypass the regulation

mechanisms in eukaryotic cells[29,30].

RNA structures

RNA is a polymeric chain that is made of nucleotides, linked together by

phosphodiester bridges[3]. The four bases in RNA, adenine (A), cytosine (C), guanine (G)

and uracil (U), are connected at the 1' position of the D-ribose via a N-glycosidic bond

to form the nucleosides adenosine, cytidine, guanosine, and uridine (Figure 1-1).
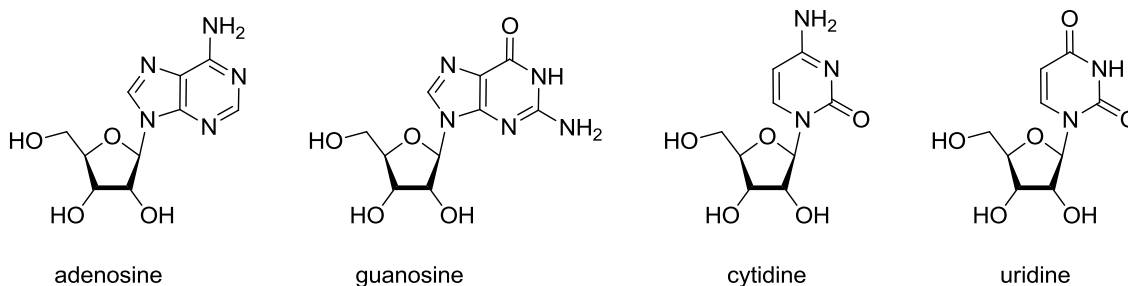
Figure 1-1: Structures of nucleosides found in RNA. *Left to right*. Purines, adenosine (A) and guanosine (G), and pyrimidines, cytidine (C), uridine (U).

The RNA sequence determines the folding of the RNA into local secondary structures. The secondary structure then folds into global three dimensional tertiary structure that is essential for its function. Compared to double-stranded DNA, a single-stranded RNA molecule has a much greater number of conformational possibilities due to higher degrees of freedom represented by rotation about each of the six single bonds along the sugar-phosphate backbone per nucleotide unit [3]. Although RNA molecules are often rich in double-stranded regions that form when complementary sequences within the chain come together and join via intra-strand base pairing (**Figure 1-2**).
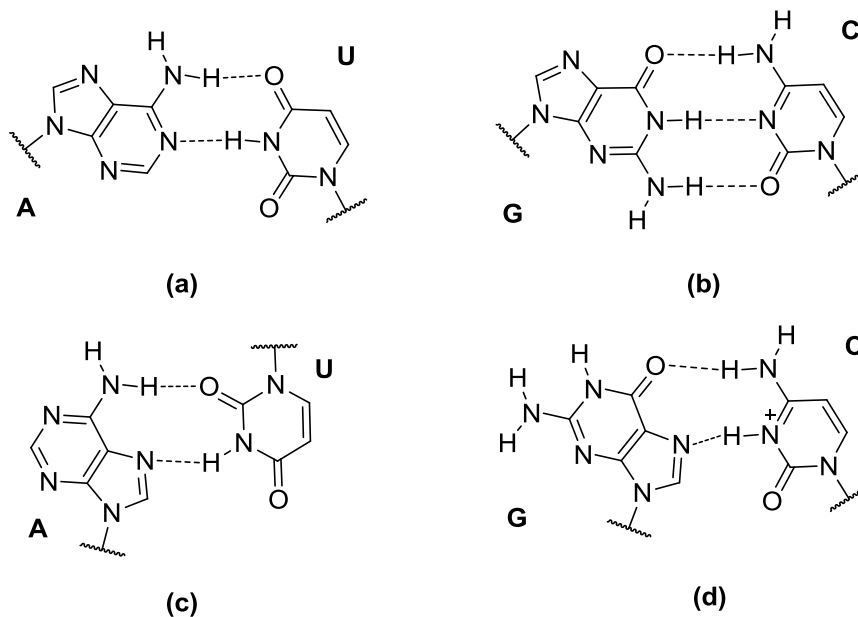
Figure 1-2: The Watson-Crick base pairs in RNA (top) and examples of non-Watson-Crick base pairs in RNA (bottom). (a) Adenosine (A) – Uridine (U) base pair has two intermolecular hydrogen bonds. (b) Guanosine (G) – Cytidine (C) base pair has three intermolecular hydrogen bonds. (c) Hoogsteen A-U base pair. (d) Hoogsteen G-C+ base pair.

These interactions create secondary structures such as 1) hairpin stem-loop structures, in which the base-paired region forms the stem and the unpaired region between base pairs forms the loop (Figure 1-3); 2) U-turns, a loop motif of consensus sequence UNRN where N is any nucleotide and R is a purine; 3) tetraloops, four nucleotide loops found at the termini of stem-loop structures; 4) internal loops where the RNA strand is forced into short single-stranded loop because one or more bases along one strand in an RNA double helix finds no base-pairing partners; 5) junctions, regions where several secondary structures meet; and 6) tertiary structural motifs such as coaxial stacking, psudoknot formation, and ribose zippers. The RNA secondary and

tertiary structures are stabilized mostly by hydrogen bonding and base stacking

interactions.
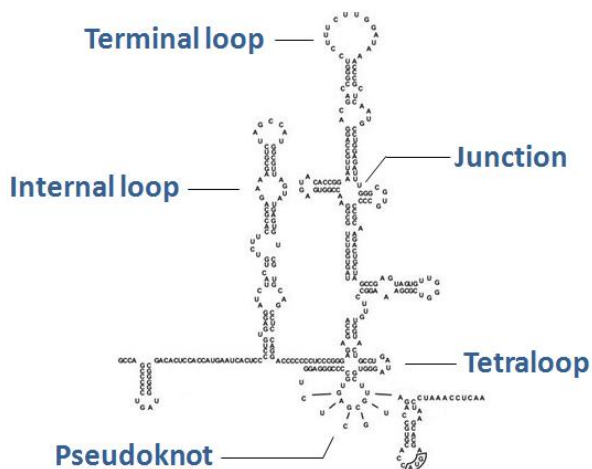
Figure 1-3: Examples of secondary structural elements found in RNA.

RNA as drug target

Being a molecule that can serve both as the genetic information depository and

as the catalytic center for many biological events, RNA has great potential to become

the next major drug target after protein and DNA[31-36]. Many key events that occur in

bacterial and viral reproductive cycles are found to be mediated by RNA and RNA-

protein complex [31,37]. A number of human diseases are associated with malfunction of

RNA-processing[38]. It is estimated that fifteen percent of human genetic diseases result

from RNA splicing defects[39]. Even inside human brain cell, it is shown that gene

expression can be regulated by alternative RNA processing and small noncoding RNAs[40].

The complex functions of RNA molecules and their association with certain diseases

make them potential targets for pharmaceutical interventions.

Like protein, RNA functions rely on their sequences and structures. The proper folding of RNA is required for its biological activity because the effective recognition between RNA and other molecules relies on the unique structural feature of the folded RNA. While a regional secondary structure maybe responsible for the binding of a small molecule, a large folded tertiary structure is probably the key for specific RNA-protein recognition. The richness in structural features of RNA makes it possible for medicinal chemists to develop molecules that can bind to a particular RNA structure with high specificity.

Indeed RNA as drug target has become the focus of research investigation in recent years[41-51]. The breakthrough in solving high resolution crystal structures of RNAs and ligand-bound RNAs provided atomic level three dimensional models of how these molecules recognize and interact with each other, helping explain some of the structure-activity-relationship (SAR) seen in the biochemical studies as well as support the design of new RNA-targeting small molecules. A number of RNA targets have been studied carefully by various research groups, such as bacterial ribosomal RNA[35,36], HIV trans activation responsive (TAR) RNA[46], and HCV internal ribosomal entry site (IRES) RNA[52]. The emergence of more and more successful examples fuels growing interests in the development of novel RNA-targeting small molecules as potential therapeutic agents for a variety of diseases.

References

(1)   Crick, F. *Nature* **1970**, *227*, 561.

(2)   Varmus, H. *Science* **1988**, *240*, 1427.

(3)   Garrett, R. H.; Grisham, C. M. *Biochemistry*; 3rd ed.; Thomson Brooks: Belmont, CA, 2007.

(4)   Noller, H. F. *Annu Rev Biochem* **1984**, *53*, 119.

(5)   Nomura, M.; Gourse, R.; Baughman, G. *Annu Rev Biochem* **1984**, *53*, 75.

(6)   Noller, H. F. *Annu Rev Biochem* **1991**, *60*, 191.

(7)   Stern, S.; Powers, T.; Changchien, L. M.; Noller, H. F. *Science* **1989**, *244*, 783.

(8)   Dahlberg, A. E. *Cell* **1989**, *57*, 525.

(9)   Noller, H. F. *Science* **2005**, *309*, 1508.

(10)   Brimacombe, R. *Eur J Biochem* **1995**, *230*, 365.

(11)   Biou, V.; Yaremchuk, A.; Tukalo, M.; Cusack, S. *Science* **1994**, *263*, 1404.

(12)   Ogle, J. M.; Brodersen, D. E.; Clemons, W. M.; Tarry, M. J.; Carter, A. P.; Ramakrishnan, V. *Science* **2001**, *292*, 897.

(13)   Mattaj, I. W.; Derobertis, E. M. *Cell* **1985**, *40*, 111.

(14)   Wassarman, D. A.; Steitz, J. A. *Science* **1992**, *257*, 1918.

(15)   Yang, Z. Y.; Zhu, Q. W.; Luo, K. X.; Zhou, Q. *Nature* **2001**, *414*, 317.

(16)   Nguyen, V. T.; Kiss, T. S.; Michels, A. A.; Bensaude, O. *Nature* **2001**, *414*, 322.

(17)   Storz, G. *Science* **2002**, *296*, 1260.

(18)   Mattick, J. S.; Makunin, I. V. *Hum Mol Genet* **2006**, *15*, R17.

(19)   Eddy, S. R. *Nat Rev Genet* **2001**, *2*, 919.

(20)   Carthew, R. W.; Sontheimer, E. J. *Cell* **2009**, *136*, 642.

(21)   Rana, T. M. *Nat Rev Mol Cell Bio* **2007**, *8*, 23.

(22)   Grosshans, H.; Slack, F. J. *J Cell Biol* **2002**, *156*, 17.

(23)   KissLaszlo, Z.; Henry, Y.; Bachellerie, J. P.; CaizerguesFerrer, M.; Kiss, T. *Cell* **1996**, *85*, 1077.

(24)   Kiss, T. *Cell* **2002**, *109*, 145.

(25)   Winkler, W.; Nahvi, A.; Breaker, R. R. *Nature* **2002**, *419*, 952.

(26)   Nudler, E.; Mironov, A. S. *Trends Biochem Sci* **2004**, *29*, 11.

(27)   Barrick, J. E.; Corbino, K. A.; Winkler, W. C.; Nahvi, A.; Mandal, M.; Collins, J.; Lee, M.; Roth, A.; Sudarsan, N.; Jona, I.; Wickiser, J. K.; Breaker, R. R. *P Natl Acad Sci USA* **2004**, *101*, 6421.

(28)   Thore, S.; Leibundgut, M.; Ban, N. N. *Science* **2006**, *312*, 1208.

(29)   Jang, S. K.; Krausslich, H. G.; Nicklin, M. J. H.; Duke, G. M.; Palmenberg, A. C.; Wimmer, E. *J Virol* **1988**, *62*, 2636.

(30)   Tsukiyamakohara, K.; Iizuka, N.; Kohara, M.; Nomoto, A. *J Virol* **1992**, *66*, 1476.

(31)   Li, S.; Z., X. In *Medicinal Chemistry of Nucleic Acids*; Zhang, L. H., Xi, Z., Chattopadhyaya, J., Eds.; John Wiley & Sons, Inc: Hoboken, NJ, USA, 2011.

(32)   Walsh, C. *Antibiotics: Actions, origins, resistance*; ASM Press: Washington, DC, 2003.

(33)   Pearson, N. D.; Prescott, C. D. *Chem Biol* **1997**, *4*, 409.

(34)   Gallego, J.; Varani, G. *Accounts Chem Res* **2001**, *34*, 836.

(35)   Hermann, T. *Curr Opin Struc Biol* **2005**, *15*, 355.

(36)   Poehlsgaard, J.; Douthwaite, S. *Nat Rev Microbiol* **2005**, *3*, 870.

(37)   Knipe, D. M.; Howley, P. M.; Griffin, D. E. *Fundamental Virology*; 4th ed.; Lippincott Williams & Wilkins: Philadelphia, 2001.

(38)   Krawczak, M.; Reiss, J.; Cooper, D. N. *Hum Genet* **1992**, *90*, 41.

(39)   Smith, C. W. J.; Valcarcel, J. *Trends Biochem Sci* **2000**, *25*, 381.

(40)   Filipowicz, W. *P Natl Acad Sci USA* **2000**, *97*, 14035.

(41)   Hermann, T.; Westhof, E. *Curr Opin Biotech* **1998**, *9*, 66.

(42)   Ecker, D. J.; Griffey, R. H. *Drug Discov Today* **1999**, *4*, 420.

(43)   Hofstadler, S. A.; Griffey, R. H. *Curr Opin Drug Discov Devel* **2000**, *3*, 423.

(44)   Xavier, K. A.; Eder, P. S.; Giordano, T. *Trends Biotechnol* **2000**, *18*, 349.

(45)   Drysdale, M. J.; Lentzen, G.; Matassova, N.; Murchie, A. I.; Aboul-Ela, F.; Afshar, M. *Prog Med Chem* **2002**, *39*, 73.

(46)   Froeyen, M.; Herdewijn, P. *Curr Top Med Chem* **2002**, *2*, 1123.

(47)   Vicens, Q.; Westhof, E. *Chembiochem* **2003**, *4*, 1018.

(48)   Willkomm, D. K.; Gruegelsiepe, H.; Goudinakis, O.; Far, R. K. K.; Bald, R.; Erdmann, V. A.; Hartmann, R. K. *Chembiochem* **2003**, *4*, 1041.

(49)   Wahlestedt, C. *Drug Discov Today* **2006**, *11*, 503.

(50)   Fanning, G. C. *Curr Drug Targets* **2006**, *7*, 1607.

(51)   Magnet, S.; Blanchard, J. S. *Chem Rev* **2005**, *105*, 477.

(52)   Zhou, S.; Rynearson, K. D.; Ding, K. J.; Brunn, N. D.; Hermann, T. *Bioorgan Med Chem* **2013**, *21*, 6139.

Chapter 2. Hepatitis C Virus Internal Ribosome Entry Site RNA as Drug Target

Hepatitis C virus infection and treatment

An estimated 180 million people worldwide are infected by hepatitis C virus (HCV) infection[1]. HCV is a major cause of chronic hepatitis, cirrhosis and ultimately hepatocellcular carcinoma[2], a primary indication for liver transplantation in the western world [3]. In the United States alone, 10,000 to 20,000 deaths a year are from HCV [4]. There is currently no vaccine against HCV. Over the past decade, the standard treatment has been pegylated interferon plus ribavirin [5], providing only moderate efficacy but causing severe side effects[6].

Two new classes of direct acting agents (DAA) including protease and polymerase inhibitors are now available. Vertex's Telaprevir and Merck's Boceprevir, both NS3/4A protease inhibitors, were approved by FDA in 2011 to be used in combination with pegylated interferon (PEG-IFN) and ribavirin for treatment of genotype 1 infection, which accounts for more than 70 percent of American cases. However along with the improved efficacy of the new line of treatments were the additional side effects patients need to bear from the new drugs [7]. Moreover, these agents don't cover all HCV genotypes and rapid drug resistance was reported in single agent studies [2,8,9].

In 2013 Gilead's Sovaldi, a polymerase inhibitor, was approved to use in combination with ribavirin for oral dual therapy of HCV genotypes 2 and 3 which accounts for 20-25 percent of cases in the US, and to be used in combination with injected PEG-IFN and ribavirin for treatment-naive patients with HCV genotypes 1 and 4 [10]. Although Sovaldi is expected to make the treatment of hepatitis C more effective and less onerous in shorter time, it comes with an almost unbearable wholesale cost of $84,000 for the 12 weeks of treatment recommended for most patients, and $168,000 for the 24 weeks needed for a hard-to-treat strain of the virus.

The current options for the treatment for HCV infections are far from ideal. In the mean time high genetic variability of the virus poses constant threat of resistance development, sabotaging the already limited treatment options [11]. As a result, there is an ongoing need to explore new targets within the virus and to develop new direct acting antiviral agents for more affordable, more effective and more sustainable treatment for hepatitis C [12,13].

HCV genome and IRES

HCV belongs to the *flavivirus* family. Its positive-stranded 9600 nucleotides long RNA genome encodes a polyprotein precursor of approximately 3000 amino acids (Figure 2-1). HCV genome translates into a polyprotein that is cleaved into ten proteins by cellular and viral proteases [14]. Three structural proteins include the core protein (C), E1 protein and E2 protein. Non-structural proteins include p7 protein (ion-channel), NS2,

NS3 (Serine-protease), NS4A, NS4B, NS5A, and NS5B (RNA-dependent RNA-polymerase). NS5B catalyzes the replication of the viral RNA [15].

In addition to the translated sequence are the highly conserved 5' and 3' untranslated regions (UTR) that flank the two ends of the genome. Within the 5' UTR contains an internal ribosome entry site (IRES) which extends from position 40 through 372 of the viral RNA genome, spanning the 5'- UTR and 30 nucleotides pass the start codon at A342 into the polyprotein coding frame [16].
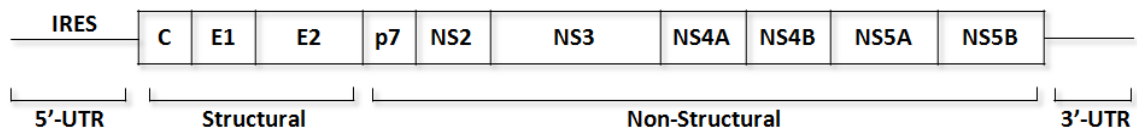
Figure 2-1: Schematic of HCV genome showing the 5' untranslated region (UTR); IRES within the 5' UTR; structural and non-structural regions; and 3' UTR.

IRES contains three independently folding domains (II-IV) that are connected by flexible linkers [17] (Figure 2-2). Domain I of 5' UTR plays a role in viral replication together with the 3' UTR but is not required for IRES-driven translation [18,19].
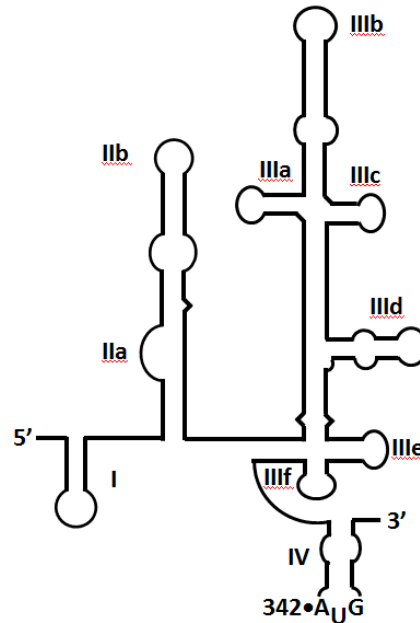
Figure 2-2: Schematic of secondary structure of the HCV 5' non-translated region that contains IRES (domain II-IV). Sub-domains are indicated. AUG start codon at 342 [20] is highlighted.

IRES and Cap-Independent Translation Initiation

HCV IRES is found to mediate the HCV protein translation initiation in a cap-independent fashion, effectively bypassing the complex eukaryotic cell translation initiation mechanisms that depend on a 5'-cap (7-methyl guanosine) structure on the mRNA. Ribosome instead is directly recruited to the viral RNA to start translation of the viral proteins [21].

Cap dependent translation initiation in eukaryotic cell is a complex process that requires highly ordered assembly of ribosomal pre-initiation complexes [22-24]. In brief, it involves 1) host initiation factor proteins (eIFs) association with the cap structure at the

5' end of the mRNA, 2) 40S ribosome binding and scanning to the start codon, and 3)
association with the 60S ribosomal subunit to form an active 80S ribosome.

By contrast, the HCV IRES mediates viral protein translation initiation in a cap-
independent fashion that bypasses most of the initiation factors required in cap-
dependent translation initiation [25-27]. In this process, IRES domain III interacts and
recruits with high affinity the small ribosomal 40S subunit directly in the absence of any
known initiation factors or the cap structure [28,29]. The IRES domain II makes close
contact to the 40S subunit near the active site of the ribosome at the 40S-60S interface
[30]. The apical loop of domain II interacts with the domain IV, the AUG codon within
which unwinds during the binding process and is placed inside the 40S subunit's
decoding site [31,32]. Via the binding surface provided by Domain III, initiation factor eIF3
(a large multiprotein complex required to prevent premature association of 40S and 60S
subunits) and eIF2/GTP (bound to Met-tRNA) bind to the surface of 40S to form a 48S
particle with already established codon-anticodon base pairing in the ribosomal P site
[27,33]. The conformational changes in the 40S subunit promote the eIF5-induced GTP
hydrolysis and subsequent eIF2/GDP release from the 48S complex [34]. Followed by the
joining of the 60S subunit, eIF5, eIF5B and GTP, the active 80S initiation complex is
formed [29].

IRES Subdomain IIa and Its Potential as a Drug Target

The correct positioning of the HCV viral mRNA at the decoding site is critical for

the viral protein translation initiation and involves interacting with the apical loop of

subdomain IIb, whose positioning instead relies on the folding of the subdomain IIa

internal loop structure [1]. The overall structure of IRES domain II RNA has been solved in

cryo-electron microscopy (cryo-EM) studies of the IRES-40S complexes, revealing L-

shaped conformation of subdomain IIa whose bent structure helps direct the apical

hairpin loop of subdomain IIb to overlap with the ribosomal E site in the close proximity

of the P site [34,35]. More recently, NMR and X-ray crystal structures of the HCV IRES

subdomain IIa becomes available and both show a 90 degree bent shape of the region.

In the high resolution crystal structure, the bulge is stabilized by divalent metal ions

(Figure 2-3) [36-38].
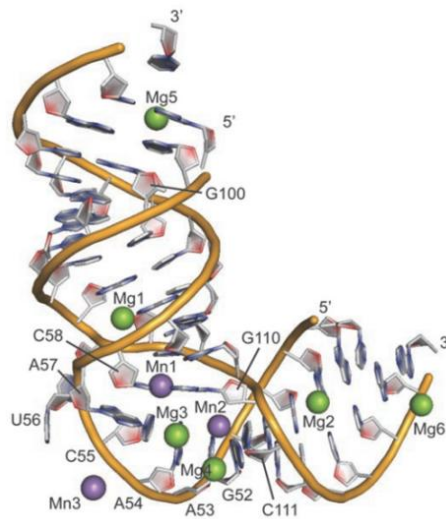
Figure 2-3: HCV IRES subdomain IIa crystal structure [36]. Metal ions are shown as spheres.

Although the bent architecture of the subdomain IIa is required for the assembly with the ribosome, the topology of the IRES-ribosomal interaction indicates that the subdomain IIb must be removed from the E-site to allow the P-site tRNA to translocate during translation initiation [34,35]. It has be suggested that the release of the domain IIb is through conformational changes in the subdomain IIa [39,40]. Indeed it has been shown in recent studies that mutations or the binding of a small molecule ligands at the subdomain IIa region that alters its bent conformation results in disruption of IRES-driven translation and inhibition of viral protein synthesis [39-41].

The subdomain IIa therefore is a dynamic structural element that plays very important roles in the HCV IRES-driven translation initiation. Its L-shape bent conformation has proven to be required for the ribosome assembly. Yet the structural alternation in the same region must occur before the translation mechanism could begin functioning.

The intricate function in conjunction with its dynamic structural element renders HCV IRES subdomain IIa a potential target of small molecule inhibitors. In theory, any conformational changes induced by the binding of a small molecule can give rise to a meltdown of the viral translation process. And similarly any small molecule binding that prevents the conformational change needed for the release of subdomain IIb from the E site may achieve the same effect.

As a key functional element in the viral translation process, the sequence of HCV IRES subdomain IIa is highly conserved. Within the 1600 clinical isolates studied previously [42], it was found that with the exception of A57, C104, and G107 subdomain IIa sequence is greater than 98 % conserved across all genotypes. The residues forming the ligand binding sites are greater than 99 % conserved.

The high sequence conservation, unique function, and structural features make HCV IRES subdomain IIa an attractive drug target for small molecule ligand.

FRET Assay

Förster Resonance Energy Transfer (FRET) is a radiationless transfer of energy between a donor chromophore and an acceptor chromophore when they are in close proximity (< 10 nm) [43,44]. The donor chromophore absorbs light at a certain wavelength and emits at a different wavelength. An acceptor chromophore, when placed close to the donor, absorbs the energy emitted by the donor and emits a fluorescent light at another distinct wavelength.

The efficiency of the energy transfer (E) between the dye pair is dependent on the distance between the dye pair and can be defined as,

$$E = \frac{R_0^6}{R_0^6 + r^6}$$

where R_0 is the Förster radius of the pair and r is the distance between the pair. The Förster radius is defined as the distance at which the efficiency of the energy transfer is 50 %.

Efficiency of the energy transfer (E) can be measured experimentally by the ratio between the measured acceptor emission via FRET and the measured acceptor emission via direct excitation (DE),

$$E = \frac{FRET}{DE}$$

where the DE is the acceptor dye emission measured by directly exciting the dye at its absorption wavelength. Based on these relationships, the FRET efficiency measured by fluorescence emission between the dyes can be used to estimate the distance between them.

A FRET assay has been developed in the lab to test the binding of the synthesized compounds to the HCV IRES subdomain IIa bulge [45]. The assay is designed based on the L shape architecture of the subdomain IIa seen in the X-ray crystal structure [36]. As already discussed in the preceding sections, the bent conformation of the HCV IRES subdomain IIa is of critical importance for the viral protein translation initiation. By using a fluorescently labeled subdomain IIa RNA construct where the cyanine dye pair Cy3 and Cy5 was covalently attached at the 5' termini of HCV IRES subdomain IIa RNA construct (Figure 2-4.a), the conformational change induced by the ligand binding can be measured through FRET efficiency.
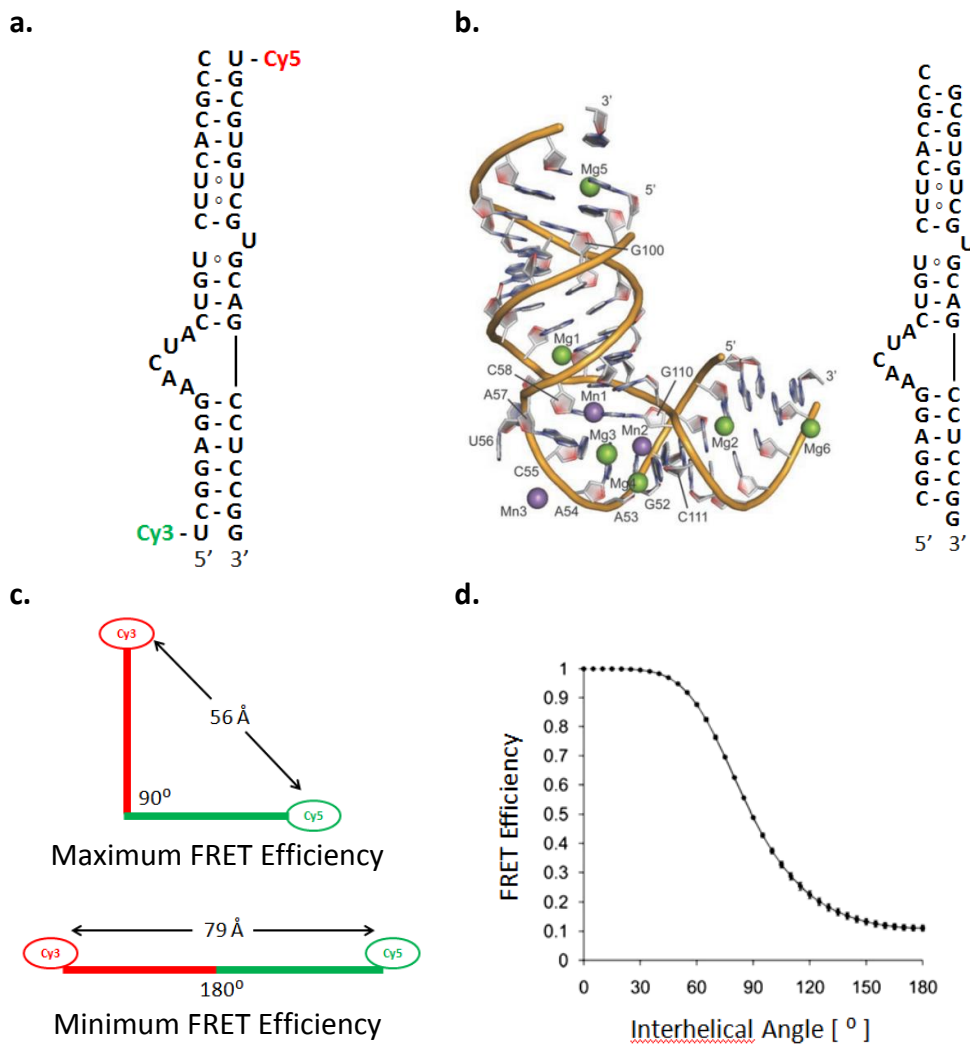
Figure 2-4: Subdomain IIa FRET construct and dependence of Cy3/Cy5 FRET efficiency on the interhelical angle and distance. **a**. Secondary structure of fluorescently labeled HCV IRES subdomain IIa RNA construct used in the FRET assay. **b**. Crystal structure and its secondary sequence showing L-shape conformation of subdomain IIa is used as reference to calculate distance between the termini [36]. **c**. Schematic drawing of the RNA conformations at maximum and minimum FRET efficiency, interhelical angels and their corresponding distances between the termini are indicated. **d**. Calculated relationship between FRET efficiency and interhelical angle of the RNA bent structure.

Using this construct and assuming the RNA geometry derived from the IIa crystal structure (Figure 2-4.b), the Cy3/Cy5 FRET efficiency dependence on the interhelical angle was calculated [45] (Figure 2-4.d). The FRET efficiency reaches its maximum when the RNA adopts a 90° bent structure and a corresponding 56 Å distance between the dyes. And the efficiency gradually decreases as the angel widens until its minimum when the construct adopts a 180° straightened conformation and a corresponding 79 Å distance between the dyes (Figure 2-4.c).

This FRET assay was used to demonstrate that benzimidazole inhibitors **1** (Figure 2-5) disrupts HCV IRES function by widening the interhelical angle of the subdomain IIa [39]. As seen in the titration curve, the normalized FRET signal decreases in response to the increase of inhibitor concentration, indicating an increased distance between the two cyanine dyes and a widened interhelical angle of the domain IIa RNA construct. The same compound was then tested in a HCV replicon assay to show the effective inhibition viral replication. The FRET assay can therefore be used for assessing the binding affinity of designed ligands to the subdomain IIa internal bulge.
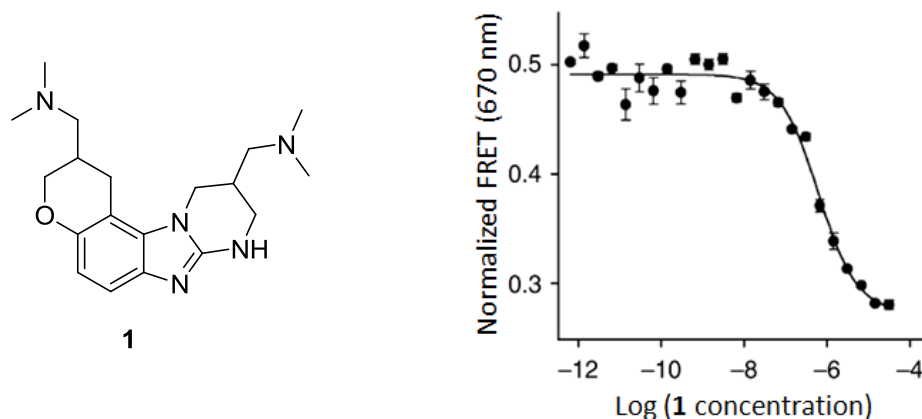
Figure 2-5: Structure of benzimidazole inhibitor **1** (left) and Normalized FRET signal for titrations of Cy3/Cy5-labeled subdomain IIa RNA with benzimidazole **1** (right). Fitting of the dose response curve resulted in EC_{50} value of 600 ± 80 nM [39].

References

(1)   Thomas, D. L. *Nat Med* **2013**, *19*, 850.

(2)   Rosen, H. R. *New Engl J Med* **2011**, *364*, 2429.

(3)   Davis, G. L.; Albright, J. E.; Cook, S. F.; Rosenberg, D. M. *Liver Transplant* **2003**, *9*, 331.

(4)   Weiss, U. *Nature* **2005**, *436*, 929.

(5)   Fried, M. W.; Shiffman, M. L.; Reddy, K. R.; Smith, C.; Marinos, G.; Goncales, F. L.; Haussinger, D.; Diago, M.; Carosi, G.; Dhumeaux, D.; Craxi, A.; Lin, A.; Hoffman, J.; Yu, J. *New Engl J Med* **2002**, *347*, 975.

(6)   Hoofnagle, J. H.; Seeff, L. B. *New Engl J Med* **2006**, *355*, 2444.

(7)   Enserink, M. *Science* **2011**, *332*, 159.

(8)   Pawlotsky, J. M. *Hepatology* **2011**, *53*, 1742.

(9)   Halfon, P.; Locarnini, S. *J Hepatol* **2011**, *55*, 192.

(10)   Pollack, A.; The New York Times: 2013; Vol. 2013.

(11)   Salvatierra, K.; Fareleski, S.; Forcada, A.; Lopez-Labrador, F. X. *World J Virol* **2013**, *2*, 6.

(12)   Bartenschlager, R.; Lohmann, V.; Penin, F. *Nat Rev Microbiol* **2013**, *11*, 482.

(13)   Scheel, T. K.; Rice, C. M. *Nat Med* **2013**, *19*, 837.

(14)   Tang, H.; Grise, H. *Clin Sci (Lond)* **2009**, *117*, 49.

(15)   Lindenbach, B. D.; Evans, M. J.; Syder, A. J.; Wolk, B.; Tellinghuisen, T. L.; Liu, C. C.; Maruyama, T.; Hynes, R. O.; Burton, D. R.; McKeating, J. A.; Rice, C. M. *Science* **2005**, *309*, 623.

(16)   Dibrov, S. M.; Parsons, J.; Carnevali, M.; Zhou, S.; Rynearson, K. D.; Ding, K.; Garcia Sega, E.; Brunn, N. D.; Boerneke, M. A.; Castaldi, M. P.; Hermann, T. *J Med Chem* **2013**.

(17)   Kieft, J. S.; Zhou, K.; Jubin, R.; Murray, M. G.; Lau, J. Y.; Doudna, J. A. *J Mol Biol* **1999**, *292*, 513.

(18)   Lukavsky, P. J. *Virus Res* **2009**, *139*, 166.

(19)   Friebe, P.; Lohmann, V.; Krieger, N.; Bartenschlager, R. *J Virol* **2001**, *75*, 12047.

(20)   Honda, M.; Brown, E. A.; Lemon, S. M. *RNA* **1996**, *2*, 955.

(21)   Niepmann, M. *Current topics in microbiology and immunology* **2013**, *369*, 143.

(22)   Merrick, W. C. *Gene* **2004**, *332*, 1.

(23)   Kapp, L. D.; Lorsch, J. R. *Annu Rev Biochem* **2004**, *73*, 657.

(24)   Pestova, T. V.; Kolupaeva, V. G.; Lomakin, I. B.; Pilipenko, E. V.; Shatsky, I. N.; Agol, V. I.; Hellen, C. U. T. *P Natl Acad Sci USA* **2001**, *98*, 7029.

(25)   Fraser, C. S.; Doudna, J. A. *Nat Rev Microbiol* **2007**, *5*, 29.

(26)   Kieft, J. S.; Zhou, K.; Jubin, R.; Doudna, J. A. *RNA* **2001**, *7*, 194.

(27)   Otto, G. A.; Puglisi, J. D. *Cell* **2004**, *119*, 369.

(28)   Rosenberg, S. *J Mol Biol* **2001**, *313*, 451.

(29)   Pestova, T. V.; Shatsky, I. N.; Fletcher, S. P.; Jackson, R. J.; Hellen, C. U. *Genes Dev* **1998**, *12*, 67.

(30)   Babaylova, E.; Graifer, D.; Malygin, A.; Stahl, J.; Shatsky, I.; Karpova, G. *Nucleic Acids Res* **2009**, *37*, 1141.

(31)   Filbin, M. E.; Kieft, J. S. *Rna-a Publication of the Rna Society* **2011**, *17*, 1258.

(32)   Berry, K. E.; Waghray, S.; Mortimer, S. A.; Bai, Y.; Doudna, J. A. *Structure* **2011**, *19*, 1456.

(33)   Ji, H.; Fraser, C. S.; Yu, Y.; Leary, J.; Doudna, J. A. *Proc Natl Acad Sci U S A* **2004**, *101*, 16990.

(34)   Spahn, C. M.; Kieft, J. S.; Grassucci, R. A.; Penczek, P. A.; Zhou, K.; Doudna, J. A.; Frank, J. *Science* **2001**, *291*, 1959.

(35)   Boehringer, D.; Thermann, R.; Ostareck-Lederer, A.; Lewis, J. D.; Stark, H. *Structure* **2005**, *13*, 1695.

(36)   Dibrov, S. M.; Johnston-Cox, H.; Weng, Y. H.; Hermann, T. *Angew Chem Int Ed Engl* **2007**, *46*, 226.

(37)   Lukavsky, P. J.; Kim, I.; Otto, G. A.; Puglisi, J. D. *Nat Struct Biol* **2003**, *10*, 1033.

(38)   Zhao, Q.; Han, Q.; Kissinger, C. R.; Hermann, T.; Thompson, P. A. *Acta Crystallogr D Biol Crystallogr* **2008**, *64*, 436.

(39)   Parsons, J.; Castaldi, M. P.; Dutta, S.; Dibrov, S. M.; Wyles, D. L.; Hermann, T. *Nat Chem Biol* **2009**, *5*, 823.

(40)   Carnevali, M.; Parsons, J.; Wyles, D. L.; Hermann, T. *Chembiochem* **2010**, *11*, 1364.

(41)   Locker, N.; Easton, L. E.; Lukavsky, P. J. *EMBO J* **2007**, *26*, 795.

(42)   Dibrov, S. M.; Ding, K.; Brunn, N. D.; Parker, M. A.; Bergdahl, B. M.; Wyles, D. L.; Hermann, T. *Proc Natl Acad Sci U S A* **2012**, *109*, 5223.

(43)   Clegg, R. M. *Methods Enzymol* **1992**, *211*, 353.

(44)   Sanchez, K. M.; Schlamadinger, D. E.; Gable, J. E.; Kim, J. E. *J Chem Educ* **2008**, *85*, 1253.

(45)   Parsons, J.; Castaldi, M. P.; Dutta, S.; Dibrov, S. M.; Wyles, D. L.; Hermann, T. *Nat Chem Biol* **2009**, *5*, 823.

Chapter 3. Design, Synthesis and Testing of Aryl-Substituted Benzimidazoles

Discovery of Benzimidazole Small Molecules Targeting HCV IRES Subdomain IIa RNA

When the projected was started in fall 2009, it was known that benzimidazole molecules bind to the HCV IRES subdomain IIa and inhibit viral translation [1]. At the time, however, it was not known how these molecules bind to the target. Nor was it clear about the mechanism through which these compounds inhibit the viral translation. The only available resource that could be used was the one article [1] that described the discovery of the benzimidazole molecules by mass-spectrometry assay. The structure-activity-relationship (SAR) study included substitutions at the terminal of N^1 propyl substitution (R_1) (Figure 3-1), substitution at C2 of the imidazole ring (R_2), and substitutions at 4,5,6,7 positions of the benzene ring (R_3). The best binding affinity was achieved to be 8 μM when dimethyl amino group is positioned at R_1, together with NH_2 at C2 and dimethylamino ethyl ether at C6. Further optimization of the benzimidazole with added ring constraints improved binding affinity (Figure 3-2). Compound **1** with two ring constraints reached $K_D = 0.72$ μM, while compound **2** with one ring constraint showing $K_D = 0.86$ μM.
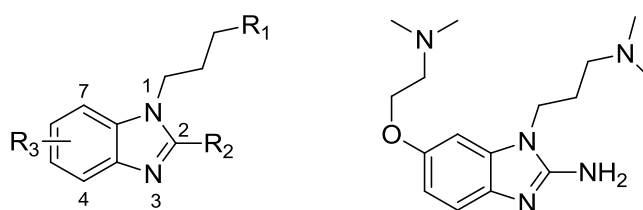
Figure 3-1: Benzimidazole scaffold that binds to the HCV IRES subdomain IIa and inhibit viral translation [1]. The benzimidazole scaffold with numbering (left), and the compound with highest binding affinity in the initial study, K_D = 8 µM (right).
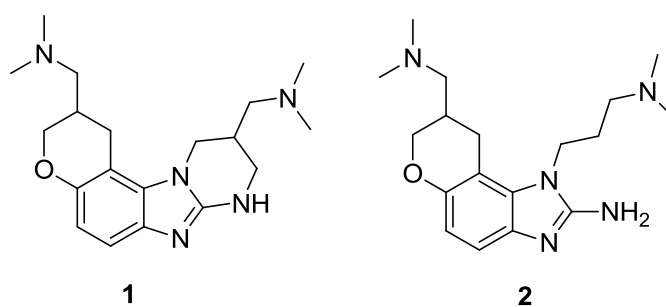
Figure 3-2: Structures of further optimized amino-benzimidazole inhibitors that possess ring constraints. Compound 1 has K_D = 0.72 µM and Compound 2 has K_D = 0.86 µM

Although compound **1** and **2** show promising binding affinities as lead structures,

their organic syntheses are lengthy and low-yielding. The reported overall yield for

compound **1** is merely 0.6 % over 12 steps. And the synthesis of compound **2** was later

modified to achieve an overall yield of 10.7 % over 8 steps [2]. However it is still difficult to

make large quantities of such compounds for future studies. Meanwhile, some of the

intermediates were reported as troublesome to purify due to the presence of aliphatic

amino groups and/or polar side chains [2]. In fact, compound **1** and **2** were both

synthesized as mixtures of stereoisomers that could not be separated using modern

purification techniques. There is a need to design more synthetically feasible compounds to support the study of HCV IRES subdomain IIa RNA as a drug target.

Challenges Faced by High-Throughput Screening of Molecules Targeting IRES RNA

Inspired by the discovery of benzimidazole **1** and like molecules, more efforts from both academia and industry have been devoted to the search for HCV translation inhibitors targeting the IRES RNA. A high throughput *in vitro* translation assay was developed using rabbit reticulocyte lysate [3]. Experiment conditions were optimized to report on HCV IRES-dependent translation relative to a 5' capped mRNA control, and a library of ~430,000 small molecules from Gilead Science Inc. was screened using this assay. However no selective HCV IRES inhibitors were discovered. Most of the ~ 1,700 initial hits were false positives resulted from off-target effects. Currently, the high throughput screen for RNA-specific inhibitors remains a great challenge. The tremendous cost of such screen as well as the poor outcome calls for alternative ways for designing new ligands targeting HCV IRES RNA.

Ligand-Based Virtual Screening

Modern virtual screening techniques provide useful guidance toward the design of new biologically active compounds when applied appropriately [4-7]. It is useful for lead identification, optimization, and scaffold hopping [8-13]. It has also been widely used to either complement or replace high throughput screenings [5,14]. The biggest advantage that virtual screening has over the traditional HTS is that it eliminates the prerequisite

for the compounds to actually exist, thereby eliminating issues that are typically associated with HTS, such as cost, assay sensitivity and specificity, presence of 'failed' compounds in the library, and challenges related with the instruments.

A large number of virtual screening methods have been developed in the past and can be classified into two categories: ligand-based and receptor-based virtual screenings. The receptor-based methods normally requires detailed structural information of the binding site but do not necessarily require experimental data on active compounds. Docking is an example of receptor-based screening method that uses the binding site structure and its chemical properties to predict binding mode and binding affinity of a given compound [15]. The ligand-based methods make use of the structures of known binders and are typically applied when limited information of the target binding site is available. Most ligand-based approaches rely on measuring similarity between compounds being compared and assume that more similar compounds are more likely to be active [16,17]. Aspects of the similarity include but are not limited to: substructure descriptor counts, atom connectivity, molecular features, and molecular shape [18].

Shape-Similarity Screening

The shape of a molecule is one of the key factors that determine its binding to the target receptor [19]. In case of an binding ligand, the negative image of the binding site resembles closely the shape of the molecule. In recent years, shape-based virtual screening methods have gained popularity due to their effectiveness in finding new

biologically active molecules and their remarkable computational efficiency as compared to traditional docking approach [20-25].

One of the shape-based virtual screening methods is ROCS developed by OpenEye Scientific Software. ROCS is a shape-based superposition method designed to perform large scale 3D database search to find structures that are chemically less intuitive but have approximately the same shape and chemical properties [26]. The shape-based superposition method used by ROCS aligns the molecules being compared by a solid-body optimization process that maximizes the overlap volume between them, where the molecular volume comprises the shape of individual atom. Followed by representing the atoms and the molecule using Gaussian functions, the shape of the molecules can then be compared through measuring the overlaps between the Gaussian functions [26].

Besides shape comparison, ROCS incorporates a 'color' feature that that was shown to be particularly beneficial for the reliable ranking of the output molecules [22,27]. In this method, the heavy atoms of the molecule are represented using steep gradient Gaussian functions while still maintaining their original volumes (Figure 3-3), where a steep gradient Gaussian is one that reaches a probability of zero within the radius of the sphere. This means that the heavy atoms are only matched if they overlap within their sphere radius. Next, the pre-defined 'color' force field included in this method assesses the chemical properties of the molecules being compared. More specifically, six

different types of chemical functionalities are considered: hydrogen bond donor,

hydrogen bond acceptor, hydrophobes, anions, cations, and rings.
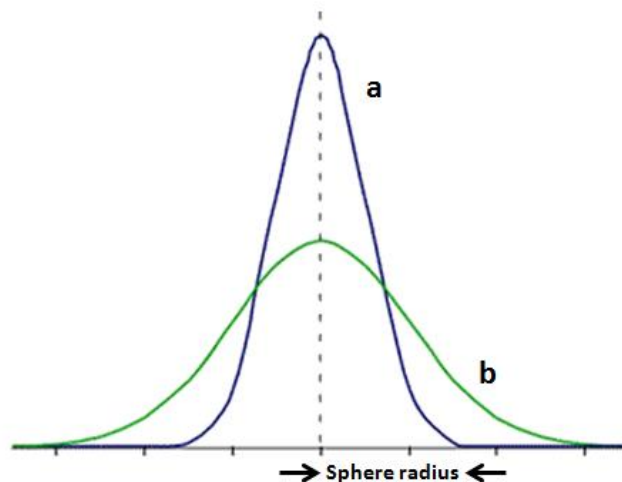
Figure 3-3: Comparison of a sphere expressed by two different Gaussian functions. Both functions have the same volume (area under the curve). **a** shows a steep gradient Gaussian and zero probability outside the radius; **b** shows a Gaussian that still has greater than zero probability outside the radius.

Query Molecule of the Screening

In principle, there are four stereo-isomers of benzimidazole **1** due to its two

chiral centers in the two six-member rings (Figure 3-2). However, the two stereo centers

are both located in fairly rigid ring structures and this as a result would limit the overall

conformational flexibility among the four isomers. The 3D structural comparison of the

four isomers prepared using the same methods as ZINC database (see below) suggests

that their overall structures are similar and the structural variations among them are

mainly due to the different orientations adopted by the terminal dimethyl amino groups

(Figure 3-4).

This structural similarity among isomers was supported by studies that became available later. In a ligand-bound HCV IRES subdomain IIa NMR structure study, the binding free energy of the two benzimidazole inhibitor (Figure 3-4) isomers to the subdomain IIa bulge was found to be comparable when measured both experimentally and by simulation [28]. And in the more recent ligand-bound subdomain IIa co-crystal structure study, the conformational analysis of benzimidazole **2** (Figure 3-2) suggested that the structure of the two enantiomers are very similar and binding of either form to the subdomain IIa bulge would be compatible with the interactions seen in the crystal structure [29]. Moreover, it was found that using multiconformer query does not increase performance in ROCS [27]. Therefore, only one of the four isomers was used as query molecule to reduce the computation time and overall complexity of the screening. Based on the evidence just provided, this should not affect the outcome of the screening. The isomer with the R,R configuration was used in the initial screening.
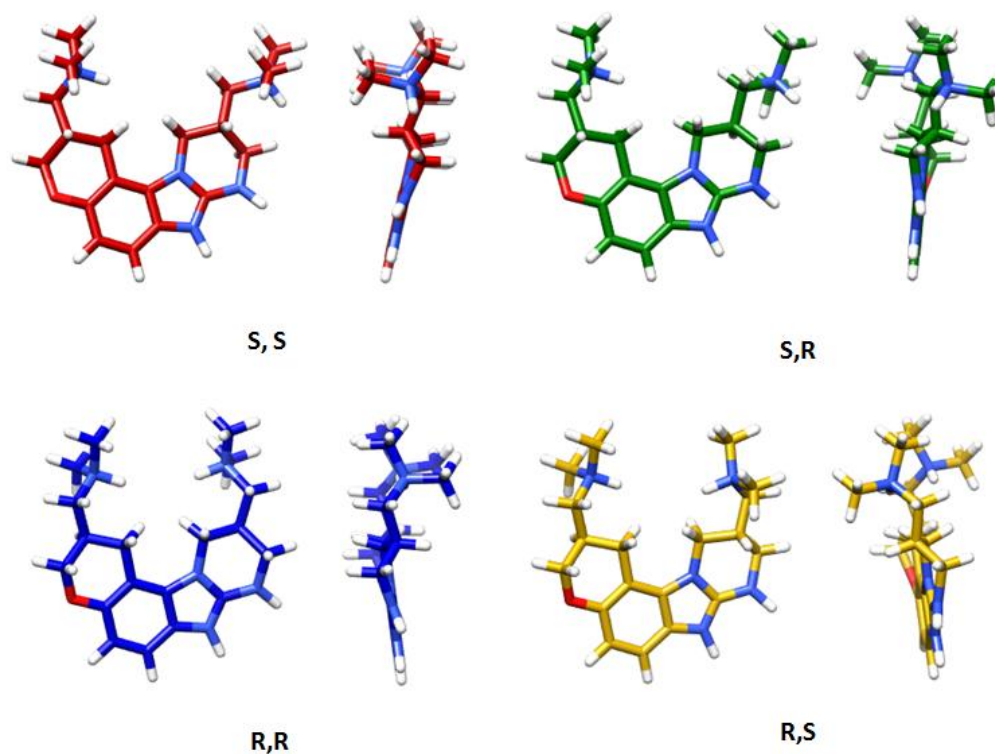
Figure 3-4: 3D structure models of four stereoisomers of the benzimidazole **1**. Both the front view (left) and side view (right) of the molecules are shown. The R,S assignments are indicated for the dihydropyran ring and the tetrahydropyrimidine ring respectively.
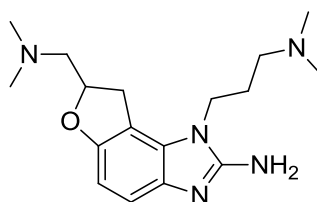
Figure 3-5: Structure of benzimidazole inhibitor used in the ligand-bound NMR structure study [28].

ZINC Database

The query molecule was searched against the ZINC database. ZINC is a

noncommercial 3D structure database that is preprocessed and ready for use in

structure based virtual screening [30,31]. ZINC compounds are divided into subsets based

on their physical and chemical properties. The drug like subset used in this study

captures the Lipinski's rule-of-five [32,33] (Table 3-1) and had 19,844,498 unique molecules

when the screening was performed (Nov 2009).

Table 3-1: Lipinski's rule of five states that in general an orally active drug has no more than one violation of the criteria and is used as a guideline in drug development process.

The molecular weight is equal or less than 500
The Log P is not greater than 5
No more than 5 H-bond donors (expressed as the sum of OHs and NHs)
No more than 10 H-bond acceptors (expressed as the sum of Ns and Os)

Ranking of the Output Molecules

The output of the ROCS search is ranked by Tanimoto Combo score, a method

used to compare the similarity and diversity of sample sets (Figure 3-6). Tanimoto

Combo is the sum of Shape Tanimoto and Color Tanimoto scores. Shape Tanimoto is a

measure of only the shape similarity between the two molecules represented by

Gaussian functions, while Color Tanimoto is a measure of the similarity defined in the

Color feature of ROCS. Both Shape Tanimoto and Color Tanimoto scores have a value

between 0 and 1 as calculated by Tanimoto equation.

$$T_{combo}(a,b) = T_{shape}(a,b) + T_{color}(a,b) \qquad (1)$$

$$T(a,b) = \frac{N_c}{N_a + N_b - N_c} \qquad (2)$$

Figure 3-6: Equations of TanimotoCombo score and Tanimoto score. Equation (1): The TanimotoCombo score is the sum of ShapeTanimoto and ColorTanimoto. Equation (2): Tanimoto score $T(a,b)$ is the ratio of the intersecting set to the union set as the measure of similarity. N represents the number of attributes in each object (a, b). c is the intersection set.

Output Review and Scaffold Selection

The top 500 hits of the search was reviewed and selected. The selection process follows a set of general guidelines that favor the RNA friendly binders (Table 3-2). More specifically, the selected scaffold should contain rigid ring structures in favor of the stacking interactions with adjacent nucleic acid base pairs, yet non-planar to avoid non-specific intercalations. The scaffold also need to contain or be able to add on later hydrogen-bond (H-bond) donors and acceptors such as Os and Ns that are capable of forming H-bond interactions with the binding site nucleobases. It is preferred that the selected scaffold is relatively easy to synthesize and contain no stereocenters to simplify the purification and compound characterization until come binding activity is seen. At that time, more complex molecules with stereocenters can be synthesized to further explore the structure-activity-relationship of the molecules. And finally, the selected scaffold should allow future modifications and optimization to facilitate the SAR study.

Table 3-2: General guidelines used for selecting scaffold from the virtual screening hit list.
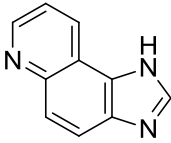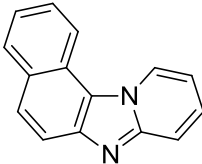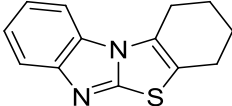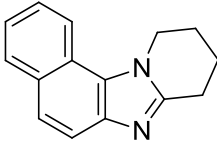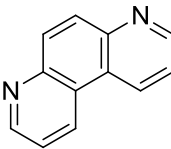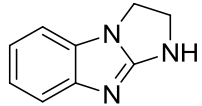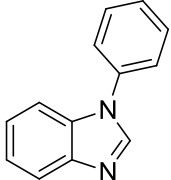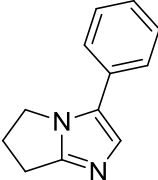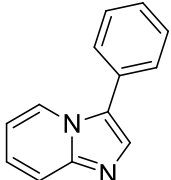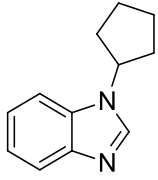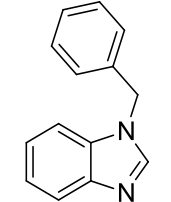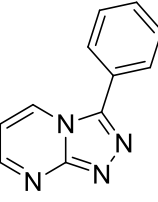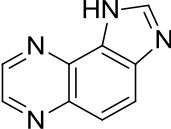
✓ rigid and non-planar
✓ be able to incorporate H-bond donors and acceptors
✓ relatively easy to synthesize
✓ allow further modification at various positions

None of the output molecules were purchased or synthesized. It is rare that the compounds obtained from the virtual screening are used directly as the lead compound. The drug-like properties have been developed based mainly on protein targets. For a nucleic acid target, additional modifications are often required for the scaffold to bind, for example, H-bond donors and acceptors. It was also not our intention to evaluate the performance of the ROCS program in searching active RNA binding molecules. The screening was used as guidance and a place to start for the ligand design. It is not a method of guaranteed success. The result must be analyzed carefully by the chemist to extract useful information towards the design of active ligands.

The top-ranked scaffold structures from the screening are shown in the table below (Table 3-3). It is noticed that the same scaffold structure may show up multiple times with different substitutions. However, the more frequent appearance of these compounds with the same core structure may simply be due to the fact that there are more such compounds deposited in the database. It is therefore not a good indication that the scaffold is more similar to the query molecule. For this reason, in the table shown below, the substitutions were removed from the molecules to yield clear view of

the core structures that are easy to compare. The rank of the scaffolds are as first seen

in the screening output.

Table 3-3: Top-ranked scaffold structures obtained from the shape similarity screen
using benzimidazole **1** as query molecule and ZINC drug-like subset.

Entry	Structure	Entry	Structure
1	1*H*-imidazo[4,5-*f*]quinoline	2	
3		4	
5		6	
7		8	
9		10	
11		12	
13			

Among the scaffolds obtained are the ones that contain benzimidazole moieties, either embedded within a fused ring system (Entry 1-4, 6, 13) or substituted at N1 (Entry 7, 10, 11). The overall shapes of the entries with fused benzimidazole moiety resemble that of the benzimidazole **1** query molecule. These scaffolds also contain nitrogen atoms that are capable of hydrogen bond formation. However they are all planar molecules that have the tendency to form non-specific intercalation with the double stranded nucleic acids. For example, they can intercalate between base pairs. These fused ring structures may also require more efforts to synthesize and functionalize at certain positions and limit optimization options in the future.

By contrast, the N^1-substituted benzimidazoles (Entry 7,10,11) are well-known scaffolds and literature examples on their synthesis are readily available. Looking at these three entries individually, entry 11 has a benzyl substitution at N1 that gives more flexibility of the substitution, while entry 10 has a cyclohexyl substitution that will give rise to chiral centers if further substituted, just like the benzimidazole **1** and **2**. On the other hand, entry 7 has a rigid phenyl substitution that can be further substituted easily. Entry 7 is also non-planar because the aryl substitution at N1 does not rest in the same plane as the benzimidazole but instead orients at an angle (Figure 3-7). The desired functional groups that improve the molecule's hydrogen bonding potential can be incorporated.

Although the synthesis of the aryl-substituted benzimidazoles was predicted to be not very difficult, the challenge remains because the design of the synthetic strategy

must also be efficient and flexible to allow quick preparation of a library of these

compounds. To achieve high synthetic efficiency, the starting materials should be readily

available and inexpensive. And it should take only a few steps to make the desired final

products. To be flexible means that the synthetic routes should consider and allow

modifications at different positions of the core structure in order to make it possible for

further optimizations. A meaningful structure-activity-relationship (SAR) is highly

valuable for the optimization of the designed ligands and requires exploration of all

spaces around the core structure using various substitutents. Finally, it is worth

mentioning that the synthesized molecules can be used in a different project later. It is

therefore best to leave the synthetic options available for maximum return from these

molecules.
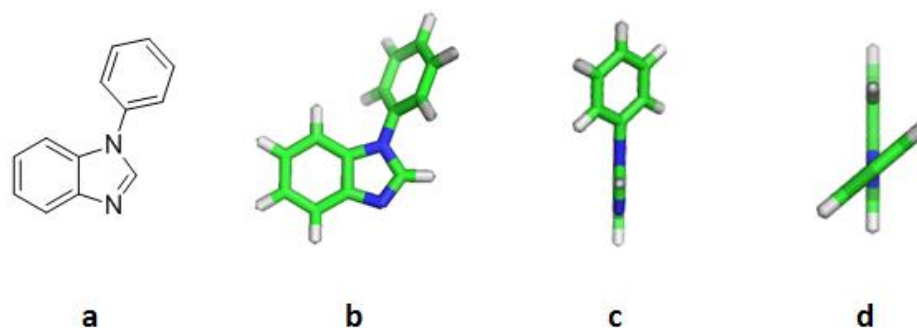
Figure 3-7: 3D structure of N^1-aryl substituted benzimidazole. The aryl substitution is orientated at an angle from the benzimidazole plane. **a**. 2D depiction of the molecule, **b**. front view of the 3D structure, **c**. side view of the structure, **d**. top view of the structure. The 3D structure model is obtained from ZINC (ID: zinc_334446) [30].

Some other scaffolds from the screen include phenanthroline (Entry 5), aryl-substituted pyrroloimidazole scaffold (Entry 8), aryl-substituted imidazopyridine (Entry 9). and substituted triazolopyrimidine (Entry 12). These scaffolds either have un-wanted biological activities or have nitrogen atoms at ring junctions that are not beneficial for the desired H-bond interactions but instead complicate the organic synthesis. For example, phenanthroline is known for coordinating with most metal ions and for its peptidase inhibition activity.

N^1-aryl substituted benzimidazole scaffold posses favorable structure and chemical features and is selected to use in the design of HCV IRES subdomain IIa RNA binding molecules.

Design of Aryl-Substituted Aminobenzimidazoles Targeting the HCV IRES IIa RNA

Previous SAR studies on the 2-aminobenzimidazoles revealed the importance of a rigid scaffold for target binding to the HCV subdomain IIa RNA [1]. Shape-similarity screening using benzimidazole **1** as query molecule resulted in the discovery of N^1-aryl-substituted benzimidazole scaffold. Compared to the query molecule **1**, the structural complexity originated from the ring structures and the two chiral centers within were reduced to a rigid aryl group that is expected to maintain the ability to form stacking interactions with the adjacent base pairs. Compared to the benzimidazole **2** (Figure 3-2), the rigid aryl substituent can function as linker for a dimethylamino substituent to form

hydrogen bond interaction with the RNA while avoiding a entropic penalty for pre-organization of the dimethylaminopropyl chain.

Several chemical series of substituted compounds were designed based on this scaffold (Figure 3-8), including the compounds **3** and the 2-amide derivatives **4**. To evaluate the importance of the 2-amino substituent, we prepared 2-hydroxy benzimidazole analogs **5**. A small number of dimethylaminopropyl-substituted compounds **6** which carried aryl substituents at the benzene ring were included as well.
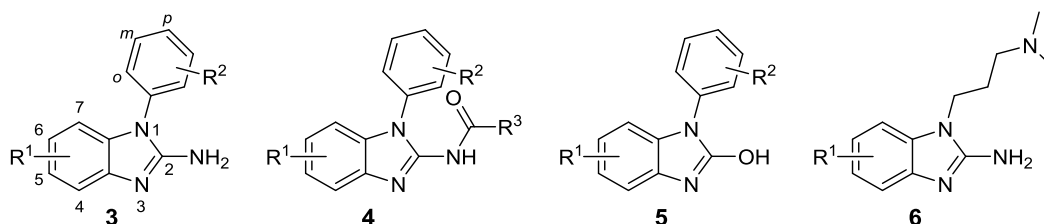
Figure 3-8: Benzimidazole derivatives for targeting the HCV IRES subdomain IIa RNA. 1-aryl-2-aminobenzimidazoles **3**, 1-aryl-2-acylaminobenzimidazoles **4**, 1-aryl-2-hydroxybenzimidazoles **5**, N,N'-dimethylaminopropyl-substituted benzimidazoles **6**.

Organic Synthesis of Aryl-substituted Aminobenzimidazoles

Synthesis of aryl ether derivatives in the series **3**, **4** and **5** ($R^1 = R^4O$, Scheme 3-1 and Table 3-4) commences from phenyl starting material **7** that is readily available and inexpensive. The ether substitution was installed first by alkylation of **7** to yield phenylether **9**, which then undergoes a palladium catalyzed Buchwald-Hartwig amination reaction [34] to obtain **11**. Catalytic reduction of the nitro group gives the common intermediate *N*-aryl-substituted *o*-phenylenediamine (**12**). In the synthesis of

phenol **3a** (R^4 = OH), *tert*-butyldimethylsilyl (TBDMS) ether linkage was used and later

removed by fluoride reagent. Cyclization of *o*-phenylenediamine **12** using

isothiocyanates provided 2-amide derivatives **4**, which could be further hydrolyzed to

furnish the 2-aminobenzimidazoles **3**. **3** could also be prepared by treating **12** with

cyanogens bromide. However, the reaction of the product with additional cyanogens

bromide was hard to avoid. Treatment of **12** with phosgene yielded 2-hydroxy

benzimidazole analogs **5**.
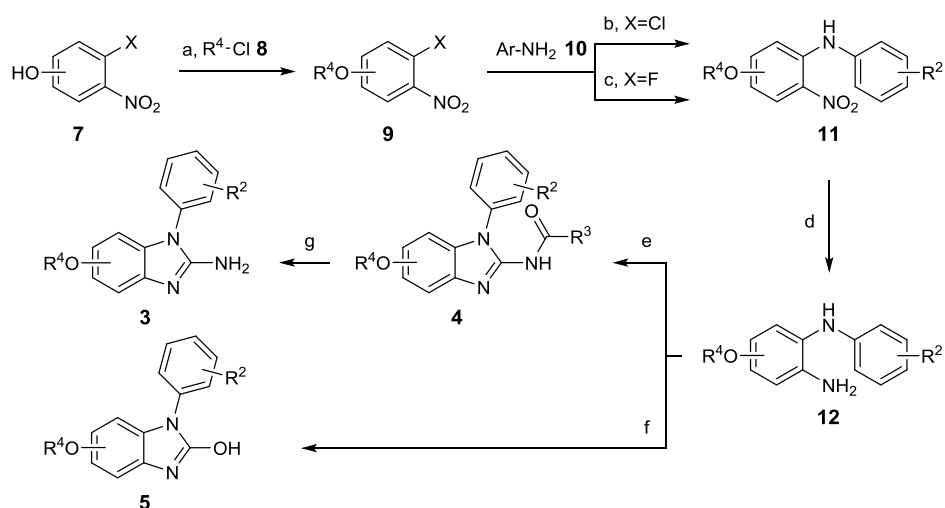
Scheme 3-1: Synthesis of 1-aryl-2-aminobenzimidazoles **3**, 1-aryl-2-acylamino-benzimidazoles **4** and 1-aryl-2-hydroxybenzimidazoles **5** from halo-nitrophenols **6**. Preparation of 5-substituted benzimidazoles commenced from 4-chloro-3-nitrophenol (X=Cl), that of 6-substituted products from 3-fluoro-4-nitrophenol (X=F). Reagents and conditions: a) (for R^4=H, **8**=TBDMSCl) K_2CO_3, ACN, reflux, 2.5-28 h, 52-94 % yield; b) Cs_2CO_3, $Pd_2(dba)_3$, (±)BINAP, 19-28 h, 31-91 % yield; c) K_2CO_3, ACN, reflux, 21-41 h, 34-36 % yield; d) H_2 (1 atm), Pd/C or PtO_2, MeOH, RT, 1.5-25 h; e) acylNCS (acyl=acetyl or benzoyl), DIPC, DIPEA, ACN, 22-48 h, 20-66 % yield over two steps; f) phosgene (20 % in toluene), pyridine, DCM, RT, 3-24 h, 50-64 % yield two steps; g) 1N HCl, H_2O, dioxane, reflux, 18-28 h, 27-96 % yield.

Two aniline derivatives **3h** and **3i** (Table 3-4) were synthesized from 2,4-

dichrloro-nitrobenzene **13** starting material through two consecutive Buchwald-Hartwig

amination reactions (Scheme 3-2). The following catalytic reduction of the nitro group

and cyclization using isothiocyanate yields 2-amide substituted derivative **18** that was

further hydrolyzed to complete synthesis of compound **3h** and **3i**.
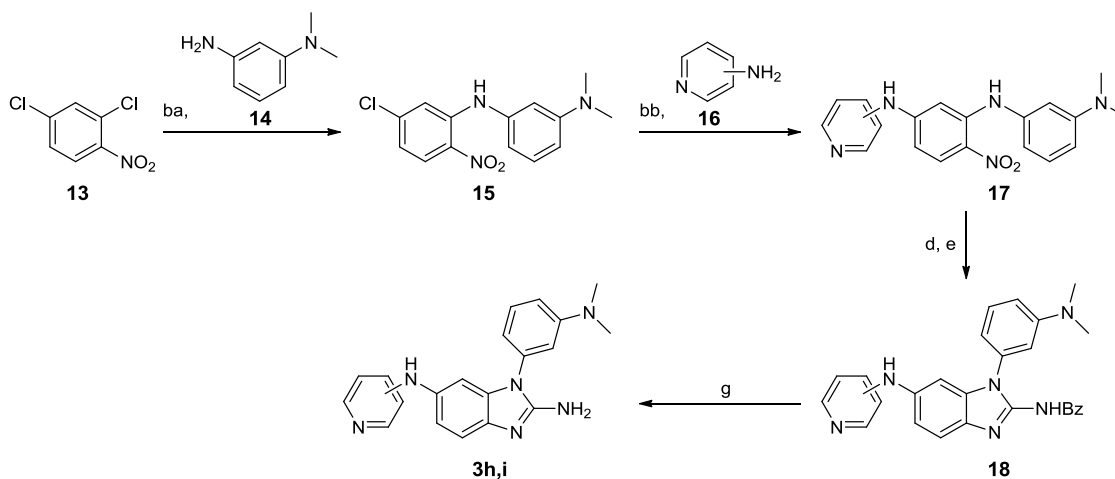
Scheme 3-2: Synthesis of 1-aryl-2-aminobenzimidazoles **3h** and **3i**. Reagents and conditions: ba) Cs_2CO_3, $Pd_2(dba)_3$, ($\pm$)BINAP, toluene, reflux, 21 h, 43 % yield two steps; **14** was synthesized from N,N-dimethyl-3-nitroaniline by reduction with H_2 (1 atm), Pd/C in MeOH, 20 hr; bb) Cs_2CO_3, $Pd_2(dba)_3$, ($\pm$)BINAP, dioxane, reflux, 20-44 h, 34-43 % yield d) H_2 (1 atm), Pd/C or PtO_2, MeOH, RT, 21-23 h h; e) BzNCS, DIPC, DIPEA, ACN, 24-26 h, 22-32 % yield over two steps; g) 1N HCl, H_2O, dioxane, reflux, 23-26 h, 27-56 % yield.

The *N,N*-dimethylaminopropyl-substituted benzimidazoles **6** (Table 3-5) were

synthesized following the route outlined in Scheme 3-3. Dichloronitrobenzene **13**

precursors were first selectively alkylated at the position *ortho* to nitro group to install

the dimethylaminopropyl substitution. Coupling with aromatic amines using Buchwald-

Hartwig chemistry led to nitro-aniline **22**, or with boronic acids using Suzuki chemistry to

yield biphenyl intermediate **23**. Catalytic reduction of the nitro group and cyclization

with isothiocyanate reagent furnish the 2-amide derivatives **24** whose hydrolysis gave

the final products **6**.
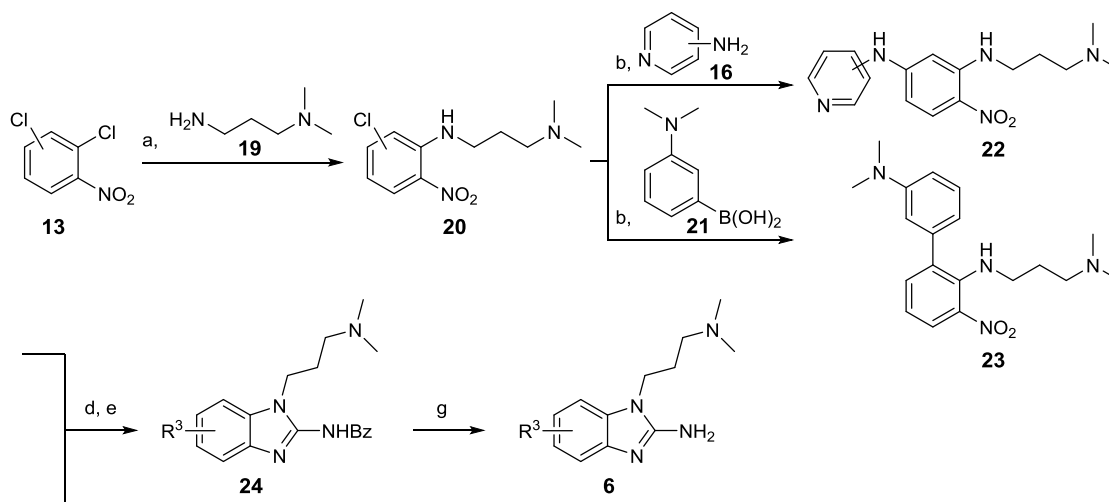
Scheme 3-3: Synthesis of *N,N'*-dimethylaminopropyl-substituted benzimidazoles **6** from dichloro-nitrobenzenes **13**. Preparation of 6-substituted benzimidazoles commenced from 1,2-dichloro-4-nitrobenzene, that of 7-substituted products from 1,2-dichloro-3-nitrobenzene. Reagents and conditions: a) K_2CO_3, ACN, reflux, 24 h, 96-97 % yield; b) Cs_2CO_3, $Pd_2(dba)_3$, (±)BINAP, 19-23 h, 37-80 % yield range; d) H_2 (1 atm), Pd/C or PtO_2, MeOH, RT, 21-25 h; e) BzNCS, DIPC, DIPEA, ACN, 19-21 h, 29-33 % yield over two steps; g) 1N HCl, H_2O, dioxane, reflux, 17-21 h, 22-46 % yield.

Testing of Compounds Using FRET Assay

The synthesized compounds were tested for binding to the IRES IIa RNA by

triplicate titration in the IIa FRET assay. Target binding affinity, expressed as EC_{50} value,

was determined from fitting of single-site binding dose response curves to the titration

data (Tables 3-5 and 3-6).Of the nine 1-aryl-2-aminobenzimidazoles **3** synthesized, all

but two showed binding to the IIa RNA target with affinities between 74–250 µM.

Exceptions were the unsubstituted phenol **3a** and the 5- picolyl ether **3d**. Inspection of

the binding pocket around **1** in the co-crystal structure suggested that while the parent

phenol **3a** is unable to form interactions beyond the amino-imidazole scaffold, in the

derivative **3d** the bulky pyridinemethylene ether substituent off the 5-position might

interfere with ligand docking at the G110 base of the RNA target (Figure 3-7). In contrast,

the more flexible aliphatic dimethylaminoalkyl ether chain was tolerated at the same

position, as attested by the binding of compounds **3b** and **3c** (250 and 210 µM,

respectively). Improvement of the affinity by 2-fold was seen in derivative **3e** (95 µM)

which carried a 5-dimethylaminopropyl ether substituent at the benzimidazole and an

additional *p*-dimethyalmino group on the imidazole-linked phenyl ring. The same

combination of functional groups, however, with the dimethylaminoalkyl ether chain

moved to the 6-position reduced activity of compond **3f** (170 µM). Relocation of the

dimethylamino substituent from the *para*- to the *meta*-position at the imidazole-linked

phenyl ring increased binding in derivative **3g** (120 µM), yet not to the level of **3e**. Finally,

aromatic substituents were tolerated at the benzimidazole 6-position as indicated by

the affinity of compounds **3h** and **3i**, which were among the most active ligands

synthesized here (74 and 100 µM, respectively). In comparison, compounds **6h** and **6i**

which carried the same aromatic pyridine substituents at the 6-position but had the *m*-

dimethyalminophenyl ring at the imidazole replaced with a flexible

dimethylaminopropyl chain showed weaker target affinity (both, 160 µM). Attachment
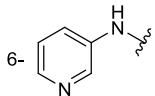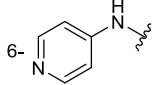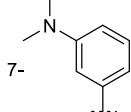
of a *m*-dimethylaminophenyl group at the 7-position of the benzimidazole retained

binding activity in compound **6j** albeit only at 290 µM.

Table 3-4: Activity of 1-aryl-benzimidazole derivatives **3**, **4** and **5** in the FRET assay.

Compound	R^1	R^2	R^3	EC_{50} [µM][a]
3a	5-OH	H	H	n.a.
3b / 5b	5- (structure)	H	H	250 ± 66
3c / 5c	5- (structure)	H	H	210 ± 39
3d	5- (structure)	H	H	n.a.
3e	5- (structure)	p- (structure)	H	95 ± 6
3f / 5f	6- (structure)	p- (structure)	H	170 ± 16
3g	6- (structure)	m- (structure)	H	120 ± 5
3h	6- (structure)	m- (structure)	H	74 ± 2
3i	6- (structure)	m- (structure)	H	100 ± 12
4ba	5- (structure)	H	CH_3	100 ± 13
4ca	5- (structure)	H	CH_3	> 500
4ab	5-OH	H	C_6H_5	n.a.
4bb	5- (structure)	H	C_6H_5	> 500
4cb	5- (structure)	H	C_6H_5	> 500
4eb	5- (structure)	p- (structure)	C_6H_5	precip.
4fb	6- (structure)	p- (structure)	C_6H_5	precip.

[a]EC_{50} values (± standard error from triplicate experiments) are shown for 2-aminobenzimdiazoles **3** and acyl derivates **4**. All tested 2-hydroxybenzimidazoles **5** precipitated RNA at a concentration between 50-100 µM.

Table 3-5: Activity of *N,N'*-dimethylaminopropyl-substituted benzimidazoles **6** in the FRET assay.

Compound	R[1]	EC$_{50}$ [μM][a]
6h		160 ± 15
6i		160 ± 29
6j		290 ± 100

[a]EC$_{50}$ values are shown ± standard error from triplicate experiments.

When the ligand-bound subdomain IIa structure became available in 2012 [29], modeling studies of the aryl-substituted benzimidazole scaffold was done and it suggested that the twist conformation between the benzimidazole and aryl ring along with an appropriate *meta*-substitution position for the dimethylamino group would provide a rigid vector for interaction with the phosphate group of residue A109 (Figure 3-9). While in comparison of the crystal structure of compound **3e** that shows a twist angle of 67° between the imidazole and the phenyl ring attached at the 1-position, a good fit of the 1-phenyl ring in **3e** and the dimethylaminopropyl chain in **1** bound to the IIa RNA target was observed in a superposition of the two compounds (Figure 3-9). The *meta* position of the phenyl ring in **3e** is pointing at the location of the dimethylamino group in **1** which forms a key hydrogen bond with the phosphate of A109 in the RNA target.
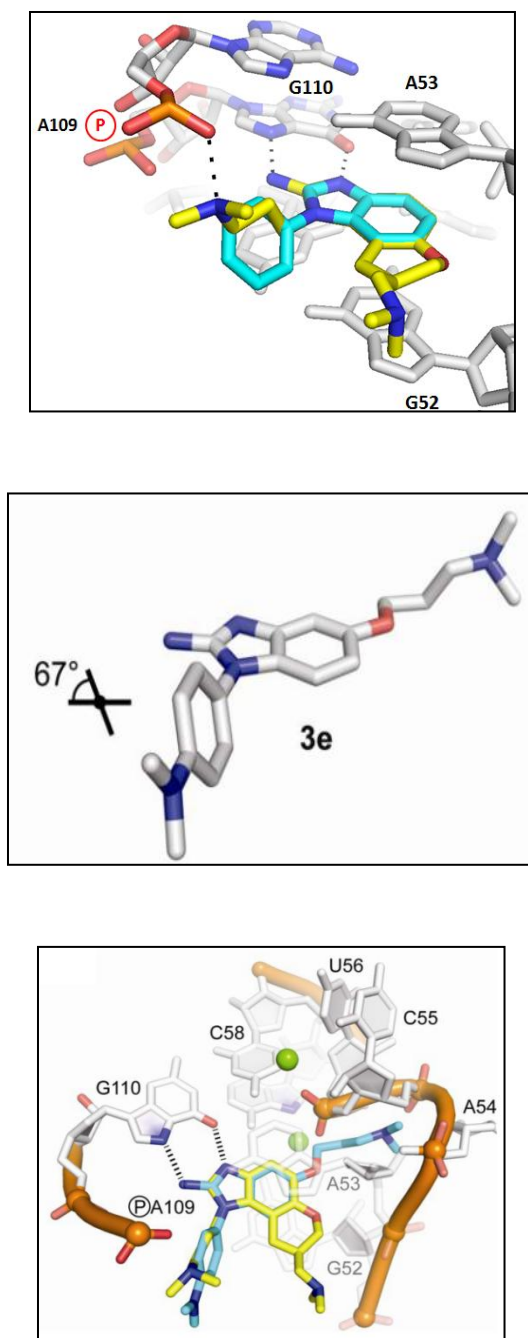
Figure 3-9: Molecular modeling of the aryl-benzimidazoles and ligand-bound HCV IRES subdomain IIa cocrystal structure. *Top*: Model of the N1-phenyl-2-aminobenzimidazole core (cyan) docked at the binding site of benzimidazole **2** (yellow) in the subdomain IIa RNA cocrystal structure [29]. *Middle:* Crystal structure of compound **3e** showing 67° twist angle between the imidazole and the phenyl ring. *Bottom*: Superposition of compound **3e** (Blue) on the inhibitor **2** (Yellow) in the subdomain IIa cocrystal structure.

Comparison of the derivatives **3f** and **3g** suggests that higher affinity is achieved by substitution of the phenyl ring with a dimethylamino group at the *meta* position compared to the *para* position. In the superposition of **3e** on the **1** target complex, the dimethylaminopropyl ether chain at the benzimidazole 5-position is directed towards a cleft lined by the sugar phosphate backbone of residues A54-U56 (Figure 3-9). This region is located in a flexible internal loop of the IIa RNA target and undergoes a large conformational change upon binding of the ligand **2**. Such adaptive binding might allow the accommodation of flexible substituents at the benzimidazole 5-position, for example, the dimethylaminopropyl ether chain in the **3e** derivative. However, as indicated by the inactivity of compound **3d**, which carries a pyridinemethylene ether substituent, bulky and more rigid groups at the 5-position may not be reconciled with target adaptation.

Acylation of the 2-amino group abolished binding as indicated by compounds in the series **4**. The acetylated derivative **4ba** was an exception for which a target affinity of 100 µM was measured, surpassing that of the parent compound **3b** (250 µM). This observation is not readily reconciled with the crystal structure of the ligand **1** RNA complex, perhaps suggesting that compound **4ba** accesses an alternative binding mode at the target. The hydroxybenzimidazoles **5** compounds showed strong precipitating properties in the FRET assay, suggesting nonspecific binding interactions with the target RNA. All tested compounds in this series led to rapid fluorescence quenching in the FRET

assay at micromolar concentration, apparently due to precipitation of the dye labeled RNA target.
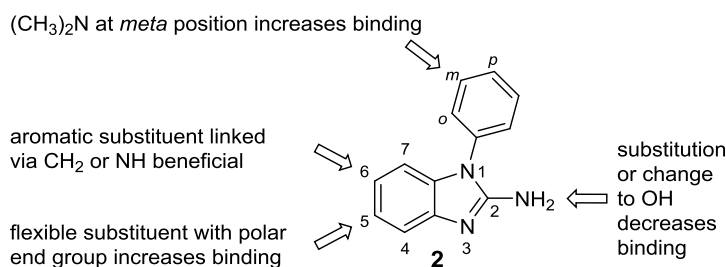
Figure 3-10: Structure activity relationships discovered for N^1-aryl-2-amino-benzimidazoles targeting the HCV IRES subdomain IIa RNA.

Summary

In summary, the N^1-aryl-substituted 2-amino-benzimidazole compounds were designed based on the aryl-benzimidazole scaffold obtained from the shape-similarity screening using inhibitor **1** as query molecule. The synthesis of the designed molecules is described. The compounds were tested using the FRET assay and binding affinities were obtained. Based on the available data, structure-activity relationship study was conducted (Figure 3-10). The observed pattern of compound activity in the FRET target binding assay were explained in the context of the cocrystal structure of benzimidazole **2** bound to the IIa RNA. Ligands with the highest affinity showed binding at EC_{50} values around 74–100 µM which is inferior to the previously studied tricyclic benzimdazoles

such as **1** although the synthetic accessibility of designed compounds is much better,

allowing further optimization of the N^1-aryl-substituted benzimidazoles in the future.

Materials and Methods

General Notes: All chemical reagents were obtained from commercial suppliers

listed on UCSD Market Place website and used without further purification. Anhydrous

solvents were obtained using a two-column purification system (Glasscontour Systems,

Irvine, CA). Non-aqueous reactions were carried out under anhydrous conditions using

oven-dried glassware under an inert atmosphere. The inert atmosphere was created via

balloons filled with Argon (Ar) gas or via Schlenk line apparatus. Analytical thin-layer

chromatography (TLC) was carried out on precoated 60 F254 aluminum backed silica gel

plates from EMD Millipore. TLC plates were visualized by UV and/or stained by ninhydrin

solution followed by heat. Flash column chromatography was performed using SiliaFlash

P60 40-63 µm 60 Å silica gel from Silicycle. Organic solvents were removed by rotary

evaporation below 30 °C at approximately 15 mmHg. NMR spectra were recorded at

room temperature (22 °C) on a Varian Mercury 400 MHz instrument with chemical shifts

reported relative to residual deuterated solvent peaks. Deuterated solvents used

include deuterochloroform ($CDCl_3$), deuteromethanol (CD_3OD), and deuterodimethyl

sulfoxide (DMSO-d6). Chemical shifts (δ) are in parts per million (ppm); multiplicities are

indicated by s (singlet), d (doublet), t (triplet), q (quartet), dd (doublet of doublet), or m

(multiplet); coupling constants (*J*) are reported in Hertz (Hz). Mass spectra were

obtained on a Micromass Quattro Ultima Triple Quadrupole using ESI method at the UCSD Molecular Mass Spectrometry Facility.

Abbreviations: ACN = acetonitrile; BINAP = 2,2'-bis(diphenylphosphino)-1,1'-binaphthalene; dba = dibenzylideneacetone; DCM = dicholormethane; DIPC = *N,N'*-diisopropylcarbodiimide; DIPEA = *N,N*-diisopropylethylamine; DMF = dimethylformamide; DMSO = dimethyl sulfoxide; Et_3N = triethylamine; EtOAc = ethyl acetate; RT = room temperature; TBAF = tetra-n-butylammonium fluoride; TBDMSCl = *tert*-butyldimethylsilyl chloride.

tert-butyl(4-chloro-3-nitrophenoxy)dimethylsilane (9a)
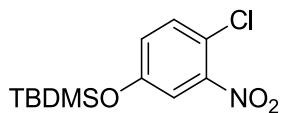
To a 100 ml round-bottom flask was added 4-chloro-3-nitrophenol (200 mg, 1.16 mmol), DCM (30 ml), *tert*-Butyldimethylchlorosilane (174 mg, 1.16 mmol), and triethylamine (161 μl, 1.16 mmol). The reaction was stirred at rt for 2.5 hours, then concentrated and purified via flash column (Hexane – DCM : 80 % - 20 %) to yield product as a clear oil (324 mg, 94 % yield). ^{1}H NMR (400 MHz, CDCl$_3$): δ 7.38 (d, *J* = 8 Hz, 1H), 7.32 (d, *J* = 2 Hz, 1H), 6.99 (dd, *J$_1$* = 8 Hz, *J$_2$* = 2Hz, 1H), 0.97 (s, 9H), 0.22 (s, 6H). ^{13}C NMR (400 MHz, CDCl$_3$): δ 155.08, 148.35, 132.56, 125.39, 118.98, 117.20, 25.70, 18.37, -4.32.

Spectrum 3-1: *tert*-butyl(4-chloro-3-nitrophenoxy)dimethylsilane (**9a**) ^{1}H NMR (400 MHz, CDCl₃)
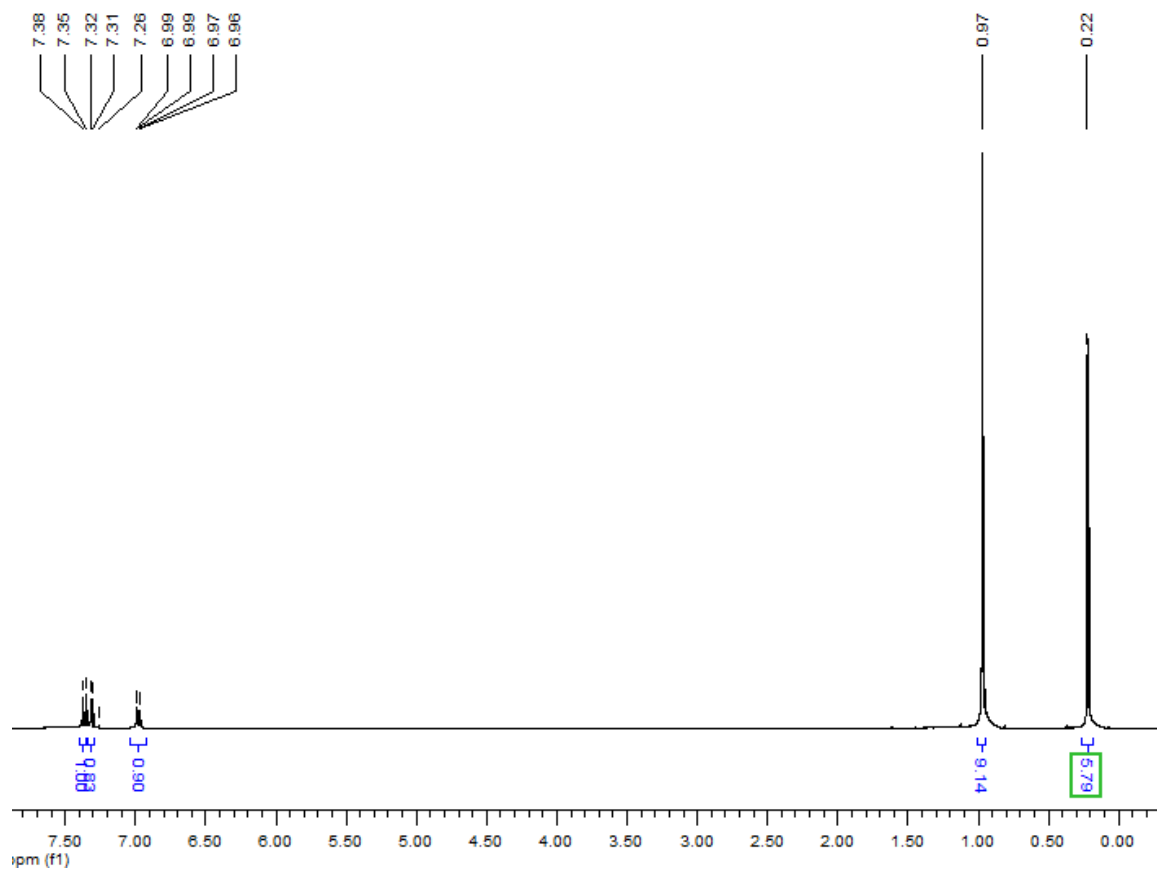
Spectrum 3-2: *tert*-butyl(4-chloro-3-nitrophenoxy)dimethylsilane (**9a**) ^{13}C NMR (400 MHz, CDCl$_3$)
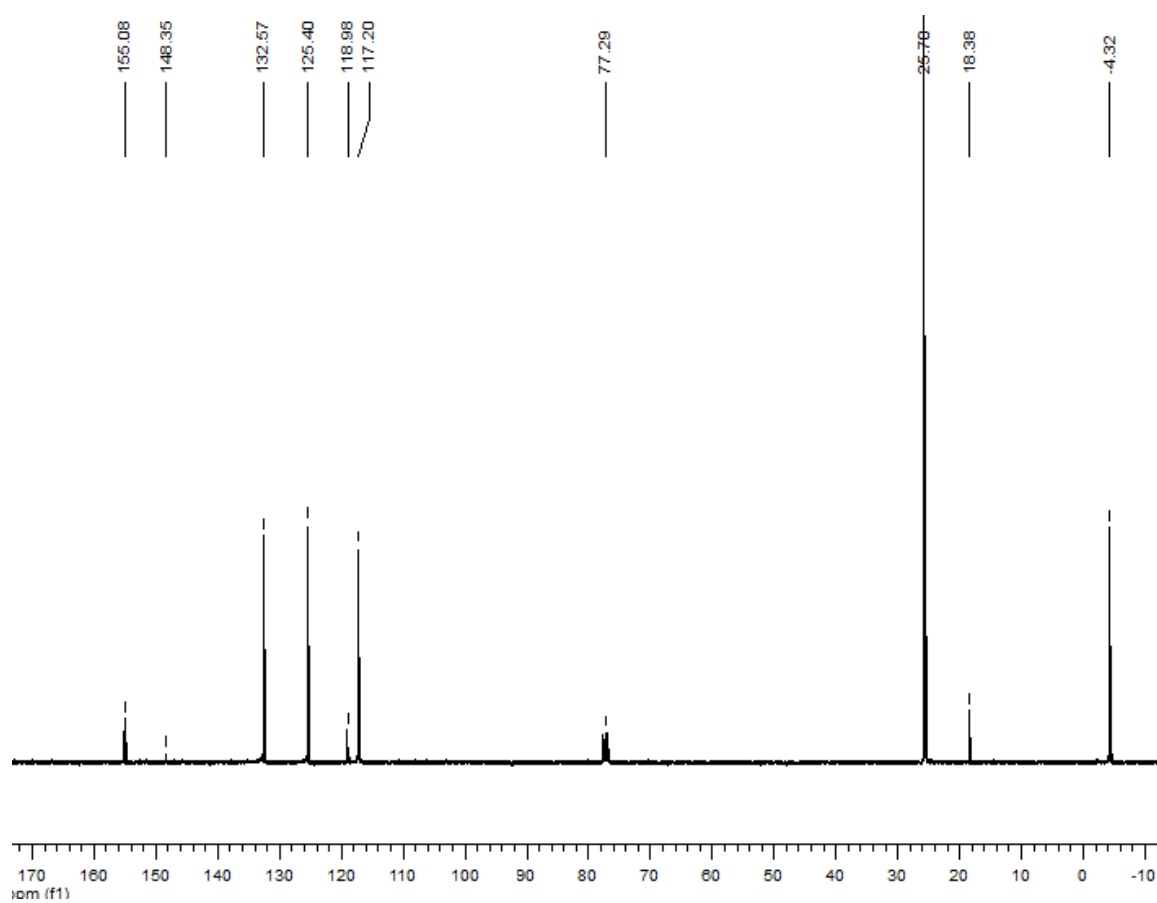
2-(4-chloro-3-nitrophenoxy)-*N*,*N*-dimethylethanamine (9b)
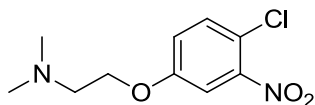
To a 100 ml round-bottom flask was added 2-dimethylaminoethyl chloride hydrochloride (1.0 g, 6.9 mmol, 1.2 eq), ACN (50 ml), 4-chloro-3-nitrophenol (1.0 g, 5.8 mmol) and finally K_2CO_3 (1.7 g, 12.7 mmol). The reaction was stirred under Ar and heated to reflux for 26 hours before cooling to RT and filtration. After removal of solvent, the residue was extracted with EtOAc and water (150 ml ea.). The water layer was extracted with additional 100 ml of EtOAc. The combined organic layers were then washed with water, brine and dried over Na_2SO_4. After filtration and concentration, the crude was purified with flash column chromatography (DCM – MeOH : 90 % - 10 %) to yield yellow oil as the product (1.3 g, 94 % yield). ^{1}H NMR (400 MHz, DMSO-d6): δ 7.65 (d, *J* = 3 Hz), 7.64 (d, *J* = 9 Hz, 1H), 7.29 (dd, J_1 = 9 Hz, J_2 = 3 Hz, 1H), 4.12 (t, *J* = 5 Hz, 2H), 2.60 (t, *J* = 5 Hz, 2H), 2.18 (s, 6H). ^{13}C NMR (400 MHz, DMSO-d6): δ 158.41, 148.96, 132.76, 121.19, 116.18, 111.72, 67.62, 58.00, 46.12.

Spectrum 3-3: 2-(4-chloro-3-nitrophenoxy)-*N,N*-dimethylethanamine (**9b**) ^{1}H NMR (400 MHz, DMSO-d6)
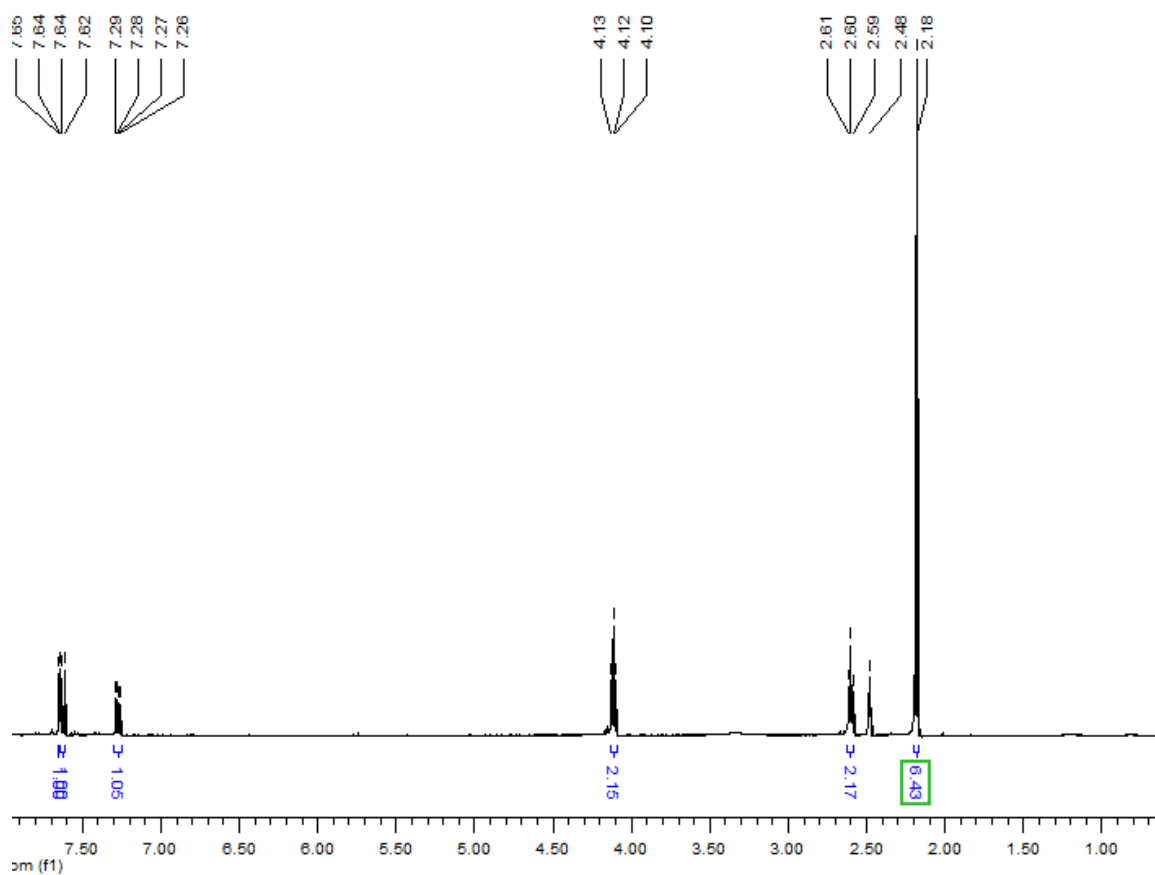
Spectrum 3-4: 2-(4-chloro-3-nitrophenoxy)-*N,N*-dimethylethanamine (**9b**) ^{13}C NMR (400 MHz, DMSO-d6)
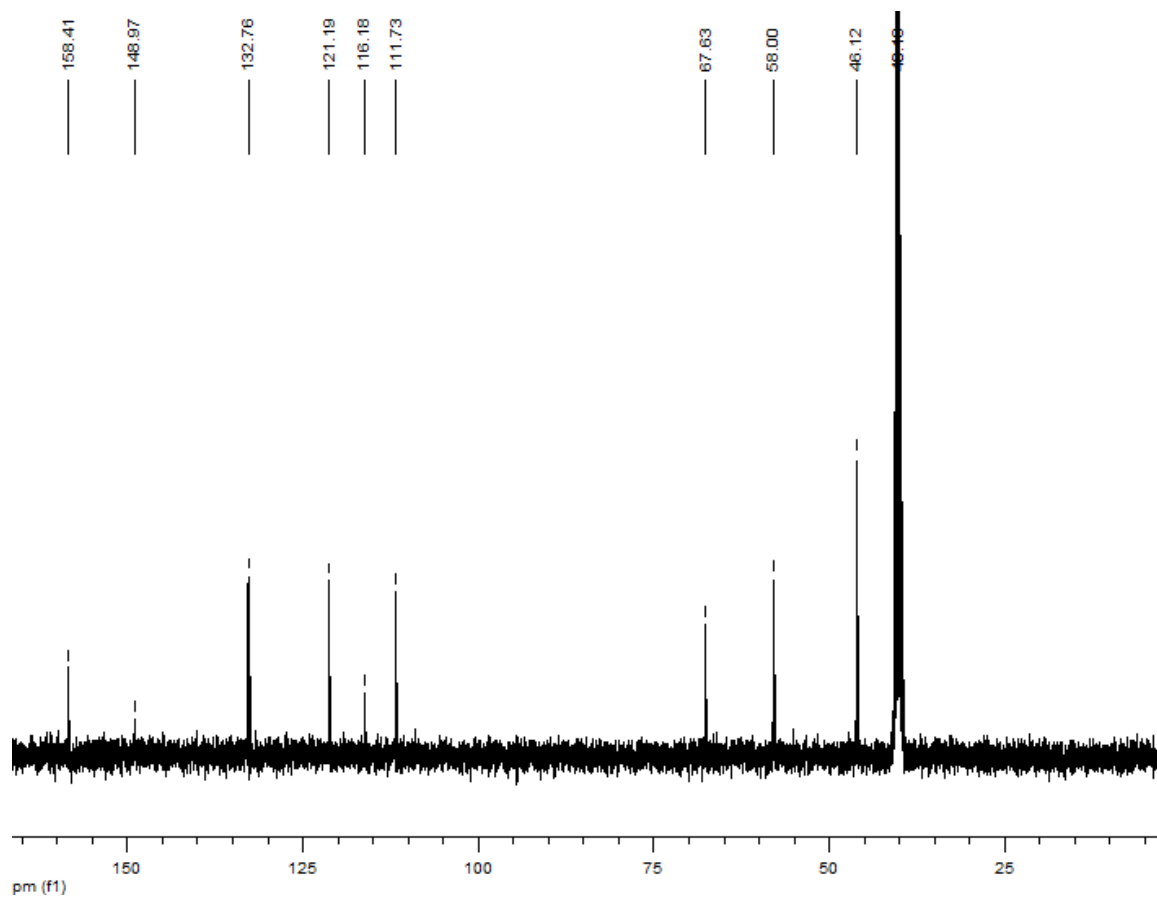
3-(4-chloro-3-nitrophenoxy)-*N*,*N*-dimethylpropan-1-amine (9c)
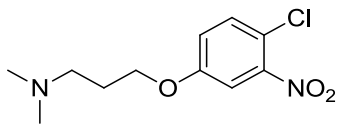
To a 250 ml round-bottom flask was added 4-chloro-3-nitrophenol (2.0 g, 11.5 mmol), DMF (100 ml), *N*,*N*,-dimethylaminopropylchloride hydrochloride (2.2 g, 13.8 mmol, 1.2 eq), and K_2CO_3 (3.1 g, 23.0 mmol). The reaction was stirred and heated to 60 °C for 16 hours before cooling to RT. It was filtered and then concentrated. The crude was purified via flash column chromatography (DCM – MeOH : 90 % - 10 %) to yield yellow oil as the product (2.4 g, 79 % yield). ^{1}H NMR (400 MHz, $CDCl_3$): δ 7.40 – 7.38 (m, 2H), 7.06 (dd, J_1 = 9 Hz, J_2 = 3 Hz, 1H), 4.06 (t, J = 6 Hz, 2H), 2.50 (t, J = 7 Hz, 2H), 2.27 (s, 6H), 2.02 (p, J = 6 Hz, 2H). ^{13}C NMR (400 MHz, $CDCl_3$): δ 158.08, 132.54, 120.41, 118.24, 111.27, 67.29, 56.10, 45.53, 27.19. MS (ESI) calculated exact mass for $C_{11}H_{15}ClN_2O_3$ = 258.08. Found $[M+H]^+$ = 259.00.

Spectrum 3-5: 3-(4-chloro-3-nitrophenoxy)-*N*,*N*-dimethylpropan-1-amine (**9c**) ^{1}H NMR (400 MHz, CDCl$_3$)
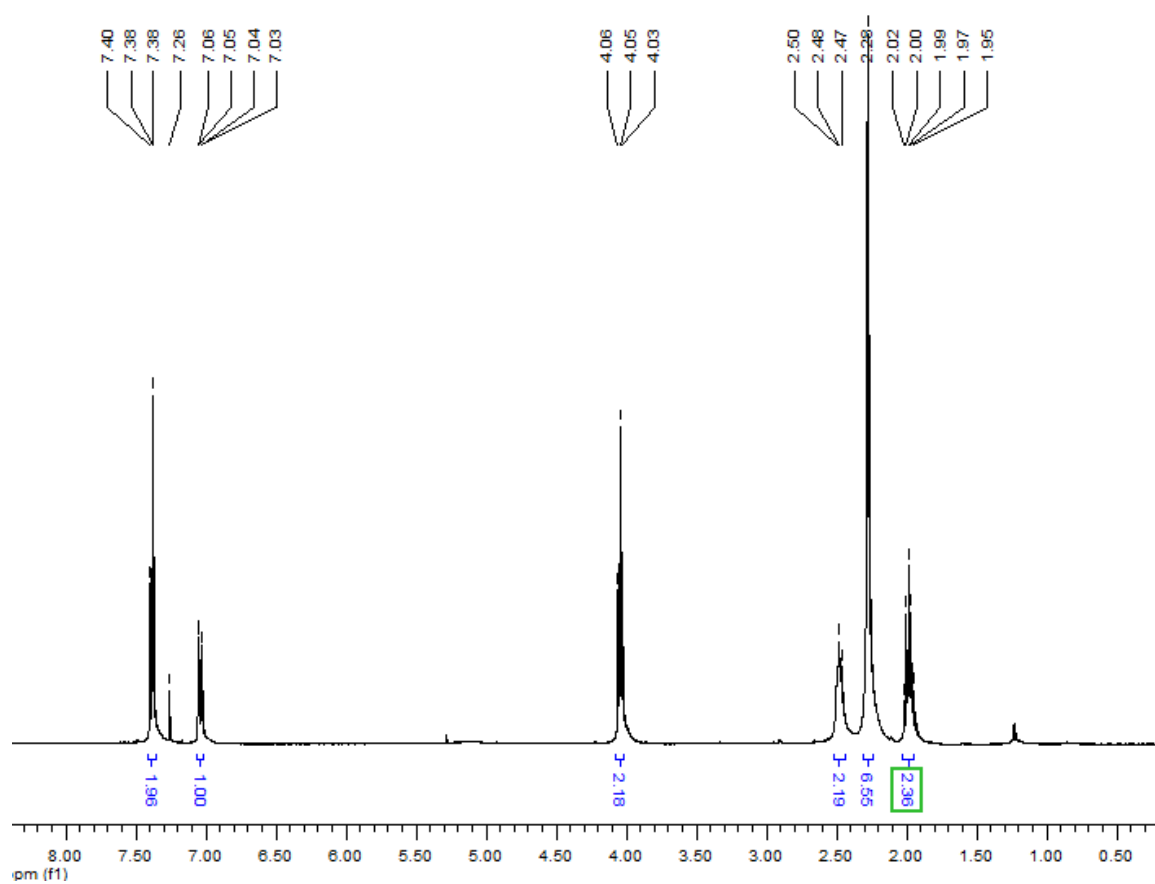
Spectrum 3-6: 3-(4-chloro-3-nitrophenoxy)-*N,N*-dimethylpropan-1-amine (**9c**) ^{13}C NMR (400 MHz, CDCl$_3$)
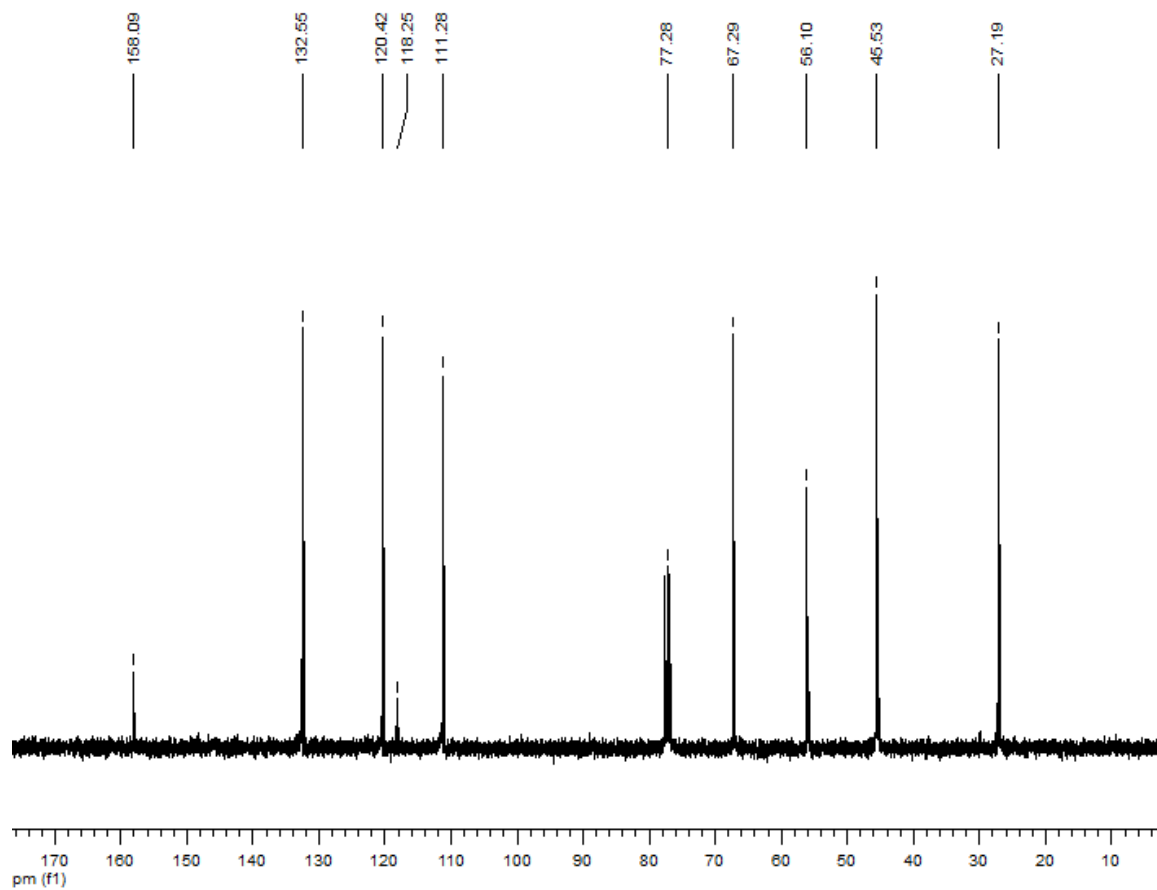
4-((4-chloro-3-nitrophenoxy)methyl)pyridine (9d)
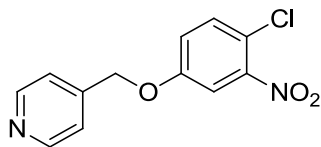
To a 250 ml round-bottom flask was added 4-chloro-3-nitrophenol (1.6 g, 9.2 mmol), DMF (100 ml), 4-picolylchloride hydrochloride (1.5 g, 9.2 mmol) and K_2CO_3 (2.54 g, 18.3 mmol). The reaction was stirred and heated to 60 °C for 28 hours before cooling to RT. It was filtered and then concentrated. The crude was purified via flash column (Hexane – EtOAc : 40 % - 60 %) to yield slight yellow solid as the product (1.3 g, 52 % yield). ^{1}H NMR (400 MHz, DMSO-d6): δ 8.59 (d, J = 6 Hz, 2H), 7.77 (d, J = 3 Hz, 1H), 7.69 (d, J = 9 Hz, 1H), 7.43 (d, J = 6 Hz, 2H), 7.38 (dd, J_1 = 9 Hz, J_2 = 3Hz, 1H), 5.28 (s, 2H). ^{13}C NMR (400 MHz, DMSO-d6): δ 157.80, 150.50, 148.89, 145.65, 132.99, 122.55, 121.41, 116.94, 112.23, 67.17. MS (ESI) calculated exact mass for $C_{12}H_9ClN_2O_3$ = 264.03. Found $[M+H]^+$ = 264.97.

Spectrum 3-7: 4-((4-chloro-3-nitrophenoxy)methyl)pyridine (**9d**) ^{1}H NMR (400 MHz, DMSO-d6)
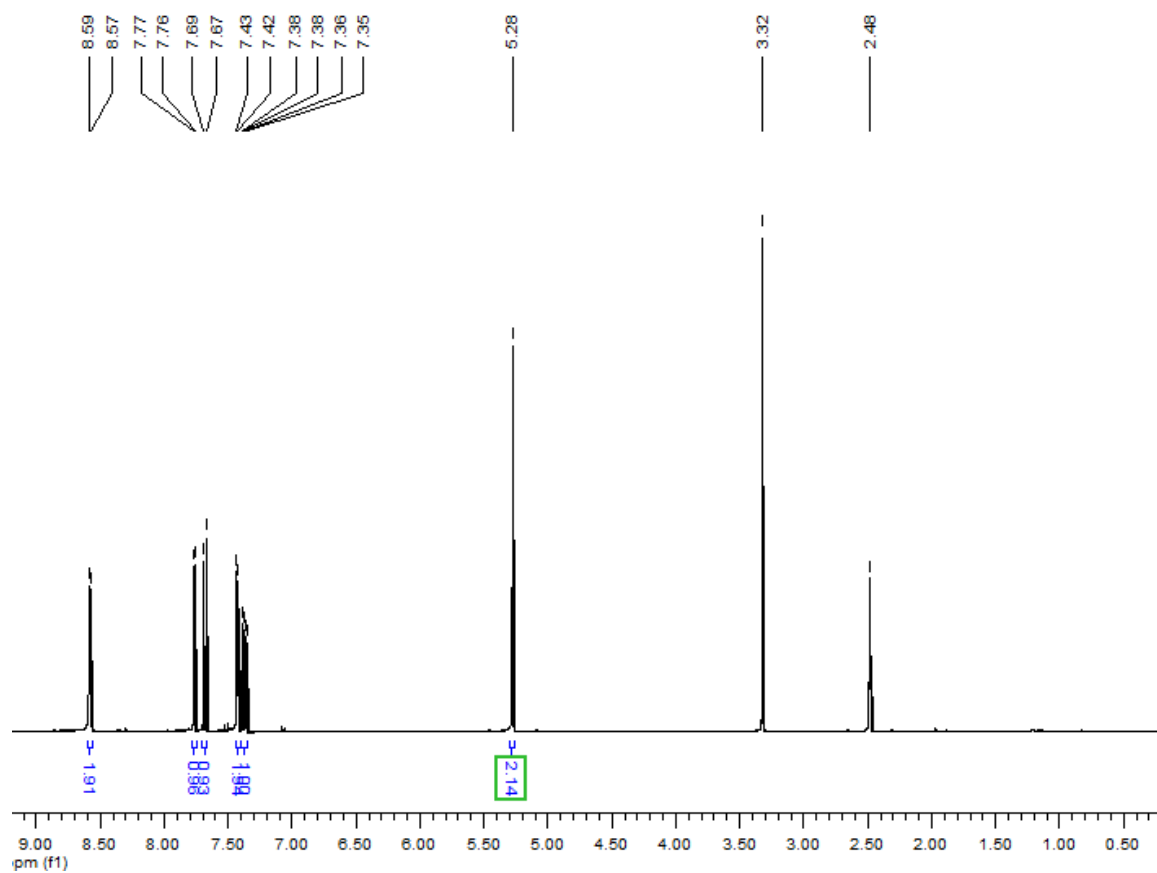
Spectrum 3-8: 4-((4-chloro-3-nitrophenoxy)methyl)pyridine (**9d**) ^{13}C NMR (400 MHz, DMSO-d6)
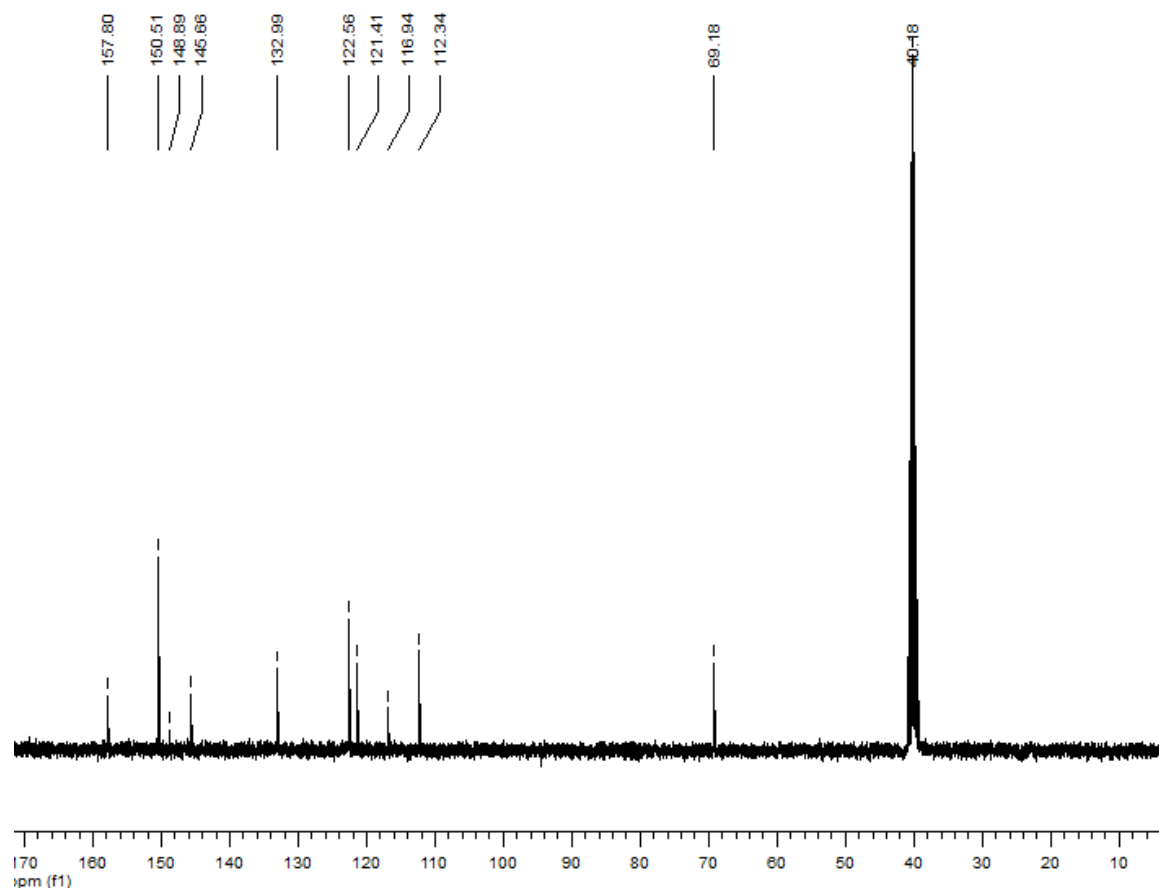
3-(3-fluoro-4-nitrophenoxyl)-*N*,*N*-dimethylpropan-1-amine (9f)
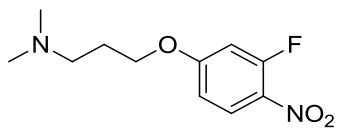
To a 250 ml round-bottom flask was added 3-fluoro-4-nitrophenol (2.0 g, 12.7 mmol), DMF (100 ml), *N*,*N*-dimethylaminopropylchloride hydrochloride (2.4 g, 15.3 mmol, 1.2 eq), and K_2CO_3 (3.9 g, 28.0 mmol). The reaction was stirred and heated to 60 °C for 18 hours before it was cooled to RT. After filtration and concentration, the crude was purified via flash column (DCM – MeOH : 90 % - 10 %) to yield yellow oil as the product (2.0 g, 64 % yield). ^{1}H NMR (400 MHz, DMSO-d6): δ 8.14 (t, *J* = 9 Hz, 1H), 7.18 (dd, J_1 = 14 Hz, J_2 = 3 Hz, 1H), 6.96 (dd, J_1 = 9 Hz, J_2 = 2 Hz, 1H), 4.15 (t, *J* = 7 Hz, 2H), 2.36 (t, *J* = 7 Hz, 2H), 2.14 (s, 6H), 1.89 (p, *J* = 6 Hz, 2H). ^{13}C NMR (400 MHz, DMSO-d6): δ 165.37, 158.72, 156.11, 128.69, 112.23, 104.59, 68.22, 55.90, 45.74, 27.05. MS (ESI) calculated exact mass for $C_{11}H_{16}FN_2O_3$ = 242.11. Found $[M+H]^+$ = 243.06.

Spectrum 3-9: 3-(3-fluoro-4-nitrophenoxyl)-*N,N*-dimethylpropan-1-amine (**9f**) ^{1}H NMR (400 MHz, DMSO-d6)
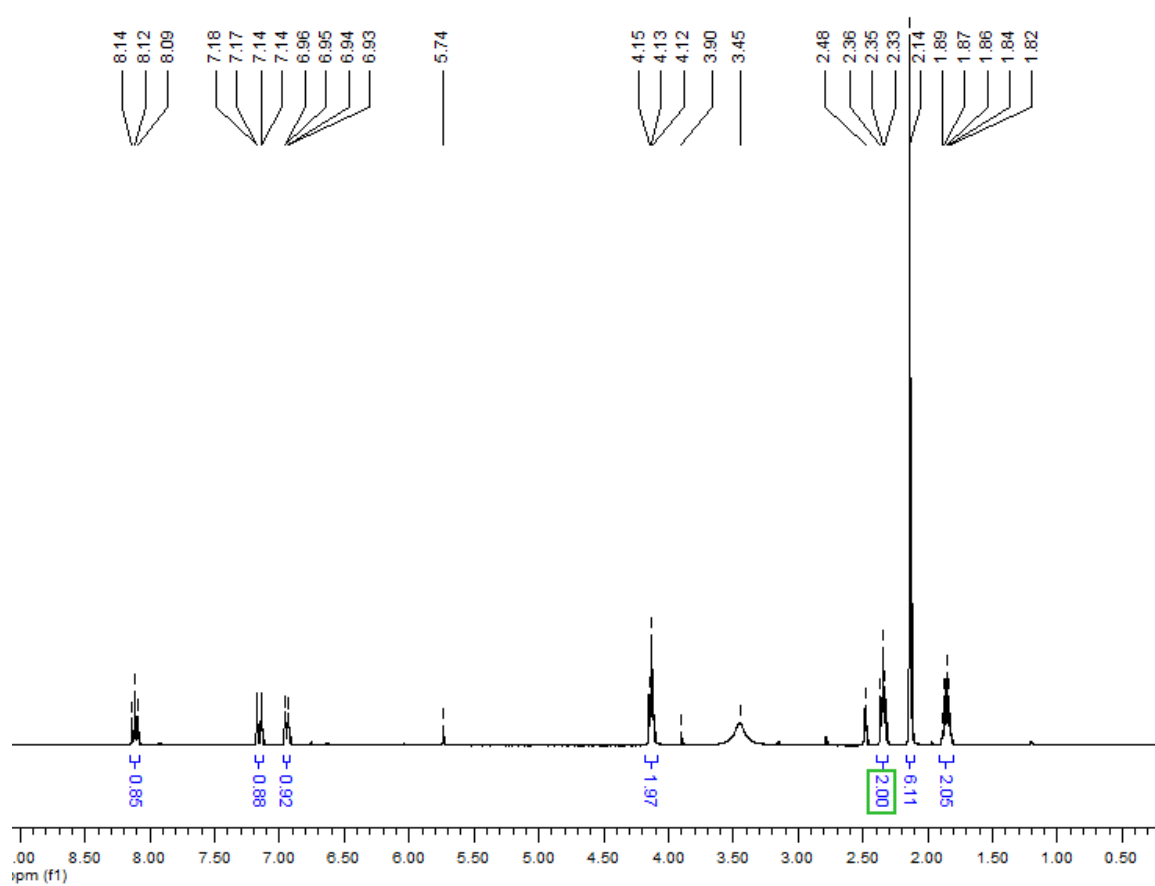
Spectrum 3-10: 3-(3-fluoro-4-nitrophenoxyl)-*N,N*-dimethylpropan-1-amine (**9f**) ^{13}C NMR (400 MHz, DMSO-d6)
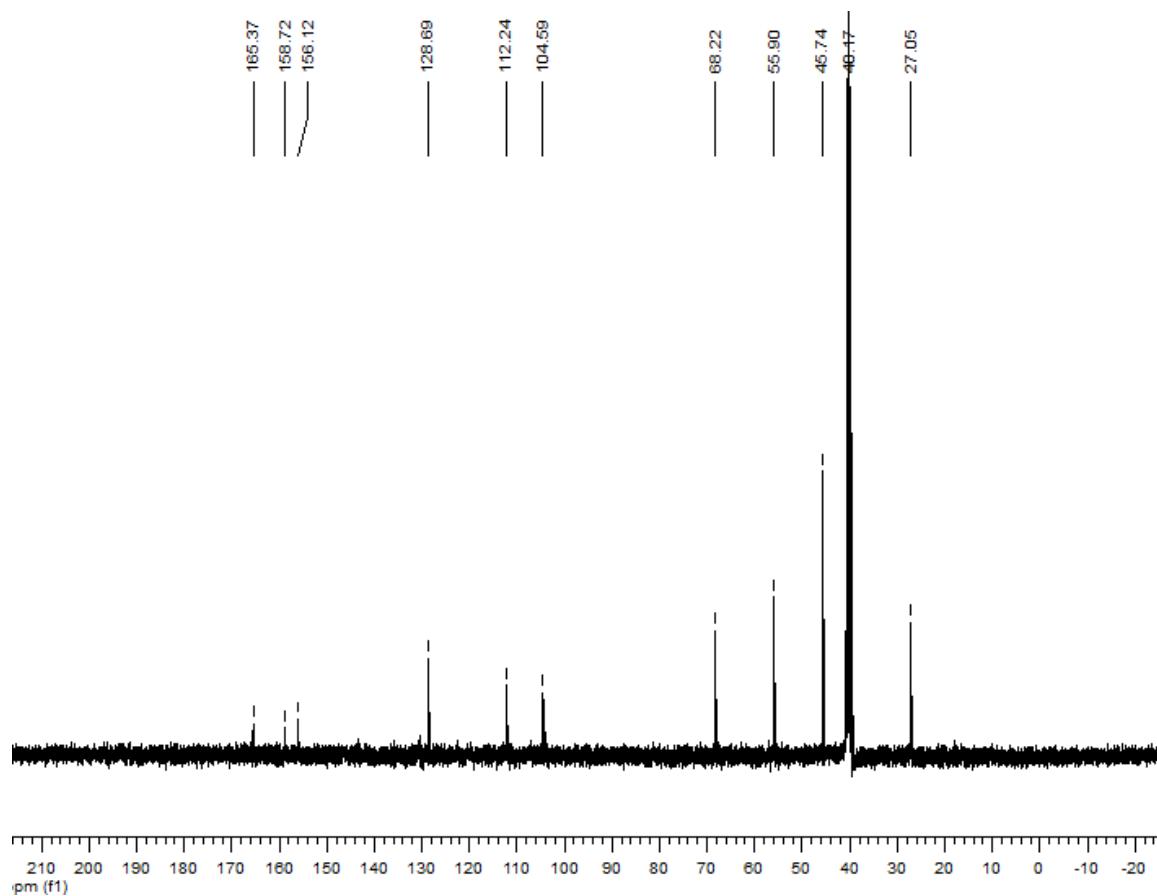
4-((*tert*-butyldimethylsilyl)oxy)-2-nitro-*N*-phenylaniline (11a)
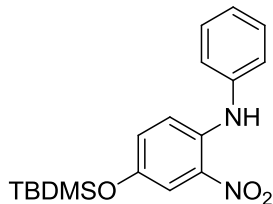
To a 100 ml round bottom flask was added *tert*-butyl(4-chloro-3-

nitrophenoxy)dimethylsilane (**9a**) (1.5 g, 5.3 mmol), toluene (40 ml), aniline (730 µl, 8

mmol), Pd$_2$(dba)$_3$ (243 mg, 0.26 mmol, 5 mol %), *rac*-BINAP (248 mg, 0.39 mmol, 7.5

mol %), and Cs$_2$CO$_3$ (2.6 g, 8 mmol). The reaction was stirred and heated to reflux under

Ar for 26 hr. It was then cooled to RT and extracted with water (2 x 100 ml). The organic

layer was washed with brine and dried over Na$_2$SO$_4$. After filtration and evaporation of

solvent, the crude was purified via flash column chromatography (DCM – Hexane : 80 %

- 20 %) to give red color oil as the product (1.38 g, 76 % yield). ^{1}H NMR (400 MHz,

DMSO-d6): δ 9.03 (s, 1H), 7.47-7.07 (m, 8H), 0.93 (s, 9H), 0.18 (s, 6H). ^{13}C NMR (400 MHz,

DMSO-d6): δ 147.23, 140.82, 137.12, 134.84, 130.13, 130.06, 124.50, 122.89, 119.86,

115.46, 26.18, 18.58, -4.01. MS (ESI) calculated exact mass for C$_{18}$H$_{24}$N$_2$O$_3$Si = 344.16.

Found [M+H]$^+$ = 345.20.

Spectrum 3-11: 4-((*tert*-butyldimethylsilyl)oxy)-2-nitro-*N*-phenylaniline (**11a**) ^{1}H NMR (400 MHz, DMSO-d6)
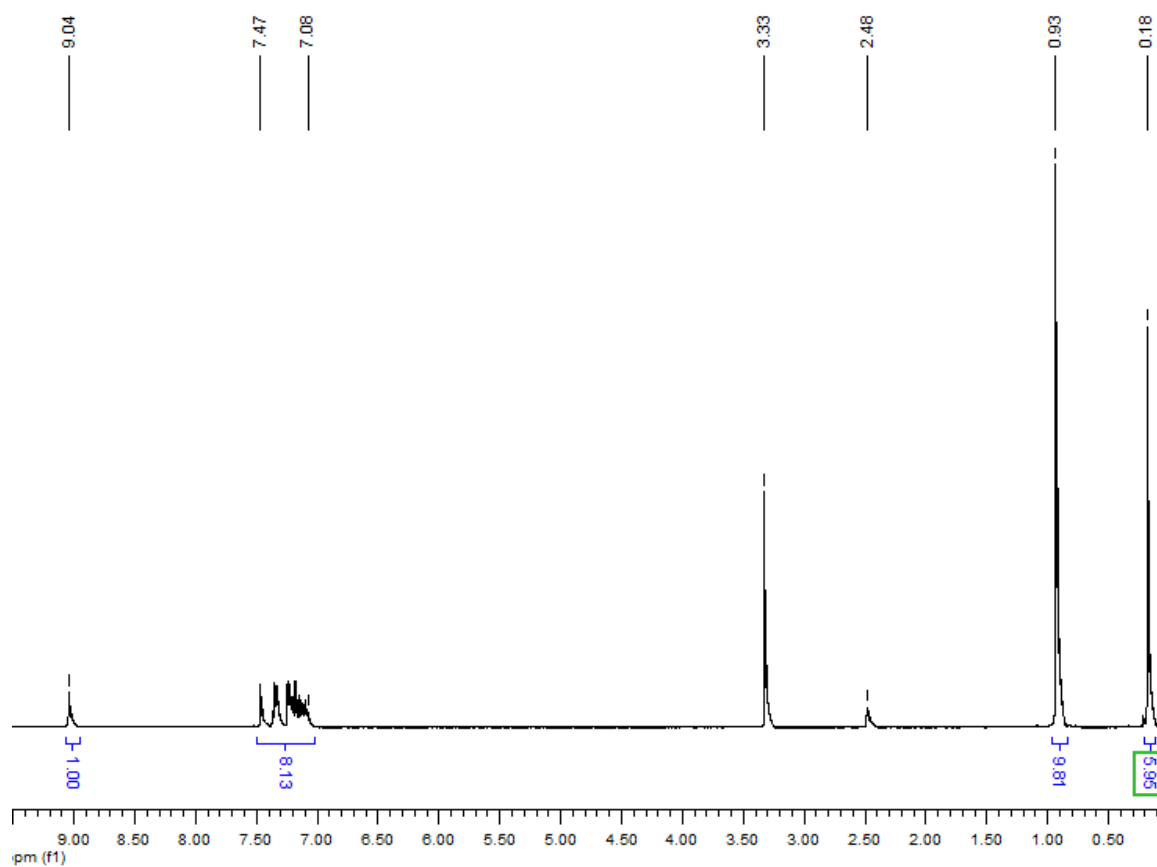
Spectrum 3-12: 4-((*tert*-butyldimethylsilyl)oxy)-2-nitro-*N*-phenylaniline (**11a**) ^{13}C NMR (400 MHz, DMSO-d6)
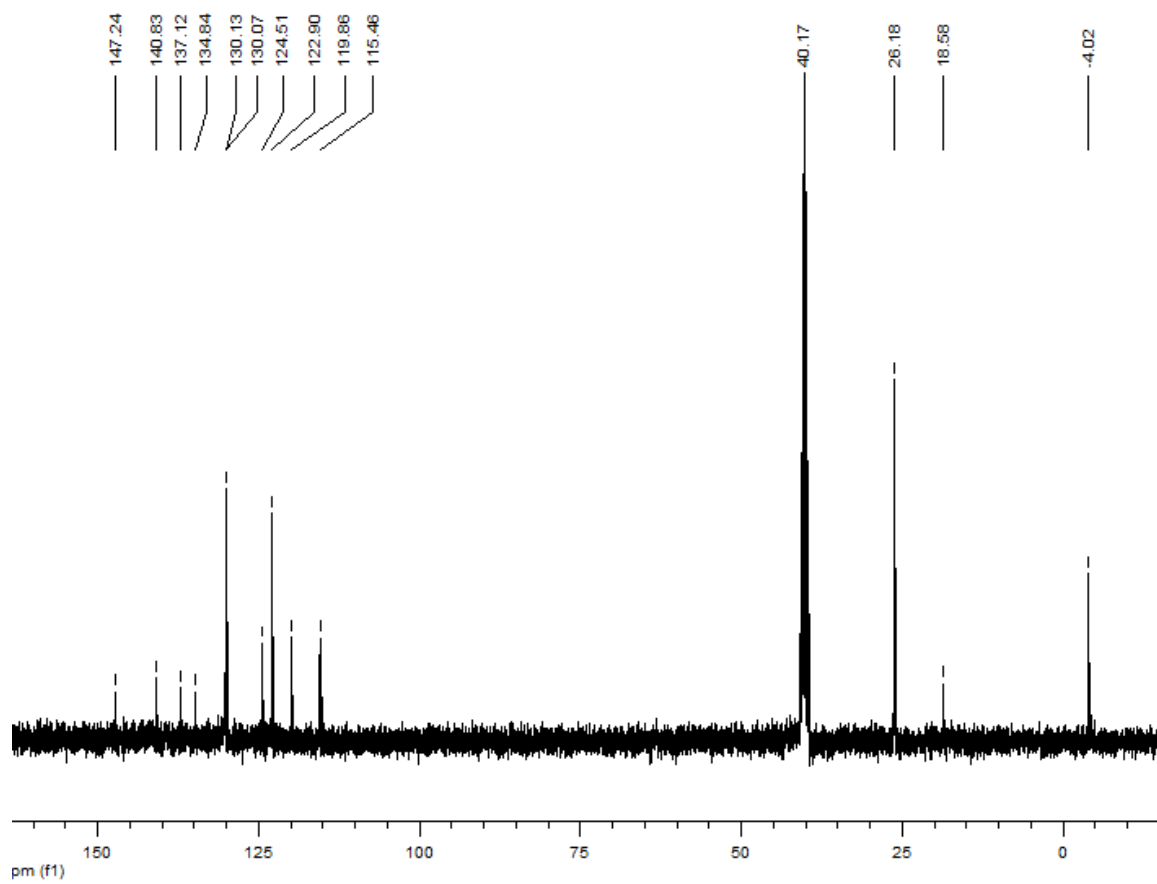
N¹-(4-(2-dimethylamino)ethoxy)-2-nitrophenyl)-N⁴,N⁴-dimethylbenzene-1,4-diamine (11x)
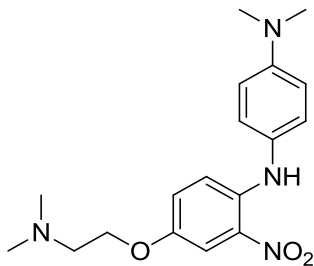
To a 50 ml round-bottom flask was added 2-(4-chloro-3-nitrophenoxy)-*N,N*-dimethylethanamine (**9b**) (290 mg, 1.2 mmol), toluene (20 ml), N^1,N^1-dimethylbenzene-1,4-diamine (162 mg, 1.2 mmol), Pd$_2$(dba)$_3$ (54 mg, 0.06 mmol, 5 mol %), rac-BINAP (55 mg, 0.09 mmol, 7.5 mol %), and Cs$_2$CO$_3$ (376 mg, 1.2 mmol). The reaction was stirred and heated to reflux under Ar for 21 hours before cooled to RT. It was then filtered and extracted with water (2 x 20 ml). The organic layer was washed with brine and dried over Na$_2$SO$_4$. After filtration and removal of solvent, the crude was purified via flash column (DCM – MeOH : 80 % - 20 %) to yield a dark red oil as the product (136 mg, 33 % yield). ^{1}H NMR (400 MHz, DMSO-d6): δ 9.22 (s, 1H), 7.53 (d, *J* = 3 Hz, 1H), 7.19 (dd, J_1 = 9 Hz, J_2 = 3 Hz, 1H), 7.11 (d, *J* = 9 Hz, 2H), 6.93 (d, *J* = 9 Hz, 1H), 6.76 (d, *J* = 9 Hz, 2H), 4.06 (t, *J* = 6 Hz, 2H), 2.88 (s, 6H), 2.71 (t, *J* = 6 Hz, 2H), 2.27 (s, 6H). ^{13}C NMR (400 MHz, DMSO-d6): δ 149.60, 149.22, 140.47, 131.59, 128.31, 127.68, 126.92, 118.46, 113.78, 108.01, 66.64, 57.89, 55.60, 45.79. MS (ESI) calculated exact mass for C$_{19}$H$_{22}$N$_4$O$_2$ = 344.18. Found [M+H]$^+$ = 345.2.

Spectrum 3-13: N^1-(4-(2-dimethylamino)ethoxy)-2-nitrophenyl)-N^4,N^4-dimethylbenzene-1,4-diamine (**11x**) ^{1}H NMR (400 MHz, DMSO-d6)
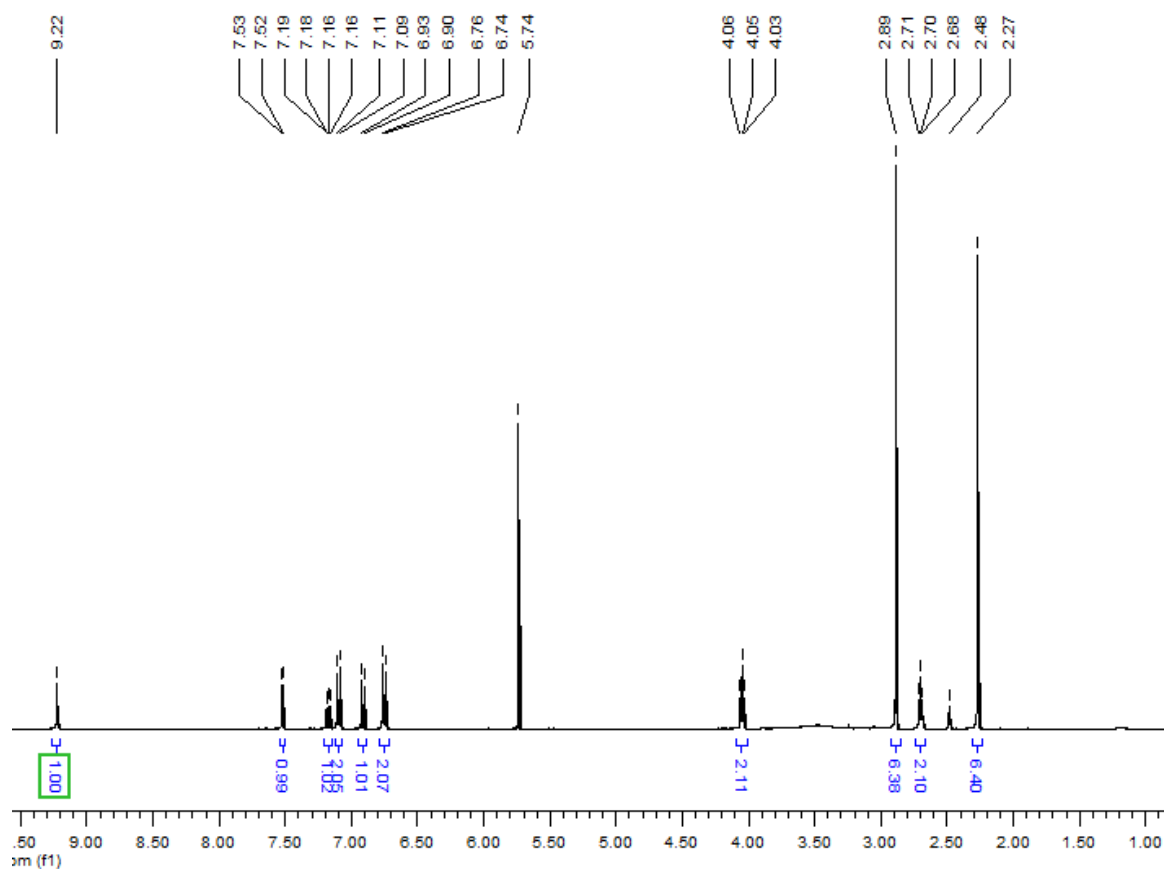
Spectrum 3-14: N^1-(4-(2-dimethylamino)ethoxy)-2-nitrophenyl)-N^4,N^4-dimethylbenzene-1,4-diamine (**11x**) ^{13}C NMR (400 MHz, DMSO-d6)
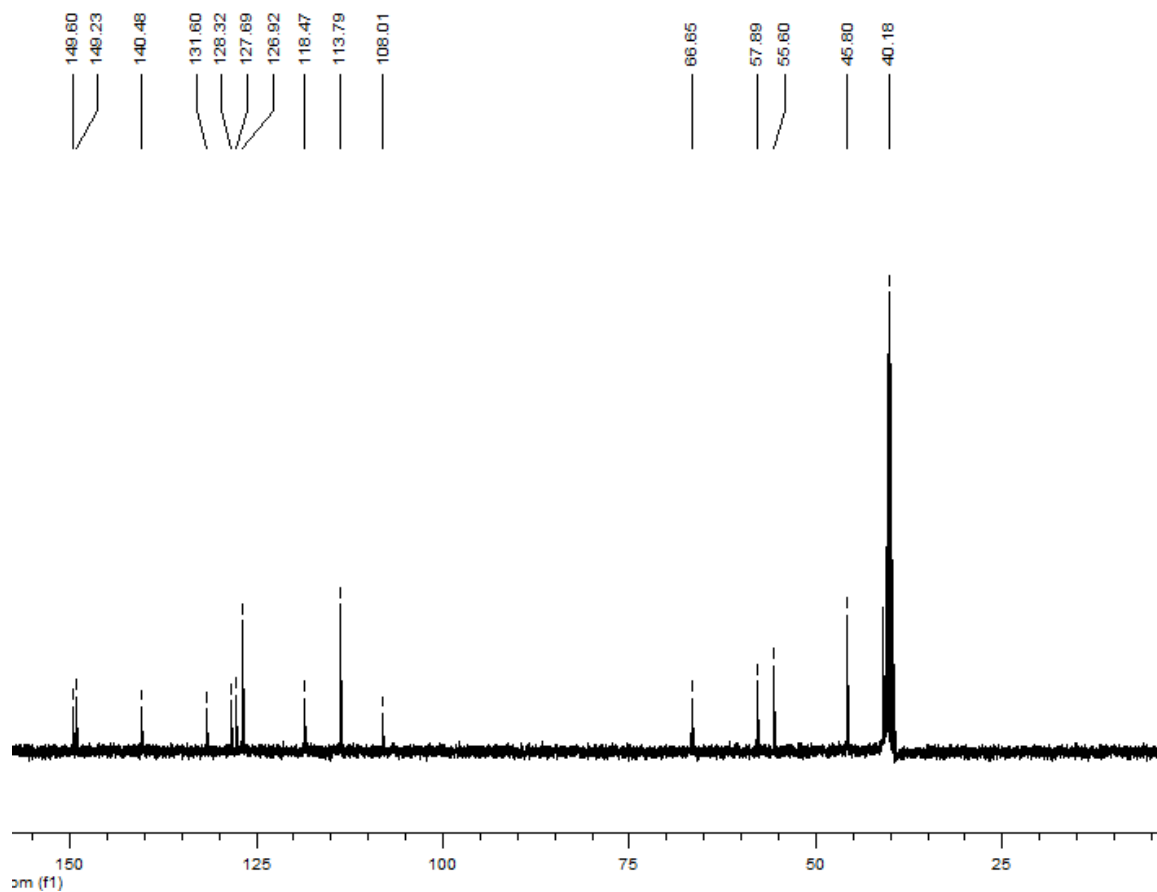
4-(3-(dimethylamino)propoxy)-2-nitro-*N*-phenylaniline (11c)
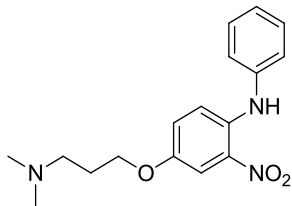
To a 100 ml round bottom flask was added 3-(4-chloro-3-nitrophenoxy)-*N,N*-dimethylpropan-1-amine (**9c**) (1.5 g, 5.7 mmol), toluene (50 ml), aniline (525 µl, 5.7 mmol), Pd$_2$(dba)$_3$ (263 mg, 0.29 mmol, 5 mol %), *rac*-BINAP (269 mg, 0.43 mmol, 7.5 mol %), and Cs$_2$CO$_3$ (1.8 g, 5.7 mmol). The reaction was stirred and heated to reflux under Ar for 24 hours before cooled to RT. It was then filtered and extracted twice with water (100 ml ea.). The organic layer was collected then washed with brine and dried over Na$_2$SO$_4$. After filtration and removal of solvent, the crude product was purified via flash column chromatography (DCM – MeOH : 90 % - 10 %) to yield red oil as the product (1.1 g, 63 % yield). ^{1}H NMR (400 MHz, DMSO-d6): δ 9.05 (s, 1H), 7.53 (s, 1H), 7.36 (t, *J* = 8 Hz, 2H), 7.22 – 7.21 (m, 4H), 7.10 (t, *J* = 7 Hz, 1H), 4.02 (t, *J* = 7 Hz, 2H), 2.44 (t, *J* = 7 Hz, 2H), 2.19 (s, 6H), 1.88 (p, *J* = 7 Hz, 2H). ^{13}C NMR (400 MHz, DMSO-d6): δ 151.37, 141.03, 136.49, 135.09, 130.12, 126.28, 124.31, 122.56, 120.35, 108.74, 67.13, 56.04, 45.55, 27.08. MS (ESI) calculated exact mass for C$_{17}$H$_{21}$N$_3$O$_3$ = 315.16. Found [M+H]$^+$ = 316.07.

Spectrum 3-15: 4-(3-(dimethylamino)propoxy)-2-nitro-*N*-phenylaniline (**11c**) ^{1}H NMR
(400 MHz, DMSO-d6)
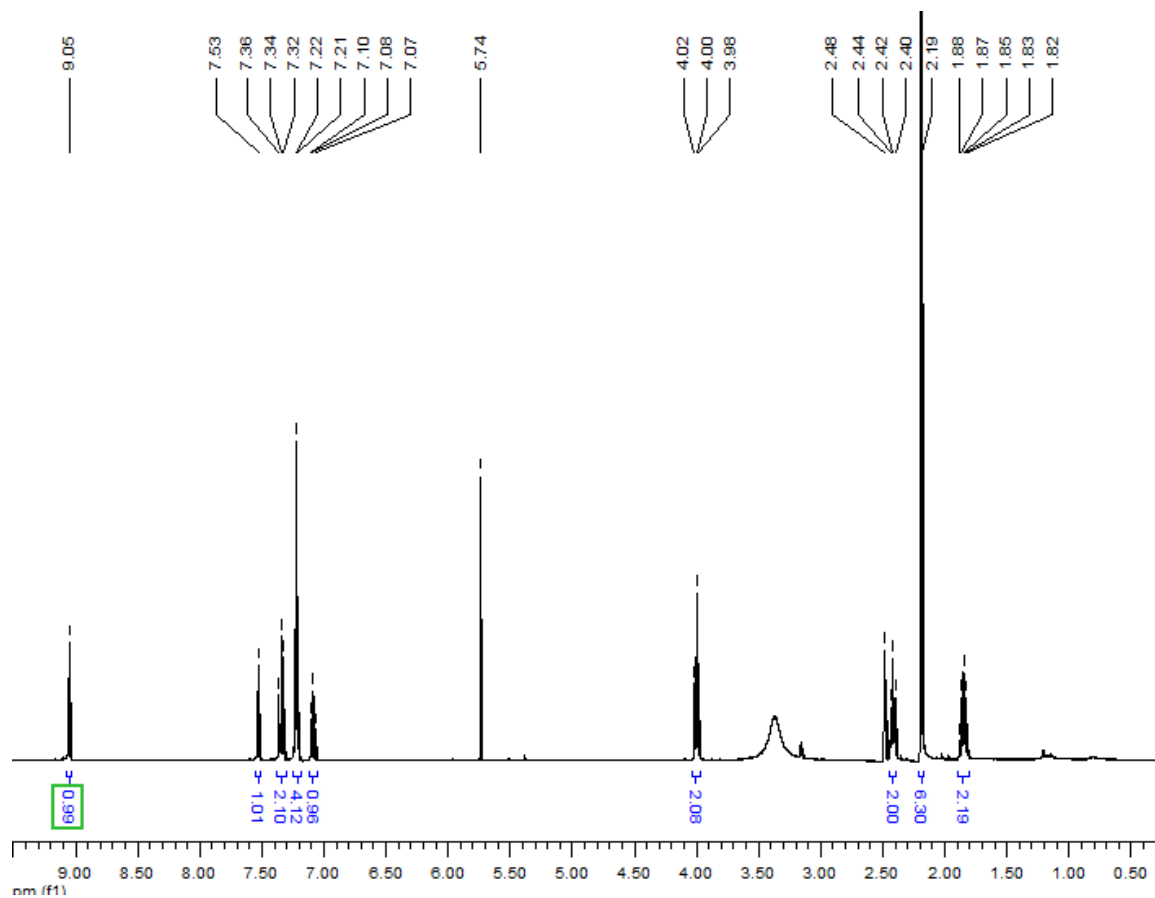
Spectrum 3-16: 4-(3-(dimethylamino)propoxy)-2-nitro-*N*-phenylaniline (**11c**) ^{13}C NMR (400 MHz, DMSO-d6)
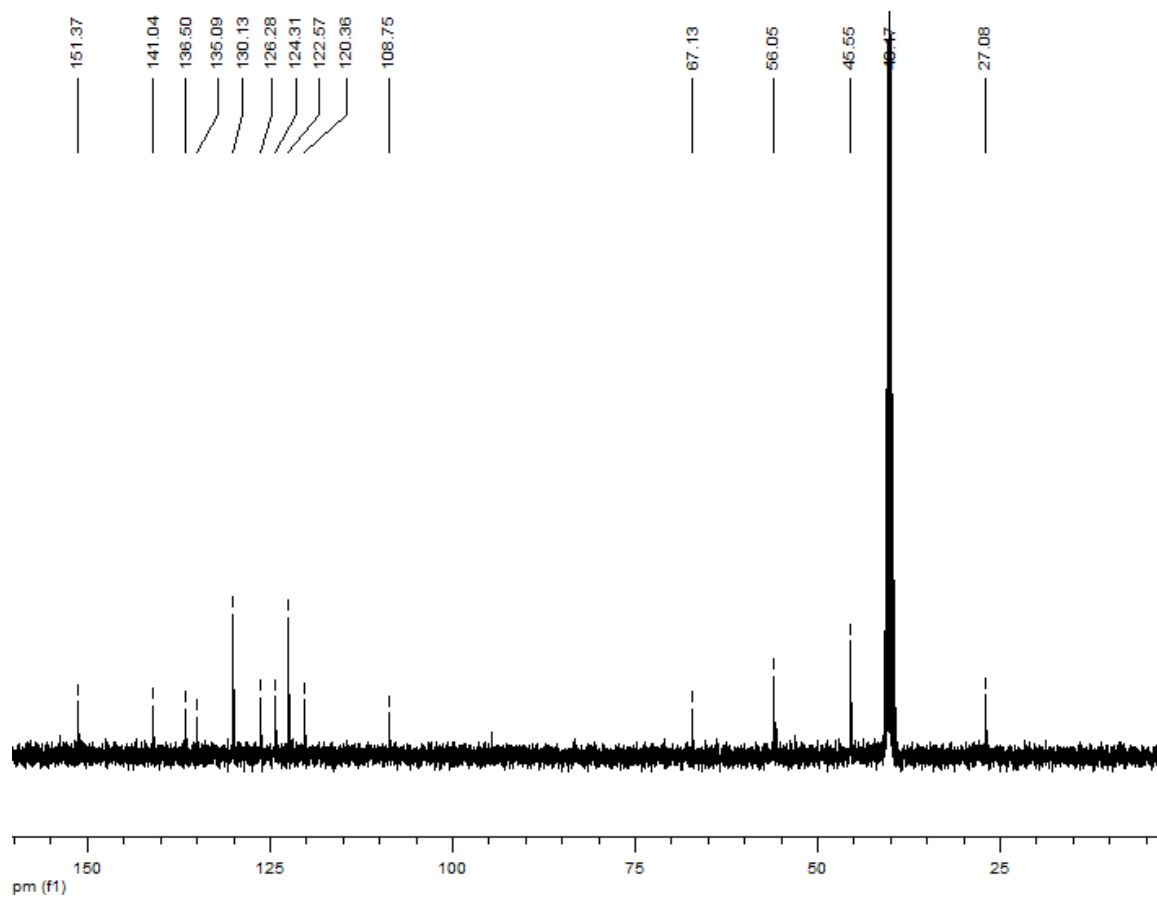
N*¹-(4-(3-(dimethylamino)propoxy)-2-nitrophenyl)-*N*⁴,*N*⁴-dimethylbenzene-1,4-diamine (11e)
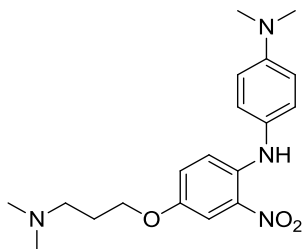
To a 250 ml round-bottom flask was added *N,N*-dimethyl-*p*-nitroaniline (957 mg, 5.7 mmol) and MeOH (100 ml). The flask was flushed with Ar gas before Pd/C (50 mg, 10 wt %) was added. The reaction was then sealed under H_2 atmosphere and stirred at RT for 3.5 hours before it was filtered and concentrated. The oil residue was dissolved in toluene (100 ml). 3-(4-chloro-3-nitrophenoxy)-*N,N*-dimethylpropan-1-amine (**9c**) (1.5 g, 5.7 mmol) was added, followed by $Pd_2(dba)_3$ (264 mg, 0.3 mmol, 5 mol %) and *rac*-BINAP (269 mg, 0.4 mmol, 7.5 mol %) and Cs_2CO_3 (1.8 g, 5.7 mmol). The reaction was stirred and heated to reflux for 24 hours before filtered and extracted with water (2 x 150 ml). The organic layer was collected and washed with brine and dried over Na_2SO_4. The crude was filtered, concentrated and purified via flash column (DCM – MeOH : 90 % - 10 %) to yield red oil as the product (637 mg, 31 % yield). ¹H NMR (400 MHz, DMSO-d6): δ 9.23 (s, 1H), 7.50 (d, J = 2 Hz, 1H), 7.18 (dd, J1 = 2 Hz, J2 = 8 Hz, 1H), 7.11 (d, J = 8 Hz, 2H), 6.93 (d, J = 10 Hz, 1H), 6.77 (d, J = 8 Hz, 2H), 3.99 (t, J = 6 Hz, 2H), 2.89 (s, 6H), 2.54 (t, J = 7 Hz, 2H), 2.27 (s, 6H), 1.90 (p, J = 7 Hz, 2H). ¹³C NMR (400 MHz, DMSO-d6): δ 149.79, 149.23, 140.43, 131.59, 128.34, 127.68, 126.93, 118.51, 113.80, 107.81, 66.92,

55.88, 45.15, 40.98, 26.70. MS (ESI) calculated exact mass for $C_{19}H_{26}N_4O_3$ = 358.20.

Found $[M+H]^+$ = 359.18.

Spectrum 3-17: N^1-(4-(3-(dimethylamino)propoxy)-2-nitrophenyl)-N^4,N^4-dimethylbenzene-1,4-diamine (**11e**) ^{1}H NMR (400 MHz, DMSO-d6)

om (f1)
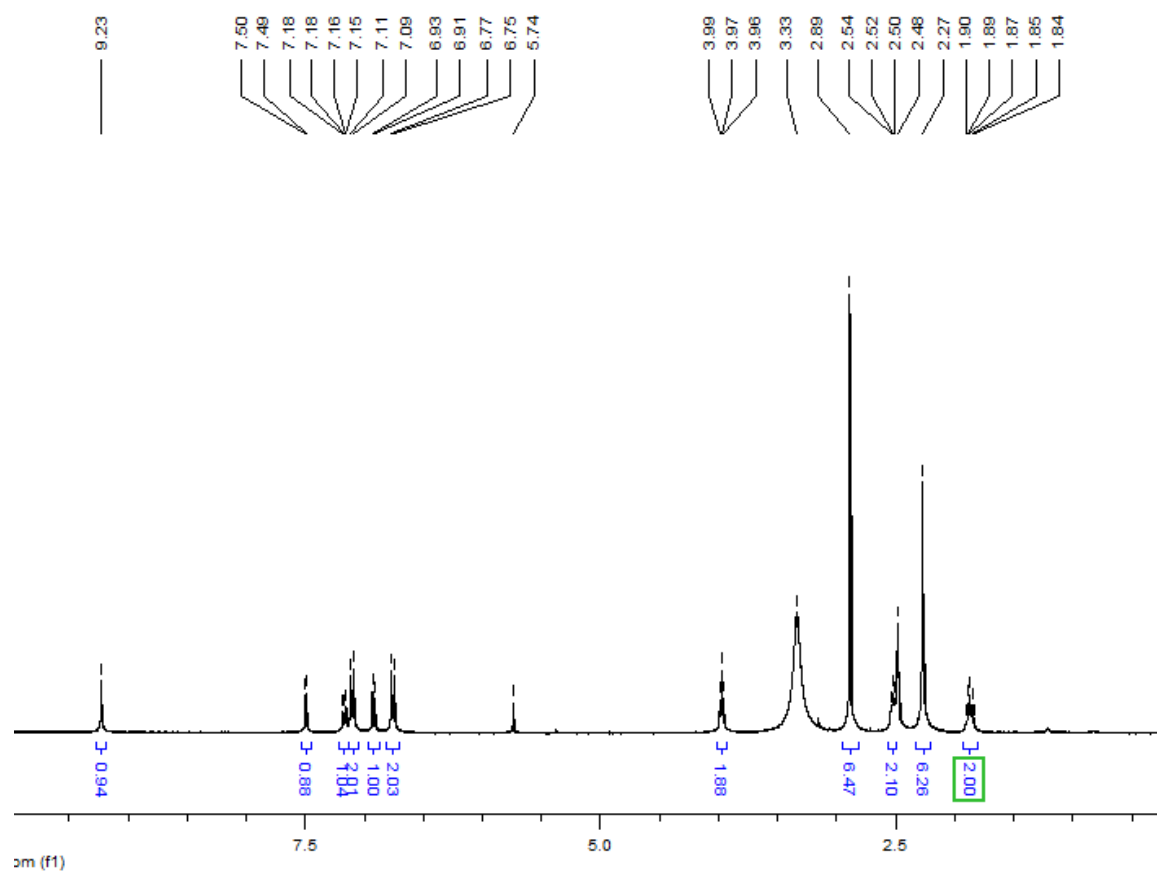
Spectrum 3-18: N^1-(4-(3-(dimethylamino)propoxy)-2-nitrophenyl)-N^4,N^4-dimethylbenzene-1,4-diamine (**11e**) ^{13}C NMR (400 MHz, DMSO-d6)
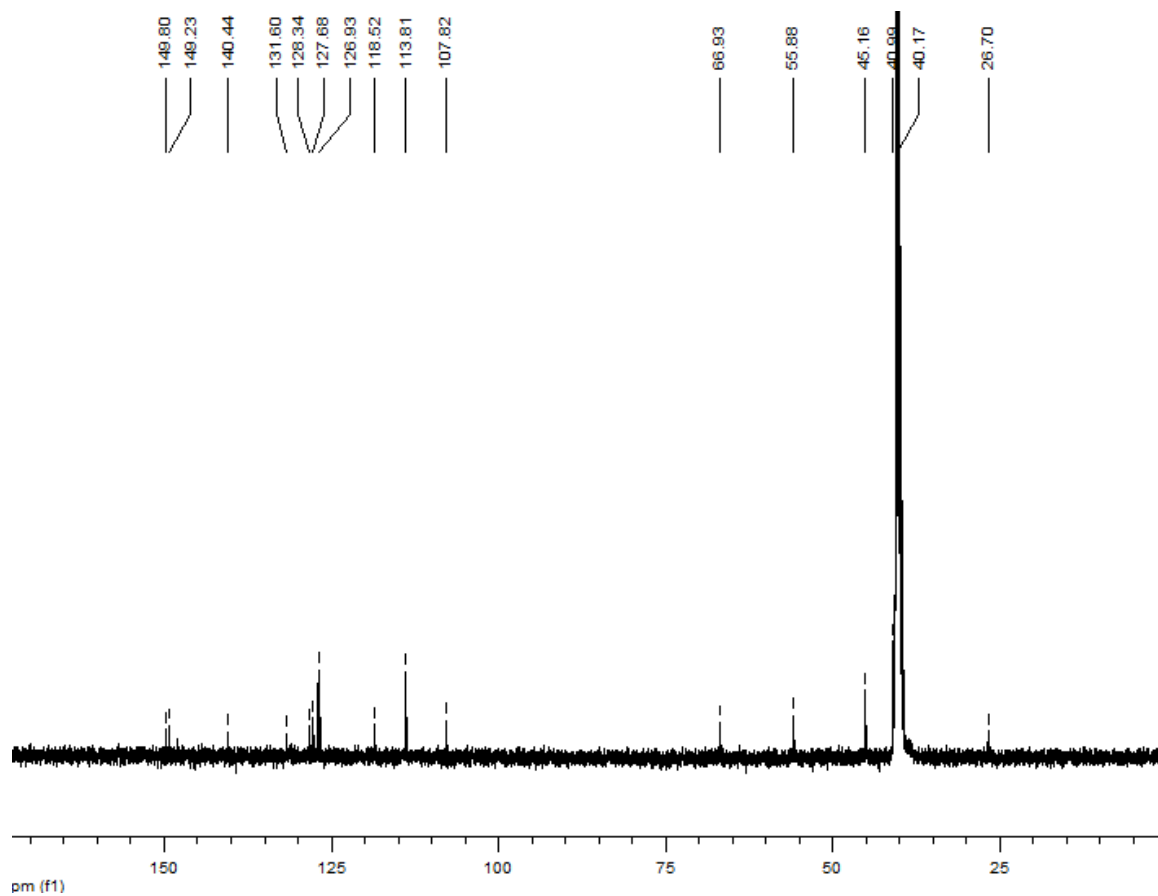
4-(2-(dimethylamino)ethoxy)-2-nitro-*N*-phenylaniline (11b)
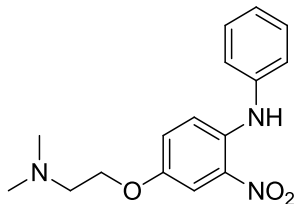
To a 100 ml round bottom flask was added 2-(4-cloro-3-nitrophenoxy)-*N,N*-dimethylethanamine (**9b**) (1.3 g, 5.3 mmol), toluene (50 ml), aniline (520 µl, 5.7 mmol), Pd$_2$(dba)$_3$ (264 mg, 0.29 mmol, 5 mol %), *rac*-BINAP (269 mg, 0.43 mmol, 7.5 mol %), Cs$_2$CO$_3$ (1.8 g, 5.7 mmol). The reaction was stirred under Ar atmosphere and heated to reflux for 28 hr before it was cooled to RT. It was then filtered and extracted with water twice (100 ml ea). The organic layer was collected and washed with brine and dried over Na$_2$SO$_4$. After filtration and concentration, the crude was purified via flash column (DCM – MeOH : 90 % - 10 %) to yield a red oil as the product (990 mg, 62 % yield). ^{1}H NMR (400 MHz, DMSO-d6): δ 9.05 (s, 1H), 7.55 (t, *J* = 2 Hz, 1H), 7.34 (t, *J* = 8 Hz, 2H), 7.23 – 7.21 (m, 4H), 7.10 (t, *J* = 8 Hz, 1H), 4.07 (t, *J* = 6 Hz, 2H), 2.64 (t, *J* = 6 Hz, 2H), 2.21 (s, 6H). ^{13}C NMR (400 MHz, DMSO-d6): δ 151.21, 141.03, 136.53, 135.10, 130.12, 126.30, 124.31, 122.57, 120.32, 108.90, 67.04, 58.10, 55.10, 55.60, 46.07. MS (ESI) calculated exact mass for C$_{16}$H$_{19}$N$_3$O$_3$ = 301.14. Found [M+H]$^+$ = 302.0.

Spectrum 3-19: 4-(2-(dimethylamino)ethoxy)-2-nitro-*N*-phenylaniline (**11b**) ^{1}H NMR (400 MHz, DMSO-d6)
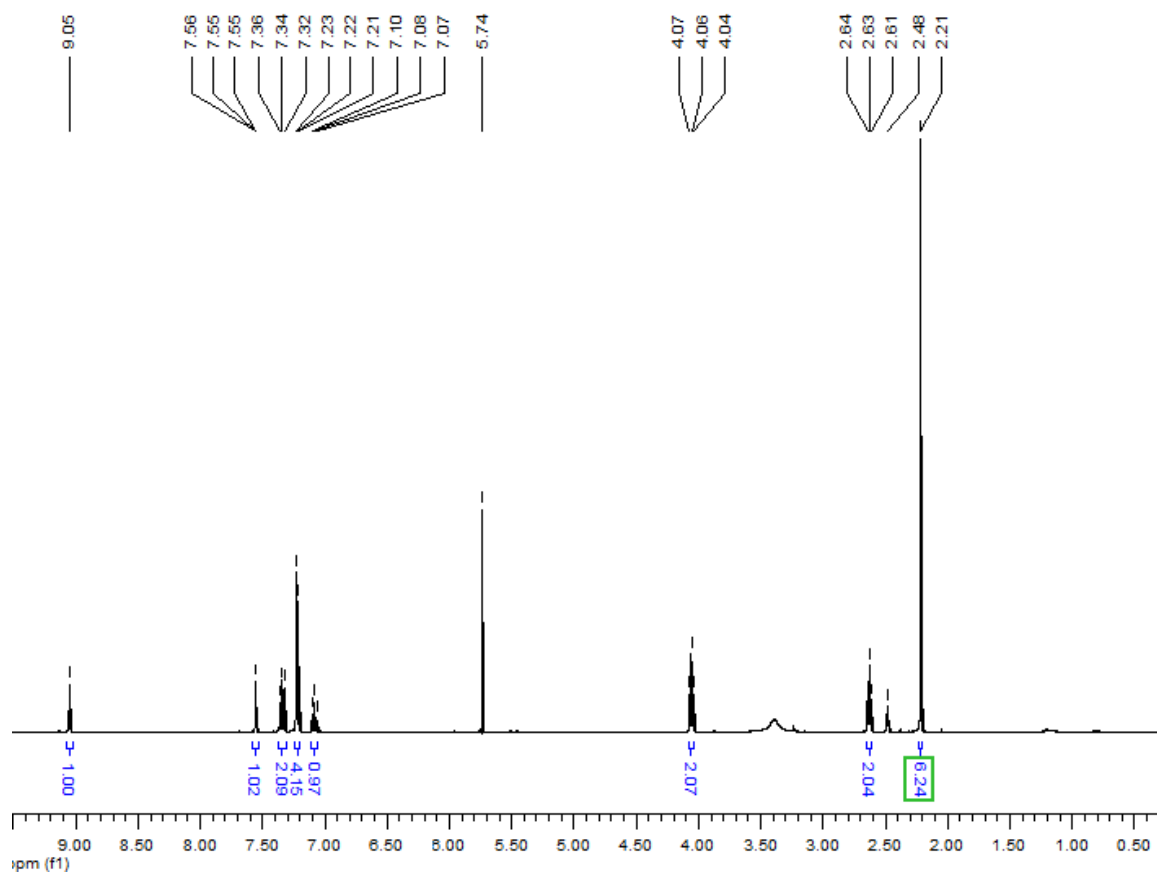
Spectrum 3-20: 4-(2-(dimethylamino)ethoxy)-2-nitro-*N*-phenylaniline (**11b**) ^{13}C NMR (400 MHz, DMSO-d6)
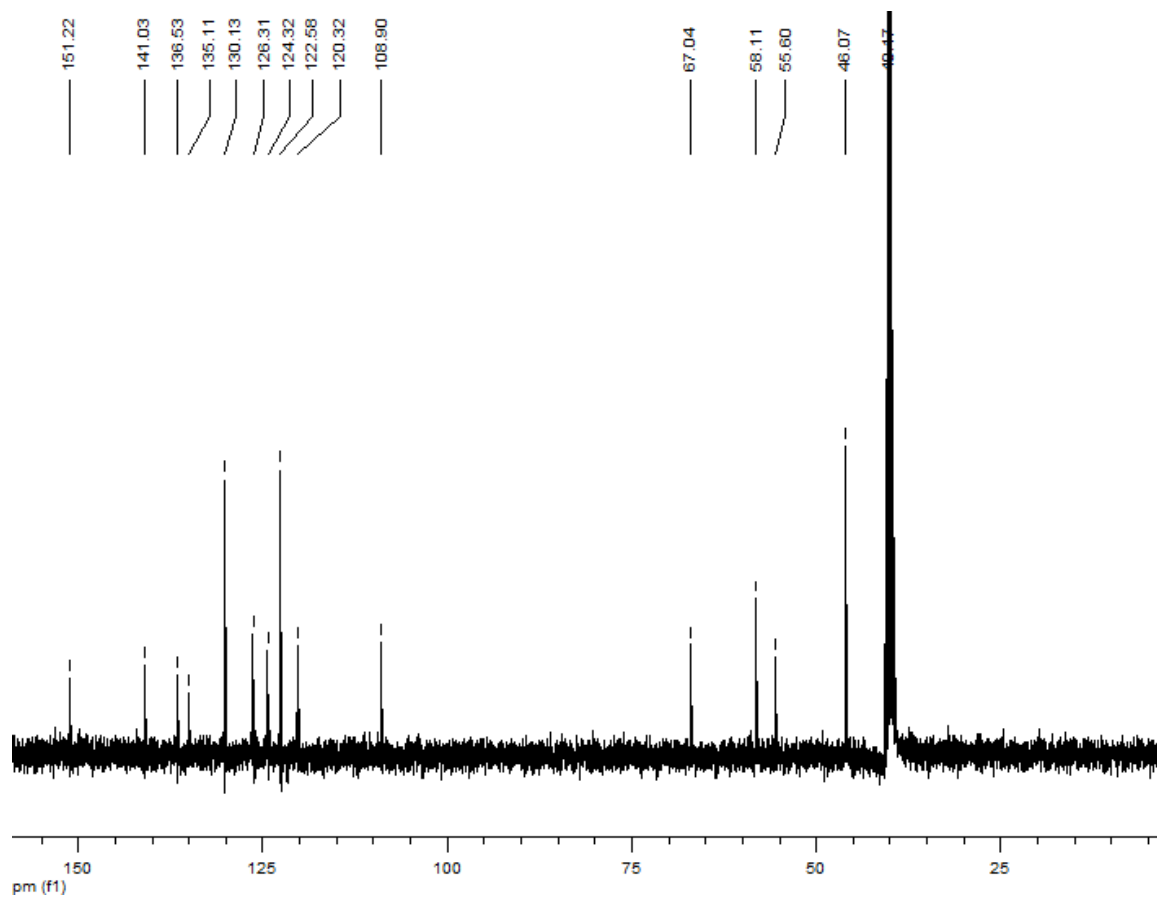
2-nitro-N-phenyl-4-(pyridine-4-ylmethoxy)aniline (11d)
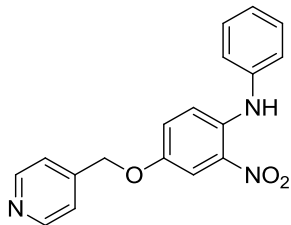
To a 250 ml round-bottom flask was added 4-((4-chloro-3-nitrophenoxy)methyl)pyridine (**9d**) (1.56 g, 5.9 mmol), toluene (100 ml), aniline (646 μl, 7.0 mmol, 1.2 eq), $Pd_2(dba)_3$ (265 mg, 0.3 mmol, 5 mol %), *rac*-BINAP (273 mg, 0.4 mmol, 7.5 mol %) and Cs_2CO_3 (1.9 g, 5.9 mmol). The reaction was stirred under Ar atmosphere and heated to reflux for 19 hours before it was cooled to RT. After filtration, it was extracted with water (2 x 100 ml). The organic layer was collected and washed with brine and dried over Na_2SO_4. After filtration and concentration, the crude was purified via flash column chromatography (DCM – EtOAc : 60 % - 40 %) to yield red solid as the product (1.73 g, 91 % yield). ^{1}H NMR (400 MHz, CDCl$_3$): δ 9.37 (s, 1H), 8.64 (d, *J* = 6 Hz, 2H), 7.69 (d, *J* = 3Hz, 1H), 7.41 – 7.36 (m, 4H), 7.26 – 7.18 (m, 4H), 7.16 (dd, J_1 = 9 Hz, J_2 = 3 Hz, 1H), 5.08 (s, 2H). ^{13}C NMR (400 MHz, CDCl$_3$): δ 150.17, 149.69, 145.76, 139.22, 138.82, 132.81, 129.97, 126.73, 125.55, 124.00, 121.81, 118.31, 108.68, 68.98. MS (ESI) calculated exact mass for $C_{18}H_{15}N_3O_3$ = 321.11. Found $[M+H]^+$ = 322.08.

Spectrum 3-21: 2-nitro-N-phenyl-4-(pyridine-4-ylmethoxy)aniline (**11d**) ^{1}H NMR (400 MHz, CDCl$_3$)
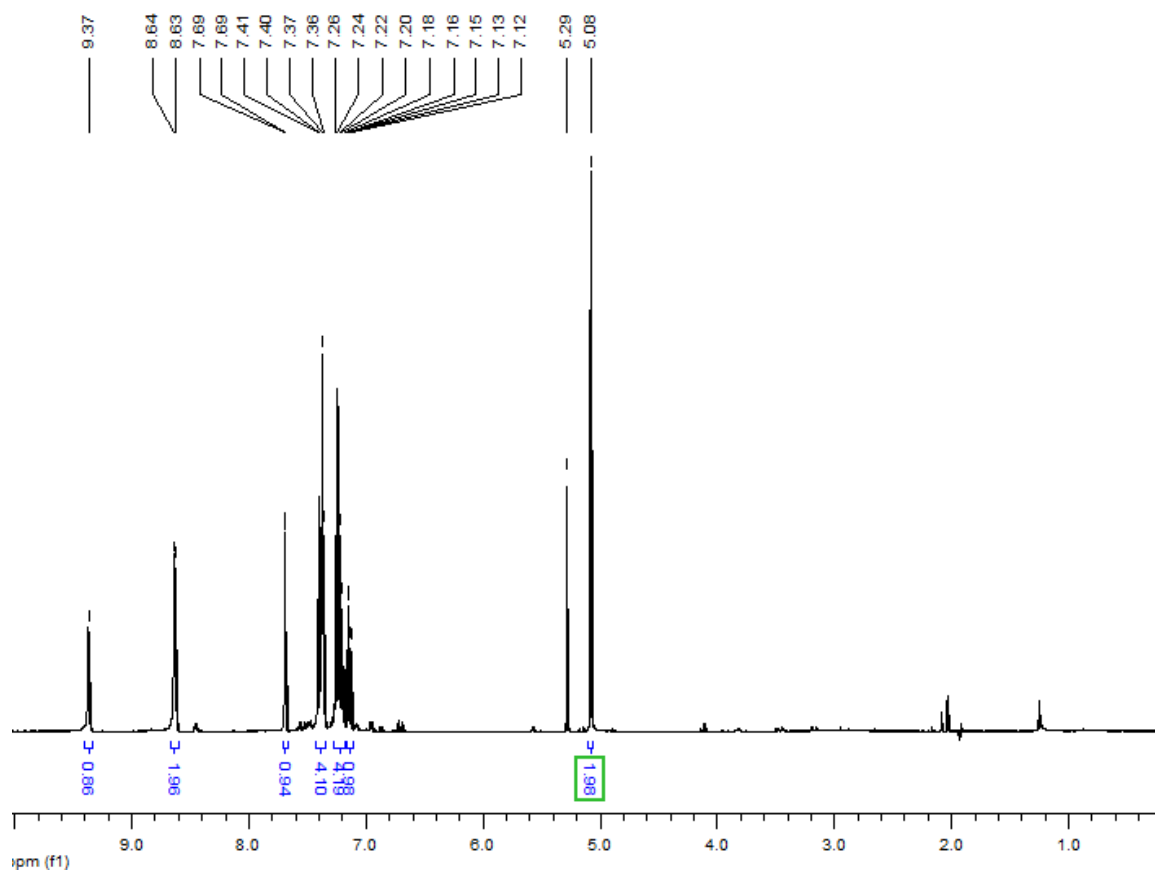
Spectrum 3-22: 2-nitro-N-phenyl-4-(pyridine-4-ylmethoxy)aniline (**11d**) ^{13}C NMR (400 MHz, CDCl$_3$)
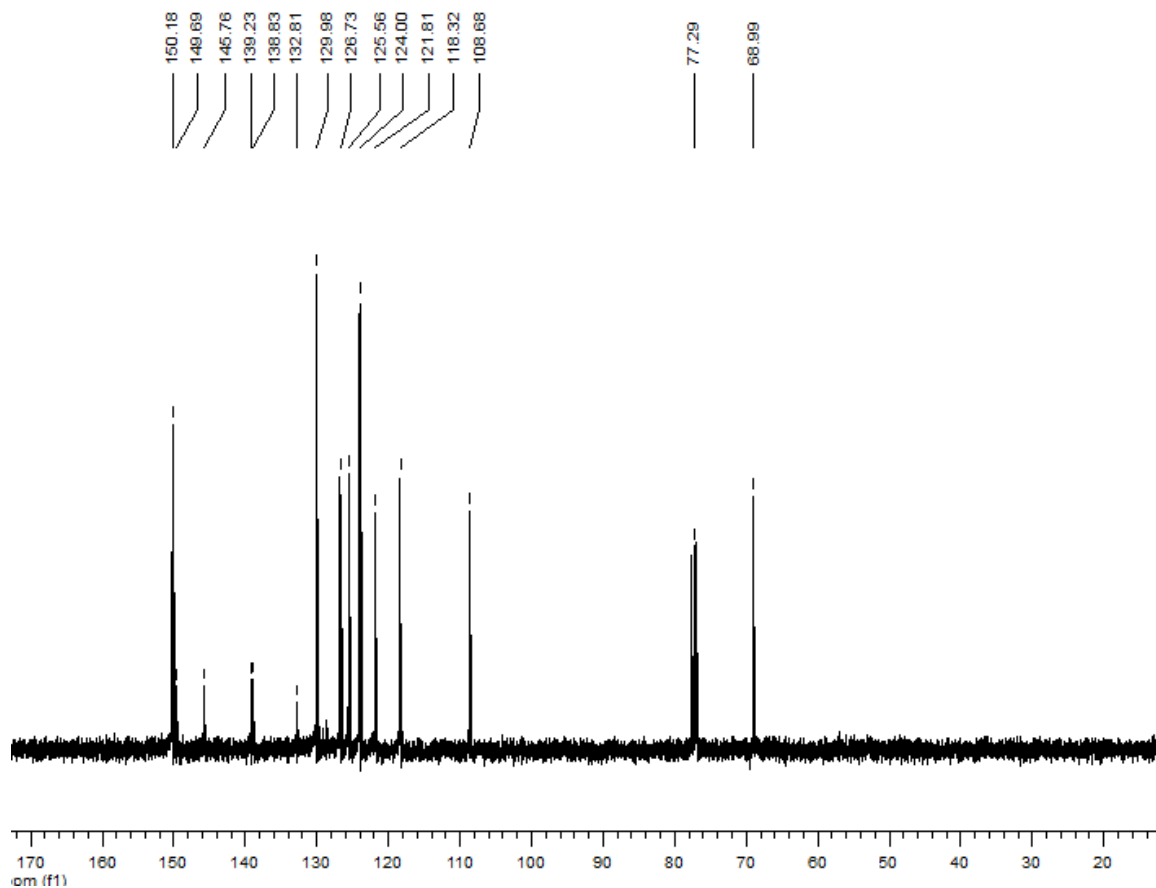
N^1-(5-(3-(dimethylamino)propoxy)-2-nitrophenyl)-N^3,N^3-dimethylbenzene-1,3-diamine (11g)
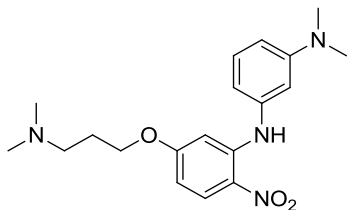
N
O
NH
N
NO2

To a 250 ml round bottom flask was added 3-(3-fluoro-4-nitrophenoxy)-*N,N*-dimethylpropan-1-amine (**9f**) (3.83 g, 15.8 mmol), ACN (100 ml), N^1,N^1-dimethylbenzene-1,3-diamine (2.05 g, 15.0 mmol), and Cs_2CO_3 (5.0 g, 15.8 mmol). The reaction was stirred and heated to reflux under Ar for 41 hr before it was cooled to RT It was then filtered and concentrated. The dark residue was dissolved in DCM (200 ml) and extracted with water (2 x 100 ml). The organic layer was collected and washed with brine and dried over Na_2SO_4. After filtration and evaporation of solvent, the crude was purified via flash column chromatography (DCM – MeOH : 90 % - 10 %) to yield yellow oil as the product (2.02 g, 36 % yield). ^{1}H NMR (400 MHz, DMSO-d6): δ 9.57 (s, 1H), 8.10 (d, J = 10 Hz, 1H), 7.23 (t, *J* = 8 Hz, 1H), 6.67 (s, 1H), 6.64 (d, *J* = 8 Hz, 1H), 6.58 (dd, J_1 = 8 Hz, J_2 = 2 Hz, 2H), 6.45 (dd, J_1 = 10 Hz, J_2 = 2Hz, 1H), 5.74 (d, *J* = 1 Hz, 1H), 3.98 (t, *J* = 6 Hz, 2H), 2.89 (s, 6H), 2.64 (t, *J* = 7 Hz, 2H), 2.34 (s, 6H), 1.94 (p, *J* = 7 Hz, 2H). ^{13}C NMR (400 MHz, DMSO-d6): δ 165.06, 152.21, 145.72, 139.82, 130.54, 129.37, 127.43, 112.29, 110.30, 108.73, 107.43, 98.97, 66.73, 55.61, 55.29, 44.44, 25.87. MS (ESI) calculated exact mass for $C_{19}H_{26}N_4O_3$ = 358.20. Found $[M+H]^+$ = 349.18.

Spectrum 3-23: N^1-(5-(3-(dimethylamino)propoxy)-2-nitrophenyl)-N^3,N^3-dimethylbenzene-1,3-diamine (**11g**) ^{1}H NMR (400 MHz, DMSO-d6)
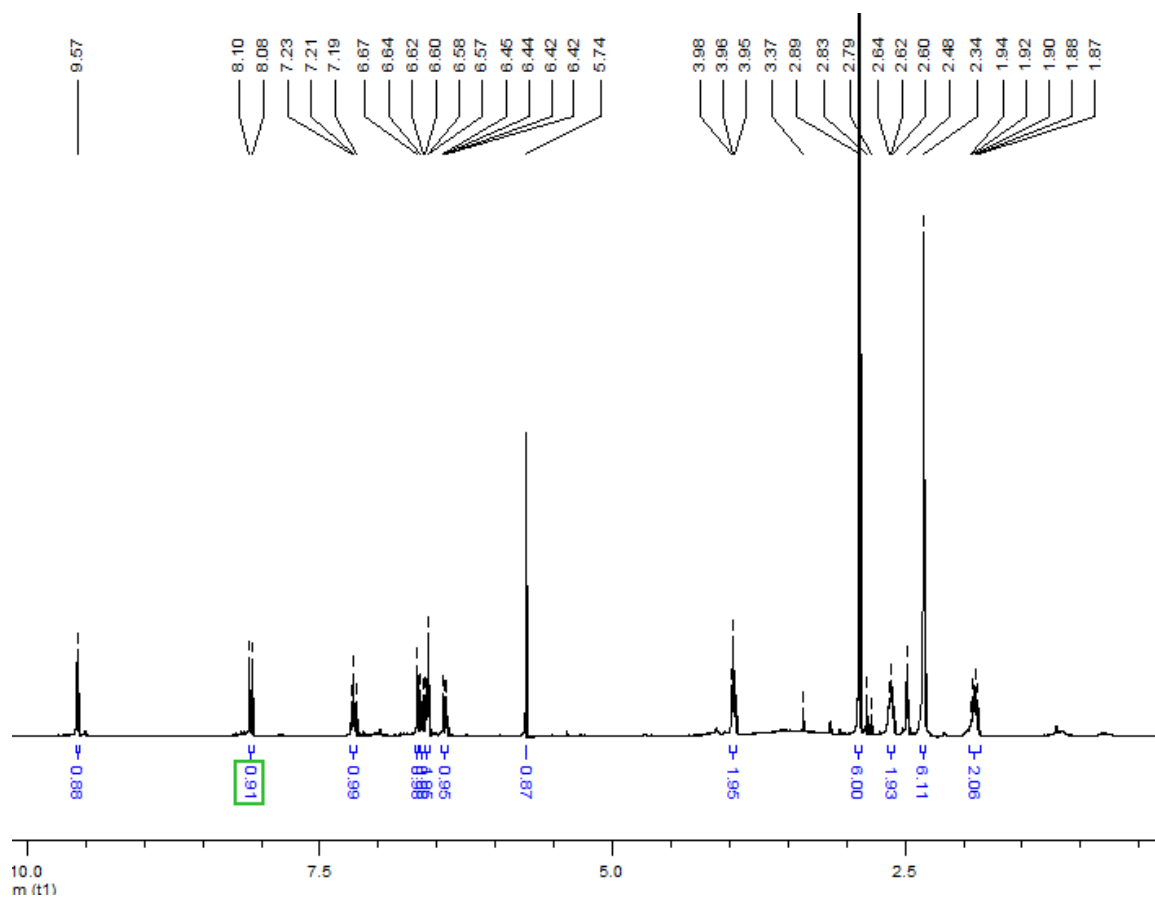
Spectrum 3-24: N^1-(5-(3-(dimethylamino)propoxy)-2-nitrophenyl)-N^3,N^3-dimethylbenzene-1,3-diamine (**11g**) ^{13}C NMR (400 MHz, DMSO-d6)
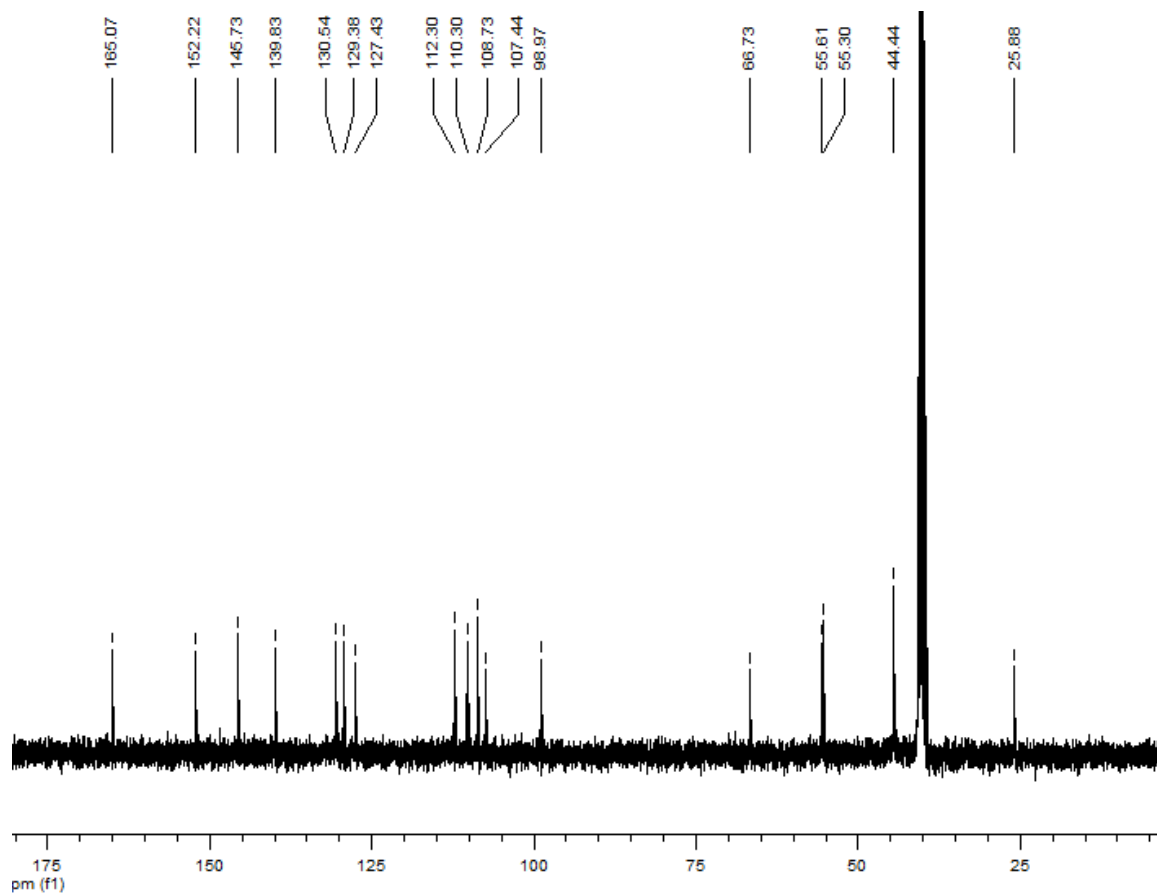
N^1-(5-(3-(dimethylamino)propoxy)-2-nitrophenyl)-N^4,N^4-dimethylbenzene-1,4-diamine (11f)
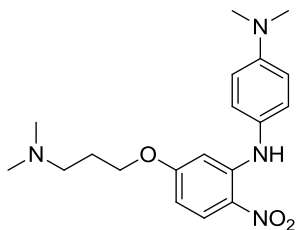
To a 250 ml round bottom flask was added 3-(3-fluoro-4-nitrophenoxy)-*N*,*N*-dimethylpropan-1-amine (**9f**) (3.6 g, 15.0 mmol), ACN (100 ml), N^1,N^1-dimethylbenzene-1,4-diamine (2.04 g, 15.0 mmol) and Cs_2CO_3 (4.7 g, 15.0 mmol). The reaction was stirred and heated to reflux under Ar for 21 hr before it was cooled to RT. After removal of solvent, the oil residue was dissolved in chloroform (100 ml) and extracted with water (2 x 100 ml). The organic layer was collected. It was washed with brine and dried over Na_2SO_4. After filtration and evaporation of solvent, the crude was purified via flash column chromatography (DCM – MeOH : 90 % - 10 %) to yield red oil as the product (1.81 g, 34 % yield). ^{1}H NMR (400 MHz, DMSO-d6): δ 9.53 (s, 1H), 8.08 (d, J = 10 Hz, 1H), 7.15 (d, J = 9 Hz, 2H), 6.78 (d, J = 9 Hz, 2H), 6.38 (dd, J1 = 9 Hz, J2 = 2 Hz, 1H), 6.24 (d, J = 2 Hz, 1H), 3.93 (t, J = 6 Hz, 2H), 2.90 (s, 6H), 2.46 (t, J = 7 Hz, 2H), 2.23 (s, 6H), 1.85 (p, J = 7 Hz, 2H). ^{13}C NMR (400 MHz, DMSO-d6): δ 165.19, 149.48, 147.40, 129.39, 127.38, 126.68, 113.63, 106.66, 98.16, 66.80, 55.61, 44.98, 40.87, 26.35. MS (ESI) calculated exact mass for $C_{19}H_{26}N_4O_3$ = 358.20. Found $[M+H]^+$ = 359.18.

Spectrum 3-25: N^1-(5-(3-(dimethylamino)propoxy)-2-nitrophenyl)-N^4,N^4-dimethylbenzene-1,4-diamine **(11f)** ^{1}H NMR (400 MHz, DMSO-d6)
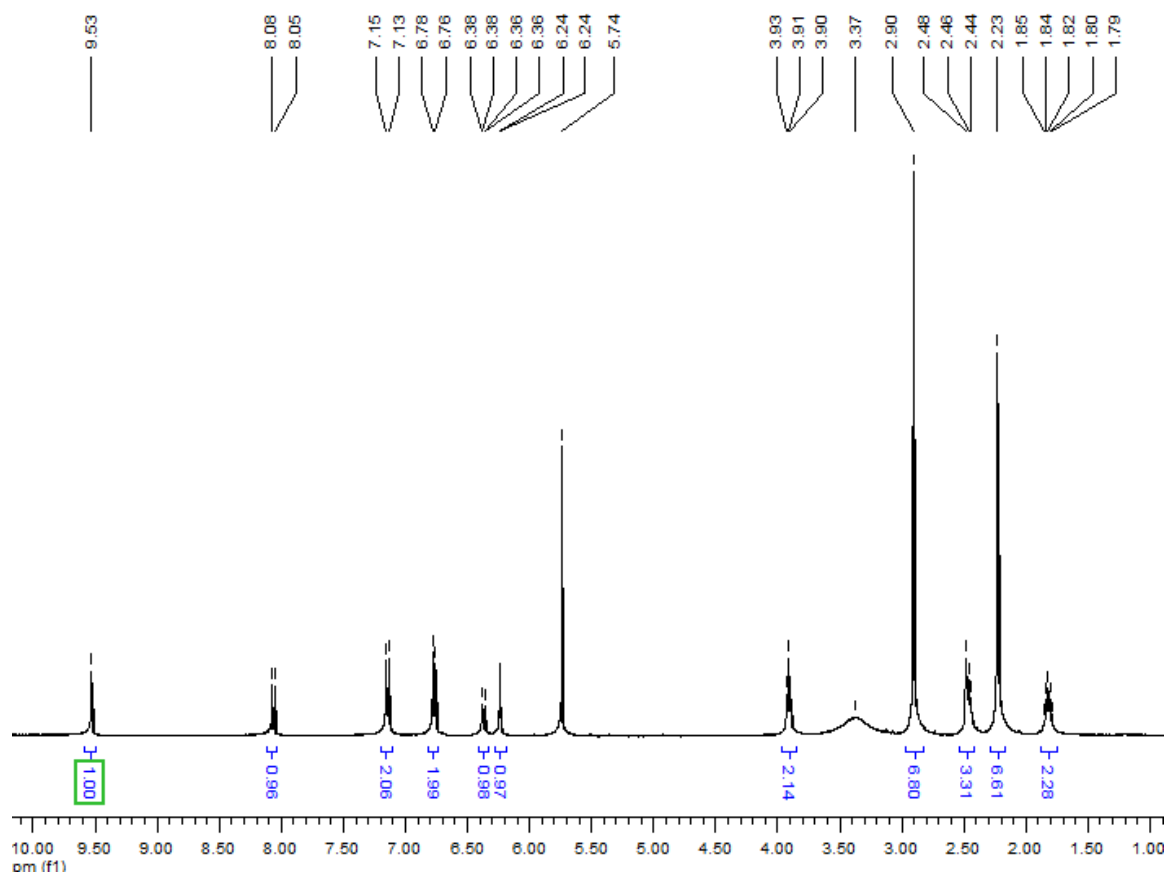
Spectrum 3-26: N^1-(5-(3-(dimethylamino)propoxy)-2-nitrophenyl)-N^4,N^4-dimethylbenzene-1,4-diamine (**11f**) ^{13}C NMR (400 MHz, DMSO-d6)
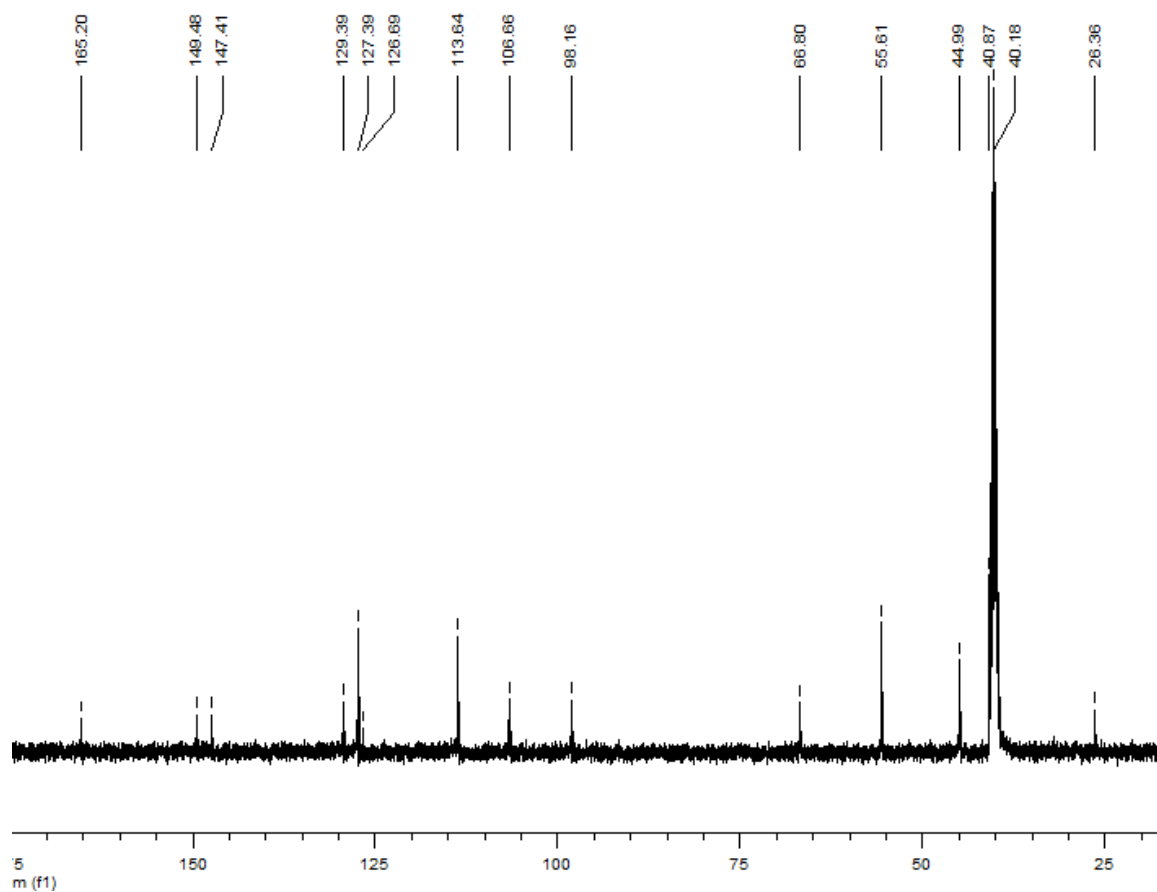
N-(5-((*tert*-butyldimethylsilyl)oxy)-1-penyl-1*H*-beno[*d*]imidazol-2-yl)benzamide (4a)
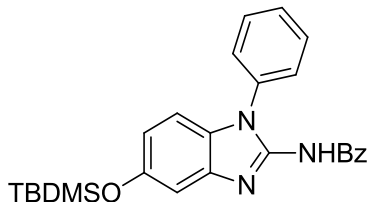
To a 100 ml round-bottom flask was added 4-((*tert*-butyldimethylsilyl)oxy)2-nitro-*N*-phenylaniline (**11a**) (3.65 g, 10.6 mmol) and methanol (60 ml). The flask was flushed with Ar gas before Pd/C (10 wt%, 100 mg) was added. The reaction was then sealed under H_2 atm and stirred at RT for 25 hours, before it was filtered and concentrated. The oil residue was dissolved in DCM (250 ml). While stirred, benzoyl isothiocyanate (1.5 ml, 10.6 mmol) was added via syringe. The reaction was then stirred at RT for 24 hours, before it was filtered, concentrated and purified via flash column to yield slight yellow foam as the intermediate product (3.4 g, 67.4 % yield), which was then dissolved in DCM (80 nml). DIPC (2.22 ml, 14.3 mmol) and DIPEA (2.49 ml, 14.3 mmol) was added. The reaction was stirred at RT for 24 hours before concentrated and purified via flash column chromatography (DCM 100 %) to yield white solid as the final product (2.1 g, 66 % yield). ^{1}H NMR (400 MHz, DMSO-d6): δ 8.02 (d, *J* = 8 Hz, 2H), 7.68 – 7.62 (m, 4H), 7.52 (t, *J* = 7 Hz, 1H), 7.43 (t, *J* = 7 Hz, 1H), 7.38 (t, *J* = 7 Hz, 2H), 7.18 (d, *J* = 2 Hz, 1H), 7.04 (d, *J* = 8 Hz, 1H), 6.73 (dd, J_1 = 8 Hz, J_2 = 2 Hz, 1H), 0.95 (s, 9H), 0.19 (s, 6H). ^{13}C NMR (400 MHz, DMSO-d6): δ 174.45, 153.22, 152.26, 138.68, 134.97, 131.69, 130.57, 130.01, 129.36, 128.92, 128.56, 127.80, 124.92, 115.97, 110.84, 104.33, 26.29, 18.67, -3.85. MS (ESI) calculated exact mass for $C_{26}H_{29}N_3O_2Si$ = 443.20. Found $[M+H]^+$ = 444.23.

Spectrum 3-27: *N*-(5-((*tert*-butyldimethylsilyl)oxy)-1-penyl-1*H*-beno[*d*]imidazol-2-yl)benzamide (**4a**) ^{1}H NMR (400 MHz, DMSO-d6)
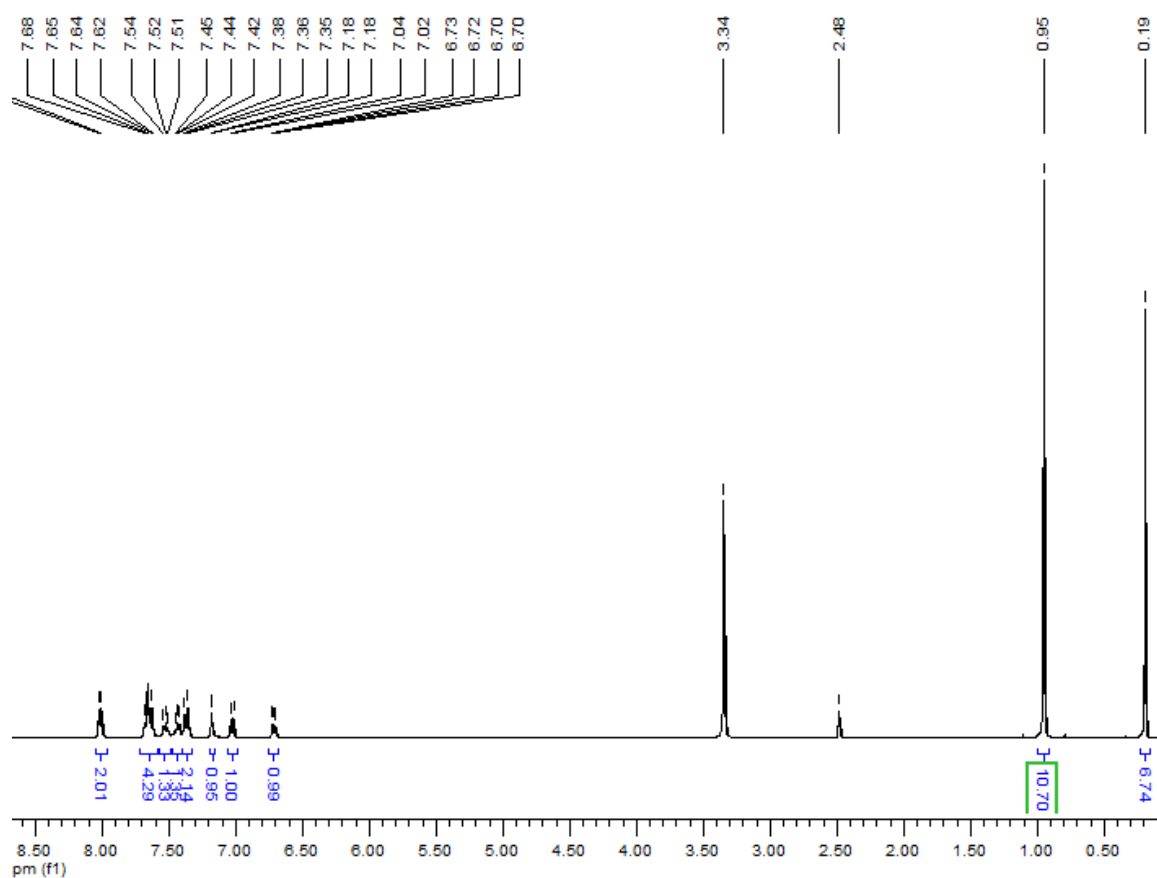
Spectrum 3-28: *N*-(5-((*tert*-butyldimethylsilyl)oxy)-1-penyl-1*H*-beno[*d*]imidazol-2-yl)benzamide **(4a)** ^{1}H NMR (400 MHz, DMSO-d6)
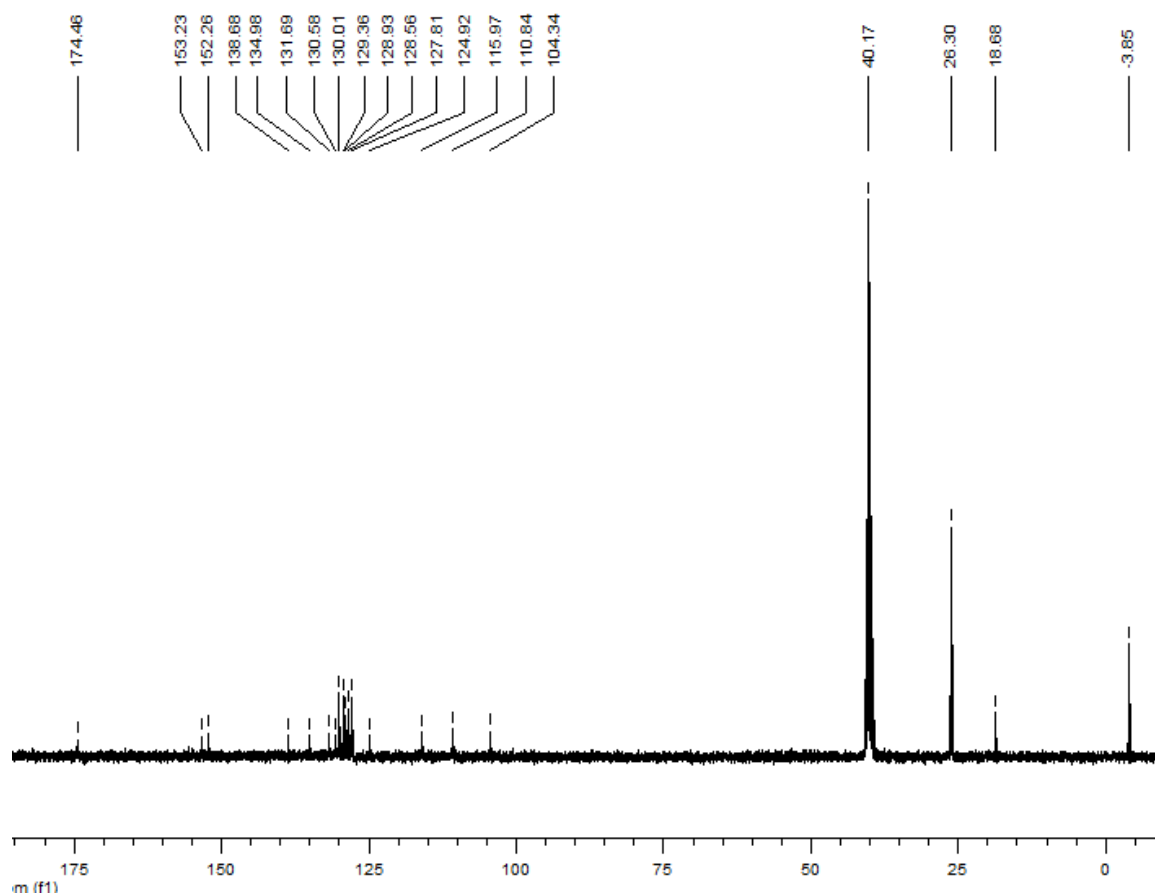
N-(5-hydroxy-1-phenyl-1H-benzo[d]imidazol-2-yl)benzamide (4ab)
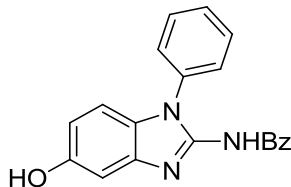
To a 50 ml round-bottom flask was added N-(5-((tert-butyldimethylsilyl)oxy)-1-penyl-1H-beno[d]imidazol-2-yl)benzamide (**4a**) (447 mg, 1.0 mmol) DCM (20 ml) and TBAF (1 ml, 1 M solution in THF, 5 wt% H_2O, 1mmol). The reaction was stirred at RT for 2 hours before it was filtered and concentrated. The crude was purified via flash column chromatography (DCM – MeOH : 90 % - 10 %) to yield white solid as the product (257 mg, 78 % yield). ^{1}H NMR (400 MHz, DMSO-d6): δ 9.48 (s, 1H), 8.02 (d, J = 8 Hz, 2H), 7.67 (m, 4H), 7.53 (t, J = 7 Hz, 1H), 7.45 (t, J = 7 Hz, 1H), 7.38 (t, J = 8 Hz, 2H), 7.06 (d, J = 2Hz, 1H), 6.99 (d, J = 9 Hz, 1H), 6.66 (dd, J_1 = 2Hz, J_2 = 9Hz, 1H), . ^{13}C NMR (400 MHz, DMSO-d6): δ 174.19, 154.91, 152.83, 138.81, 135.14, 131.60, 130.70, 129.97, 129.31, 128.79, 128.55, 127.74, 123.18, 111.73, 110.86, 99.61. MS (ESI) calculated exact mass for $C_{20}H_{15}N_3O_2$ = 329.12. Found $[M+H]^+$ = 330.12.

Spectrum 3-29: *N*-(5-hydroxy-1-phenyl-1*H*-benzo[*d*]imidazol-2-yl)benzamide **(4ab)** ¹H NMR (400 MHz, DMSO-d6)
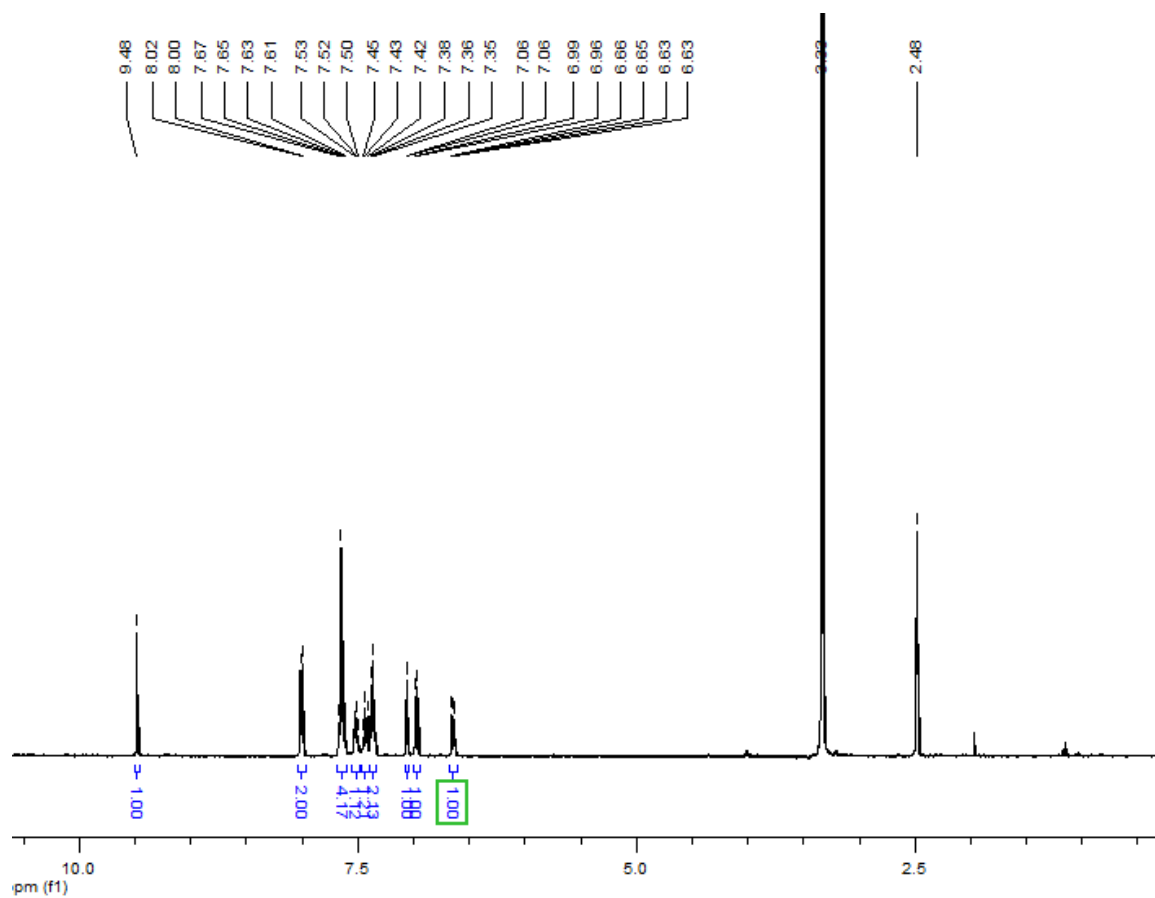
Spectrum 3-30: *N*-(5-hydroxy-1-phenyl-1*H*-benzo[*d*]imidazol-2-yl)benzamide **(4ab)** ^{13}C NMR (400 MHz, DMSO-d6)
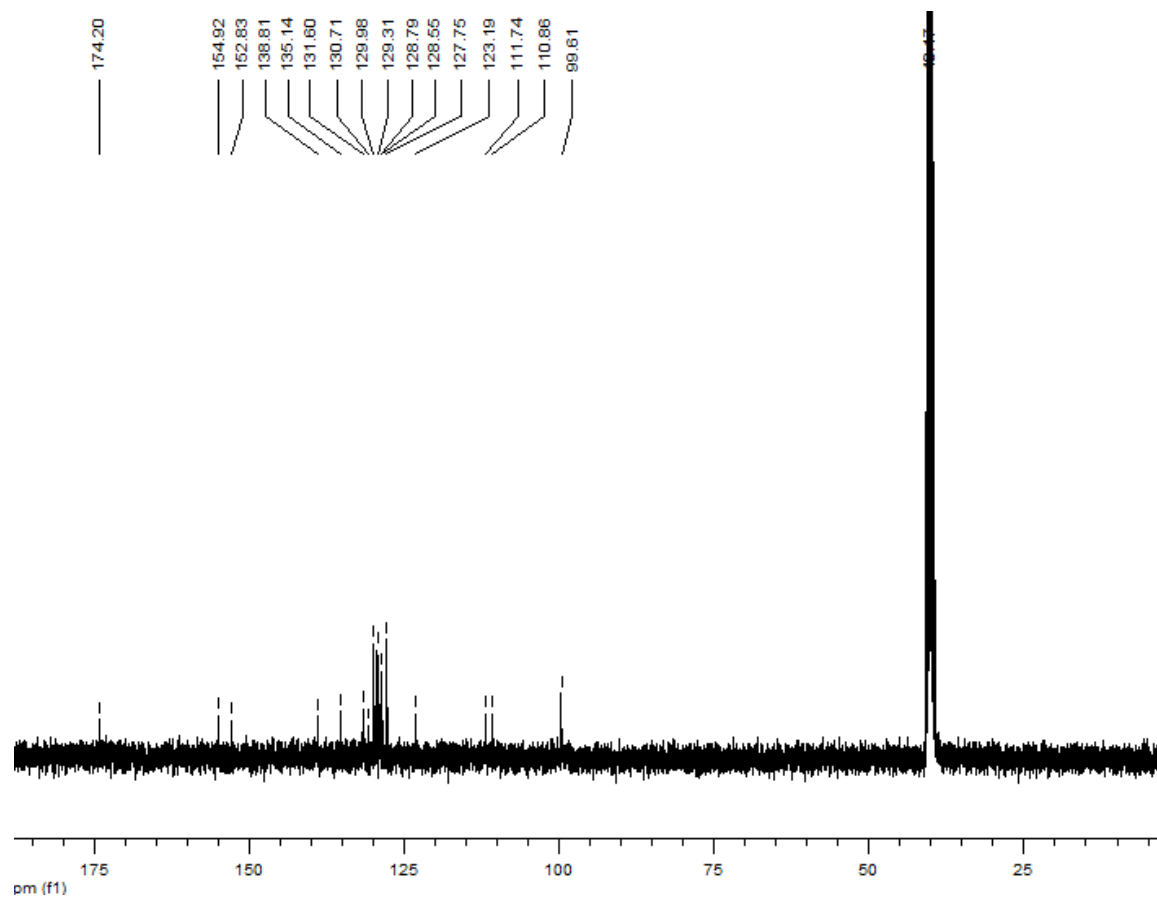
N-(5-(2-(dimethylamino)ethoxy)-1-phenyl-1H-benzo[d]imidazol-2-yl)benzamide (4bb)
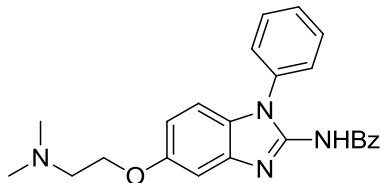
To a 250 ml round-bottom flask was added 4-(2-dimethylamino)ethoxy)-2-nitro-

N-phenylaniline (**11b**) (897 mg, 2.9 mmol) and methanol (100 ml). The flask was flushed

with Ar gas before Pd/C (90 mg, 10 wt %) was added. The reaction was then sealed

under H_2 atmosphere. It was stirred at RT for 1.5 hours before filtered and concentrated.

To the oil residue was added ACN (100 ml) followed by Benzoyl isothiocyanate (432 µl,

2.9 mmol). The reaction was stirred at RT for 2 hours before DIPC (463 µl, 2.9 mmol) and

K_2CO_3 (411 mg, 2.9 mmol) were added. The reaction was then stirred at RT for 20 hours

before it was filtered and concentrated. The crude was purified via flash column (DCM –

MeOH : 90 % - 10 %) to yield off white foam as the product (572 mg, 48 % yield two

steps). ^{1}H NMR (400 MHz, CDCl$_3$): δ 8.07 (d, J = 8 Hz, 2H), 7.57 – 7.35 (m, 10 H), 6.85 (dd,

J1 = 8 Hz, J2 = 4 Hz, 1H), 6.70 (d, J = 9 Hz, 1H), 6.32 (s, 1H), 4.06 (s, 2H), 2.66 (s, 2H), 2.22

(s, 6H). ^{13}C NMR (400 MHz, CDCl$_3$): δ 158.28, 143.98, 131.46, 129.95, 129.56, 129.43,

129.15, 128.99, 128.08, 128.01, 127.14, 119.62, 115.42, 111.81, 105.63, 102.32, 65.36,

57.97, 45.51. MS (ESI) calculated exact mass for $C_{24}H_{24}N_4O_2$ = 400.19. Found [M+H]$^+$ =

401.07.

Spectrum 3-31: *N*-(5-(2-(dimethylamino)ethoxy)-1-phenyl-1*H*-benzo[*d*]imidazol-2-yl)benzamide **(4bb)** ^{1}H NMR (400 MHz, CDCl$_3$)
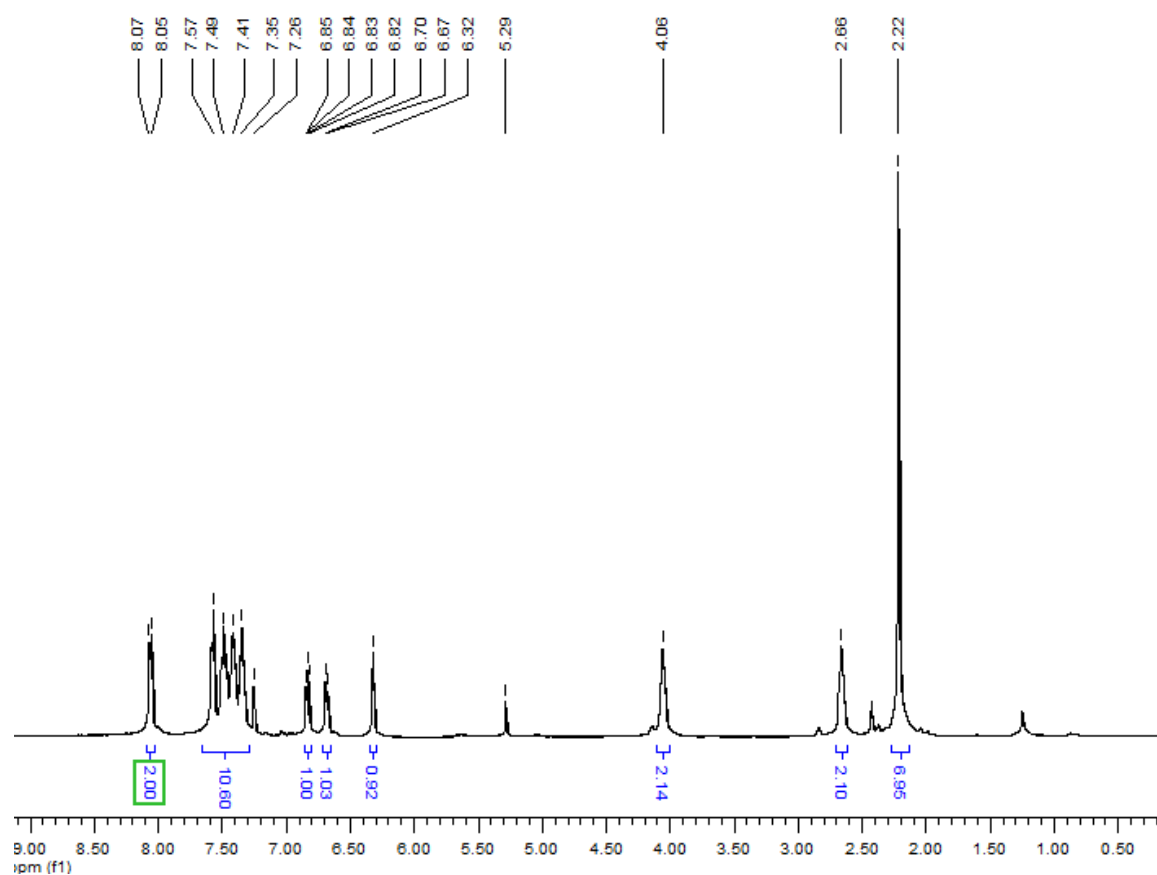
Spectrum 3-32: *N*-(5-(2-(dimethylamino)ethoxy)-1-phenyl-1*H*-benzo[*d*]imidazol-2-yl)benzamide (**4bb**) ¹³C NMR (400 MHz, CDCl₃)
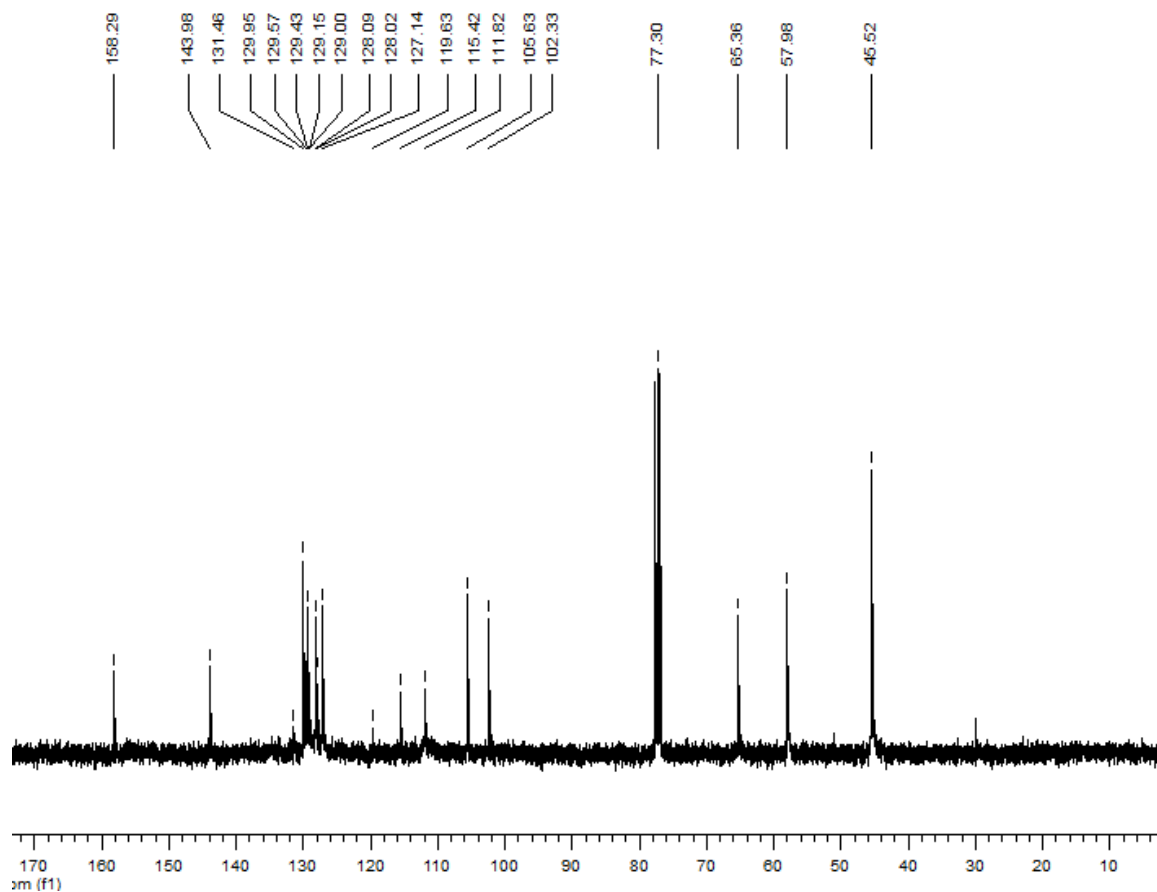
N-(5-(3-(dimethylamino)propoxy)-1-phenyl-1H-benzo[d]imidazol-2-yl)benzamide (4cb)
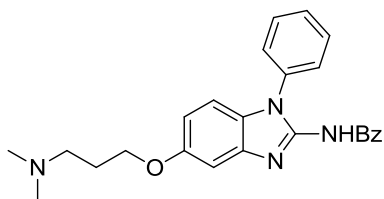
To a 50 ml round-bottom flask was added *N*-(5-hydroxy-1-phenyl-1H-benzo[*d*]imidazol-2-yl)benzamide (**4ab**) (214 mg, 0.65 mmol), ACN (15 ml), 3-dimethylamino-1-propyl chloride (200 mg, 1.26 mmol, 2 eq), and Cs_2CO_3 (616 mg, 1.95 mmol). The reaction was stirred and heated to reflux under Ar atmosphere for 6 hours before it was cooled to RT. It was then filtered and concentrated. The crude was purified via flash column chromatography (DCM – MeOH – 90 % - 10 %) to yield clear oil as the product (229 mg, 86 %). ^{1}H NMR (400 MHz, $CDCl_3$): δ 8.07 (d, J = 8 Hz, 2H), 7.56 (d, J = 8 Hz, 2H), 7.49 (t, J = 7 Hz, 2H), 7.42-7.40 (m, 2H), 7.37 (t, 7 Hz, 2H), 6.86 (d, J = 8 Hz, 1H), 6.66 (d, J = 8 Hz, 1H), 6.37 (s, 1H), 4.01 (t, J = 7 Hz, 2H), 2.32 (s, 2H), 2.18 (s, 6H), 1.93 (m, 2H). MS (ESI) calculated exact mass for $C_{25}H_{26}N_4O_2$ = 414.21. Found $[M+H]^+$ = 415.1.

Spectrum 3-33: *N*-(5-(3-(dimethylamino)propoxy)-1-phenyl-1*H*-benzo[*d*]imidazol-2-yl)benzamide (**4cb**) ^{1}H NMR (400 MHz, CDCl₃)
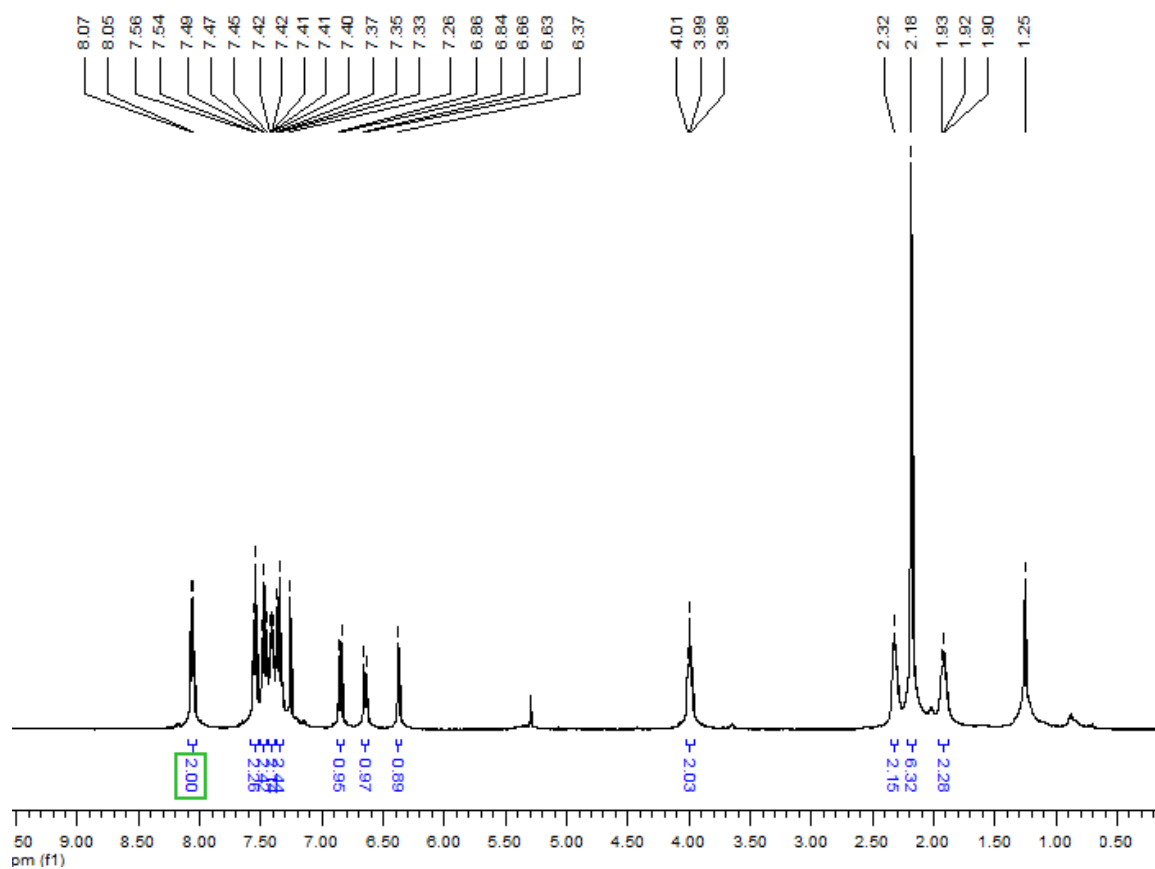
***N*-(5-(2-(dimethylamino)ethoxy)-1-phenyl-1*H*-benzo[*d*]imidazol-2-yl)acetamide (4ba)**
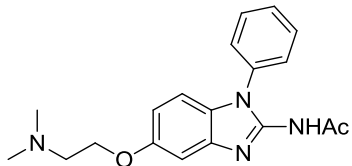
To a 100 ml round-bottom flask was added 4-(2-dimethylamino)ethoxy)-2-nitro-*N*-phenylaniline (**11b**) (564 mg, 1.87 mmol) and MeOH (50 ml). The flask was flushed with Ar gas before Pd/C (50 mg, 10 wt %) was added. The reaction was then stirred at RT under H_2 for 26 hr before it was filtered and concentrated. The resulting residue dissolved in DCM (50 ml). Acetyl isothiocyanate (164 μl, 1.87 mmol) was added. The reaction was sirred at RT for 2 hrs when DIPC (298 μl, 1.87 mmol) and Et_3N (262 μl, 1.87 mmol) were added. The reaction was then stirred at RT for 46 hrs before it was filtered and concentrated. The residue was extracted with water and DCM (150 ml ea.). The organic layer was collected and washed with water (100 ml), brine and dried with Na_2SO_4. After filtration and removal of solvent, the crude was purified via flash column chromatography (DCM – MeOH : 80 % - 20 %) to yield clear oil as the product (144 mg, 23 % yield). ^{1}H NMR (400 MHz, DMSO-d6): δ 7.58 (t, *J* = 8 Hz, 2H), 7.48-7.42 (m, 3H), 7.23 (d, *J* = 2 Hz, 1H), 7.09 (d, *J* = 9 Hz, 1H), 6.88 (dd, J_1 = 9 Hz, J_2 = 2 Hz, 1H), 4.17 (t, *J* = 5 Hz, 2H), 2.90 (t, *J* = 5 Hz, 2H), 2.39, (s, 6H), 1.91 (s, 3H). ^{13}C NMR (400 MHz, DMSO-d6): δ 171.31, 155.41, 146.10, 141.26, 135.76, 130.31, 128.90, 126.65, 113.14, 111.15, 103.19, 66.09, 57.62, 45.36, 40.13, 23.67. MS (ESI) calculated exact mass for $C_{19}H_{22}N_4O_2$ = 338.17. Found $[M+H]^+$ = 339.15.

Spectrum 3-34: *N*-(5-(2-(dimethylamino)ethoxy)-1-phenyl-1*H*-benzo[*d*]imidazol-2-yl)acetamide (**4ba**) ¹H NMR (400 MHz, DMSO-d6)

Spectrum 3-35: *N*-(5-(2-(dimethylamino)ethoxy)-1-phenyl-1*H*-benzo[*d*]imidazol-2-yl)acetamide (**4ba**) ^{13}C NMR (400 MHz, DMSO-d6)

_N_-(5-(3-dimethylamino)propoxy)-1-phenyl-1_H_-benzo[_d_]imidazol-2-yl)acetamide (4ca)
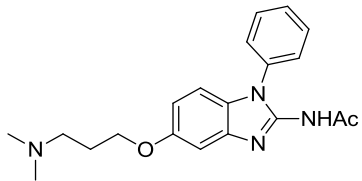
To a 100 ml round-bottom flask was added 4-(3-(dimethylamino)propoxy)-2-nitro-_N_-phenylaniline (**11c**) (682 mg, 2.16 mmol) and MeOH (50 ml). The flask was flushed with Ar gas before Pd/C (50 mg, 10 wt %) was added. The reaction was sealed under H_2 atm and stirred at RT for 7 hr. The metal was filtered and the solvent was removed. The oil residue was dissolved in ACN, and ethyl isothiocyanate (196 μl, 2.16 mmol) was added dropwise. The reaction was heated to reflux for 19 hr under Ar. After cooled to RT, the reaction was filtered and concentrated. The crude was purified by flash column chromatography (DCM – MeOH : 90 % - 10 %) to yield clear oil as the product (77 mg, 10 % yield). ^{1}H NMR (400 MHz, CD_3OD): δ 7.59 (t, _J_ = 7 Hz, 2H), 7.52 (d, _J_ = 7 Hz, 1H), 7.43 – 7.40 (m, 2H), 7.15 (d, _J_ = 2 Hz, 1H), 7.06 (d, _J_ = 9 Hz, 1H), 5.89 (dd, J_1 = 2 Hz, J_2 = 9 Hz, 1H), 4.04 (t, _J_ = 6 Hz, 2H), 2.59 (t, _J_ = 8 Hz, 2H), 2.30 (s, 6H), 2.02 (s, 3H), 2.00 (p, _J_ = 7 Hz, 2H). ^{13}C NMR (400 MHz, CD_3OD): δ 173.40, 156.32, 145.56, 139.33, 134.97, 129.78, 128.88, 128.67, 126.56, 113.21, 110.76, 101.38, 66.51, 56.24, 44.21, 26.97, 22.14. MS (ESI) calculated exact mass for $C_{20}H_{24}N_4O_2$ = 352.19. Found [M+H][+] = 353.1.

Spectrum 3-36: *N*-(5-(3-dimethylamino)propoxy)-1-phenyl-1*H*-benzo[*d*]imidazol-2-yl)acetamide **(4ca)** ^{1}H NMR (400 MHz, CD$_3$OD)
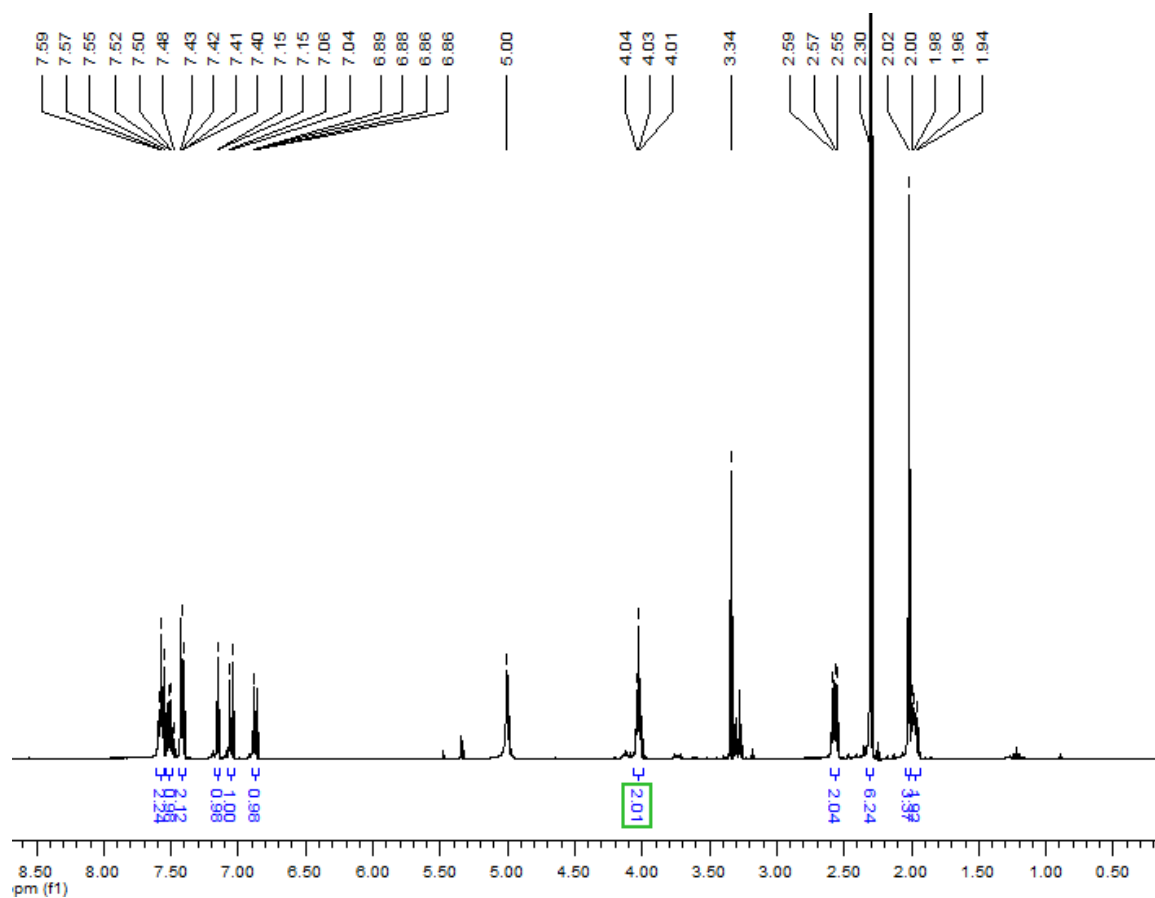
Spectrum 3-37: *N*-(5-(3-dimethylamino)propoxy)-1-phenyl-1*H*-benzo[*d*]imidazol-2-yl)acetamide (**4ca**) ^{13}C NMR (400 MHz, CD$_3$OD)
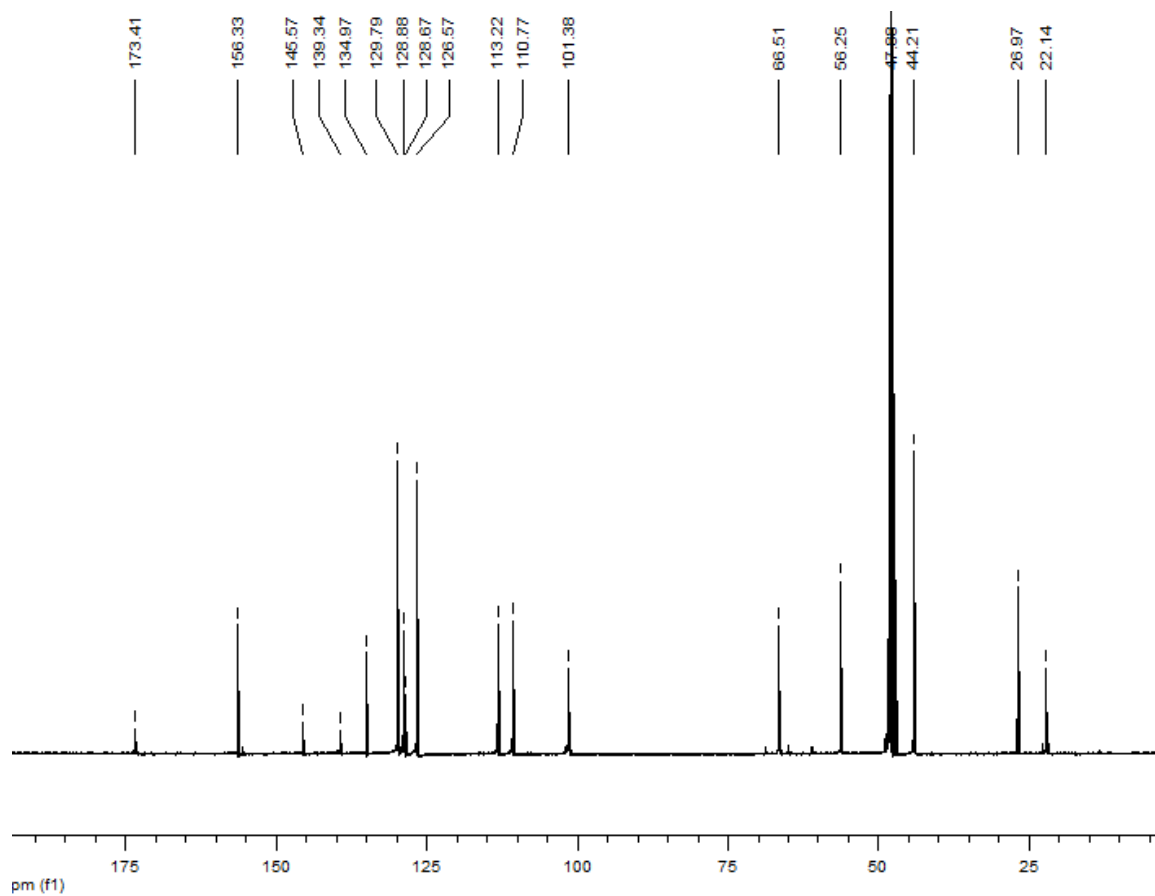
N-(1-(4-(dimethylamino)phenyl)-5-(3-(dimethylamino)propoxy)-1H-benzo[d]imidazol-2-yl)benzamide (4eb)
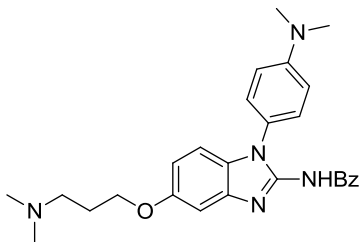
To a 100 ml round-bottom flask was added *N*¹-(4-(3-(dimethylamino)propoxy)-2-nitrophenyl)-*N*⁴,*N*⁴-dimethylbenzene-1,4-diamine (**11e**) (157 mg, 0.4 mmol) and methanol (30 ml). The flask was flushed with Ar gas before Pd/C (10 mg, 10 wt %) was added. The reaction was then sealed under H_2 atm and stirred at RT for 2 hours before it was filtered and concentrated. The oil residue was dissolved in 50 ml of DCM. Benzoyl isothiocyanate (65 μl, 0.4 mmol) was then added. The reaction was stirred at RT for 1 hour before DIPC (68 μl, 0.4 mmol) and DIPEA (76 μl, 0.4 mmol) were added. The reaction was stirred at RT for 25 hours before pouring into the water (50 ml) and extracted. The organic layer was collected and washed with water (50 ml), brine and dried over Na_2SO_4. After filtration and removal of solvent, the crude was purified via flash column chromatography (DCM- MeOH : 80 % - 20 %) to yield slight yellow solid as the product (38 mg, 20 % yield over two steps). ¹H NMR (400 MHz, CDCl₃): δ 8.23 (d, *J* = 7 Hz, 2H), 7.44 – 7.36 (m, 5H), 7.10 (d, *J* = 9 Hz, 1H), 6.88 (m, 3H), 6.76 (d, *J* = 7 Hz, 1H), 3.95 (t, *J* = 5 Hz, 2H), 3.07 (s, 6H), 2.91 (m, 2H), 2.61 (s, 6H), 2.19 (m, 2H). ¹³C NMR (400 MHz, CDCl₃): δ 155.82, 150.34, 138.31, 131.33, 129.10, 128.94, 128.08, 127.81, 125.40,

122.97, 112.56, 111.11, 111.00, 97.44, 66.16, 56.20, 44.21, 40.80, 25.90. MS (ESI)

calculated exact mass for $C_{27}H_{31}N_5O_2$ = 457.25. Found $[M+H]^+$ = 458.20 .

Spectrum 3-38: *N*-(1-(4-(dimethylamino)phenyl)-5-(3-(dimethylamino)propoxy)-1*H*-benzo[*d*]imidazol-2-yl)benzamide **(4eb)** ^{1}H NMR (400 MHz, CDCl₃)
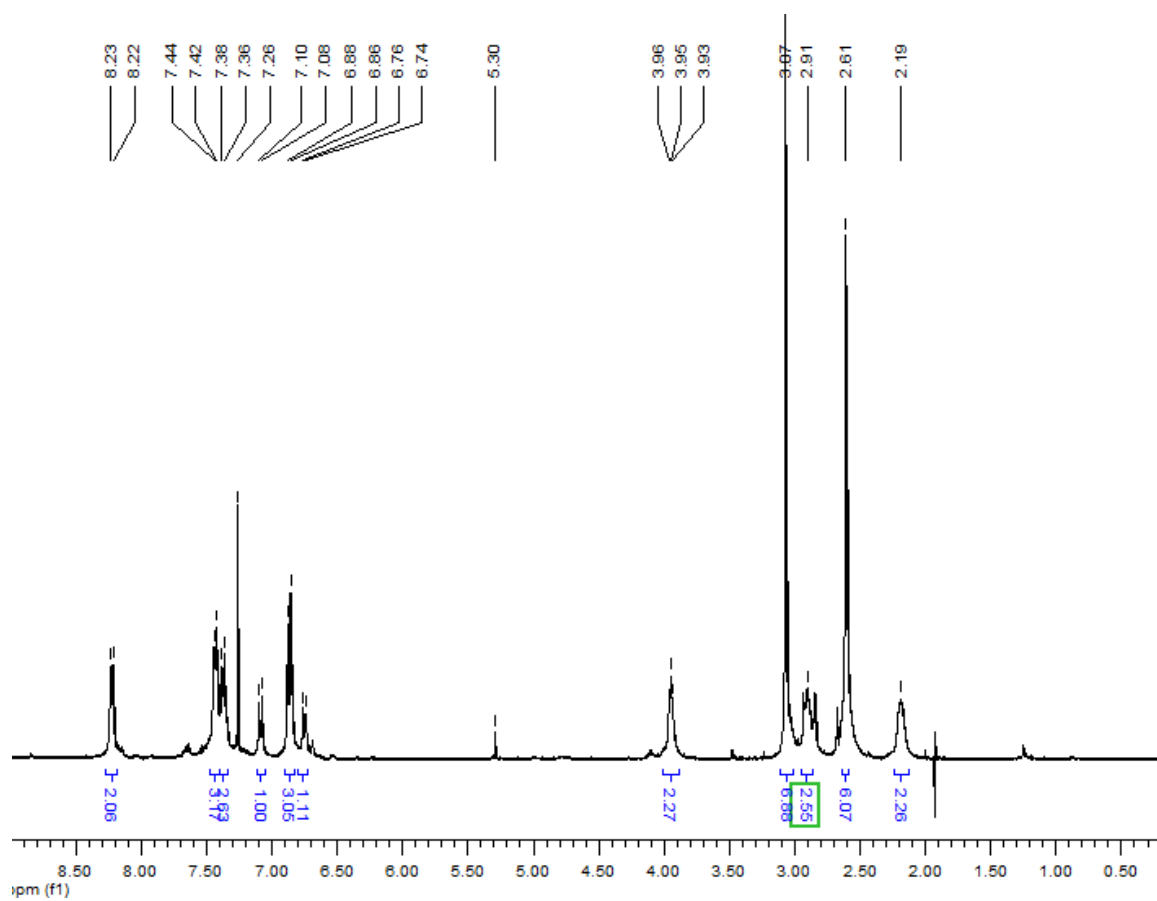
Spectrum 3-39: *N*-(1-(4-(dimethylamino)phenyl)-5-(3-(dimethylamino)propoxy)-1*H*-benzo[*d*]imidazol-2-yl)benzamide (**4eb**) ¹³C NMR (400 MHz, CDCl₃)
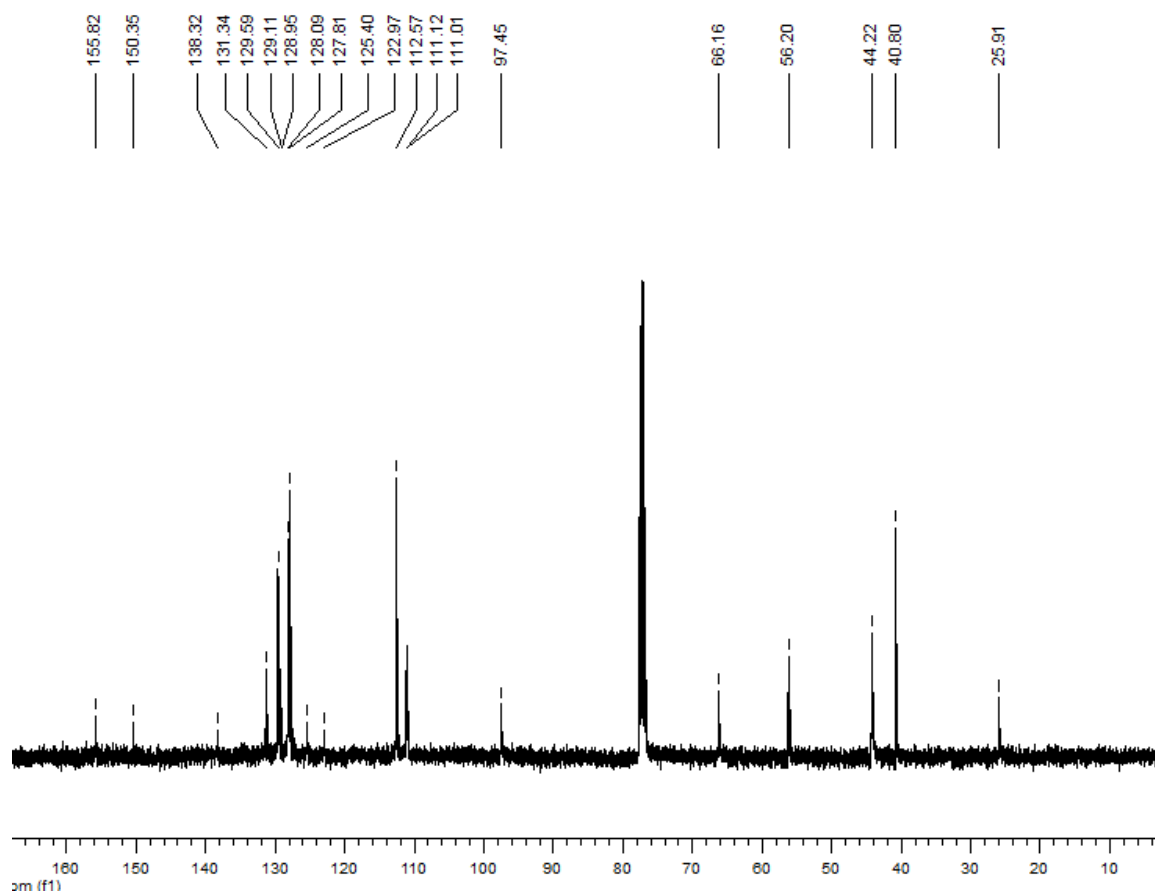
N-(1-phenyl-5-(pyridin-4-ylmethoxy)-1H-benzo[d]imidazol-2-yl)benzamide (4da)
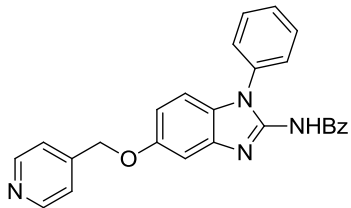
To a 50 ml round-bottom flask was added N-(5-hydroxy-1-phenyl-1H-benzo[d]imidazol-2-yl)benzamide (**4ab**) (71 mg, 0.21 mmol), ACN (20 ml) and Cs_2CO_3 (76 mg, 0.24 mmol). The reaction was stirred at RT under Ar atmosphere for 27 hours before it was filtered and concentrated. The crude was purified via flash column chromatography (EtOAc – DCM : 40 % - 60 %) to yield white solid as the product (54 mg, 60 % yield). ^{1}H NMR (400 MHz, DMSO-d6): δ 8.58 (d, J = 4 Hz, 2H), 8.01 (d, J = 8 Hz, 2H), 7.66 (m, 4H), 7.54 (m, 1H), 7.46 (m, 4H), 7.38 (m, 2H), 7.25 (s, 1H), 7.10 (d, J = 9 Hz, 1H), 6.92 (d, J = 6 Hz, 1H), 5.21 (s, 2H). MS (ESI) calculated exact mass for $C_{26}H_{20}N_4O_2$ = 420.16. Found $[M+H]^+$ = 421.1.

Spectrum 3-40: *N*-(1-phenyl-5-(pyridin-4-ylmethoxy)-1*H*-benzo[*d*]imidazol-2-yl)benzamide **(4da)** ^{1}H NMR (400 MHz, DMSO-d6)
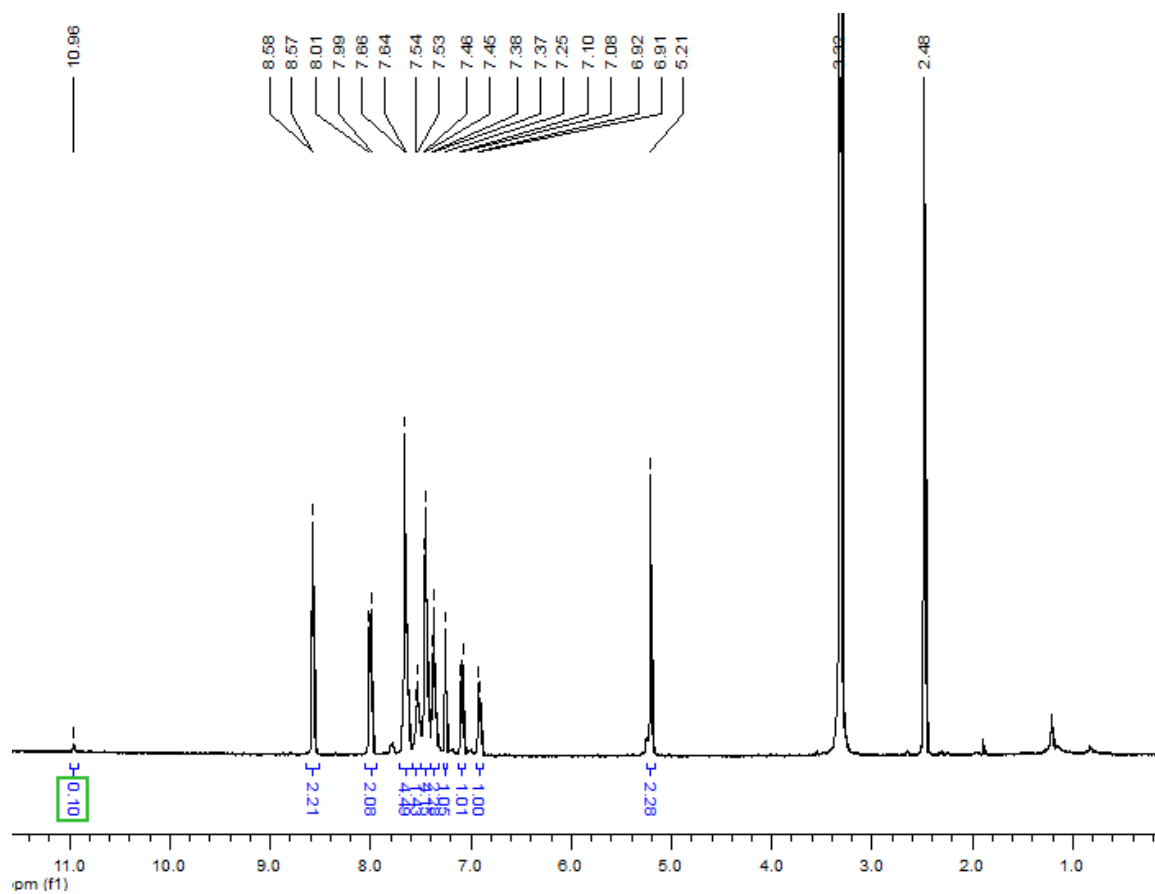
N-(1-(3-(dimethylamino)phenyl)-6-(3-(dimethylamino)propoxy)-1H-benzo[d]imidazol-2-yl)benzamide (4gb)

To a 250 ml round-bottom flask was added N^1-(5-(3-(dimethylamino)propoxy)-2-nitrophenyl)-N^3,N^3-dimethylbenzene-1,3-diamine (**11g**) (1.2 g, 3.2 mmol), methanol (100 ml). The flask was flushed with Ar gas before Pd/C (100 mg, 10 wt %) was added. The reaction was sealed under H_2 atmosphere and stirred at RT for 22 hours before it was filtered and concentrated. The dark oil residue was dissolved in ACN (100 ml). Benzoylisothiocyanate (386 µl, 3.2 mmol) was added. The reaction was stirred at RT for 3 hours when DIPC (522 µl, 3.2 mmol) and DIPEA (566 µl, 3.2 mmol) were added. The reaction was stirred at RT for 21 hours before it was filtered, concentrated. The crude was purified via flash column (DCM – MeOH : 90 % - 10 %) to yield yellow brown foam as the product (557 mg, 38 % yield). ^{1}H NMR (400 MHz, DMSO-d6): δ 8.03 (d, J = 7 Hz, 2H), 7.52 (d, J = 8 Hz, 1H), 7.46 – 7.36 (m, 4H), 6.92 (s, 1H), 6.88 – 6.82 (m, 3H), 6.70 (d, J = 2 Hz, 1H), 3.97 (t, J = 6 Hz, 2H), 2.93 (s, 6H), 2.81 (t, J = 7Hz, 2H), 2.45 (s, 6H), 2.00 (m, 2H). ^{13}C NMR (400 MHz, DMSO-d6): δ 155.97, 151.73, 137.98, 135.74, 132.68, 132.05, 131.82, 130.36, 129.41, 129.20, 129.11, 128.62, 114.70, 112.75, 111.72, 111.36, 96.23, 66.51, 55.34, 44.00, 40.73, 25.81. MS (ESI) calculated exact mass for $C_{27}H_{31}N_5O_2$ = 457.57. Found $[M+H]^+$ = 458.30.

Spectrum 3-41: *N*-(1-(3-(dimethylamino)phenyl)-6-(3-(dimethylamino)propoxy)-1*H*-benzo[*d*]imidazol-2-yl)benzamide (**4gb**) ^{1}H NMR (400 MHz, DMSO-d6)

Spectrum 3-42: *N*-(1-(3-(dimethylamino)phenyl)-6-(3-(dimethylamino)propoxy)-1*H*-benzo[*d*]imidazol-2-yl)benzamide (**4gb**) ^{13}C NMR (400 MHz, DMSO-d6)

N-(1-(4-(dimethylamino)phenyl)-6-(3-(dimethylamino)propoxy)-1H-benzo[d]imidazol-2-yl)benzamide (4fb)

To a 250 ml round bottom flask was added N^1-(5-(3-(dimethylamino)propoxy)-2-nitrophenyl)-N^4,N^4-dimethylbenzene-1,4-diamine (**11f**) (1.2 g, 3.35 mmol) and MeOH (100 ml). The flask was flushed with Ar gas before Pd/C (120 mg, 10 wt %) was added. The reaction was then sealed under H_2 atmosphere and was stirred at RT for 4.5 hr. The reaction was filtered and concentrated. The oil residue was dissolved in 100 ml of DCM and benzoyl isothiocyanate (509 µl, 3.35 mmol) was added. The reaction was stirred at RT under Ar for 1 hr when DIPC (600 µl, 3.85 mmol) and DIPEA (567 µl, 3.35 mmol) were added. The reaction was stirred at RT under Ar for 21 hr. It was then extracted with water (2 x 100 ml). The organic layer was collected. It was washed with brine and dried over Na_2SO_4. After filtration and evaporation of solvent, the crude was purified via flash column chromatography (DCM – MeOH : 90% - 10 %) to yield white solid as the product (393 mg, 26 % yield over two steps). ^{1}H NMR (400 MHz, CDCl₃): δ 8.21 (d, *J* = 7 Hz, 2H), 7.44 – 7.40 (m, 3H), 7.37 (t, *J* = 7 Hz, 2H), 7.22 (d, *J* = 9 Hz, 1H), 6.89 (d, *J* = 9 Hz, 2H), 6.83 (dd, *J₁* = 9 Hz, *J₂* = 2 Hz, 1H), 6.74 (d, *J* = 2 Hz, 1H), 3.98 (t, *J* = 6 Hz, 2H), 3.07 (s, 6H), 2.49 (t, *J* = 7 Hz, 2H), 2.26 (s, 6H), 1.98 (p, *J* = 7 Hz, 2H). ^{13}C NMR (400 MHz, CDCl₃): δ 176.65, 156.29, 154.58, 150.43, 138.28, 131.97, 131.24, 129.49, 128.01, 122.85, 112.65, 111.91,

111.20, 96.64, 67.12, 56.52, 45.59, 40.78, 27.60. MS (ESI) calculated exact mass for

$C_{27}H_{31}N_5O_2$ = 457.25. Found $[M+H]^+$ = 458.24.

Spectrum 3-43: *N*-(1-(4-(dimethylamino)phenyl)-6-(3-(dimethylamino)propoxy)-1*H*-benzo[*d*]imidazol-2-yl)benzamide (**4fb**) ^{1}H NMR (400 MHz, CDCl$_3$)

Spectrum 3-44: *N*-(1-(4-(dimethylamino)phenyl)-6-(3-(dimethylamino)propoxy)-1*H*-benzo[*d*]imidazol-2-yl)benzamide (**4fb**) ^{13}C NMR (400 MHz, CDCl$_3$)
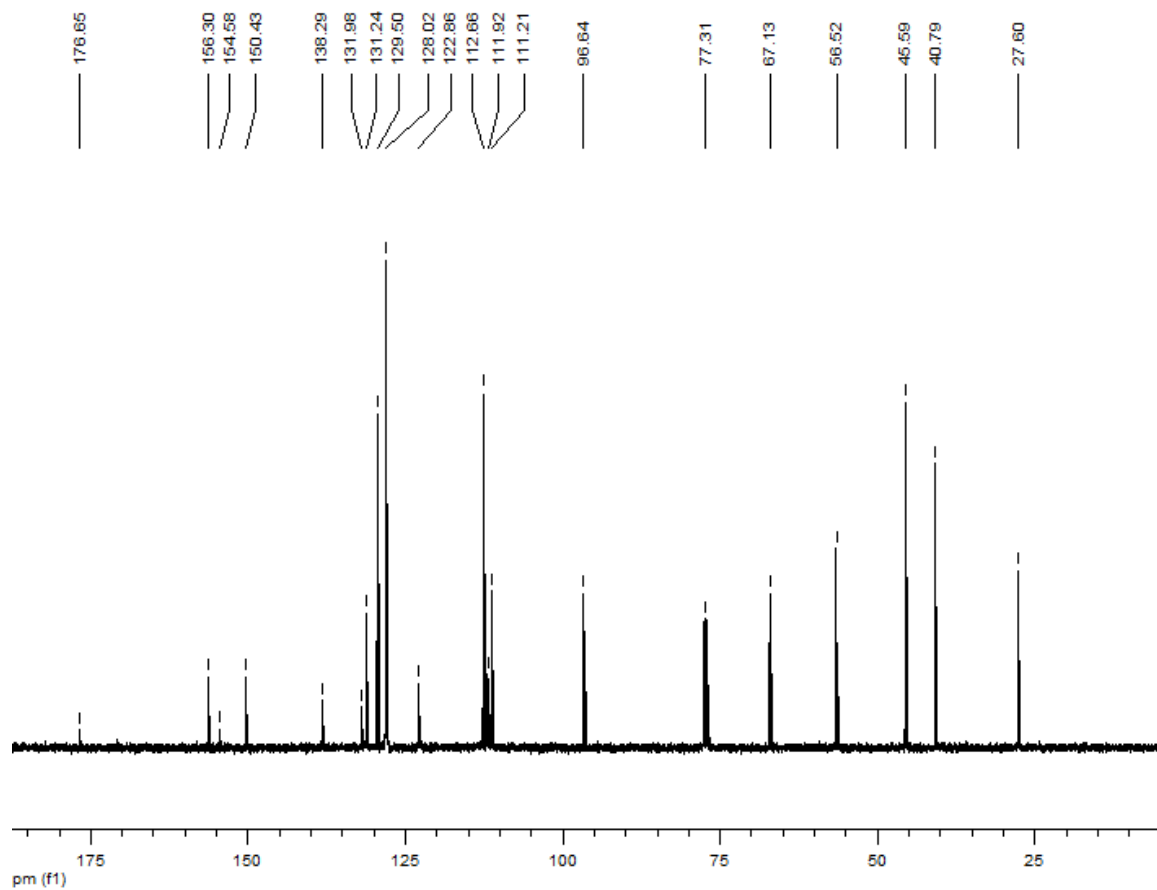
2-amino-1-phenyl-1*H*-bnzo[*d*]imidazol-5-ol (3a)
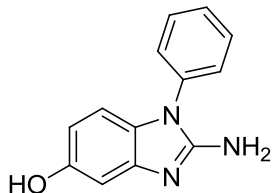
To a 50 ml round-bottom flask was added *N*-(5-hydroxy-1-phenyl-1*H*-benzo[d]imidazole-2-yl)benzamide (**4ab**) (300 mg, 0.68 mmol), 2N HCl (aq, 10 ml), dioxane (10ml). The reaction was stirred and heated to reflux for 22 hours before it was cooled to RT. It was then poured into water (100 ml) and extracted with chloroform (150 ml x 2). The organic layers were collected and combined. It was dried with brine and Na_2SO_4. After filtration and concentration, the crude was purified with flash column (DCM – MeOH : 80 % - 20 %) to yield clear oil as the product (120 mg, 78 % yield). ^{1}H NMR (400 MHz, DMSO-d6): δ 7.58 (t, *J* = 7 Hz, 2H), 7.47 (m, 3 H), 6.71 – 6.64 (m, 4 H), 6.42 (dd, J_1 = 9 Hz, J_2 = 2Hz, 1H). ^{13}C NMR (400 MHz, DMSO-d6): δ 154.13, 153.90, 141.79, 135.35, 130.78, 128.84, 128.19, 127.15, 108.70, 108.14, 101.88. MS (ESI) calculated exact mass for $C_{13}H_{11}N_3O$ = 225.09. Found $[M+H]^+$ = 226.10.

Spectrum 3-45: 2-amino-1-phenyl-1*H*-bnzo[*d*]imidazol-5-ol **(3a)** ^{1}H NMR (400 MHz, DMSO-d6)
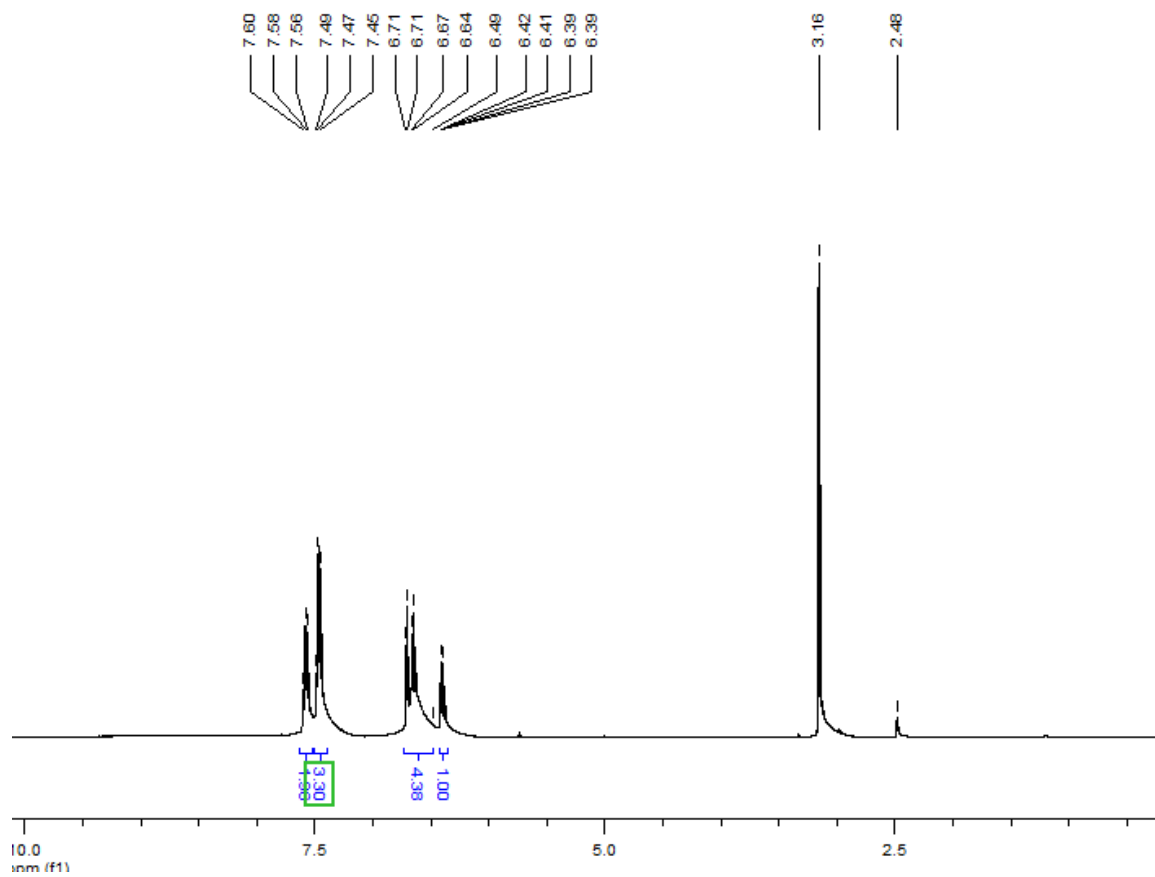
**Spectrum 3-46**: 2-amino-1-phenyl-1*H*-bnzo[*d*]imidazol-5-ol **(3a)** ^{13}C NMR (400 MHz, DMSO-d6)
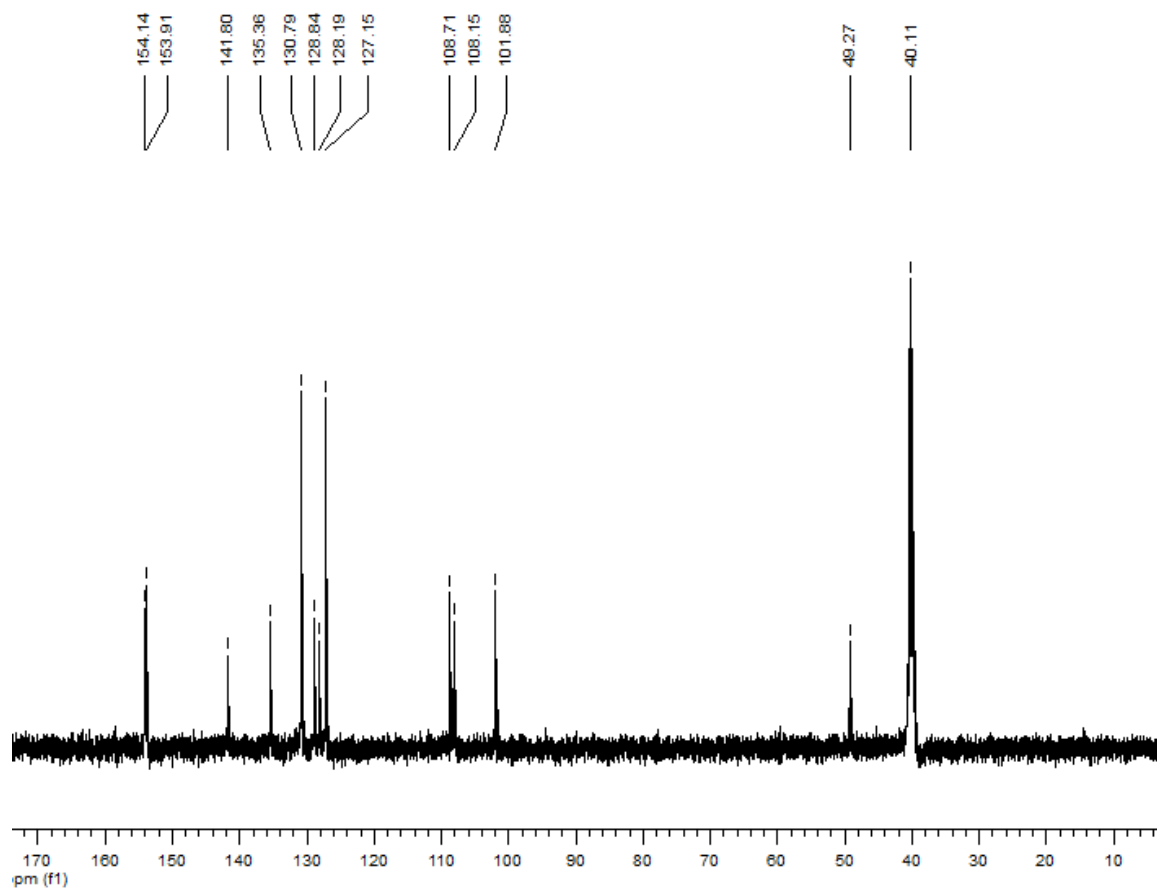
5-(3-(dimethylamino)propoxy)-1-phenyl-1*H*-benzo[*d*]imidazol-2-amine (3c)
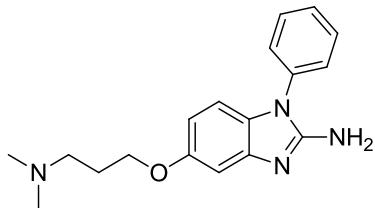
To a 100 ml round-bottom flask was added *N*-(5-(3-(dimethylamino)propoxy)-1-phenyl-1*H*-benzo[*d*]imidazol-2-yl)benzamide (**4cb**) (264 mg, 0.6 mmol) and 1N HCl aq (40 ml). The reaction was stirred and heated to reflux for 26 hours before it was cooled to RT. It was then extracted with saturated $NaHCO_3$ (100 ml). The organic layer was collected and washed with brine and dried over Na_2SO_4. After filtration and evaporation, the crude was purified using flash column chromatography (DCM – MeOH : 80 % - 20 %) to yield slight yellow oil as the product (190 mg, 94 % yield). ^{1}H NMR (400 MHz, $CDCl_3$): δ 7.55 (t, *J* = 8 Hz, 2H), 7.44-7.41 (m, 3H), 6.94 (s, 1H), 6.83 (d, *J* = 8 Hz, 1H), 6.59 (dd, J_1 = 8 Hz, J_2 = 2 Hz, 1H), 5.71 (broad, 1H), 4.00 (t, *J* = 7 Hz, 2H), 2.45 (t, *J* = 7 Hz, 2H), 2.22 (s, 6H), 1.95 (p, *J* = 7 Hz, 2H). ^{13}C NMR (400 MHz, $CDCl_3$): δ 155.61, 154.24, 143.23, 135.37, 130.48, 129.51, 128.68, 126.69, 108.50, 108.42, 101.92, 67.29, 56.76, 45.73, 27.91. MS (ESI) calculated exact mass for $C_{18}H_{22}N_4O$ = 310.18. Found $[M+H]^+$ = 311.1.

Spectrum 3-47: 5-(3-(dimethylamino)propoxy)-1-phenyl-1*H*-benzo[*d*]imidazol-2-amine
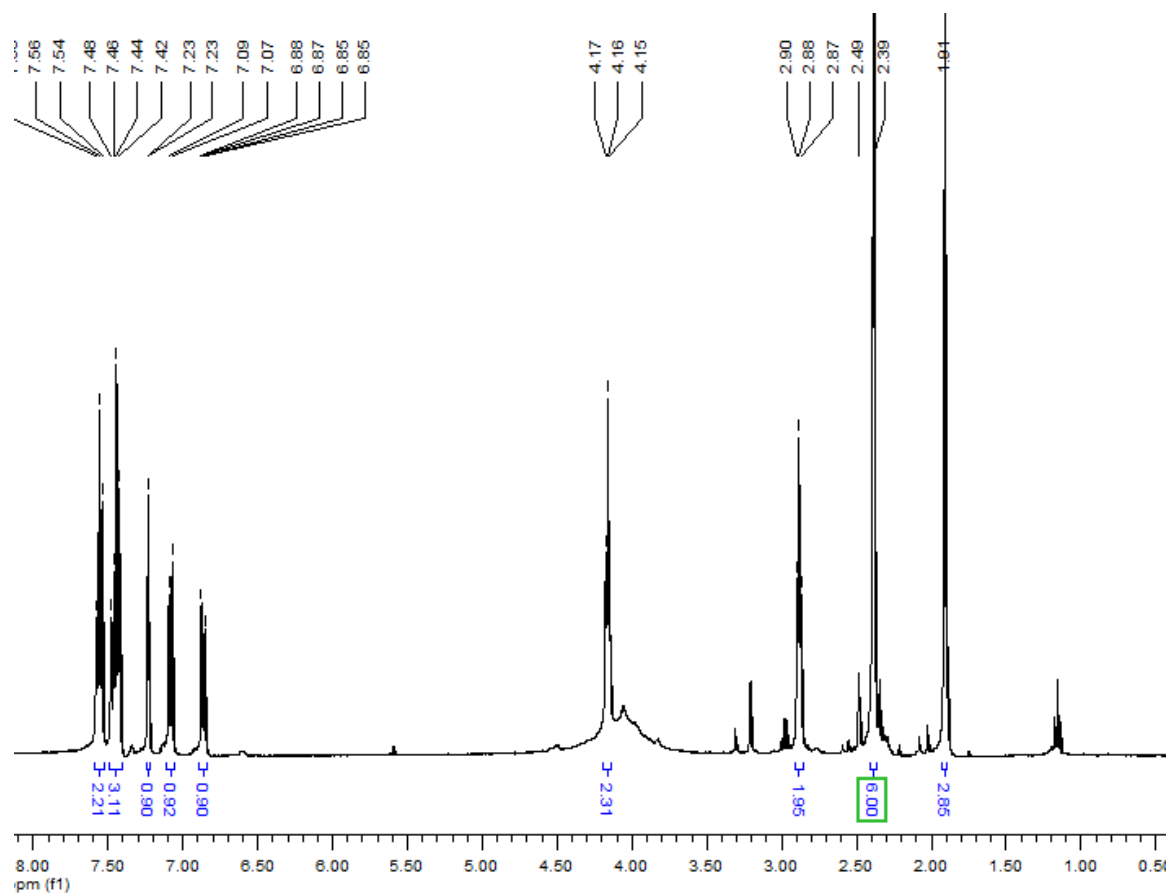(**3c**) ^{1}H NMR (400 MHz, CDCl$_3$)

Spectrum 3-48: 5-(3-(dimethylamino)propoxy)-1-phenyl-1*H*-benzo[*d*]imidazol-2-amine (**3c**) ^{13}C NMR (400 MHz, CDCl$_3$)
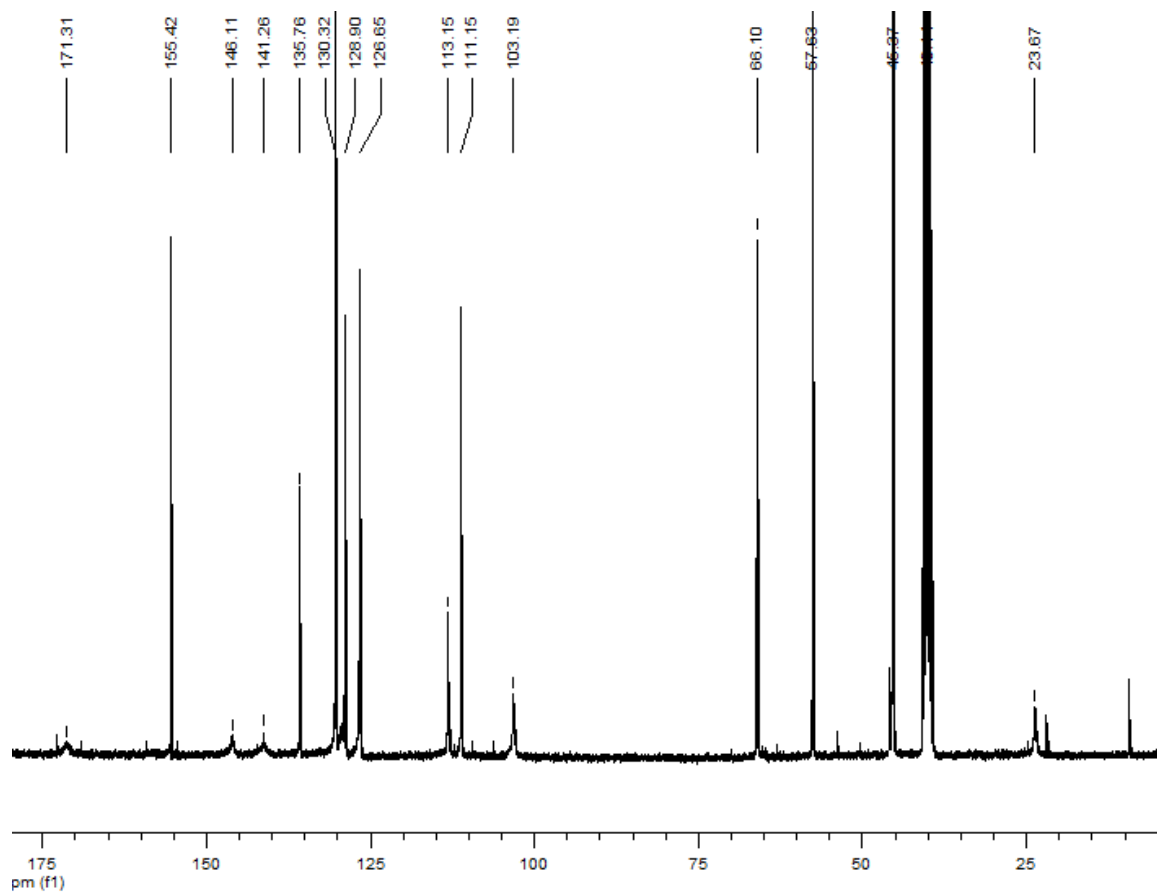
5-(2-(dimethylamino)ethoxy)-1-phenyl-1*H*-benzo[*d*]imidazol-2-amine (3b)
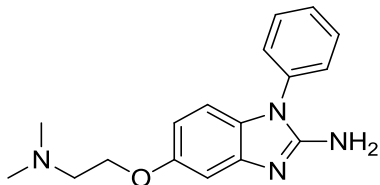
Into a 50 ml round bottom flask was added *N*-(5-2-(dimethylamino)ethoxy)-1-phenyl-1*H*-benzo[*d*]imidazol-2-amine (**4bb**) (320 mg, 0.8 mmol) and 1N HCl aq (20 ml). The reaction was stirred and heated to reflux for 24 hr before it was cooled to RT. It was then extracted with saturated $NaHCO_3$ and DCM (100 ml ea.). The aqueous layer was extracted with additional DCM (100 ml). The combined organic layers was washed with brine and dried over Na_2SO_4. After filtration and evaporation of solvent, the crude was purified via flash column chromatography (DCM – MeOH : 80 % - 20 %) to yield white solid as the product (193 mg, 65 % yield). ^{1}H NMR (400 MHz, $CDCl_3$): δ 7.55 (t, *J* = 7 Hz, 2H), 7.45 – 7.41 (m, 3H), 6.97 (d, *J* = 2 Hz, 1H), 6.84 (d, *J* = 8 Hz, 1H), 6.63 (dd, J_1 = 8 Hz, J_2 = 2 Hz, 1H), 4.08 (t, *J* = 6 Hz, 2H), 2.74 (t, *J* = 6 Hz, 2H), 2.32 (s, 6H). ^{13}C NMR (400 MHz, $CDCl_3$): δ 155.47, 154.03, 142.75, 135.19, 130.52, 129.51, 128.80, 126.68, 108.78, 108.63, 101.86, 66.86, 58.53, 45.99. MS (ESI) calculated exact mass for $C_{17}H_{20}N_4O$ = 296.16. Found $[M+H]^+$ = 297.15.

Spectrum 3-49: 5-(2-(dimethylamino)ethoxy)-1-phenyl-1*H*-benzo[*d*]imidazol-2-amine (**3b**) ^{1}H NMR (400 MHz, CDCl$_3$)

Spectrum 3-50: 5-(2-(dimethylamino)ethoxy)-1-phenyl-1*H*-benzo[*d*]imidazol-2-amine (**3b**) ^{13}C NMR (400 MHz, CDCl$_3$)
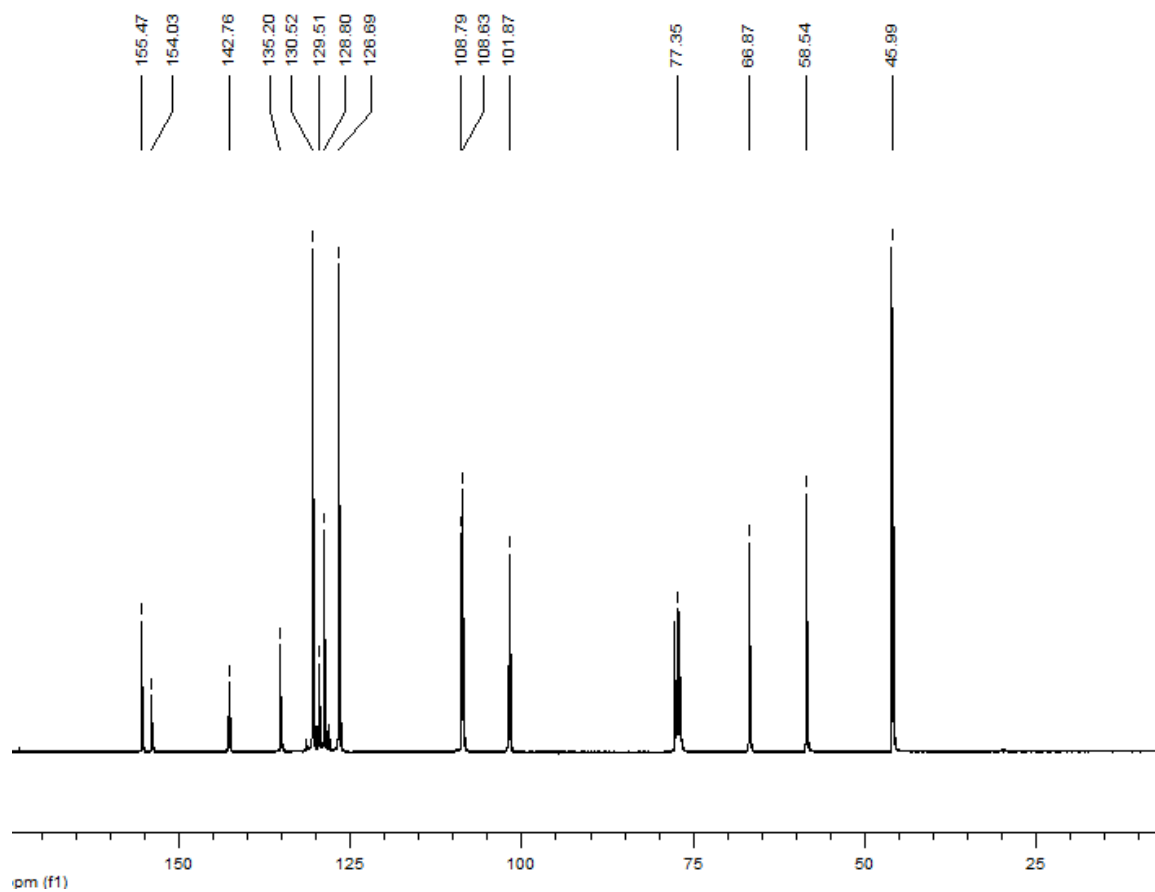
5-(2-(dimethylamino)ethoxy)-1-(4-(dimethylamino)phenyl)-1*H*-benzo[*d*]imidazol-2-amine (3e)

To a 100 ml round-bottom flask was added *N*-(5-(2-(dimetylamino)ethoxy)-1-(4-(dimethylamino)phenyl)-1*H*-benzo[*d*]imidazol-2-yl)benzamide (**4eb**) (320 mg, 0.7 mmol) and 1N HCl aq (25 ml). The reaction was stirred and heated to reflux for 19 hours before it was cooled to RT. It was then basified with 1 M NaOH aq until white precipitate formed. It was then extracted with chloroform-ethanol (2 x 100 ml, 2 : 1). The organic layers were collected and combined. It was then dried over Na_2SO_4. After filtration and evaporation of solvent, the crude was purified with flash column chromatography (DCM – MeOH : 80 % - 20 %) to yield white solid as the product (174 mg, 73 % yield). ^{1}H NMR (400 MHz, CD_3OD): δ 7.23 (d, *J* = 9 Hz, 2H), 6.92 – 6.90 (m, 3H), 6.74 (d, *J* = 8 Hz, 1H), 6.63 (dd, J_1 = 8 Hz, J_2 = 2 Hz, 1H), 4.09 (t, *J* = 6 Hz, 2H), 3.15 (t, *J* = 8 Hz, 2H), 3.02 (s, 6H), 2.75 (s, 6H), 2.17 – 2.10 (m, 2H). ^{13}C NMR (400 MHz, CD_3OD): δ 155.22, 154.91, 151.24, 140.70, 130.15, 127.63, 122.37, 113.18, 108.54, 108.08, 100.52, 65.96, 64.12, 55.97, 42.99, 39.49, 15.44. MS (ESI) calculated exact mass for $C_{19}H_{25}N_5O$ = 353.22. Found $[M+H]^+$ = 354.3.

Spectrum 3-51: 5-(2-(dimethylamino)ethoxy)-1-(4-(dimethylamino)phenyl)-1*H*-benzo[*d*]imidazol-2-amine (**3e**) ^{1}H NMR (400 MHz, CD$_3$OD)
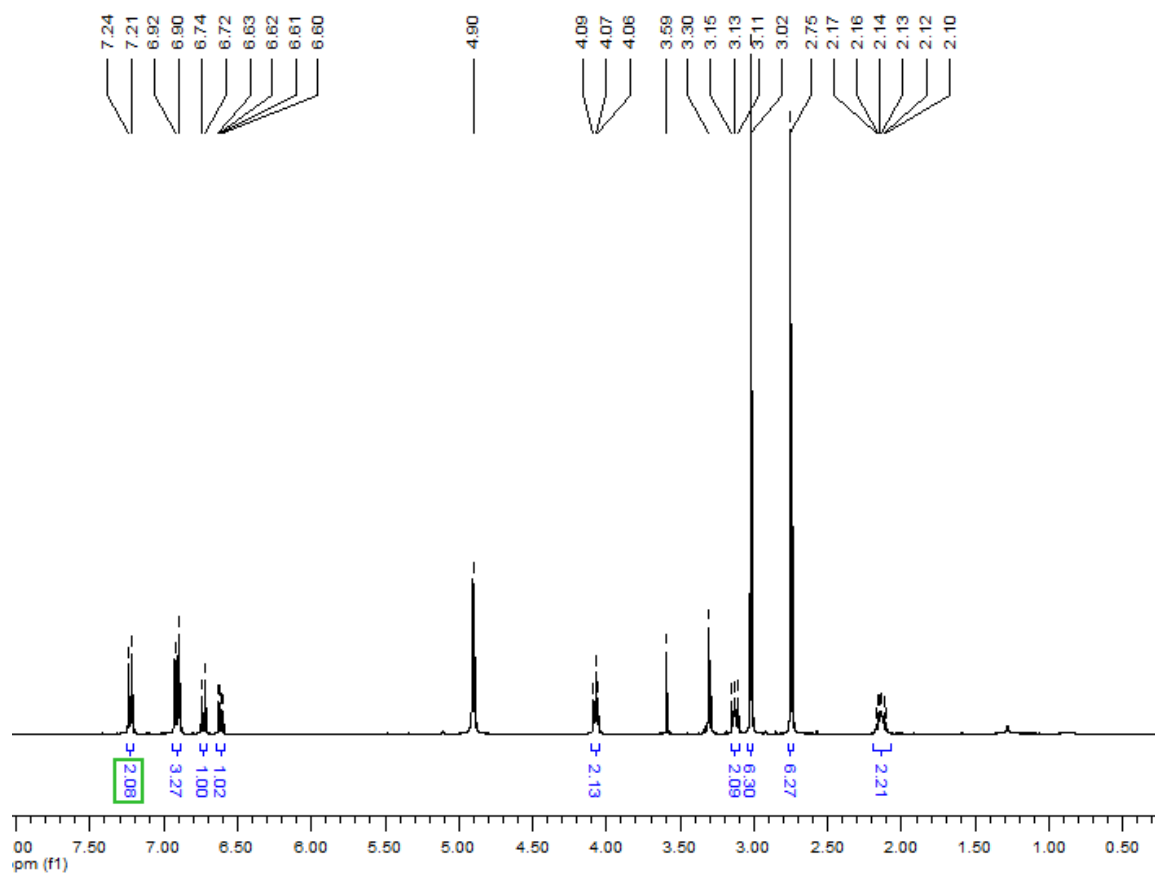
Spectrum 3-52: 5-(2-(dimethylamino)ethoxy)-1-(4-(dimethylamino)phenyl)-1*H*-benzo[*d*]imidazol-2-amine (**3e**) ^{13}C NMR (400 MHz, CD$_3$OD)
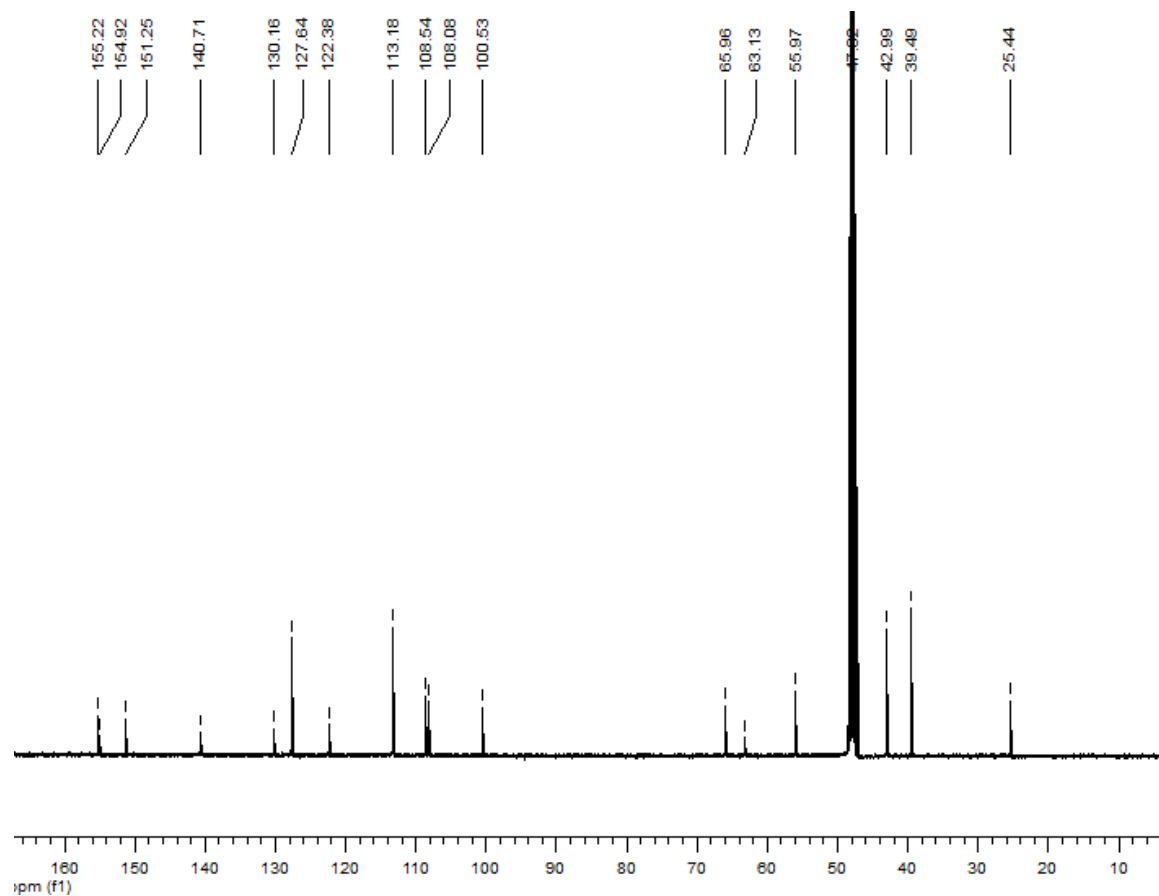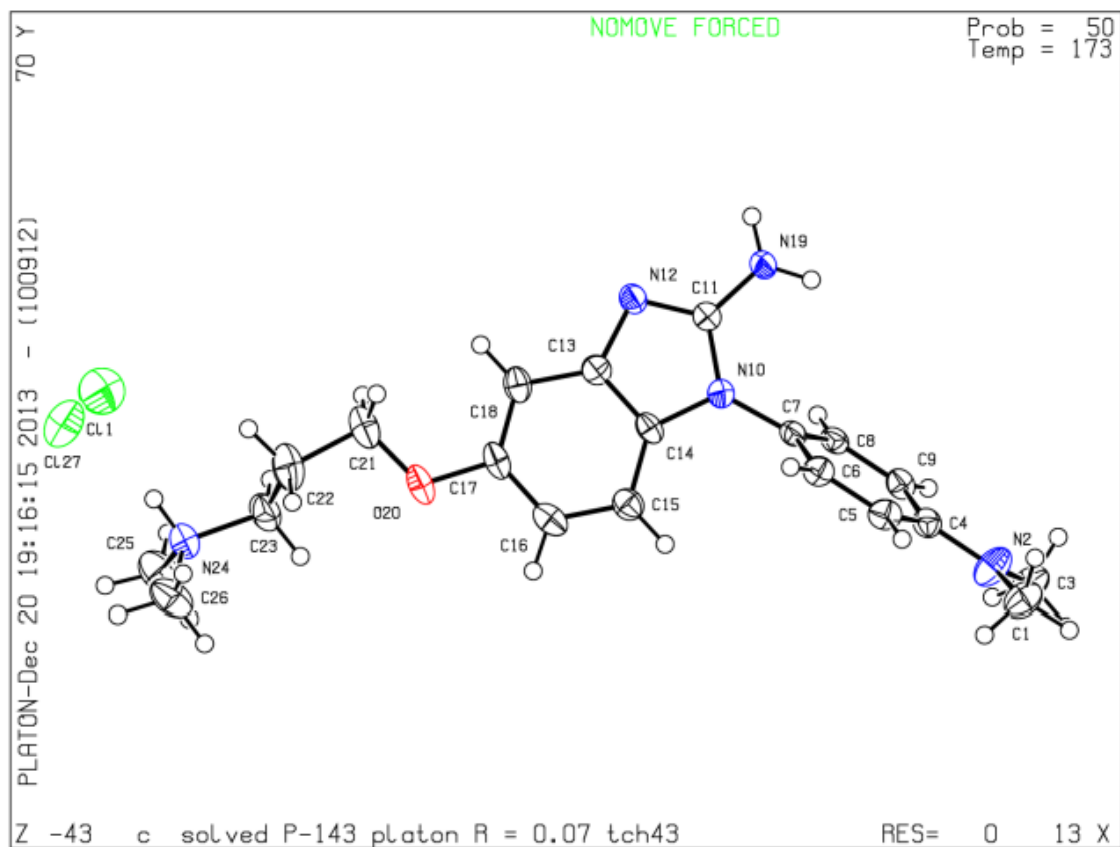
Figure 3-11: Crystal structure of 1-(4-(dimethylamino)phenyl)-5-(3-(dimethylamino)propoxy)-1H-benzo[d]imidazole-2-amine, hydrochloride

1-phenyl-5-(pyridine-4-ylmethoxy)-1*H*-benzo[*d*]imidazol-2-amine (3d)
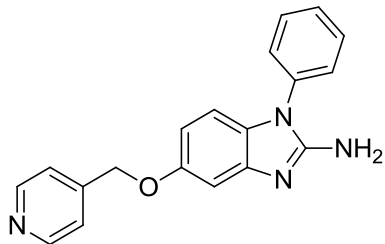
To a 50 ml round-bottom flask was added *N*-(1-phenyl-5-(pyridin-4-ylmethoxy)-1*H*-benzo[*d*]imidazol-2-yl)benzamide (**4da**) (30 mg, 0.07 mmol))and 1N HCl (20 ml). The reaction was stirred and heated to reflux for 18 hours before it was cooled to RT. It was basified by 1M NaOH until the cloudiness appears. It was then extracted with EtOAc (2 x 20 ml). The organic layers were collected and combined. It was washed with brine and dried over Na_2SO_4. After filtration and evaporation of solvent, the crude was purified via flash column chromatography (DCM – MeOH : 90 % - 10 %) to yield white solid as the product (15 mg, 68 % yield). ^{1}H NMR (400 MHz, DMSO-d6): δ 8.56 (d, *J* = 6 Hz, 2H), 7.61 (t, *J* = 7 Hz, 2H), 7.50 – 7.42 (m, 5H), 6.88 (d, *J* = 2 Hz, 1H), 6.75 (d, *J* = 9 Hz, 1H), 6.59 (dd, J_1 = 9 Hz, J_2 = 2Hz, 1H), 6.33 (s, broad, 2H), 5.15 (s, 2H). MS (ESI) calculated exact mass for $C_{19}H_{16}N_4O$ = 316.13. Found $[M+H]^+$ = 317.09.

Spectrum 3-53: 1-phenyl-5-(pyridine-4-ylmethoxy)-1*H*-benzo[*d*]imidazol-2-amine (**3d**) ^{1}H NMR (400 MHz, DMSO-d6)
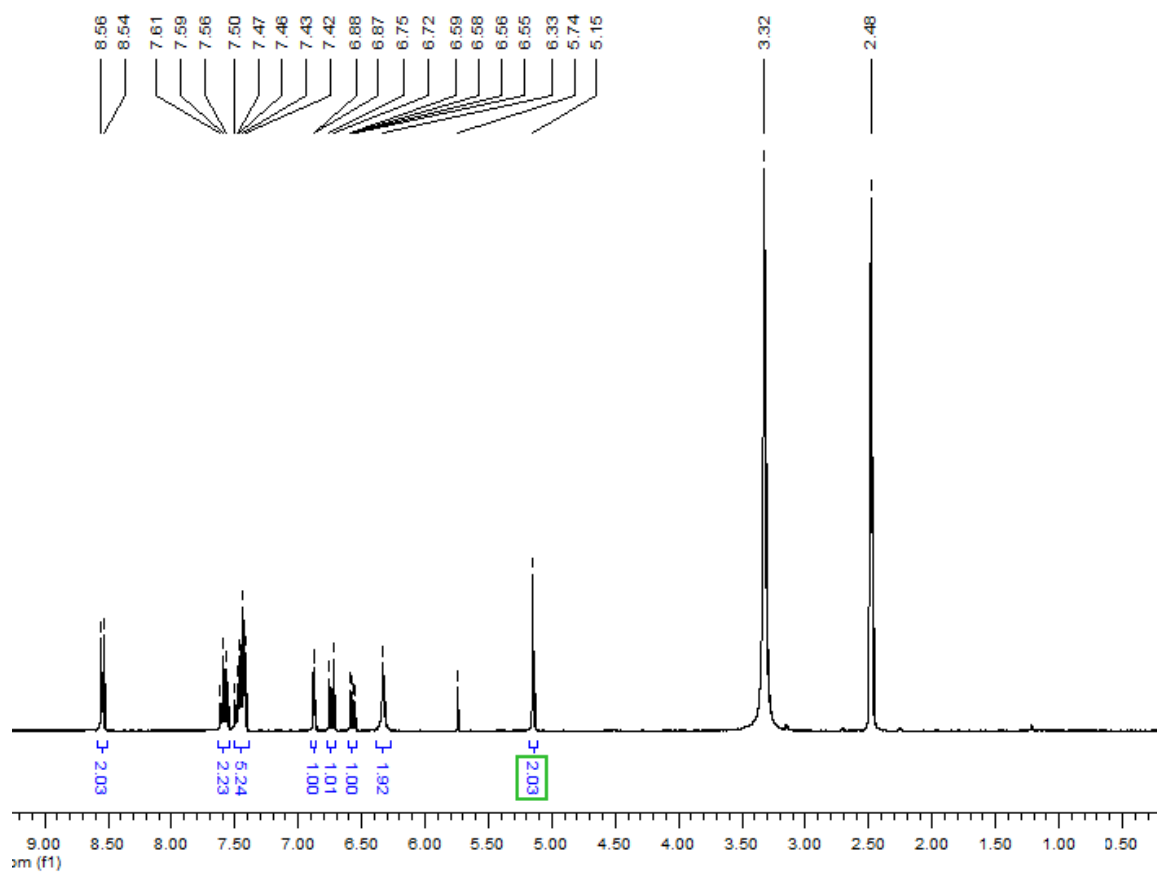
1-(4-(dimethylamino)phenyl)-6-(3-(dimethylamino)propoxy)-1*H*-benzo[*d*]imidazol-2-amine (3f)
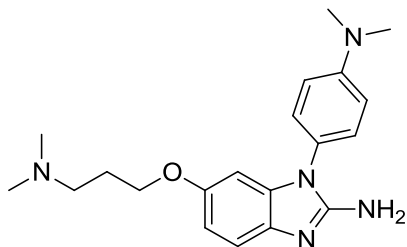
To a 100 ml round-bottom flask was added N-(1-(4-(dimethylamino)phenyl)-6-(3-(dimethylamino)propoxy)-1H-benzo[d]imidazol-2-yl)benzamide (**4fb**) (375 mg, 0.82 mmol) and 1N HCl aq (25 ml). The reaction was stirred and heated to reflux for 19 hr before cooled to RT. It was basified with saturated $NaHCO_3$ aq and 1M NaOH aq until the white precipitate formed. It was then extracted with $CHCl_3$ - EtOH (2 : 1, 3 x 150 ml). The organic layers were collected and combined. It was then dried over Na_2SO_4. After filtration and concentration, the crude was purified using flash column chromatography (DCM – MeOH : 80 % - 20 %) to yield white solid as the product (240 mg, 83 % yield). ^{1}H NMR (400 MHz, CD_3OD): δ 7.24 (d, *J* = 9 Hz, 2H), 7.16 (d, *J* = 8 Hz, 1H), 6.92 (d, *J* = 9 Hz, 2H), 6.71 (dd, J_1 = 9 Hz, J_2 = 2 Hz, 1H), 6.42 (d, *J* = 2 Hz, 1H), 3.93 (t, *J* = 6 Hz, 2H), 3.02 (s, 6H), 2.73 (t, *J* = 7 Hz, 2H), 2.43 (s, 6H), 2.00 (p, *J* = 6 Hz, 2H). ^{13}C NMR (400 MHz, DMSO-d6): δ 154.56, 154.13, 151.24, 136.04, 135.20, 127.76, 122.56, 114.89, 113.21, 109.62, 95.00, 66.46, 56.10, 47.81, 43.70, 39.49, 26.41. MS (ESI) calculated exact mass for $C_{20}H_{27}N_5O$ = 353.22. Found $[M+H]^+$ = 354.25.

Spectrum 3-54: 1-(4-(dimethylamino)phenyl)-6-(3-(dimethylamino)propoxy)-1*H*-benzo[*d*]imidazol-2-amine (**3f**) ^{1}H NMR (400 MHz, CD$_3$OD)
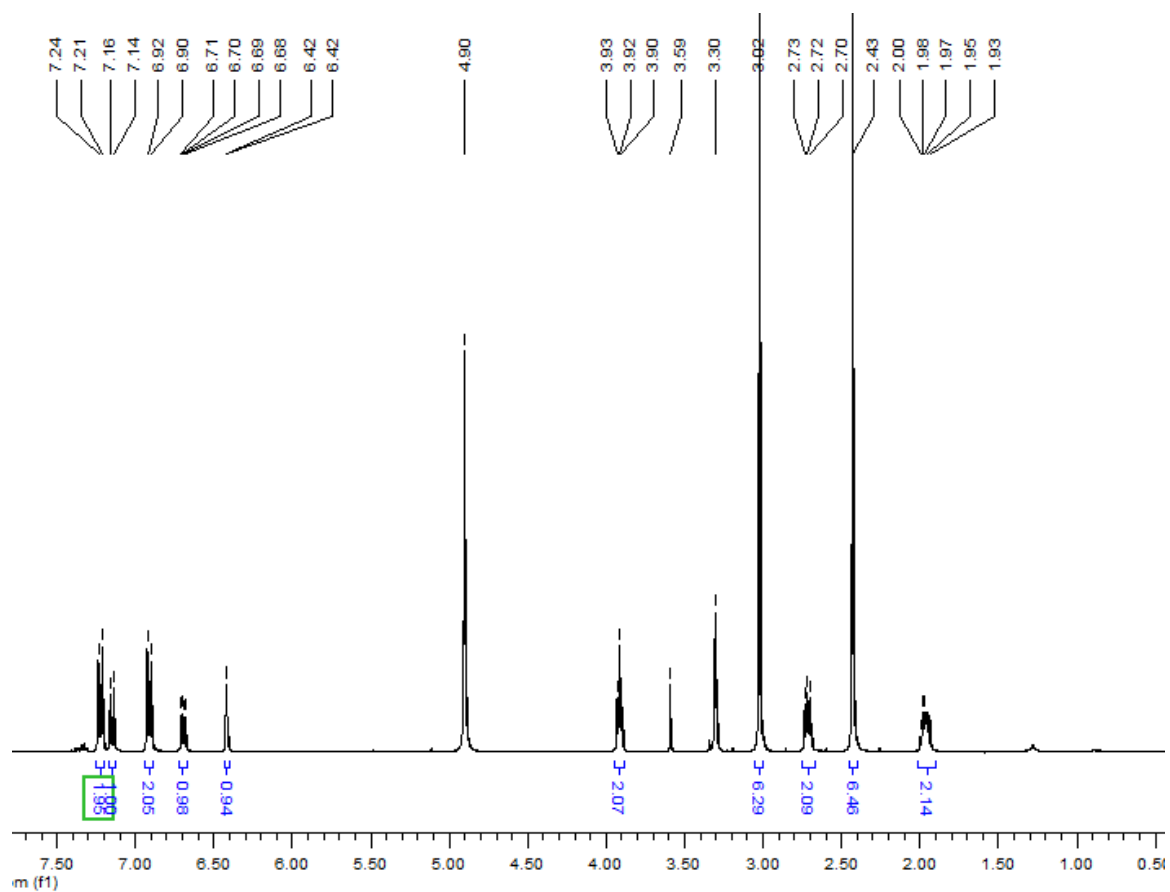
Spectrum 3-55: 1-(4-(dimethylamino)phenyl)-6-(3-(dimethylamino)propoxy)-1*H*-benzo[*d*]imidazol-2-amine (**3f**) ^{13}C NMR (400 MHz, CD$_3$OD)
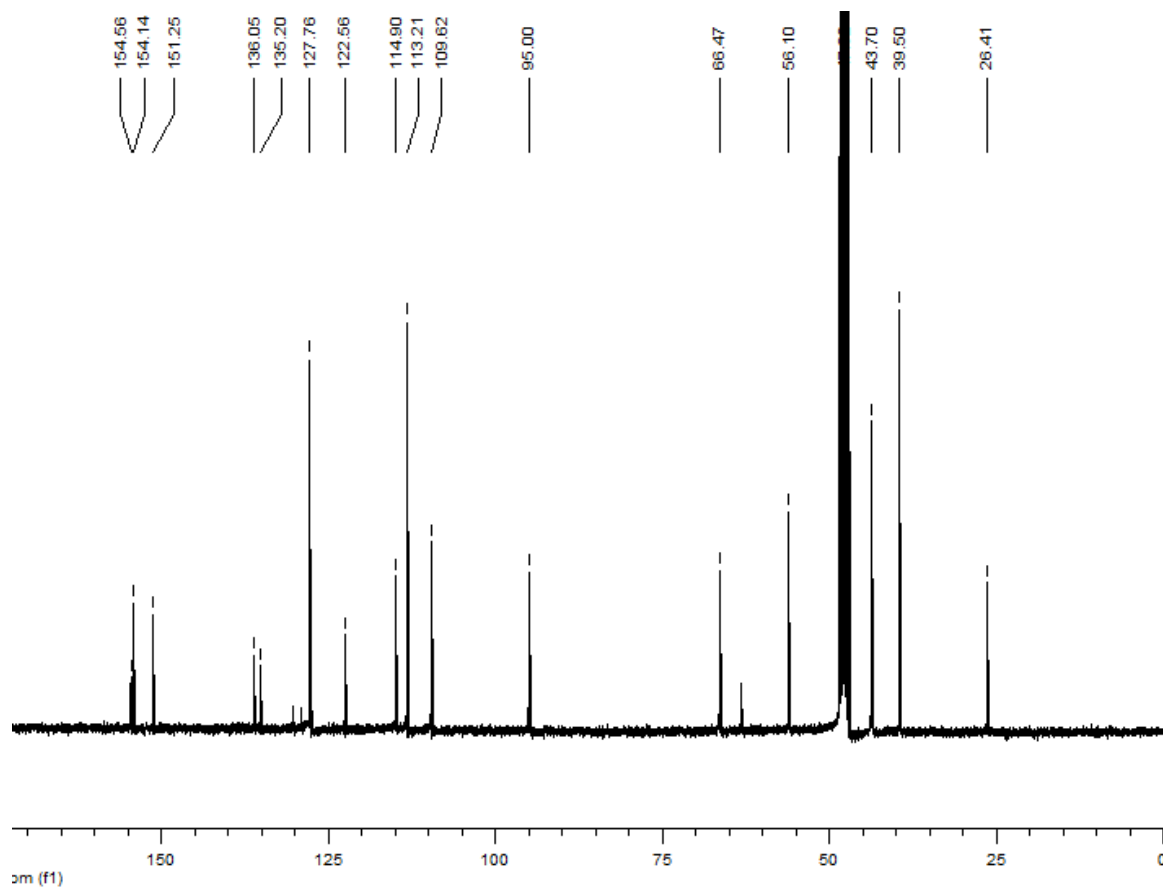
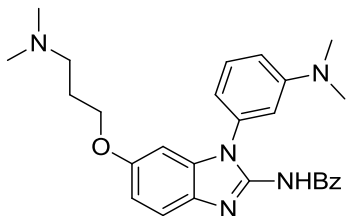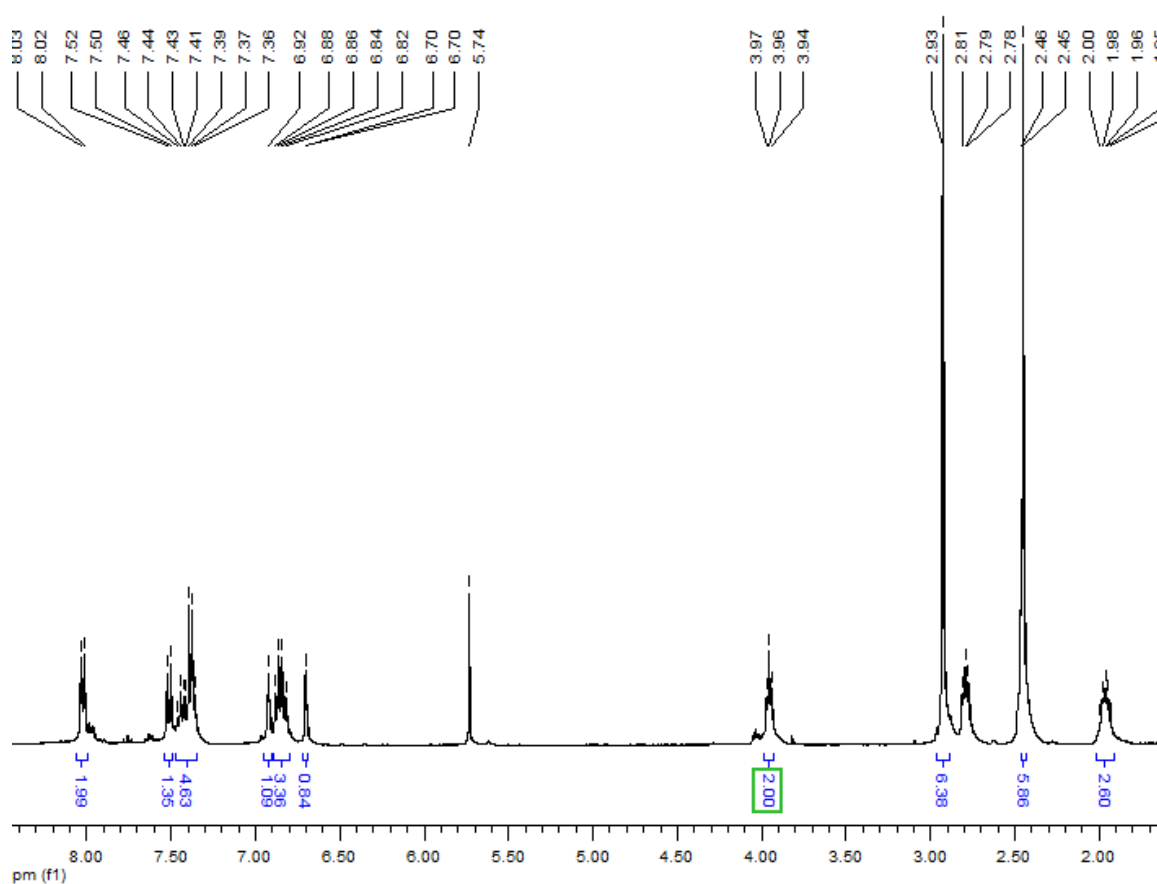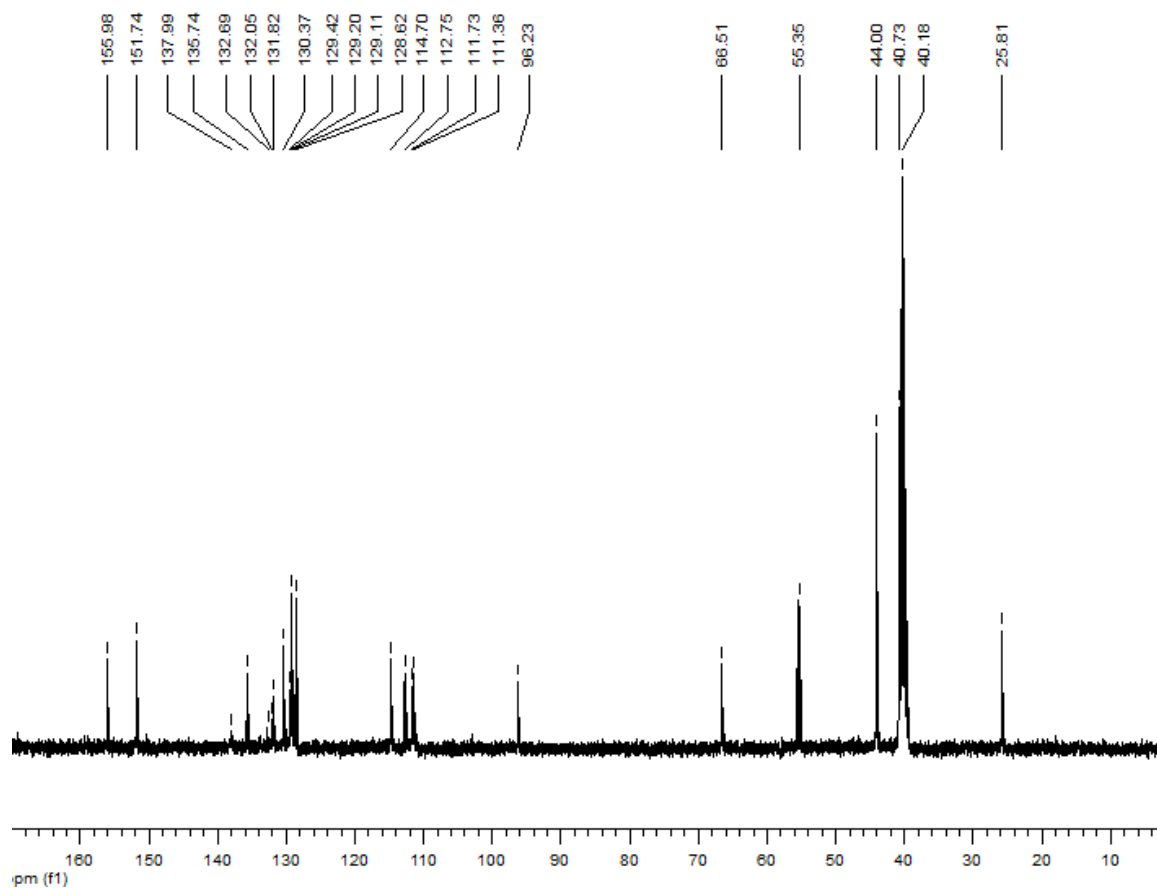**1-(3-dimethylamino)phenyl)-6-(3-(dimethylamino)propoxy)-1*H*-benzo[*d*]imidazol-2-amine (3g)**
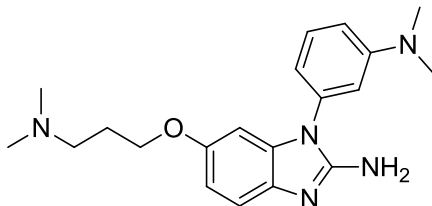
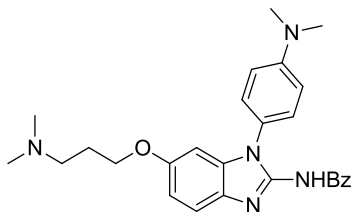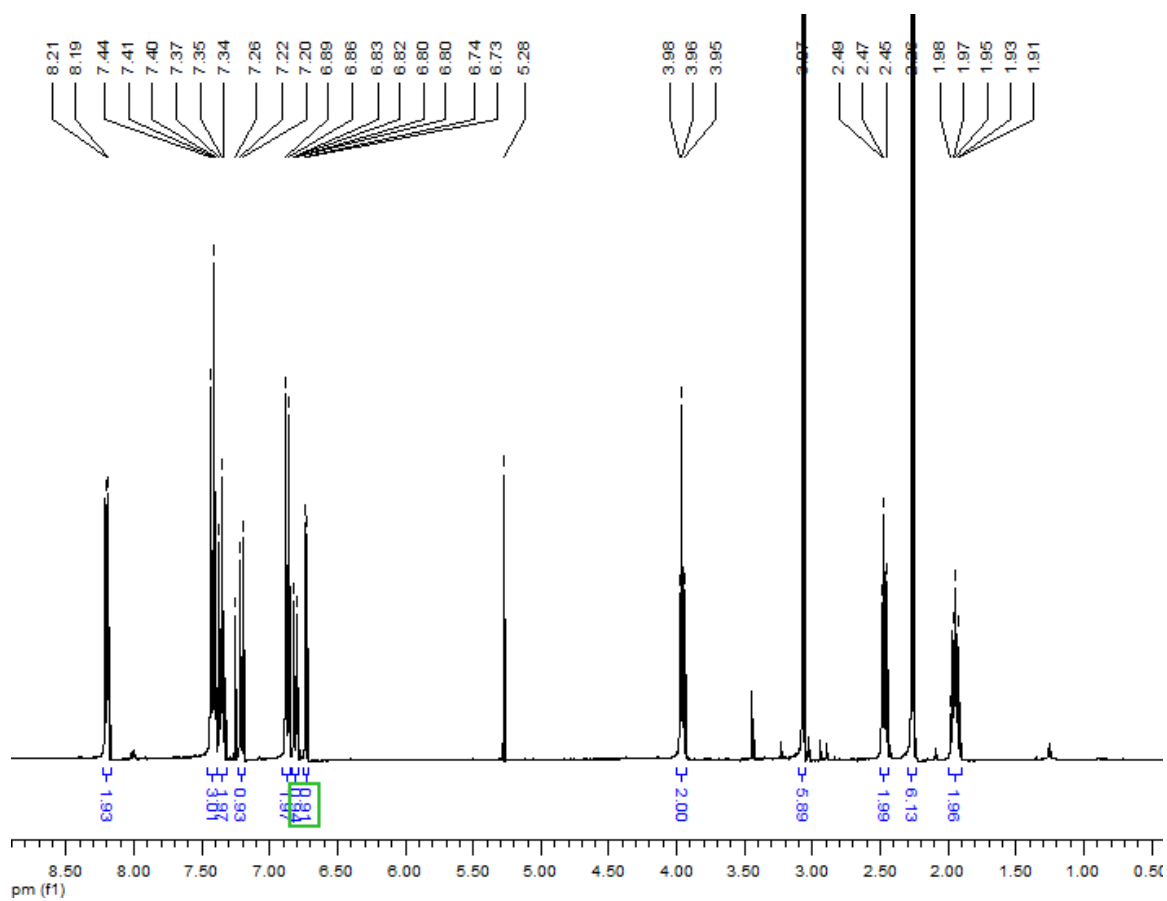To a 100 ml round bottom flask was added *N*-(1-(3-(dimethylamino)phenyl)-6-(3-(dimethylamino)propoxy)-1*H*-benzo[*d*]imidazol-2-yl)benzamide (**4gb**) (432 mg, 0.94 mmol) and 1N HCl aq (50 ml). The reaction was stirred and heated to reflux for 21 hr before it was cooled to RT. It was then extracted with saturated $NaHCO_3$ aq (100 ml) and $CHCl_3$-EtOH (2 : 1, 2 x 100 ml). The organic layers were collected and combined. It was dried over Na_2SO_4. After filtration and concentration, the crude was purified via flash column chromatography (DCM – MeOH : 80 % - 20 %) to yield yellow oil as the product (90.7 mg, 27 % yield). ^{1}H NMR (400 MHz, DMSO-d6): δ 7.39 (t, *J* = 9 Hz, 1H), 7.07 (d, *J* = 9 Hz, 1H), 6.82 (dd, J_1 = 9 Hz, J_2 = 2 Hz, 1H), 6.66 (t, *J* = 2 Hz, 2H), 6.59 (dd, J_1 = 9 Hz, J_2 = 2 Hz, 1H), 6.43 (d, *J* = 2 Hz, 1H), 5.98 (s, 2H), 3.86 (t, *J* = 6 Hz, 2H), 2.94 (s, 6H), 2.34 (t, *J* = 7 Hz, 2H), 2.11 (s, 6H), 1.80 (p, *J* = 7 Hz, 2H). ^{13}C NMR (400 MHz, DMSO-d6): δ 154.27, 153.46, 152.19, 137.57, 135.44, 135.99, 131.01, 115.86, 114.00, 112.48, 110.41, 109.46, 95.26, 67.05, 63.47, 56.34, 55.60, 45.69, 27.56.. MS (ESI) calculated exact mass for $C_{20}H_{27}N_5O$ = 353.22. Found $[M+H]^+$ = 353.46.

Spectrum 3-56: 1-(3-dimethylamino)phenyl)-6-(3-(dimethylamino)propoxy)-1*H*-benzo[*d*]imidazol-2-amine (**3g**) ^{1}H NMR (400 MHz, DMSO-d6)
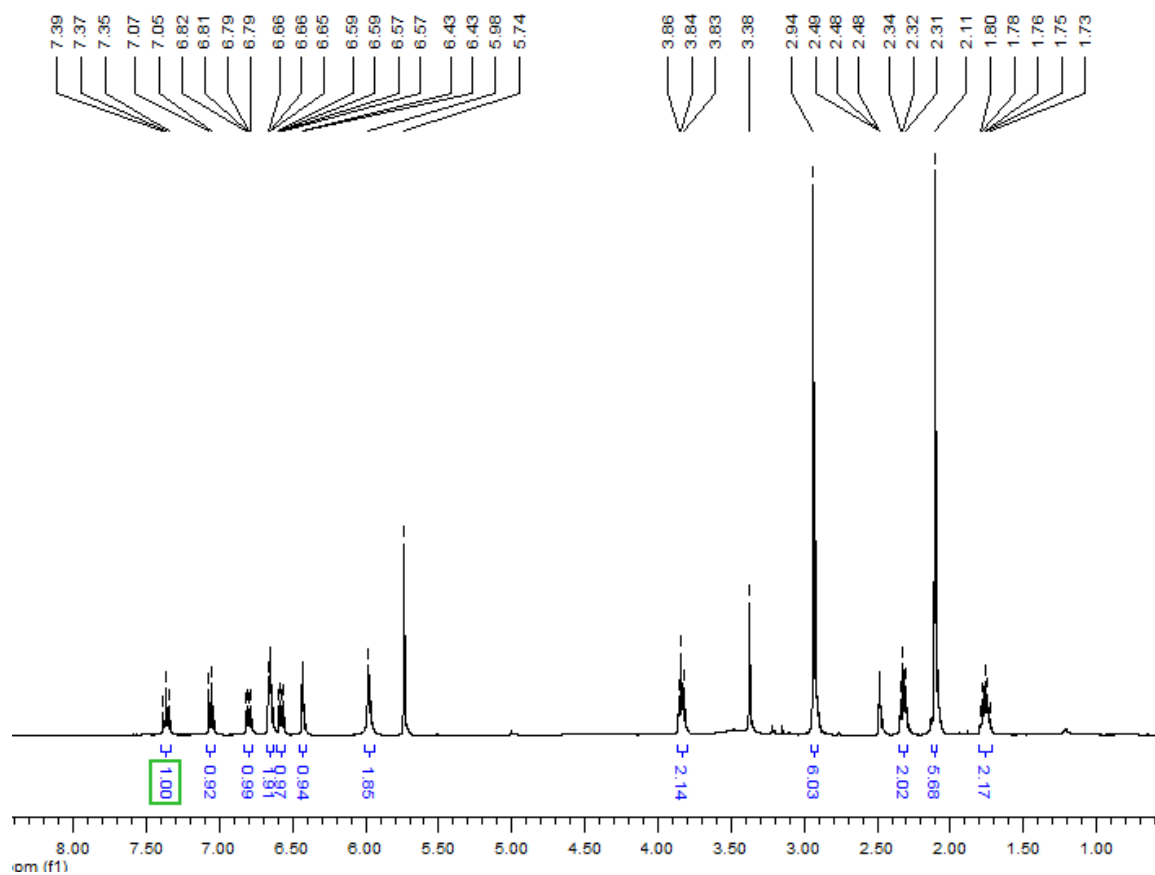
Spectrum 3-57: 1-(3-dimethylamino)phenyl)-6-(3-(dimethylamino)propoxy)-1*H*-benzo[*d*]imidazol-2-amine (**3g**) ^{13}C NMR (400 MHz, DMSO-d6)
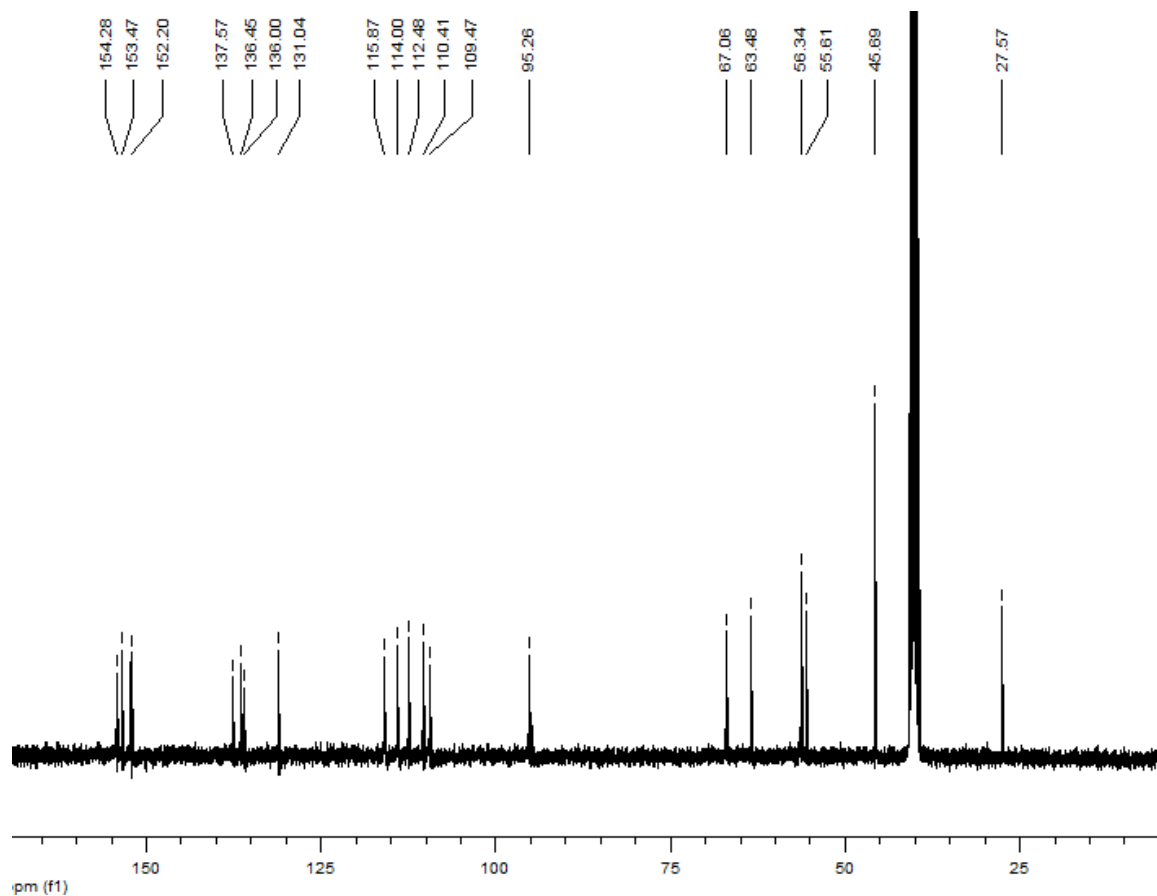
5-(2-(dimethylamino)ethoxy)-1-phenyl-1*H*-benzo[*d*]imidazol-2-ol (5b)
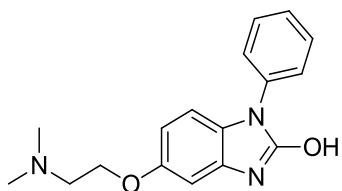
To a 25 ml round bottom flask was added 4-(2-(dimethylamino)ethoxy)-2-nitro-*N*-phenylaniline (**11b**) (56 mg, 0.2 mmol) and MeOH (15 ml). The flask was flushed with Ar gas before Pd/C (5 mg, 10 wt %) was added. The reaction was then sealed under Ar and stirred at RT for 26 hr before it was filtered and concentrated. The oil residue obtained was dissolved in DCM (20 ml). While stirred, phosgene (20 % in toluene, 102 μl, 0. 2mmol) was added via syringe dropwise, followed by pyridine (31 μl, 0.4 mmol). The reaction was stirred at RT for 3 hr before poured into 20 ml of water and extracted. The DCM layer was collected and the water layer was extracted with additional 20 ml of DCM. The combined organic layer was washed with brine and dried over Na_2SO_4. After filtration and evaporation of solvent, the crude was purified via flash column chromatography (DCM – MeOH : 60 % - 40 %) to yield oil as the product (32 mg, 50 % yield). ^{1}H NMR (400 MHz, CD$_3$OD): δ 7.57 (t, *J* = 7 Hz, 2H), 7.50 (d, *J* = 7 Hz, 2H), 7.44 (t, *J* = 7 Hz, 1H), 6.92 (d, *J* = 8 Hz, 1H), 6.78 (d, *J* = 2 Hz, 1H), 6.69 (dd, J_1 = 8 Hz, J_2 = 2 Hz, 1H), 4.10 (t, *J* = 5 Hz, 2H), 2.79 (t, *J* = 5 Hz, 2H), 2.35 (s, 6H). ^{13}C NMR (400 MHz, CD$_3$OD): δ 155.44, 154.89, 134.81, 129.43, 129.28, 127.62, 126.00, 124.86, 109.11, 107.94, 96.92, 66.08, 57.96, 44.62. MS (ESI) calculated exact mass for $C_{17}H_{19}N_3O_2$ = 297.15. Found $[M+H]^+$ = 298.04.

Spectrum 3-58: 5-(2-(dimethylamino)ethoxy)-1-phenyl-1*H*-benzo[*d*]imidazol-2-ol (**5b**) ^{1}H NMR (400 MHz, CD$_3$OD)
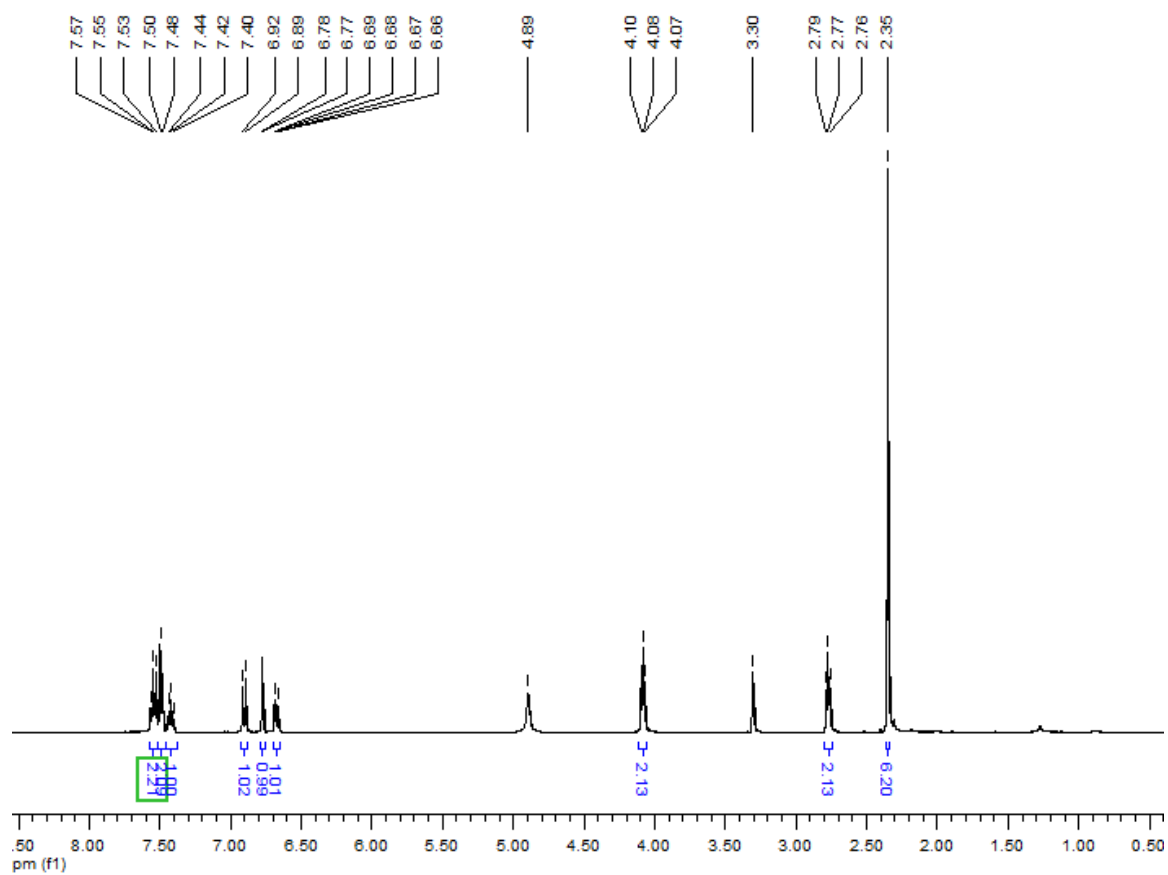
Spectrum 3-59: 5-(2-(dimethylamino)ethoxy)-1-phenyl-1*H*-benzo[*d*]imidazol-2-ol (**5b**)
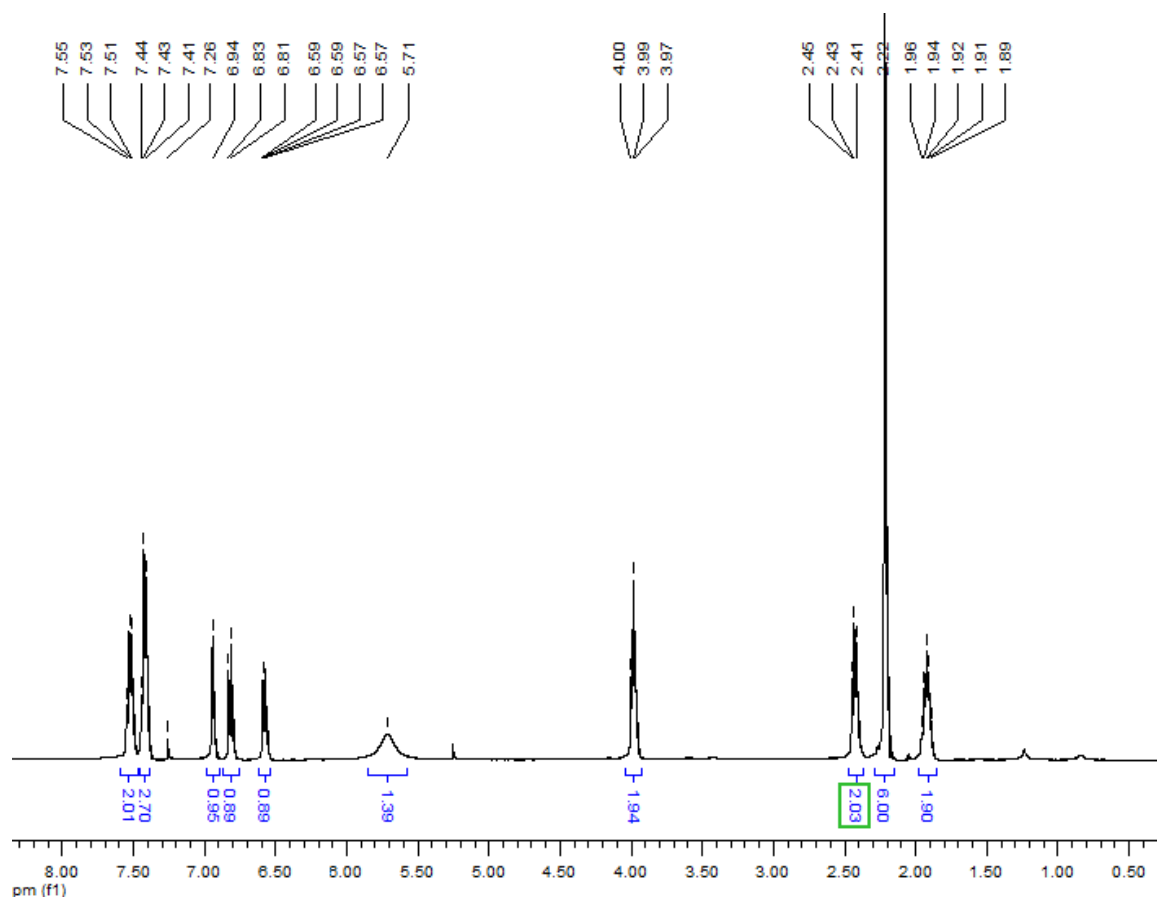^{13}C NMR (400 MHz, CD$_3$OD)
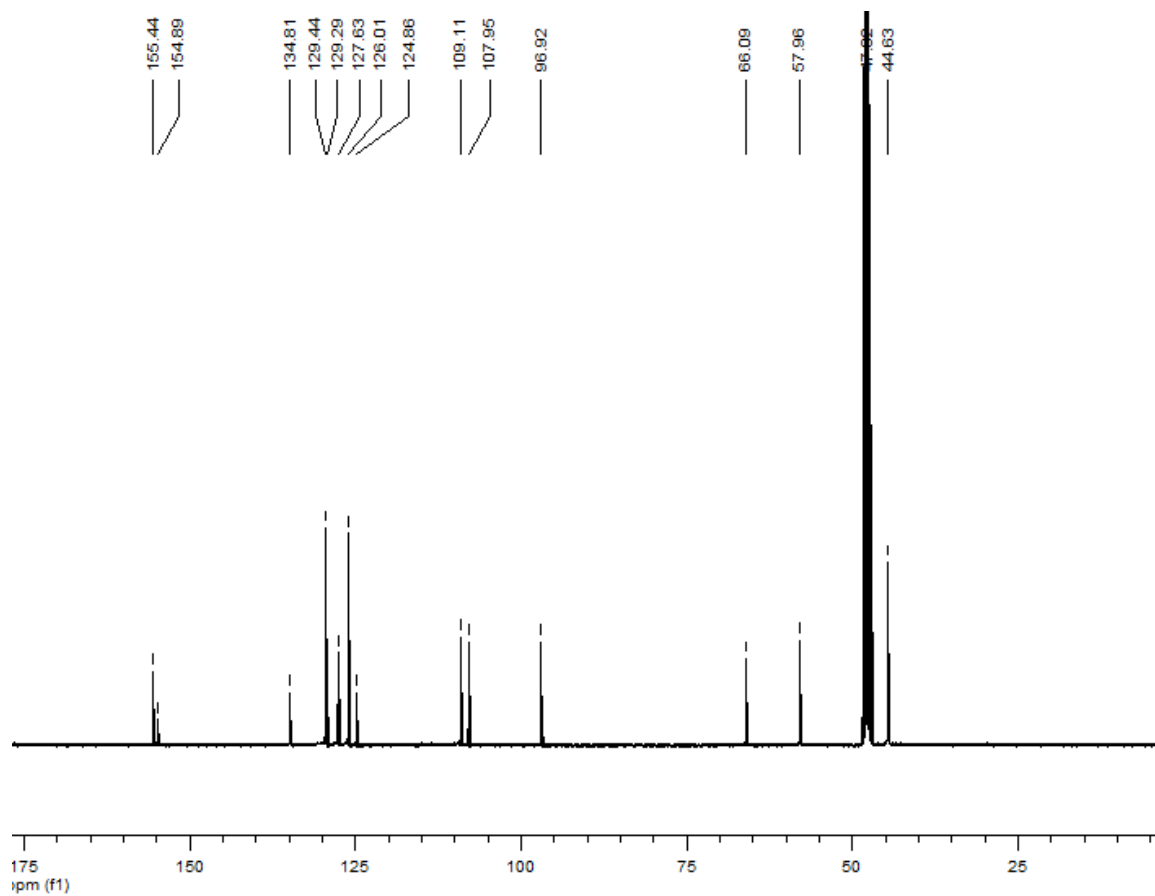
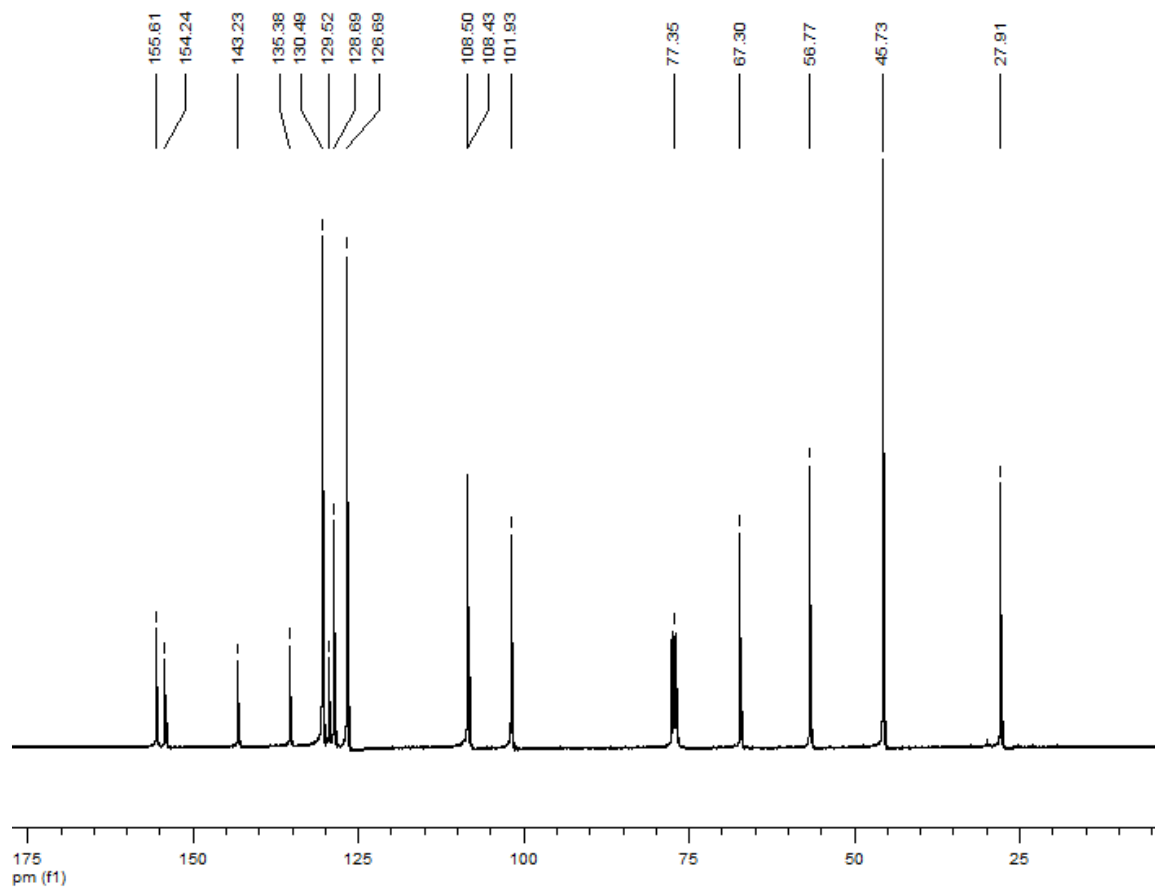**5-(3-(dimethylamino)propoxy)-1-phenyl-1*H*-benzo[*d*]imidazol-2-ol (5c)**
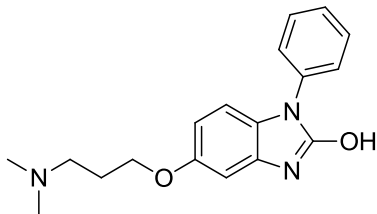
To a 100 ml round-bottom flask was added 4-(3-dimethylamino)propoxy)-2-nitro-*N*-phenylaniline (**11c**) (123 mg, 0.4 mmol) and Methanol (30 ml). The flask was flushed with Ar gas before Pd/C (10 mg, 10 wt %) was added. The reaction was then sealed under H_2 atm and stirred at RT for 1.5 hours before filtration and concentration. The oil residue was dissolved in DCM. Pyridine (63 µl, 0.8 mmol) and phosgene (214 µl, 0.4 mmol, 20 wt % solution in toluene) were added. The reaction was stirred at RT for 24 hours before it was concentrated. The crude was purified via flash column (DCM – MeOH : 80 % - 20 %) to yield clear oil as the product (79 mg, 64 % yield two steps). ^{1}H NMR (400 MHz, CD_3OD): δ 7.58 (t, J = 8 Hz, 2H), 7.50 (d, J = 9 Hz, 2H), 7.45 (t, J = 7 Hz, 1H), 6.92 (d, J = 6 Hz, 1H), 6.79 (d, J = 2 Hz, 1H), 6.70 (dd, J1 = 9 Hz, J2 = 2 Hz, 1H), 4.11 (t, J = 6 Hz, 2H), 3.37 (t, J = 8 Hz, 2H), 2.93 (s, 6H), 2.25 (p, J = 6 Hz, 2H). ^{13}C NMR (400 MHz, CD_3OD): δ 155.14, 154.85, 134.76, 129.47, 129.26, 127.70, 126.02, 125.04, 109.11, 107.99, 96.90, 65.53, 55.67, 47.82, 24.67. MS (ESI) calculated exact mass for $C_{18}H_{21}N_3O_2$ = 311.16. Found $[M+H]^+$ = 312.03.

Spectrum 3-60: 5-(3-(dimethylamino)propoxy)-1-phenyl-1*H*-benzo[*d*]imidazol-2-ol (**5c**)
^{1}H NMR (400 MHz, CD$_3$OD)
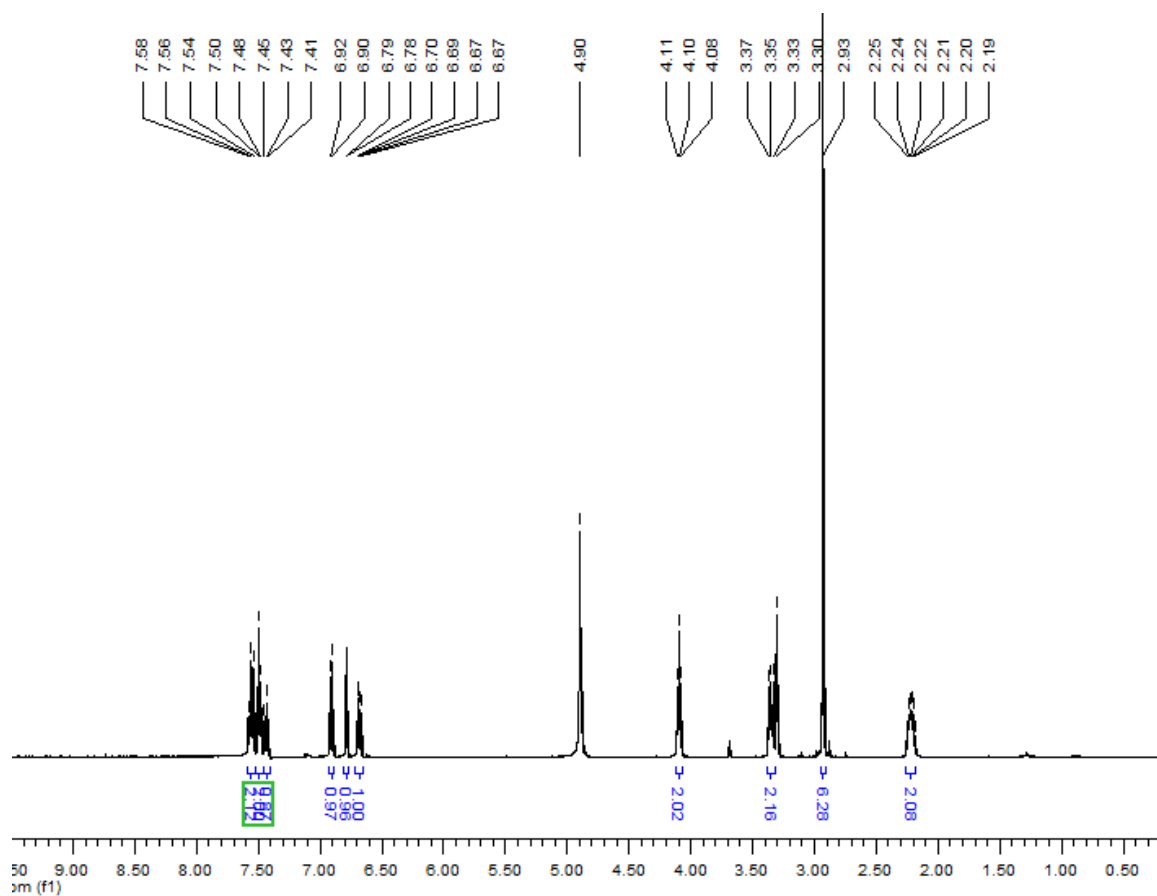
**Spectrum 3-61:** 5-(3-(dimethylamino)propoxy)-1-phenyl-1*H*-benzo[*d*]imidazol-2-ol (**5c**)
^{13}C NMR (400 MHz, CD$_3$OD)

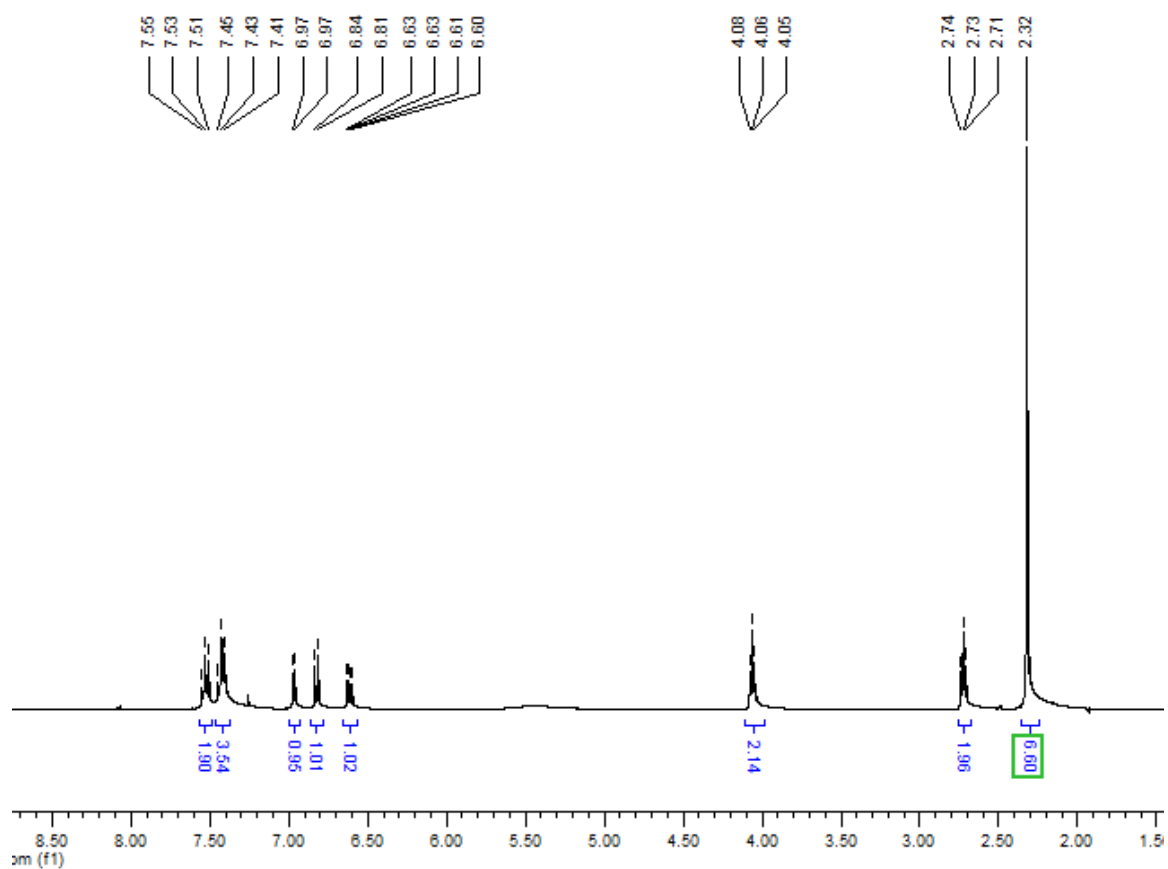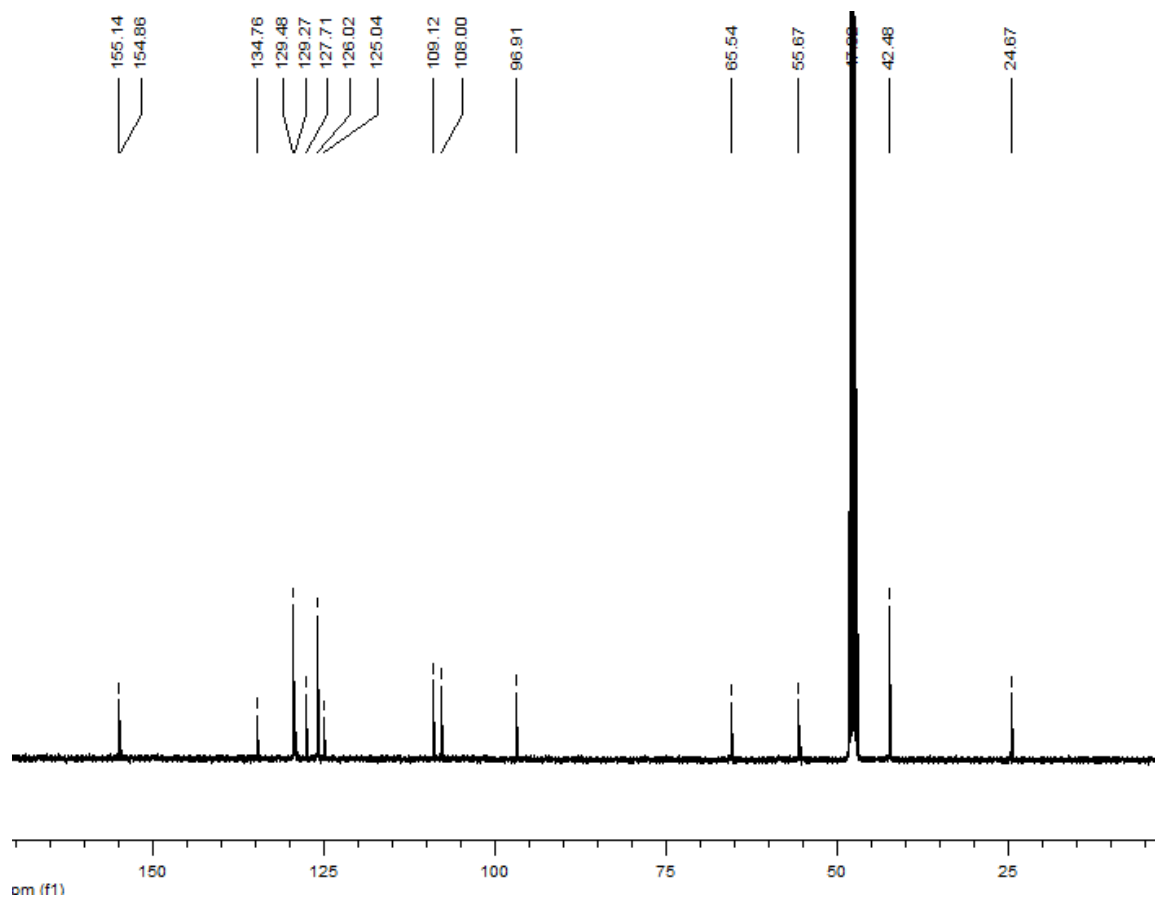**1-(4-(dimethylamino)phenyl)-6-(3-(dimethylamino)propoxy)-1*H*-benzo[*d*]imidazol-2-ol (5f)**
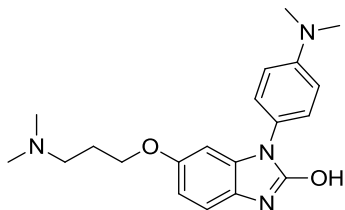
To a 50 ml rb flask was added N^1-(5-(3-(dimethylamino)propoxy)-2-nitrophenyl)-N^4,N^4-dimethylbenzene-1,4-diamine (**11f**) (63 mg, 0.17 mmol) and 20 ml of MeOH. The flask was flushed with Ar gas before Pd/C (6 mg, 10 wt %) was added. The reaction was then sealed under H_2 atm and stirred at RT for 1 hour before filtration and concentration. The oil residue was then dissolved in DCM (20 ml). Phosgene (96.4 µl, 20 % in toluene, 0.17 mmol) was added followed by pyridine (28 µl, 0.25 mmol). The reaction was stirred at RT for 5 minutes. The reaction was poured into water and extracted. The organic layer was collected and washed with brine and then dried over Na_2SO_4. After filtration and removal of solvent, the crude was purified via flash column chromatography (DCM – MeOH : 80 % - 20 %) to yield clear oil as the product (26 mg, 43 % yield). ^{1}H NMR (400 MHz, CDCl$_3$): δ10.00 (s, 1H), 7.33 (d, J = 9 Hz, 2H), 6.98 (d, J = 9 Hz, 1H), 6.84 (d, J = 9 Hz, 2H), 6.62 (dd, J1 = 9 Hz, J2 = 2 Hz, 1H), 6.53 (d, J = 2 Hz, 1H), 3.94 (t, J = 6 Hz, 2H), 3.01 (s, 6H), 2.51 (t, J = 7 Hz, 2H), 2.29 (s, 6H), 1.98 (m, 2H). ^{13}C NMR (400 MHz, CDCl$_3$): δ 156.06, 154.87, 150.45, 132.57, 127.68, 122.96, 122.14, 113.25, 110.15, 108.37, 96.54, 67.05, 56.58, 45.45, 40.85, 27.52. MS (ESI) calculated exact mass for $C_{27}H_{31}N_5O_2$ = 354.21. Found $[M+H]^+$ = 355.12.

Spectrum 3-62: 1-(4-(dimethylamino)phenyl)-6-(3-(dimethylamino)propoxy)-1*H*-benzo[*d*]imidazol-2-ol (**5f**) ^{1}H NMR (400 MHz, CDCl$_3$)
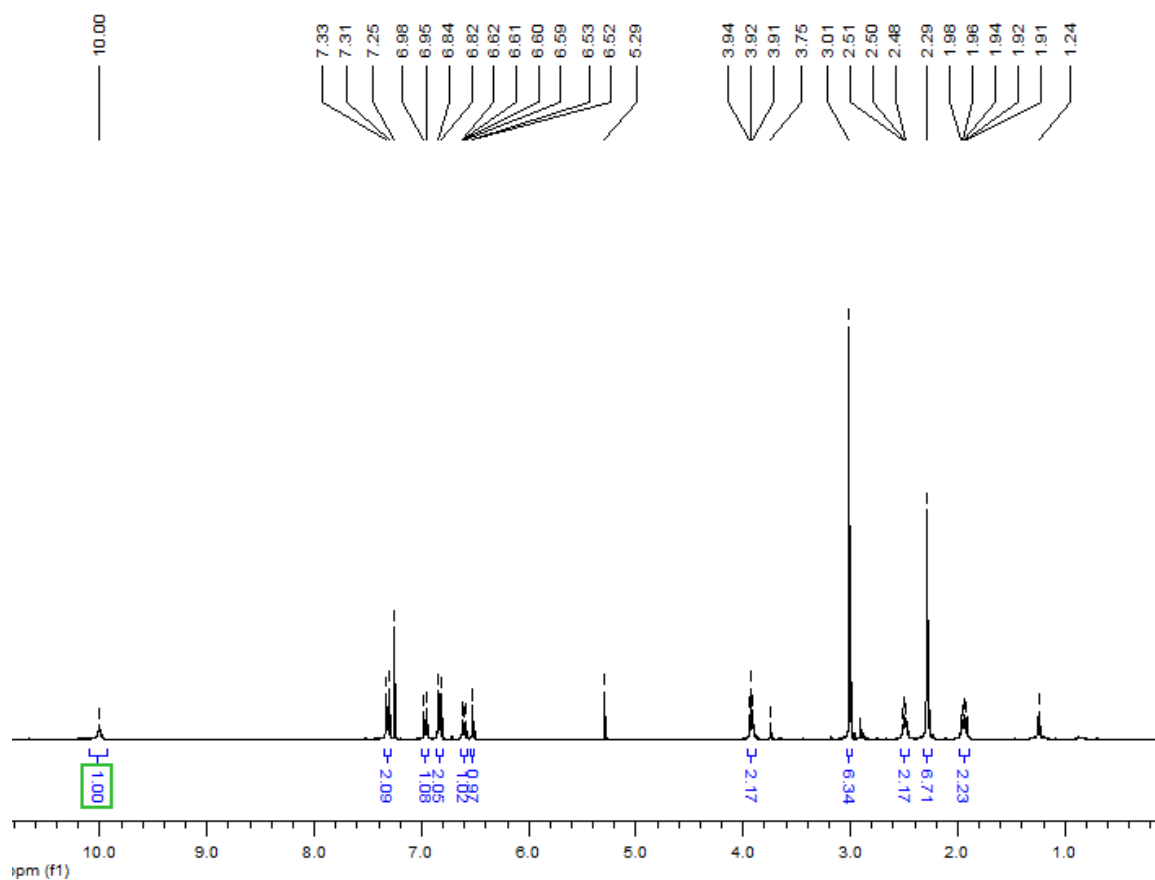
Spectrum 3-63: 1-(4-(dimethylamino)phenyl)-6-(3-(dimethylamino)propoxy)-1*H*-benzo[*d*]imidazol-2-ol (**5f**) ^{13}C NMR (400 MHz, CDCl$_3$)
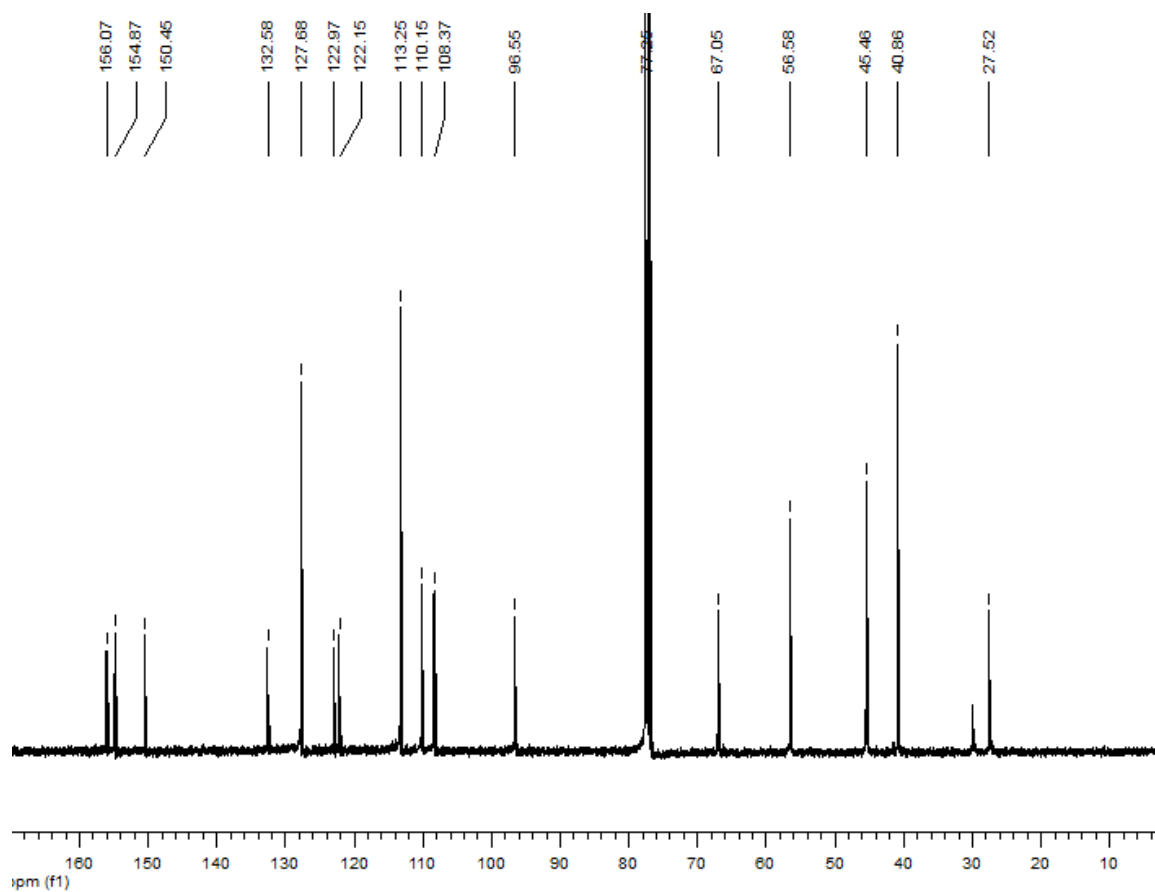
N^1-(5-chloro-2-nitrophenyl)-N^3,N^3-dimethylbenzene-1,3-diamine (15)
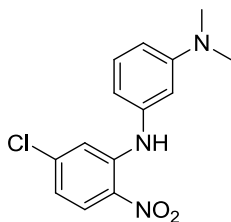
To a 250 ml round-bottom flask was added *N,N*-dimethyl-3-nitroaniline (**14**) (1.2 g, 7.2 mmol) and methanol (100 ml). The flask was flushed with Ar gas before Pd/C (120 mg, 10 wt %) was added. The reaction was then stirred at RT for 20 hours. After filtration and concentration, an oil residue was obtained. Toluene (100 ml) was added followed by 2,4-dichloronitrobenzene (1.4 g, 7.2 mmol), $Pd_2(dba)_3$ (330 mg, 0.36 mmol, 5 mol %), *rac*-BINAP (337 mg, 0.54 mmol, 7.5 mol %), and Cs_2CO_3 (2.3 g, 7.2 mmol). The reaction was stirred and heated to reflux under Ar for 21 hours before it was cooled to RT. It was filtered and extracted with water (twice, 150 ml ea.) The organic layer was collected and washed with brine and dried over Na_2SO_4. After filtration and concentration, the crude was purified via flash column (Hexane : EtOAc – 80 % - 20 %) to yield red oil as the product (900 mg, 43 % two steps). ^{1}H NMR (400 MHz, DMSO-d6) δ: 9.43 (s, 1H), 8.12 (d, *J* = 9 Hz, 1H), 7.24 (t, *J* = 8 Hz, 1H), 7.03 (d, *J* = 2 Hz, 1H), 6.83 (dd, J_1 = 9 Hz, J_2 = 2 Hz, 1H), 6.65-6.58 (m, 3H), 2.89 (s, 6H). ^{13}C NMR (400 MHz, DMSO-d6) δ: 152.28, 144.36, 141.37, 139.58, 132.09, 130.62, 128.97, 117.88, 116.06, 112.66, 110.72, 109.28, 40.67. MS (ESI) calculated exact mass for $C_{14}H_{14}ClN_3O_2$ = 291.08. Found [M+H]$^+$ = 292.0.

Spectrum 3-65: N^1-(5-chloro-2-nitrophenyl)-N^3,N^3-dimethylbenzene-1,3-diamine (**15**) ^{1}H NMR (400 MHz, DMSO-d6)
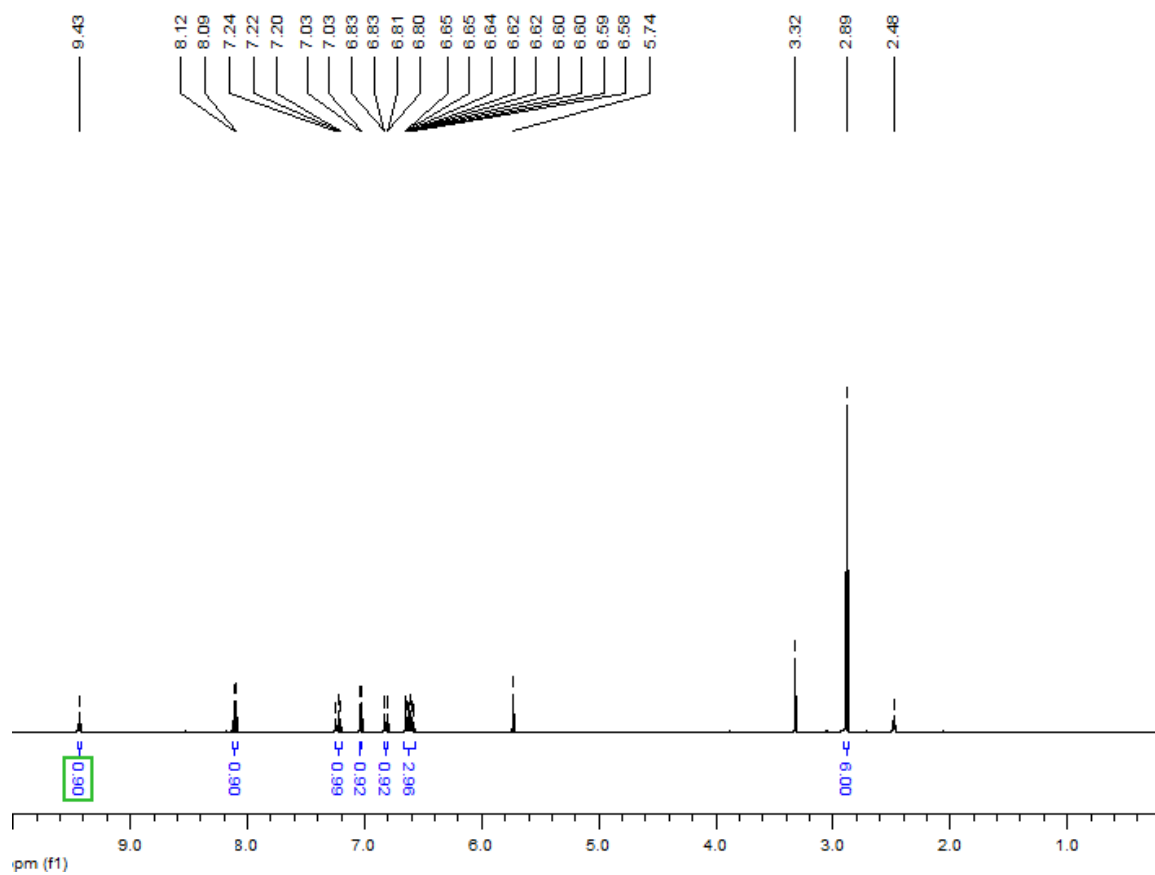
Spectrum 3-66: N^1-(5-chloro-2-nitrophenyl)-N^3,N^3-dimethylbenzene-1,3-diamine (**15**) ^{13}C NMR (400 MHz, DMSO-d6)
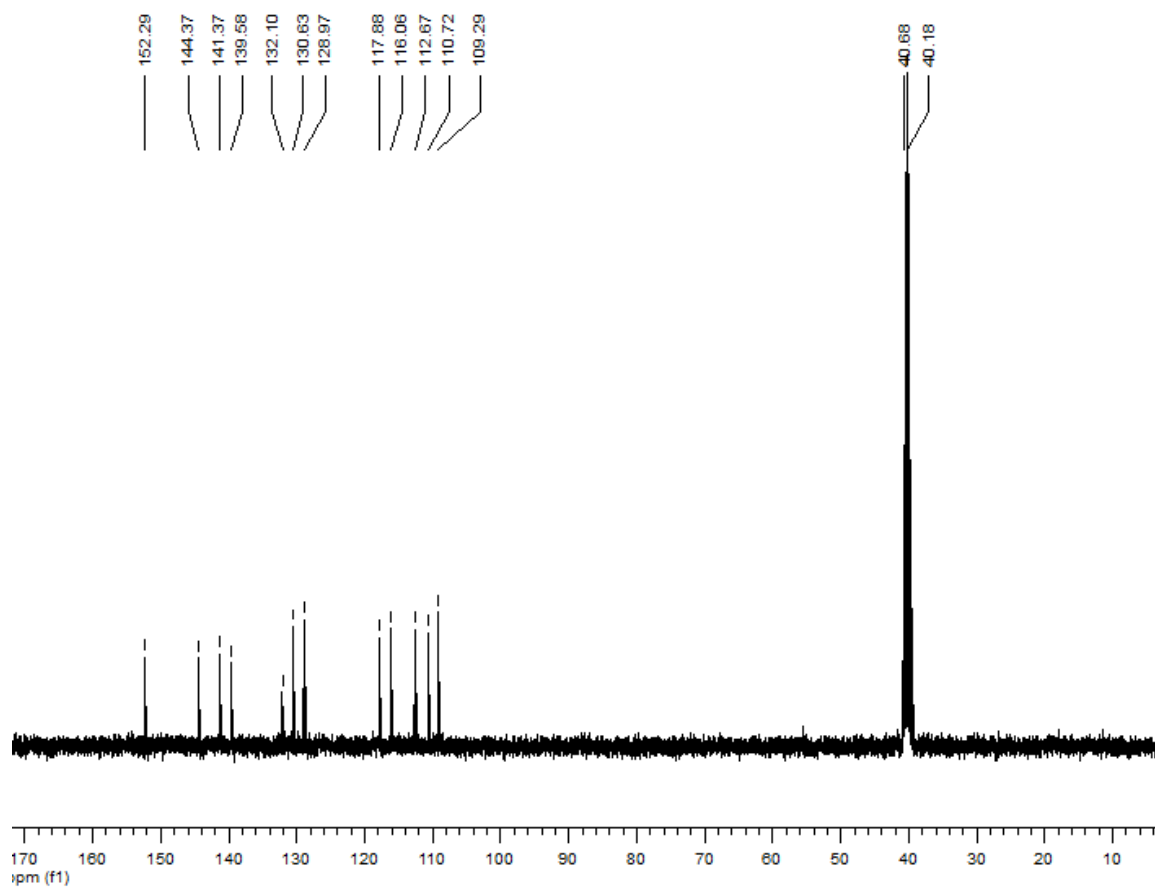
N^1,N^1-dimethyl-N^3-(2-nitro-5-(pyridin-3-ylamino)phenyl)benzene-1,3-diamine (17h)
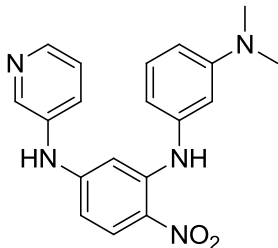
To a 250 ml round-bottom flask was added N^1-(5-chloro-2-nitrophenyl)-N^3,N^3-dimethylbenzene-1,3-diamine (**15**) (1.47 g, 5.04 mmol), dioxane (100 ml), 3-aminopyridine (569 mg, 6.05 mmol, 1.2 eq), $Pd_2(dba)_3$ (229 mg, 0.25 mmol, 5 mol %), *rac*-BINAP (235 mg, 0.38 mmol, 7.5 mol %), and Cs_2CO_3 (1.59 g, 5.04 mmol). The reaction was stirred and heated to reflux under Ar for 21 hours before it was cooled to RT. It was filtered and concentrated. The oil residue was extracted with chloroform and water (150 ml ea). The organic layer was collected and washed with additional water (150ml), brine and was dried over Na_2SO_4. After filtration and concentration, the oil crude was purified via flash column chromatography (DCM – MeOH : 90 % – 10 %) to yield red oil as the product (757 mg, 43 % yield). ^{1}H NMR (400 MHz, CDCl$_3$) δ: 9.79 (s, 1H), 8.38 (d, *J* = 2 hz, 1H), 8.28 (d, *J* = 6 Hz, 1H), 8.12 (d, *J* = 9 Hz, 1H), 7.48 (d, *J* = 8 Hz, 1H), 7.22 (t, *J* = 5 Hz, 2H), 6.85 (s, 1H), 6.64 – 6.53 (m, 4H), 6.32 (dd, J_1 = 9 Hz, J_2 = 2 Hz, 1H), 2.92 (s, 6H). MS (ESI) calculated exact mass for $C_{19}H_{19}N_5O_2$ = 349.15. Found $[M+H]^+$ = 350.3.

Spectrum 3-67: N^1,N^1-dimethyl-N^3-(2-nitro-5-(pyridin-3-ylamino)phenyl)benzene-1,3-diamine (**17h**) ^{1}H NMR (400 MHz, CDCl$_3$)

N^1,N^1-dimethyl-N^3-(2-nitro-5-(pyridin-4-ylamino)phenyl)benzene-1,3-diamine (17i)

To a 250 ml round-bottom flask was added N^1-(5-chloro-2-nitrophenyl)-N^3,N^3-dimethylbenzene-1,3-diamine (**15**) (944 mg, 3.24 mmol), dioxane (100 ml), 4-aminopyridine (335 mg, 3.56 mmol, 1.1 eq), Pd$_2$(dba)$_3$ (148 mg, 0.16 mmol, 5 mol %), *rac*-BINAP (151 mg, 0.24 mmol, 7.5 mol %), and Cs$_2$CO$_3$ (1.02 g, 3.24 mmol). The reaction was stirred and heated to reflux under Ar for 44 hours before it was cooled to RT. It was then filtered and concentrated. The oil residue was extracted with chloroform and water (150 ml ea). The organic layer was collected and washed with water (150ml), brine and was dried over Na$_2$SO$_4$. After filtration and concentration, the crude was purified via flash column chromatography (DCM – MeOH : 95 % – 5 %) to yield red oil as the product (390 mg, 34 % yield). ^{1}H NMR (400 MHz, DMSO-d6) δ: 9.59 (s, 1H), 9.51 (s, 1H), 8.29 (d, *J* = 4 Hz, 2H), 8.09 (d, *J* = 9 Hz, 1H), 7.26 (t, *J* = 8 Hz, 1H), 7.02 (d, *J* = 6 Hz, 2H), 6.78 (d, *J* = 2Hz, 1H), 6.67 – 6.56 (m, 4H), 2.89 (s, 6H). ^{13}C NMR (400 MHz, DMSO-d6) δ: 152.24, 150.82, 148.98, 148.28, 145.75, 139.90, 130.45, 129.21, 126.87, 113.11, 112.82, 110.34, 109.23, 108.91, 100.68, 40.70. MS (ESI) calculated exact mass for C$_{19}$H$_{19}$N$_5$O$_2$ = 349.15. Found [M+H]$^+$ = 350.3.

Spectrum 3-68: N^1,N^1-dimethyl-N^3-(2-nitro-5-(pyridin-4-ylamino)phenyl)benzene-1,3-diamine (**17i**) ^{1}H NMR (400 MHz, DMSO-d6)
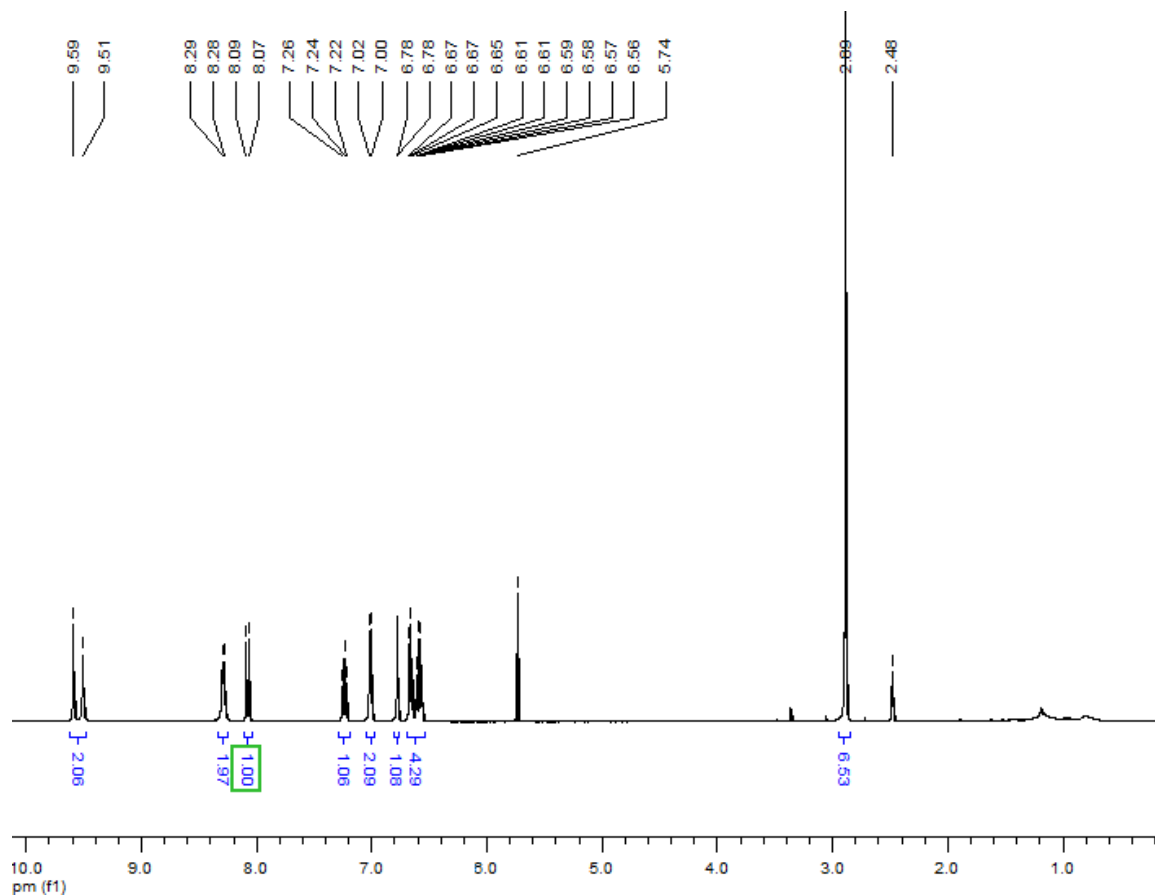
Spectrum 3-69: N^1,N^1-dimethyl-N^3-(2-nitro-5-(pyridin-4-ylamino)phenyl)benzene-1,3-diamine (**17i**) ^{13}C NMR (400 MHz, DMSO-d6)
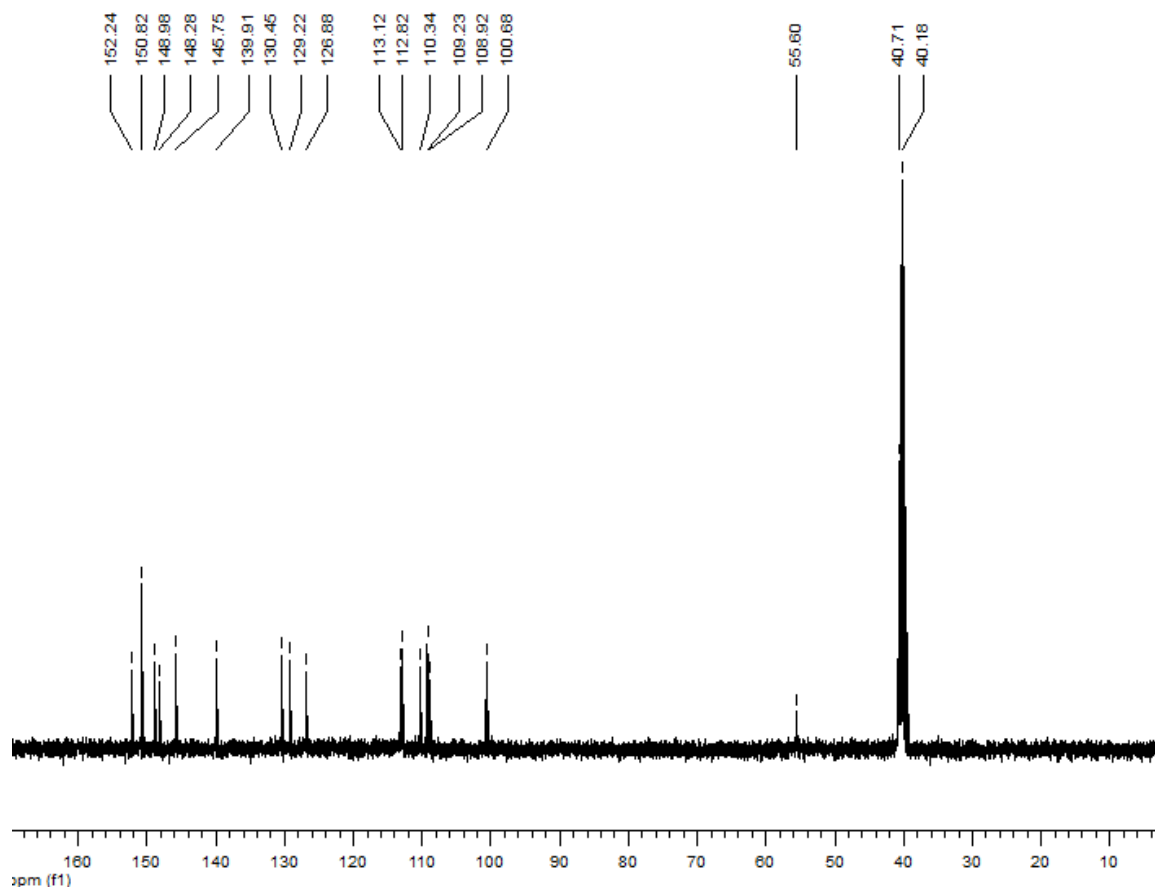
_N_-(1-(3-isopropylphenyl)-6-(pyridin-3-ylamino)-1_H_-benzo[_d_]imidazol-2-yl)benzamide (18h)
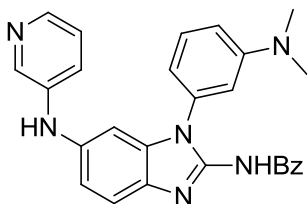
To a 250 ml round bottom flask was added N^1,N^1-dimethyl-N^3-(2-nitro-5-(pyridin-3-ylamino)phenyl)benzene-1,3-diamine (**17h**) (757 mg, 2.17 mmol) and methanol (100 ml). The flask was flushed with Ar gas before Pd/C (75 mg, 10 wt%) was added. The reaction was stirred at RT under H_2 atm for 23 hours before it was filtered and concentrated. The oil residue was dissolved in ACN (200 ml). Benzoyl isothiocyanate (322 µl, 2.17 mmol) was added via syringe. The reaction was stirred at RT for 9 hours when DIPC (338 µl, 2.17 mmol) and K_2CO_3 (300 mg, 2.17 mmol) were added. The reaction was stirred at RT for 24 hours before it was filtered and concentrated. The crude was purified via flash column chromatography (DCM – MeOH : 90 % - 10 %) to yield yellow oil as the product (312 mg, 32 % yield). ^{1}H NMR (400 MHz, CDCl$_3$) δ: 8.28 (s, 1H), 8.22 (d, _J_ = 7 Hz, 2H), 8.06 (d, _J_ = 4 Hz, 1H), 7.41 – 7.33 (m, 5H), 7.21 (d, _J_ = 8 Hz, 1H), 7.07 (m, 2H), 6.96 (m, 3H), 6.79 (dd, J_1 = 8 Hz, J_2 = 2 Hz, 1H), 6.41 (s, 1H), 2.97 (s, 6H). MS (ESI) calculated exact mass for $C_{28}H_{25}N_5O$ = 448.20. Found [M+H]$^+$ = 449.3.

Spectrum 3-70: *N*-(1-(3-isopropylphenyl)-6-(pyridin-3-ylamino)-1*H*-benzo[*d*]imidazol-2-yl)benzamide (**18h**) ¹H NMR (400 MHz, CDCl₃)
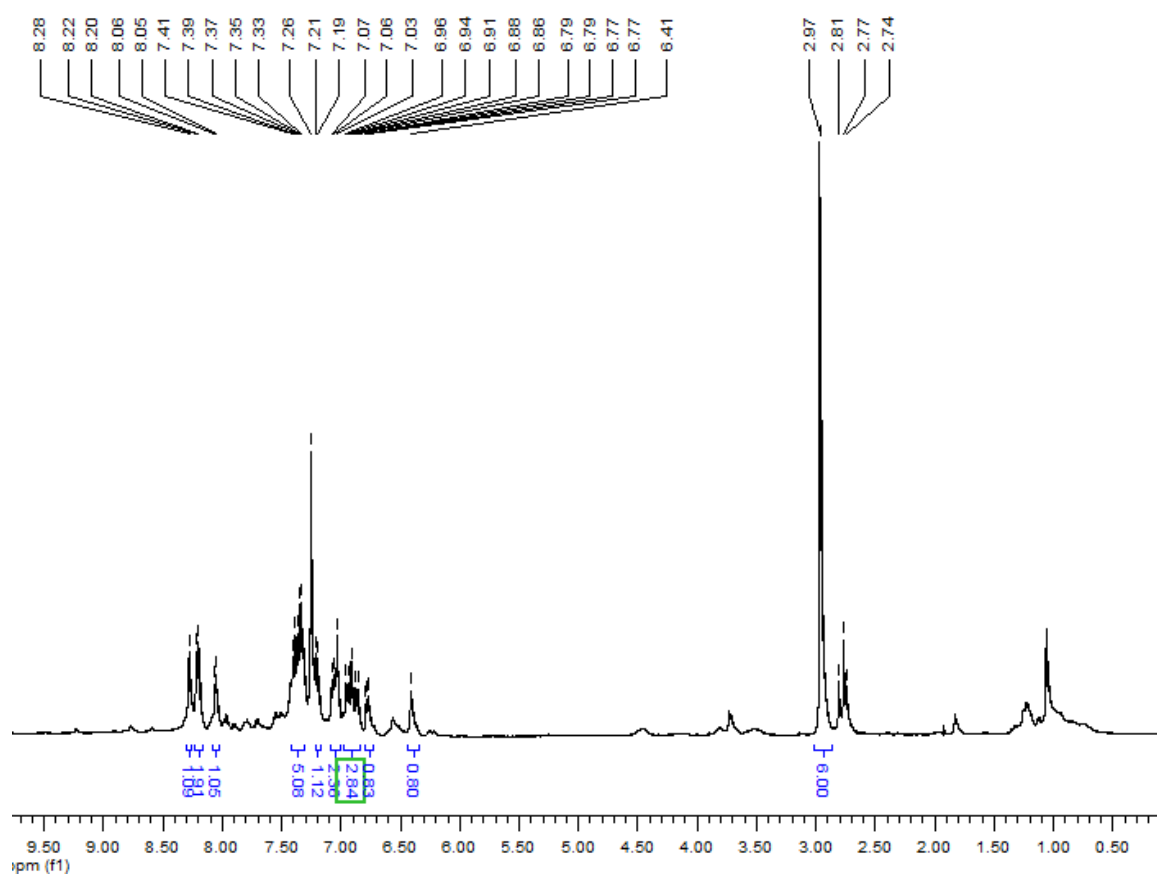
N-(1-(3-(dimethylamino)phenyl)-6-(pyridin-4-ylamino)-1H-benzo[d]imidazol-2-yl)benzamide (18i)
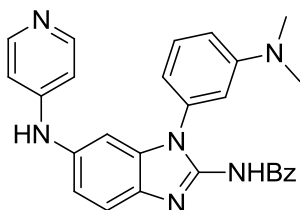
To a 250 ml round bottom flask was added N^1,N^1-dimethyl-N^3-(2-nitro-5-(pyridin-4-ylamino)phenyl)benzene-1,3-diamine (**17i**) (390 mg, 1.12 mmol) and methanol (100 ml). The flask was flushed with Ar gas before Pd/C (40 mg, 10 wt%) was added. The reaction was stirred at RT under H_2 atm for 22 hours before filtration and concentration. The oil residue was dissolved in ACN (200 ml) and benzoyl isothiocyanate (166 µl, 1.12 mmol) was added via syringe. The reaction was stirred at RT for 20 hours when DIPC (174 µl, 1.12 mmol) and K_2CO_3 (155 mg, 1.12 mmol) were added. The reaction was stirred at RT for 24 hours before filtration and concentration. The crude was purified via flash column chromatography (DCM – MeOH : 90 % - 10 %) to yield yellow viscous oil as the product (108 mg, 22 % yield). ^{1}H NMR (400 MHz, CD$_3$OD) δ: 8.07 (d, J = 5 Hz, 2H), 8.01 (d, J = 7 Hz, 2H), 7.62 (d, J = 8 Hz, 1H), 7.48 (t, J = 7 Hz, 1H), 7.37 (m, 3H), 7.21 (d, J = 8 Hz, 1H), 7.12 (s, 1H), 6.95 (d, J = 5 Hz, 2H), 6.89 (s, 1H), 6.86 (m, 2H), 2.94 (s, 6H). MS (ESI) calculated exact mass for C$_{28}$H$_{25}$N$_5$O = 448.20. Found [M+H]$^+$ = 449.3.

Spectrum 3-71: *N*-(1-(3-(dimethylamino)phenyl)-6-(pyridin-4-ylamino)-1*H*-benzo[d]imidazol-2-yl)benzamide (**18i**) ^{1}H NMR (400 MHz, CD$_3$OD)

1-(3-(dimethylamino)phenyl)-*N*⁶-(pyridin-3-yl)-1*H*-benzo[*d*]imidazole-2,6-diamine (3h)
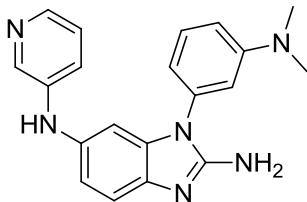
To a 100 ml round bottom flask was added *N*-(1-(3-(dimethylamino)phenyl)-6-(pyridin-3-ylamino)-1*H*-benzo[*d*]imidazol-2-yl)benzamide (**18h**) (312 mg, 0.69 mmol) and 1N HCl aq (50 ml). The reaction was heated to reflux while stirred for 24 hours before cooled to RT. It was extracted with saturated NaHCO$_3$ aq and Chloroform-EtOH 2:1 (100 ml and 3 x 100 ml). The organic layers were collected and combined and dried over Na$_2$SO$_4$. After filtration and concentration, the crude was purified via flash column chromatography (DCM – MeOH : 80 % - 20 %) to yield slight brown/yellow oil as the product (92 mg, 39 % yield). ^{1}H NMR (400 MHz, CD$_3$OD) δ: 8.12 (d, *J* = 2 Hz, 1H), 7.82 (dd, *J*$_1$ = 5 Hz, *J*$_2$ = 1 Hz, 1H), 7.42 (t, *J* = 8 Hz, 1H), 7.33 (m, 1H), 7.25 (d, *J* = 8 Hz, 1H), 7.15 (dd, *J*$_1$ = 8 Hz, *J*$_2$ = 5 Hz, 1H), 6.94 (dd, *J*$_1$ = 8 Hz, *J*$_2$ = 2 Hz, 1H), 6.88 (dd, *J*$_1$ = 8 Hz, *J*$_2$ = 2 Hz, 1H), 6.77 (d, *J* = 2 Hz, 1H), 6.75 (t, *J* = 2Hz, 1H), 6.72 (d, *J* = 8 Hz, 1H), 2.97 (s, 6H). ^{13}C NMR (400 MHz, CD$_3$OD) δ: 154.33, 152.35, 143.56, 138.05, 137.38, 136.38, 135.57, 135.39, 135.04, 130.55, 124.21, 121.11, 115.85, 115.20, 113.66, 112.69, 110.00, 101.69, 39.40. MS (ESI) calculated exact mass for C$_{20}$H$_{20}$N$_6$ = 344.17. Found [M+H]$^+$ = 345.2.

Spectrum 3-72: 1-(3-(dimethylamino)phenyl)-N^6-(pyridin-3-yl)-1H-benzo[d]imidazole-2,6-diamine (**3h**) ^{1}H NMR (400 MHz, CD$_3$OD)
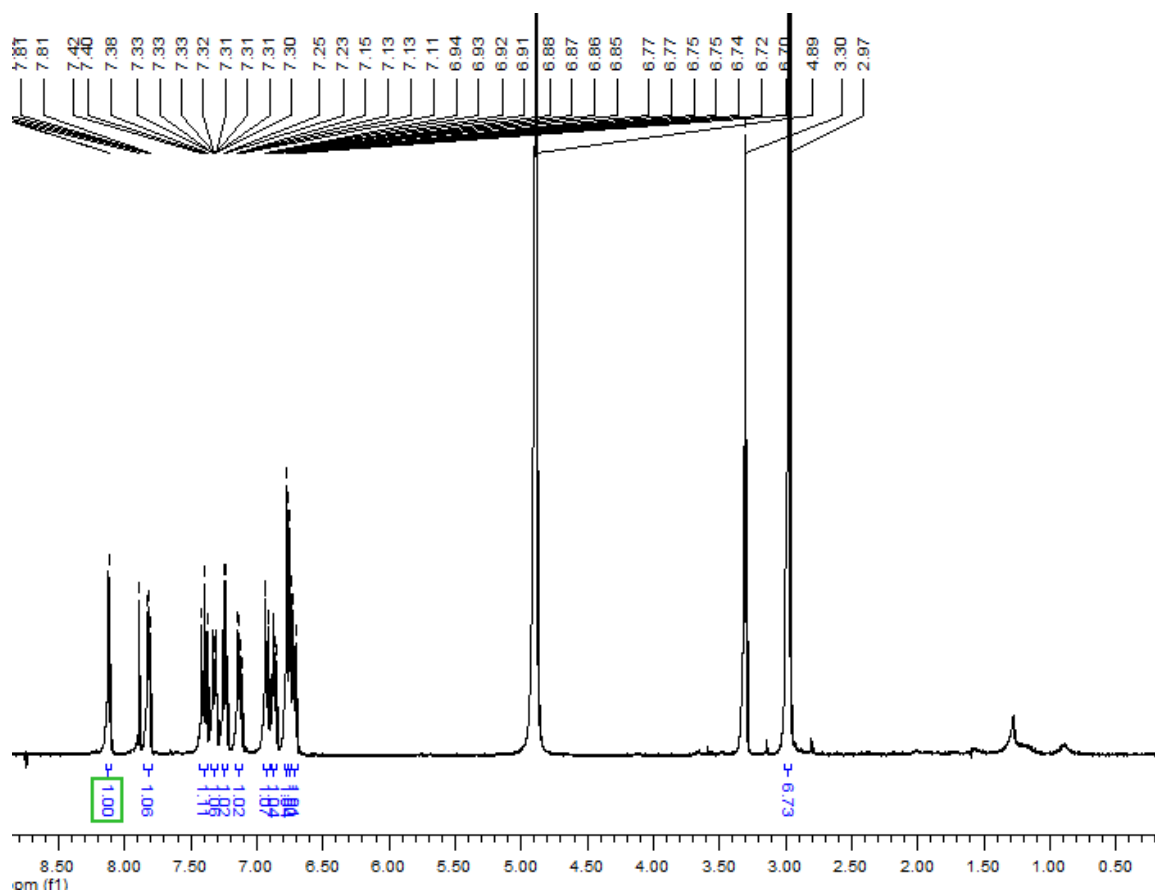
Spectrum 3-73: 1-(3-(dimethylamino)phenyl)-N^6-(pyridin-3-yl)-1H-benzo[d]imidazole-2,6-diamine (**3h**) ^{13}C NMR (400 MHz, CD$_3$OD)
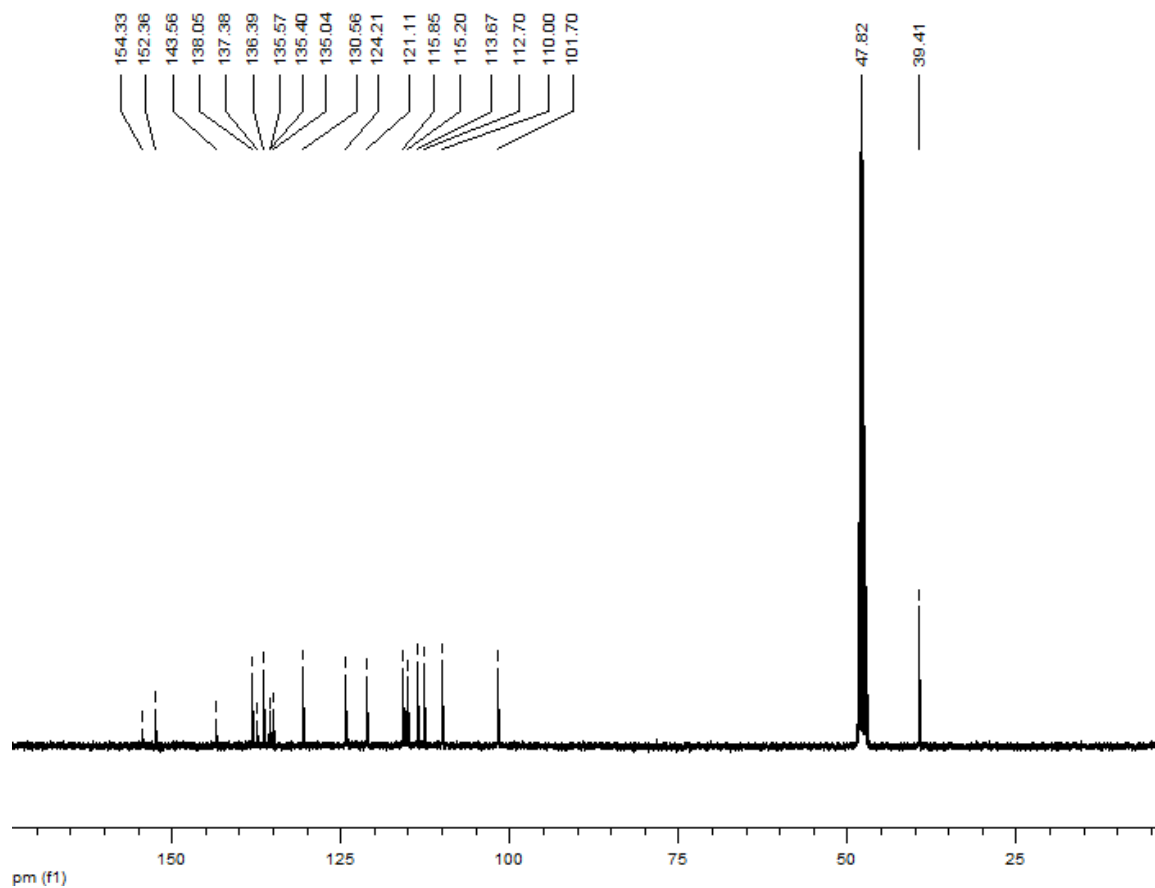
1-(3-(dimethylamino)phenyl)-*N*⁶-(pyridin-4-yl)-1*H*-benzo[*d*]imidazole-2,6-diamine (3i)
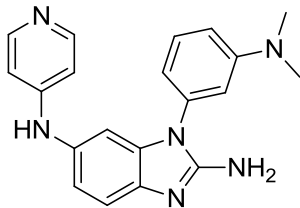
To a 100 ml round bottom flask was added *N*-(1-(3-(dimethylamino)phenyl)-6-

(pyridin-4-ylamino)-1*H*-benzo[*d*]imidazol-2-yl)benzamide (**18i**) (108 mg, 0.24 mmol) and

1N HCl aq (50 ml). The reaction was heated to reflux while stirred for 28 hours before

cooling to RT. It was extracted with saturated $NaHCO_3$ aq and Chloroform-EtOH 2:1 (100

ml and 3 x 100 ml). The organic layers were collected and combined. It was dried over

Na_2SO_4. After filtration and concentration the crude was purified via flash column

chromatography (DCM – MeOH : 80 % - 20 %) to yield slight yellow oil as the product (22

mg, 27 % yield). ^{1}H NMR (400 MHz, CD_3OD) δ: 7.99 (d, J = 5Hz, 2H), 7.43 (t, J = 8 Hz, 1H),

7.30 (d, J = 8 Hz, 1H), 6.98 (d, J = 8 Hz, 1H), 6.89 (d, J = 8 Hz, 1H), 6.80 (s, 1H), 6.78 – 6.71

(m, 4H), 2.98 (s, 6H). ^{13}C NMR (400 MHz, CD_3OD) δ: 154.99, 154.33, 152.37, 147.33,

139.35, 135.60, 135.34, 132.09, 130.59, 117.76, 115.24, 113.63, 112.75, 109.96, 108.31,

104.03, 39.39. MS (ESI) calculated exact mass for $C_{20}H_{20}N_6$ = 344.17. Found [M+H]$^+$ =

345.2.

Spectrum 3-74: 1-(3-(dimethylamino)phenyl)-N^6-(pyridin-4-yl)-1H-benzo[d]imidazole-2,6-diamine (**3i**) ^{1}H NMR (400 MHz, CD$_3$OD)

Spectrum 3-75: 1-(3-(dimethylamino)phenyl)-N^6-(pyridin-4-yl)-1*H*-benzo[*d*]imidazole-2,6-diamine (**3i**) ^{13}C NMR (400 MHz, CD$_3$OD)
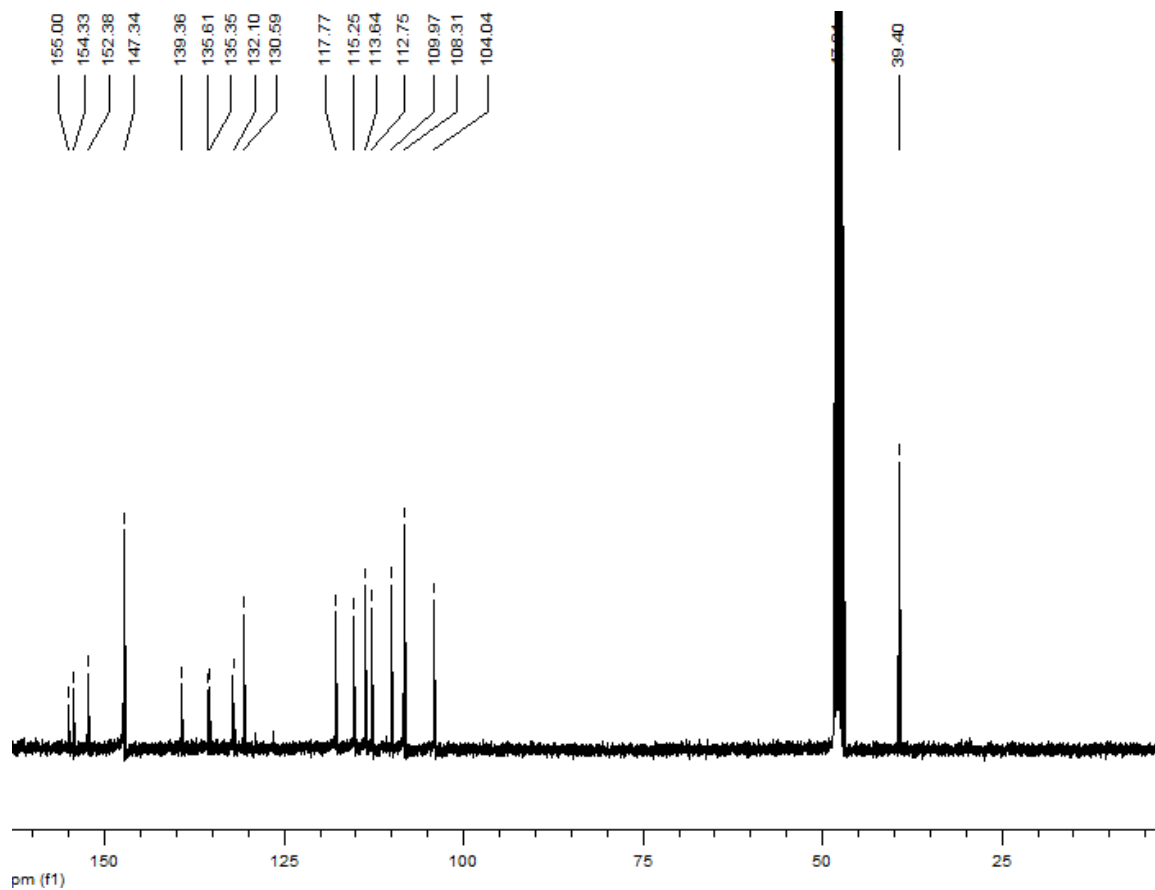
N^1-(5-chloro-2-nitrophenyl)-N^3,N^3-dimethylpropane-1,3-diamine (20h)
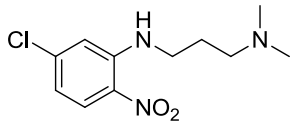
Into a 250 ml round-bottom flask was added 2,4-dichloronitrobenzen (4.0 g, 20.8 mmol), CAN (100 ml) and N^1,N^1-dimethyl-1,3-propanediamine (**19**) (2.6 ml, 21.0 mmol), and K_2CO_3 (2.9 g, 21.0 mmol). The reaction was stirred and heated to reflux for 24 hours before cooling to RT. It was then filtered, concentrated and extracted with DCM (150 ml) and water (150 ml x 2). The organic layer was washed with brine and dried over Na_2SO_4. After filtration and evaporation of solvent, the oil crude was purified via flash column (DCM – MeOH : 90 % - 10 %) to yield orange color oil as the product (5.2 g, 97 % yield). ^{1}H NMR (400 MHz, DMSO-d6) δ: 8.61 (t, J = 5 Hz, 1H), 8.04 (d, J = 9 Hz, 1H), 7.08 (d, J = 2 Hz, 1H), 6.65 (dd, J_1 = 9 Hz, J_2 = 2 Hz, 1H), 3.38 (q, J = 5 Hz, 2H), 2.39 (t, J = 6 Hz, 2H), 2.19 (s, 6H), 1.76 (p, J = 6 Hz, 2H). ^{13}C NMR (400 MHz, DMSO-d6) δ: 146.33, 142.24, 130.49, 128.88, 115.64, 114.09, 57.32, 45.50, 42.03, 26.00. MS (ESI) calculated exact mass for $C_{11}H_{16}ClN_3O_2$ = 257.09. Found $[M+H]^+$ = 258.0.

Spectrum 3-76: N^1-(5-chloro-2-nitrophenyl)-N^3,N^3-dimethylpropane-1,3-diamine (**20h**)
^{1}H NMR (400 MHz, DMSO-d6)
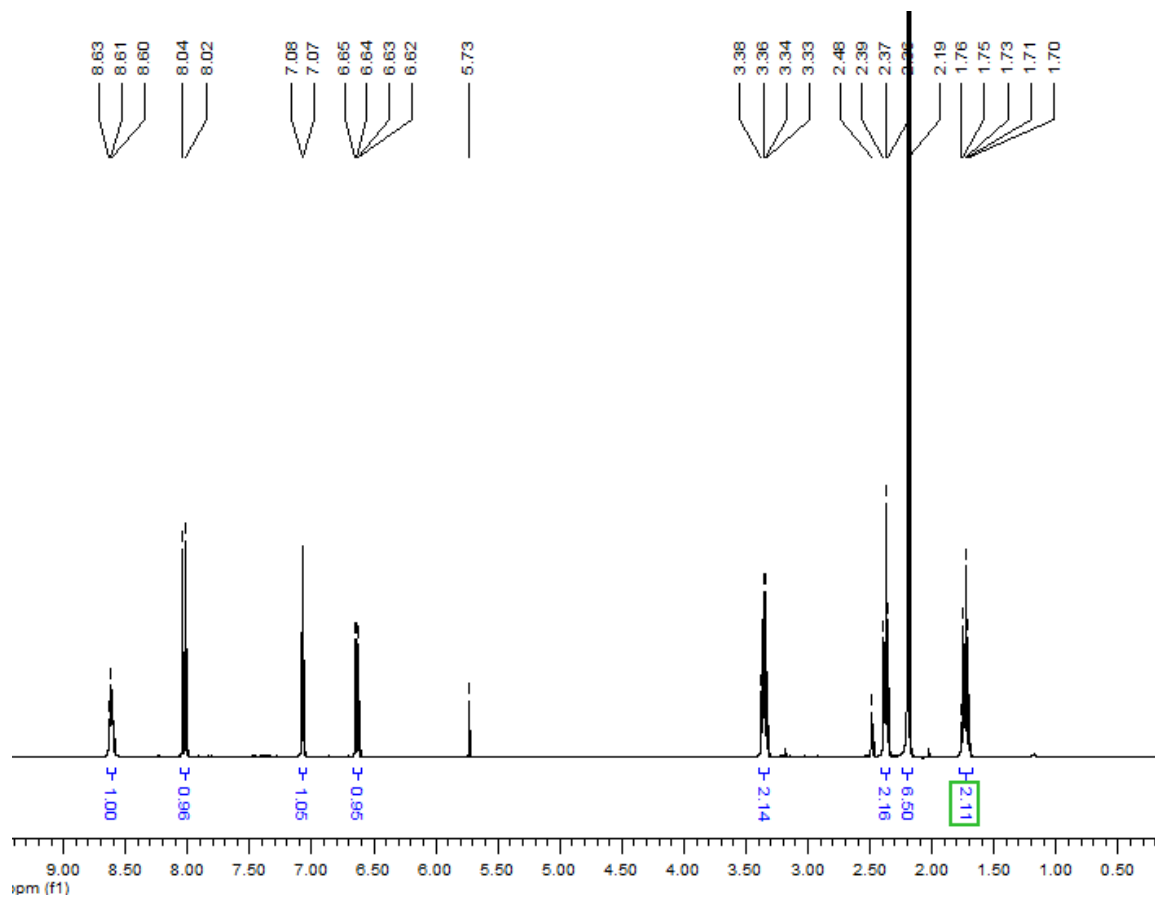
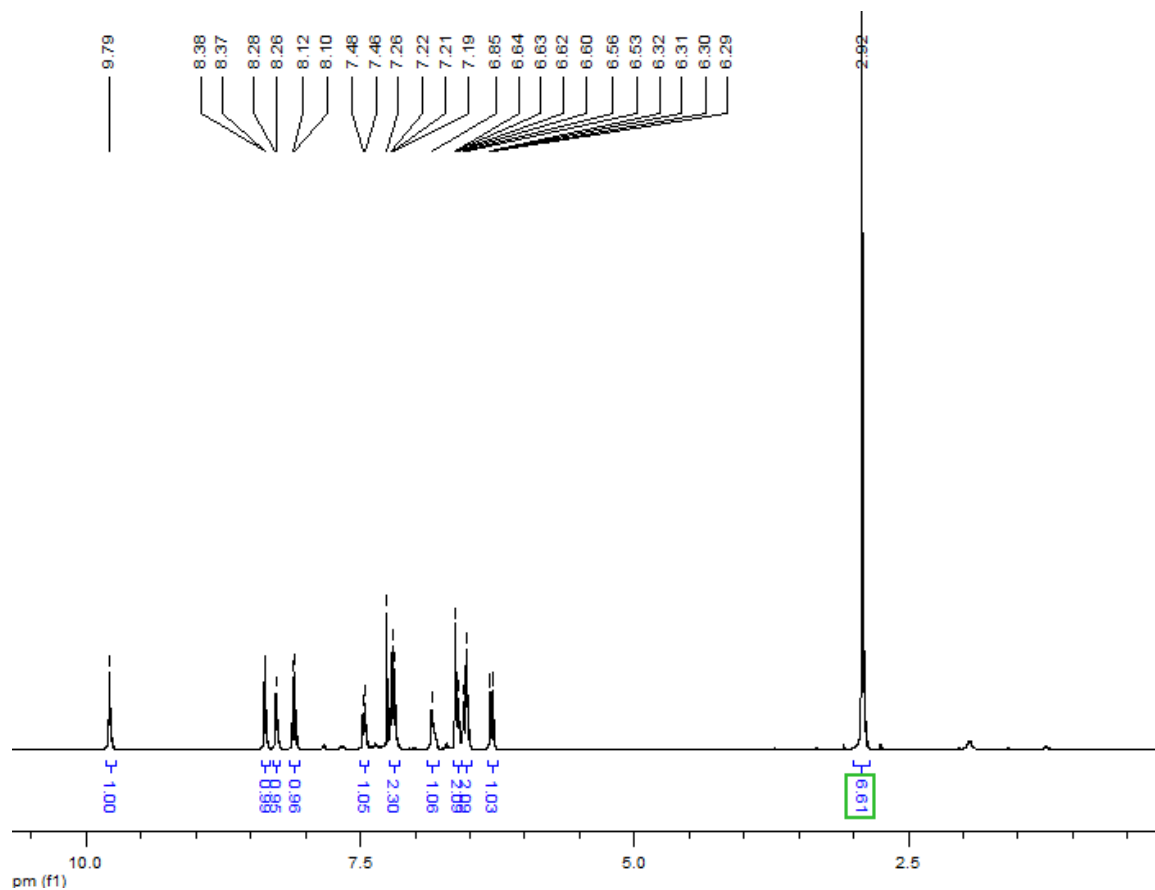**Spectrum 3-77:** N^1-(5-chloro-2-nitrophenyl)-N^3,N^3-dimethylpropane-1,3-diamine (**20h**)
^{13}C NMR (400 MHz, DMSO-d6)
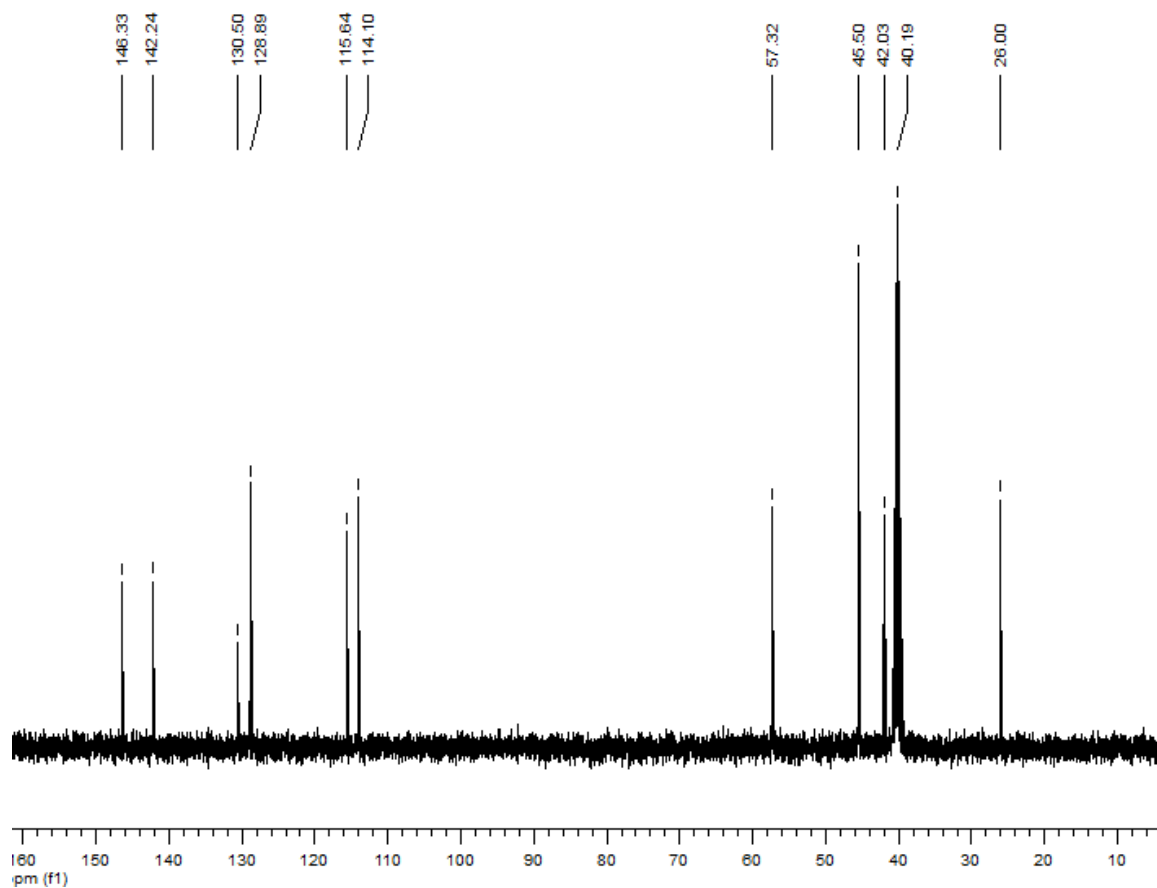
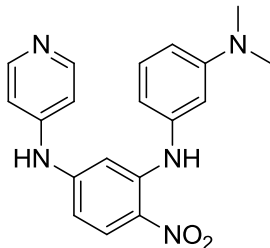**N^1-(2-chloro-6-nitrophenyl)-N^3,N^3-dimethylpropane-1,3-diamine (20j)**
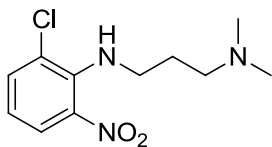
To a 250 ml round bottom flask was added 1,2-dichloro-3-nitrobenzene (7.0 g, 36.5 mmol), ACN (120 ml), *N,N*-dimethyl-1,3-propandiamine (**19**) (4.5 ml, 37.0 mmol), and K_2CO_3 (5.1 g, 37.0 mmol). The reaction was stirred and heated to reflux under Ar atmosphere for 16 hours before cooling to RT. It was then filtered and concentrated. The crude was purified via flash column chromatography (DCM – MeOH : 95 % - 5 %) to yield yellow oil as the product (7.98 g, 96 % yield). ^{1}H NMR (400 MHz, CDCl$_3$) δ: 7.83 (dd, J_1= 9 Hz, J_2 = 2 Hz, 1H), 7.46 (dd, J_1 = 8 Hz, J_2 = 2 Hz, 1H), 7.38 (s, broad, 1H), 6.69 (t, J = 8 Hz, 1H), 3.36 (q, J = 5 Hz, 2H), 2.44 (t, J = 6 Hz, 2H), 2.26 (s, 6H), 1.79 (p, J = 6 Hz, 2H). ^{13}C NMR (400 MHz, CDCl$_3$) δ: 142.46, 135.54, 125.60, 124.19, 116.79, 58.09, 46.71, 45.72, 27.71. MS (ESI) calculated exact mass for $C_{11}H_{16}ClN_3O_2$ = 257.09. Found [M+H]$^+$ = 258.1.

Spectrum 3-78: N^1-(2-chloro-6-nitrophenyl)-N^3,N^3-dimethylpropane-1,3-diamine (**20j**) ^{1}H NMR (400 MHz, CDCl$_3$)
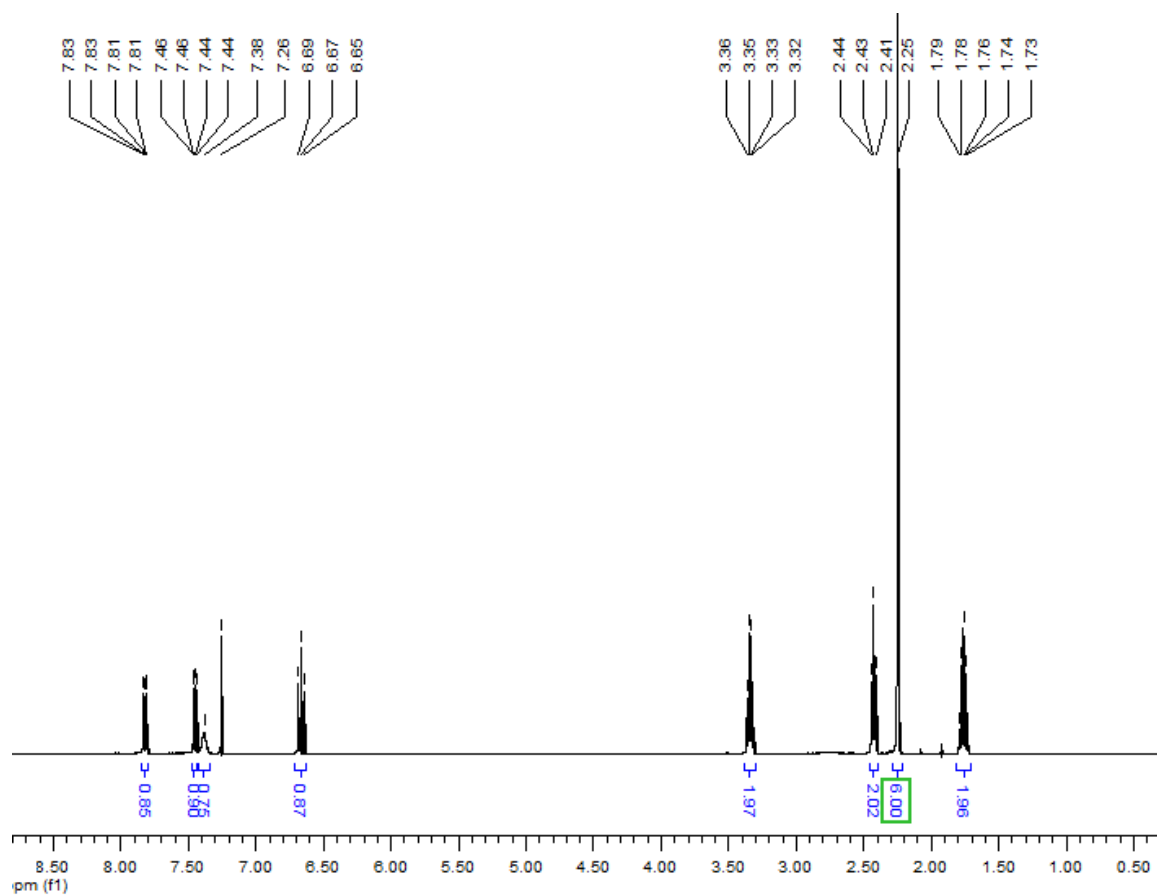
Spectrum 3-79: N^1-(2-chloro-6-nitrophenyl)-N^3,N^3-dimethylpropane-1,3-diamine (**20j**)
^{13}C NMR (400 MHz, CDCl$_3$)
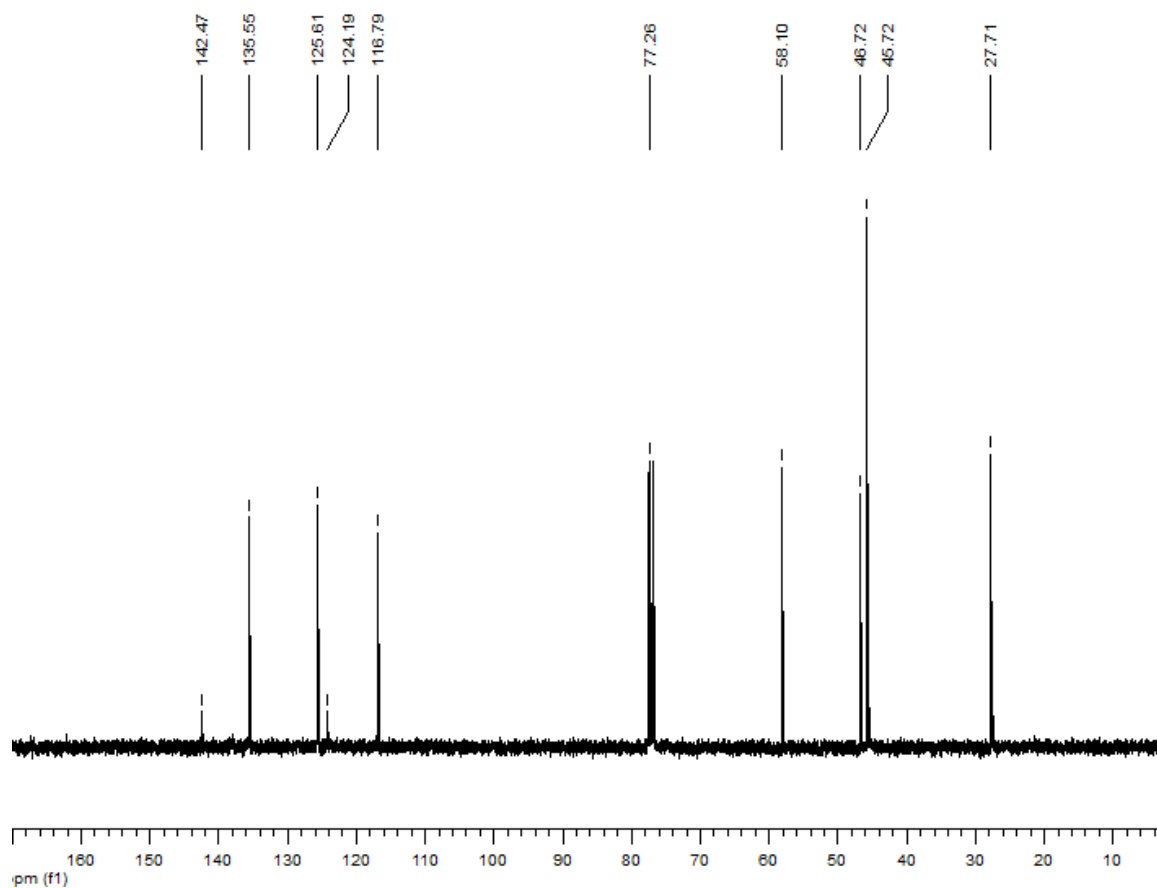
***N³*-(3-(dimethylamino)propyl)-4-nitro-*N¹*-(pyridin-4-yl)benzene-1,3-diamine (22i)**
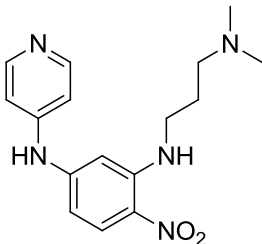
Into a 100 ml round-bottom flask was added N^1-(5-chloro-2-nitrophenyl)-N^3,N^3-dimethylpropane-1,3-diamine (**22h**) (934 mg, 3.6 mmol), dioxane (50 ml), Pd$_2$(dba)$_3$ (166 mg, 0.18 mmol, 5 mol %), *rac*-BINAP (170 mg, 0.27 mmol, 7.5 mol %), and Cs$_2$CO$_3$ (1.1 g, 3.6 mmol). The reaction was stirred and heated to reflux under Ar for 20 hours before cooling to RT. It was then filtered and concentrated. The crude was purified via flash column (DCM – MeOH : 90 % -10 %) to yield yellow oil as the product (908 mg, 80 % yield). ^{1}H NMR (400 MHz, CDCl$_3$) δ: 8.63 (s, 1H), 8.43 (d, *J* = 6Hz, 2H), 8.15 (d, *J* = 9 Hz, 1H), 7.28 (s, 1H), 7.05 (d, *J* = 6 Hz, 2H), 6.55 (d, *J* = 2 Hz, 1H), 6.42 (dd, *J$_1$* = 9 hz, *J$_2$* = 2Hz, 1H), 3.34 (p, *J* = 5 Hz, 2H), 2.46 (t, *J* = 7 Hz, 2H), 2.25 (s, 6H), 1.90 (p, *J* = 7 Hz, 2H). ^{13}C NMR (400 MHz, CDCl$_3$) δ: 150.96, 148.27, 148.21, 147.61, 129.50, 127.06, 112.73, 106.89, 99.12, 57.40, 45.57, 41.86, 26.62. MS (ESI) calculated exact mass for C$_{16}$H$_{21}$N$_5$O$_2$ = 315.17. Found [M+H]$^+$ = 316.2.

Spectrum 3-80: N^3-(3-(dimethylamino)propyl)-4-nitro-N^1-(pyridin-4-yl)benzene-1,3-diamine **(22i)** ^{1}H NMR (400 MHz, CDCl$_3$)
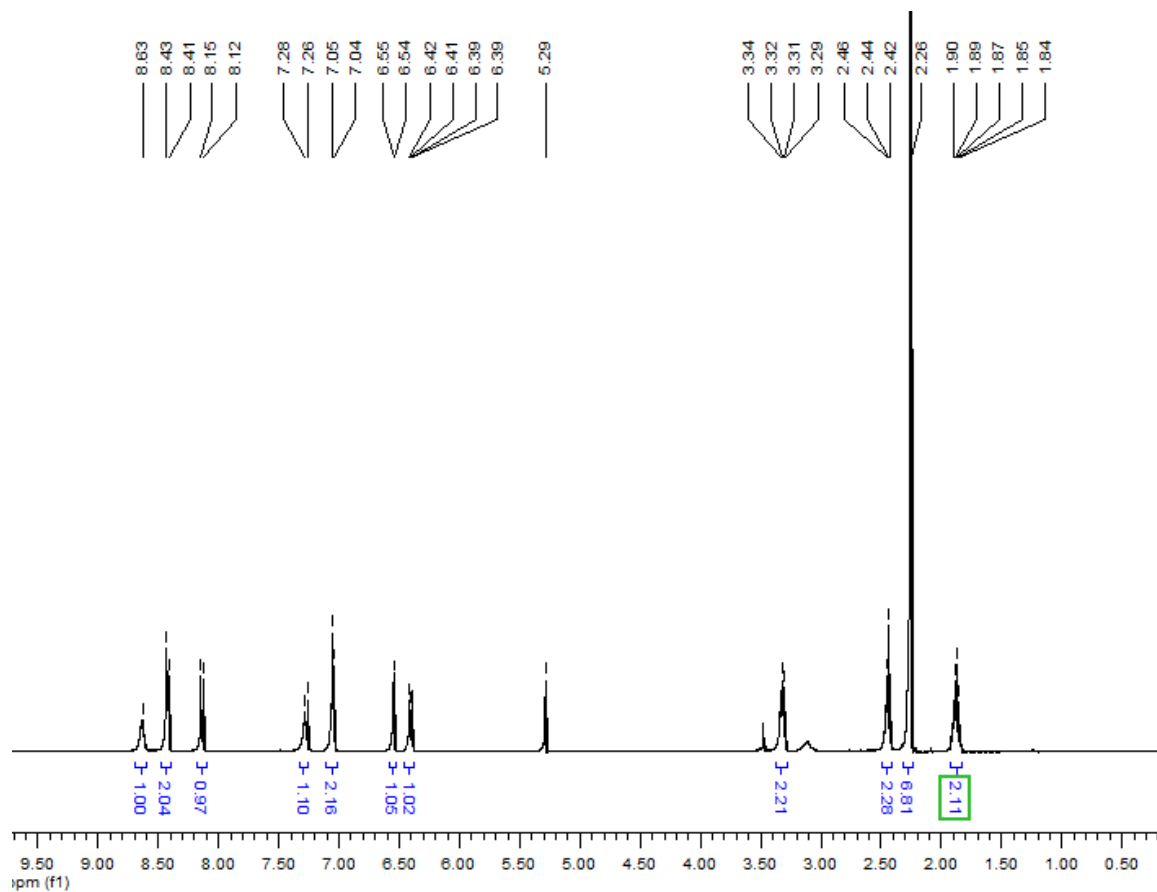
Spectrum 3-81: N^3-(3-(dimethylamino)propyl)-4-nitro-N^1-(pyridin-4-yl)benzene-1,3-diamine **(22i)** ^{13}C NMR (400 MHz, CDCl$_3$)
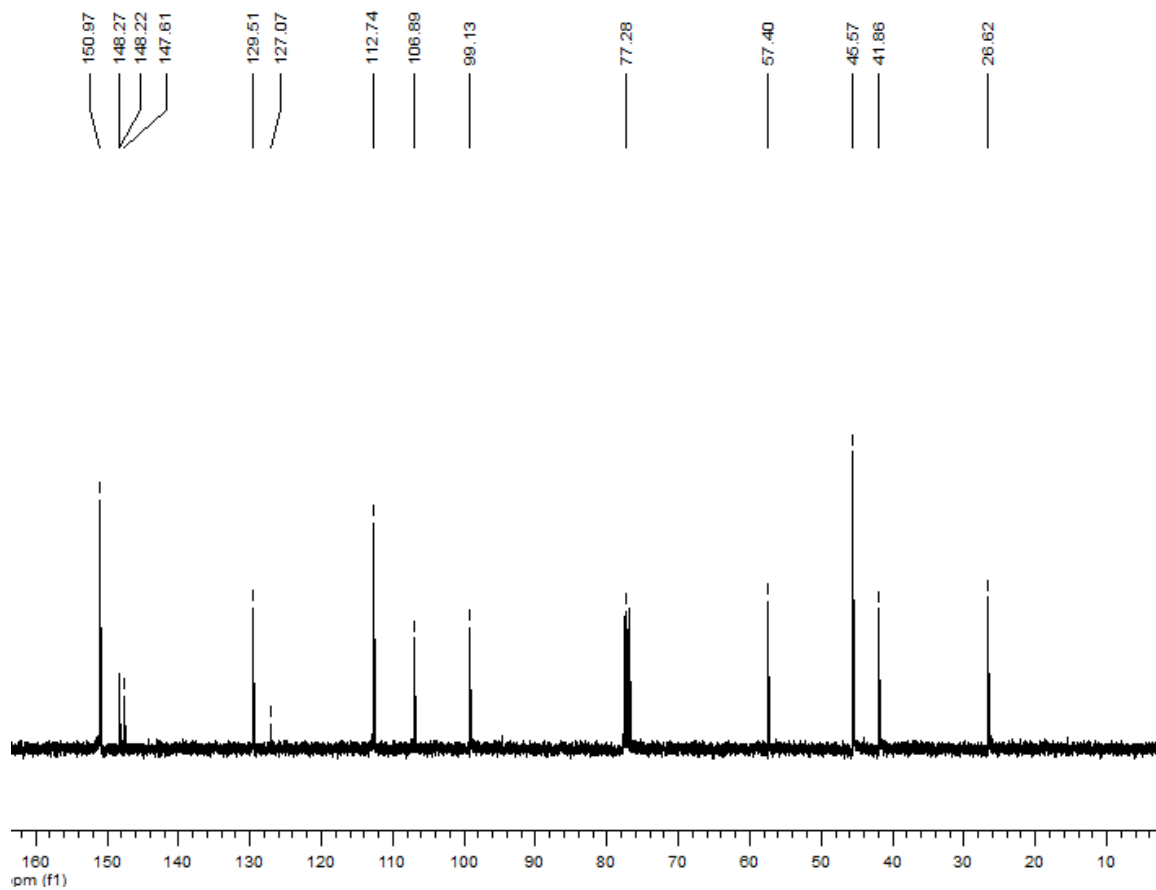
N*³-(3-(dimethylamino)propyl)-4-nitro-*N*¹-(pyridin-3-yl)benzene-1,3-diamine (22h)
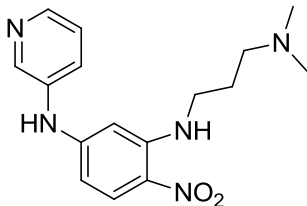
To a 100 ml round-bottom flask was added N^1-(5-chloro-2-nitrophenyl)-N^3,N^3-

dimethylpropane-1,3-diamine (**20h**) (489 mg, 2.16 mmol), Toluene (40 ml), 3-

aminopyridine (223 mg, 2.37 mmol), Pd$_2$(dba)$_3$ (99 mg, 0.11 mmol, 5 mol %), *rac*-BINAP

(101 mg, 0.16 mmol, 7.5 mol%), and Cs$_2$CO$_3$ (748 mg, 2.37 mmol, 1.1 eq). The reaction

was stirred and heated to reflux under Ar atmosphere for 19 hours before cooling to RT.

It was then filtered and concentrated. The crude was purified via flash column

chromatography (DCM – MeOH (80 % - 20 %) to yield yellow oil as the product (269 mg,

40 % yield). ^{1}H NMR (400 MHz, CDCl$_3$) δ: 8.64 (s, 1H), 8.53 (d, *J* = 2 Hz, 1H), 8.38 (d, *J* = 5

Hz, 1H), 8.11 (d, *J* = 9 Hz, 1H), 7.58 (d, *J* = 7 Hz, 1H), 7.33 (dd, J_1 = 8 Hz, J_2 = 5 Hz, 1H), 6.43

(s, 1H), 6.25 (d, *J* = 2 Hz, 1H), 6.22 (dd, J_1 = 9 Hz, J_2 = 2 Hz, 1H), 3.28 (q, *J* = 5 Hz, 2H), 2.40

(t, *J* = 7 Hz, 2H), 2.21 (s, 6H), 1.86 – 1.79 (m, 2H). MS (ESI) calculated exact mass for

C$_{16}$H$_{21}$N$_5$O$_2$ = 315.17. Found [M+H]$^+$ = 316.2.

Spectrum 3-82: N^3-(3-(dimethylamino)propyl)-4-nitro-N^1-(pyridin-3-yl)benzene-1,3-diamine **(22h)** ^{1}H NMR (400 MHz, CDCl$_3$)
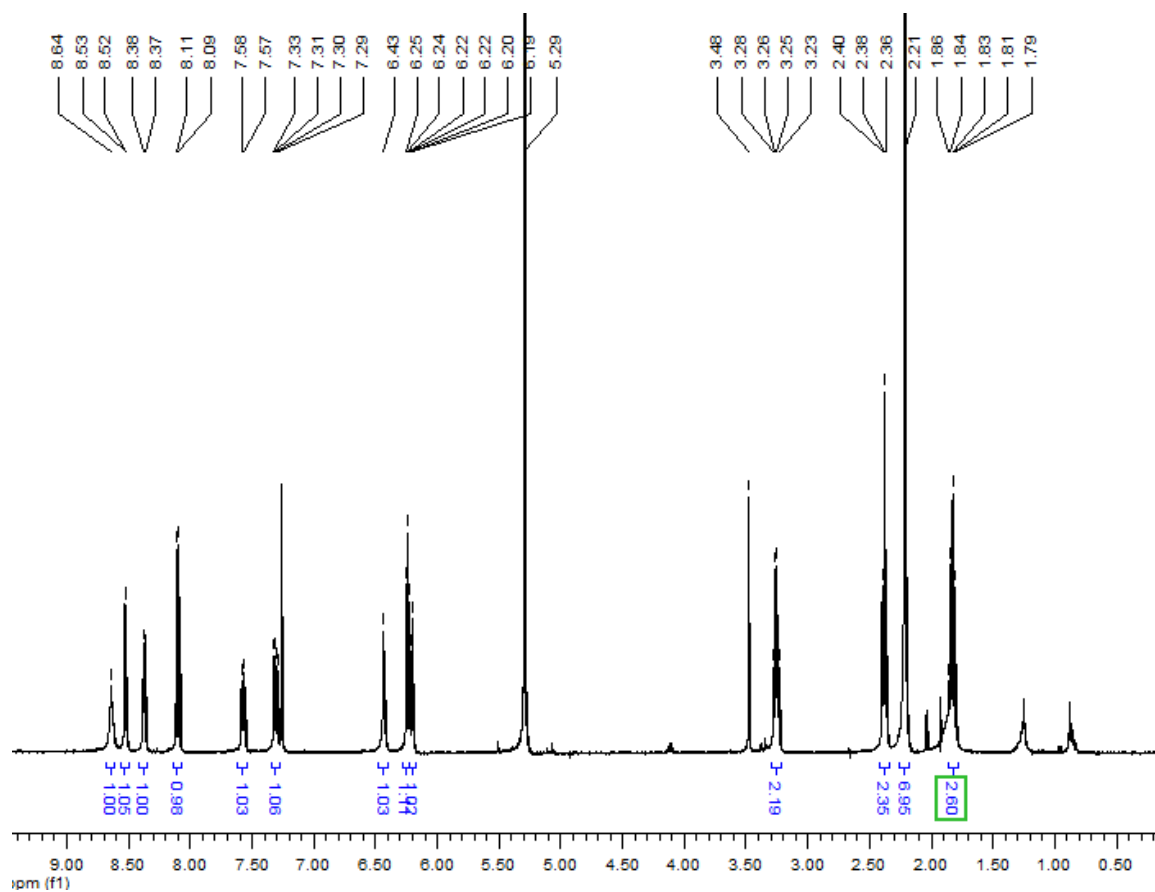
***N*²-(3-(dimethylamino)propyl)-*N*^{3'},*N*^{3'}-dimethyl-3-nitro-[1,1'-biphenyl]-2,3'-diamine (23)**
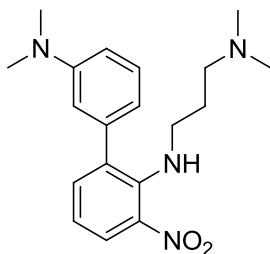
To a 100 ml round bottom flask was added *N*¹-(2-chloro-6-nitrophenyl)-*N*³,*N*³-dimethylpropane-1,3-diamine (**20j**) (1.0 g, 3.9 mmol), dioxane (40 ml), 3-(*N*,*N*-dimethylamino)phenylboronic acid (768 mg, 4.6 mmol, 1.2 eq), $Pd_2(dba)_3$ (178 mg, 0.19 mmol, 5 mol %), *rac*-BINAP (181 mg, 0.29 mmol, 5 mol %), and Cs_2CO_3 (1.47 g, 4.6 mmol). The reaction was stirred and heated to reflux under Ar atmosphere for 53 hours before cooling to RT. It was then filtered and concentrated. The crude was purified via flash column chromatography (DCM – MeOH : 90 % - 10 %) to yield red color oil as the product (803 mg, 60 % yield). ^{1}H NMR (400 MHz, DMSO) δ: 7.94 (dd, J_1 = 8 Hz, J_2 = 2 Hz, 1H), 7.36 – 7.31 (m, 2H), 7.25 (t, J = 8 Hz, 1H), 6.83 (dd, J_1 = 7 Hz, J_2 = 8 Hz, 1H), 6.74 (dd, J_1 = 9 Hz, J_2 = 2 Hz, 1H), 6.69 (s, 1H), 6.66 (d, J = 7 Hz, 1H), 2.90 (s, 6H), 2.71 (q, J = 6 Hz, 2H), 2.08 (t, J = 7 Hz, 2H), 1.99 (s, 6H), 1.42 (p, J = 6 Hz, 2H). ^{13}C NMR (400 MHz, DMSO) δ: 151.14, 144.44, 141.00, 138.27, 133.91, 129.90, 125.92, 117.52, 116.99, 112.83, 112.19, 57.20, 45.56, 45.28, 40.76, 27.33. MS (ESI) calculated exact mass for $C_{19}H_{26}N_4O_2$ = 342.21. Found [M+H]$^+$ = 343.2.

Spectrum 3-83: N^2-(3-(dimethylamino)propyl)-$N^{3'},N^{3'}$-dimethyl-3-nitro-[1,1'-biphenyl]-2,3'-diamine **(23)** ^{1}H NMR (400 MHz, DMSO)
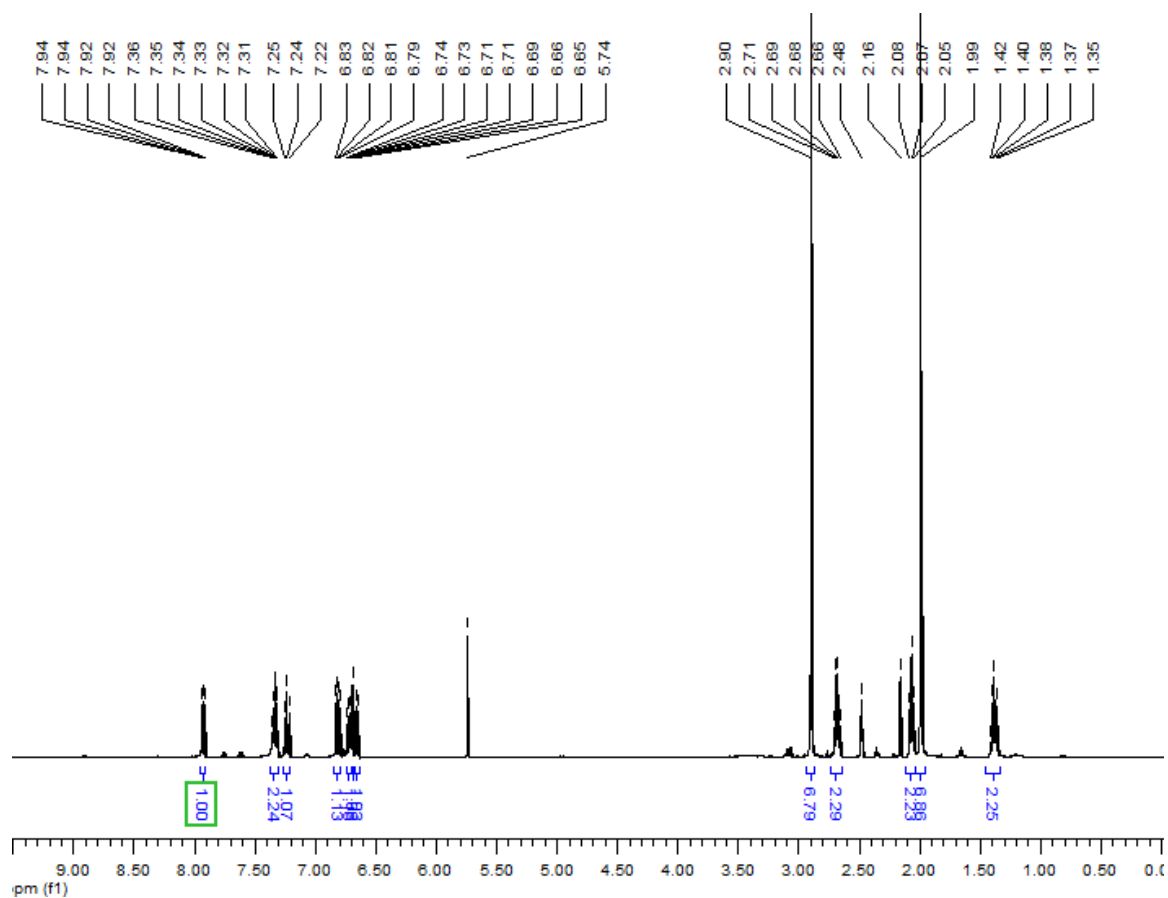
Spectrum 3-84: N^2-(3-(dimethylamino)propyl)-$N^{3'}$,$N^{3'}$-dimethyl-3-nitro-[1,1'-biphenyl]-2,3'-diamine **(23)** ^{13}C NMR (400 MHz, DMSO)
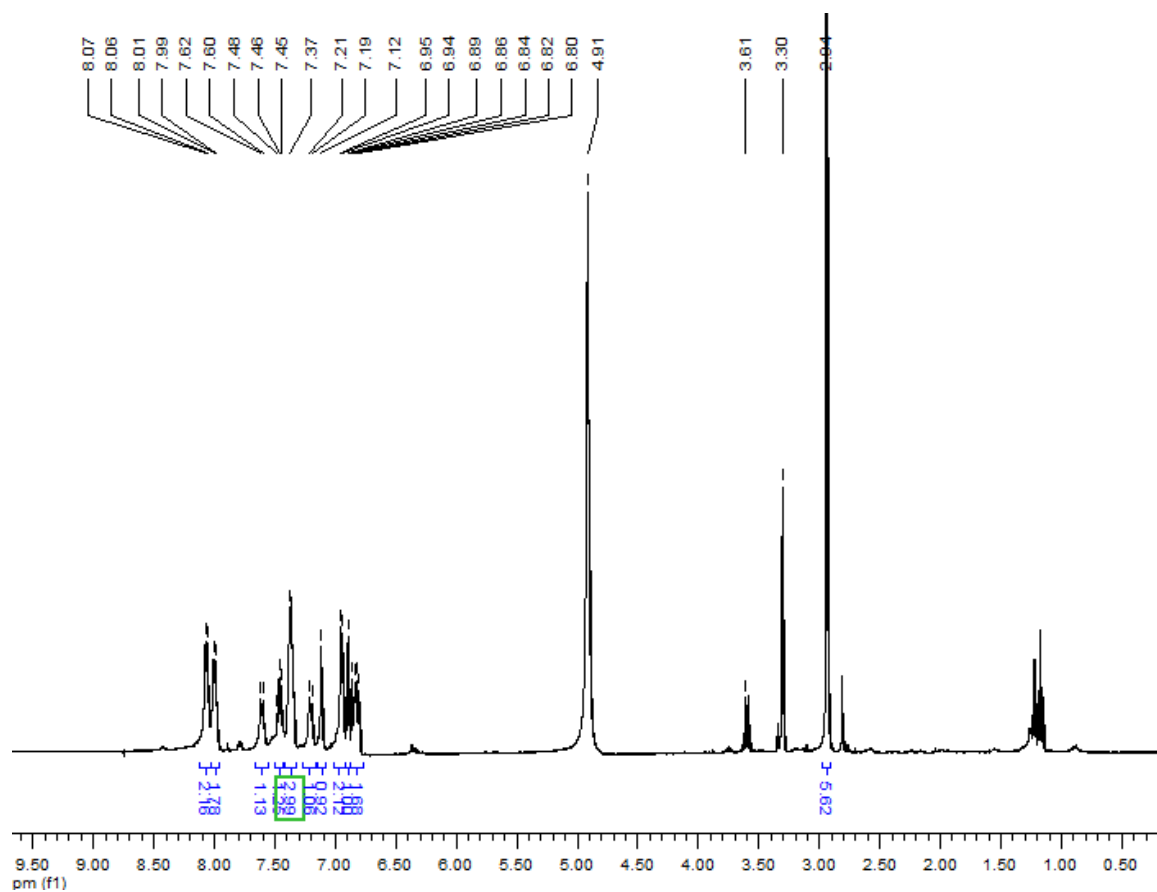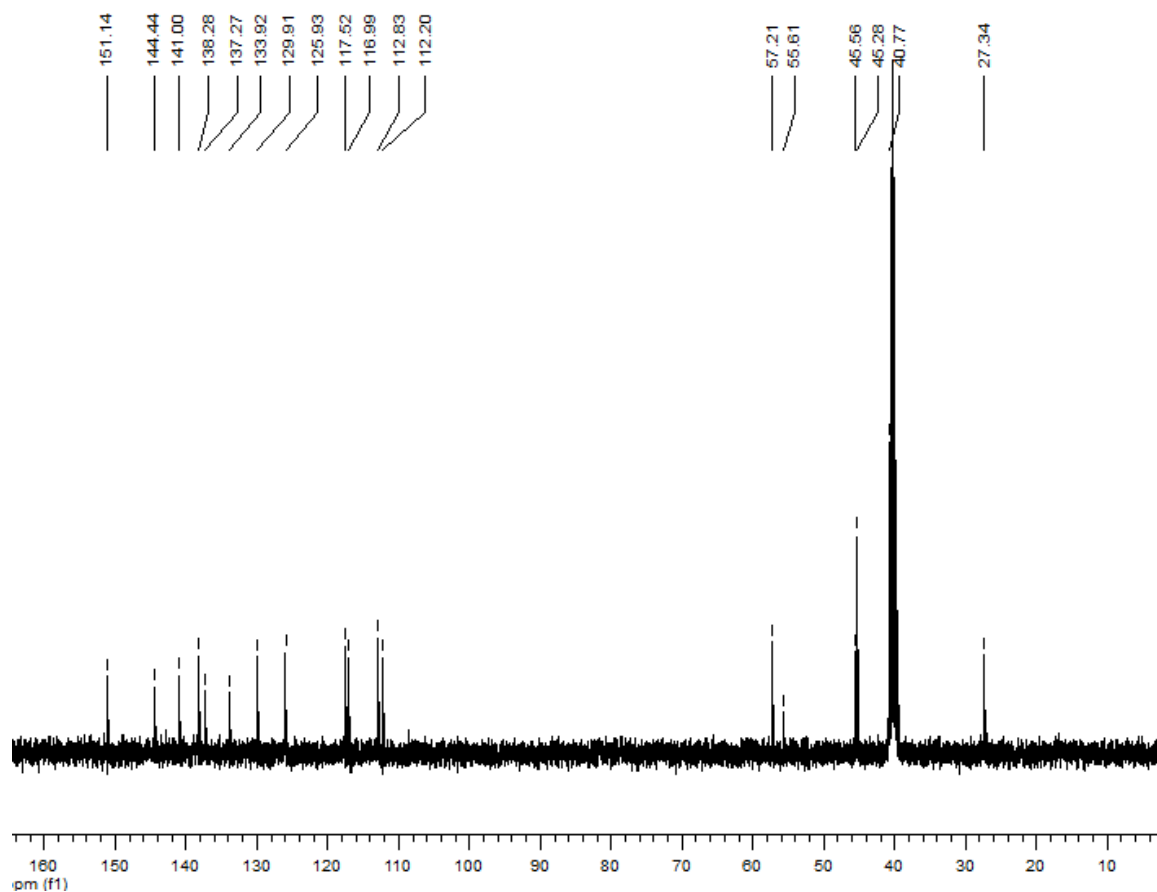
_N_-(1-(3-(dimethylamino)propyl)-6-(pyridin-3-ylamino)-1_H_-benzo[_d_]imidazol-2-yl)benzamide (24h)
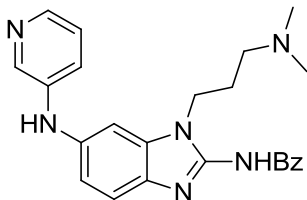
Into a 250 ml round-bottom flask was added _N³_-(3-(dimethylamino)propyl)-4-nitro-_N¹_-(pyridine-3-yl)benzene-1,3-diamine (**22h**) (474 mg, 1.5 mmol) and methanol (100 ml). The flask was flushed with Ar gas before Pd/C (40 mg, 10 wt %) was added. The flask was then sealed under H_2 atmosphere and stirred at RT for 1.5 hours before it was filtered and concentrated. The oil residue was dissolved in ACN (100 ml) and benzoylisothiocyanate (222 μl, 1.5 mmol) was added. The reaction was stirred at RT for 18 hours when DIPC (233 μl, 1.5 mmol) and K_2CO_3 (207 mg, 1.5 mmol) were added. The reaction was stirred at RT for 24 hours before filtration and concentration. It was purified via flash column chromatography (DCM – MeOH : 90 % - 10 % to 70 % - 30 %) to yield white solid as the product (403 mg, 65 % yield). ^{1}H NMR (400 MHz, DMSO-d6) δ: 8.40 (s, 1H), 8.36 (d, _J_ = 3 Hz, 1H), 7.98 (d, _J_ = 5 Hz, 1H), 7.74 (d, _J_ = 8 Hz, 2H), 7.59 – 7.53 (m, 4H), 7.46 (d, _J_ = 8 Hz, 1H), 7.33 (s, 1H), 7.21 (dd, _J₁_ = 8 Hz, _J₂_ = 5 Hz, 1H), 7.02 (d, _J_ = 8 Hz, 1H), 4.25 (t, _J_ = 7 Hz, 2H), 2.09 (t, _J_ = 6 Hz, 2H), 1.95 (s, 6H), 1.77 (p, _J_ = 7 Hz, 2H). ^{13}C NMR (400 MHz, DMSO-d6) δ: 152.96, 141.84, 140.42, 138.93, 138.70, 138.40, 137.12, 131.37, 130.07, 129.66, 129.34, 124.48, 121.65, 120.52, 116.03, 100.05, 94.54, 56.48, 45.62, 42.83, 27.83. MS (ESI) calculated exact mass for $C_{24}H_{26}N_6O$ = 414.22. Found $[M+H]^+$ = 415.3.

Spectrum 3-85: *N*-(1-(3-(dimethylamino)propyl)-6-(pyridin-3-ylamino)-1*H*-benzo[*d*]imidazol-2-yl)benzamide **(24h)** ^{1}H NMR (400 MHz, DMSO-d6)
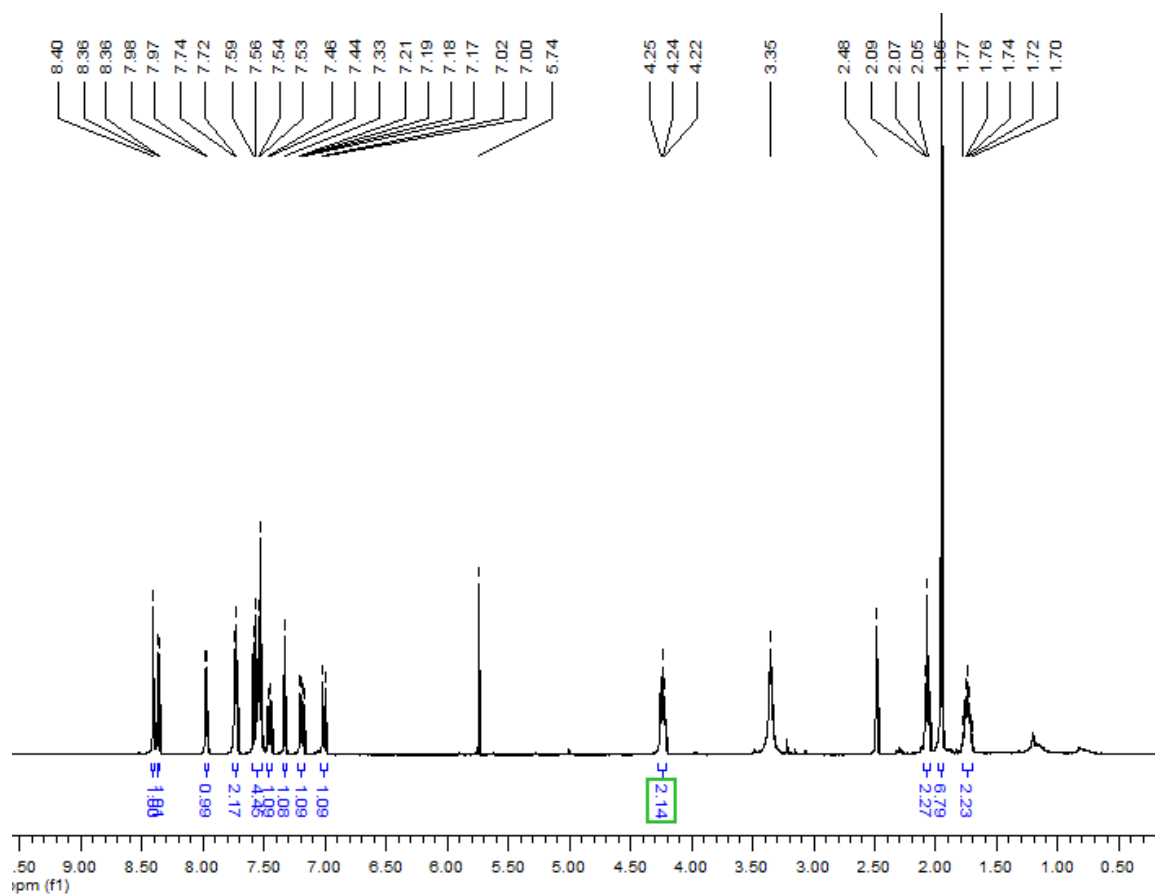
Spectrum 3-86: *N*-(1-(3-(dimethylamino)propyl)-6-(pyridin-3-ylamino)-1*H*-benzo[*d*]imidazol-2-yl)benzamide **(24h)** ¹³C NMR (400 MHz, DMSO-d6)
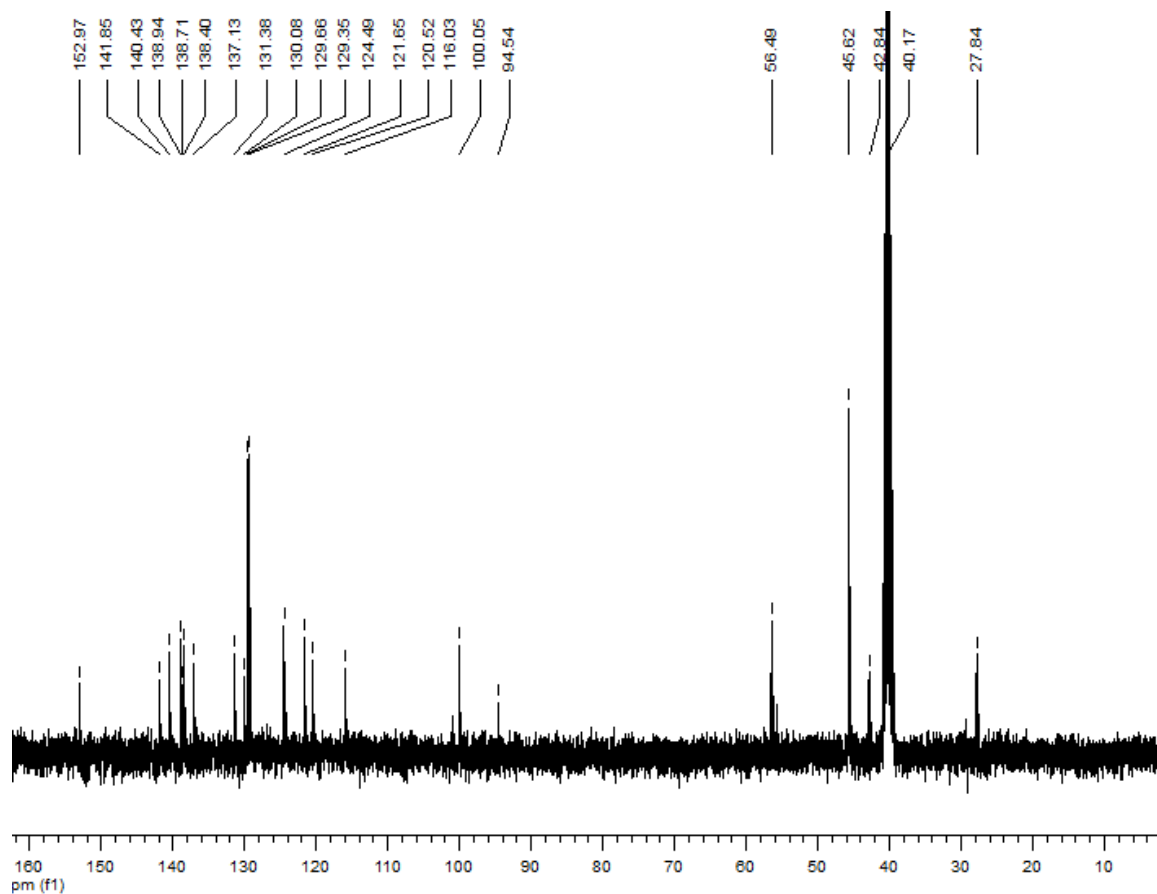
N-(1-(3-(dimethylamino)propyl)-6-(pyridin-4-ylamino)-1H-benzo[d]imidazol-2-yl)benzamide (24i)
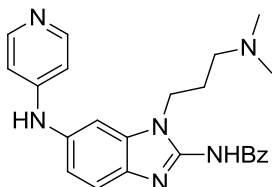
To a 250 ml round-bottom flask was added N^3-(3-(dimethylamino)propyl)-4-nitro-N^1-(pyridin-4-yl)benzene-1,3-diamine (**22i**) (907 mg, 2.87 mmol) and methanol (100 ml). The flask was flushed with Ar gas before Pd/C was added. The reaction was then stirred under H_2 atmosphere for 19 hours before filtration and concentration. The oil residue was dissolved in ACN (250 ml) and benzoyl isothiocyanate (425 µl, 2.87 mmol) was added. The reaction was stirred at RT for 24 hours when DIPC (446 µl, 2.87 mmol) and K_2CO_3 (396 mg, 2.87 mmol) were added. The reaction was stirred at RT for 25 hours before filtration and concentration. The crude was purified via flash column chromatography (DCM – MeOH : 90 % - 10 %) to yield dark yellow viscous oil as the product (398mg, 33% yield). ^{1}H NMR (400 MHz, DMSO) δ: 8.32 (d, J = 7 Hz, 2H), 8.24 (d, J = 6 Hz, 2H), 7.51 – 7.41 (m, 3H), 7.23 (d, J = 9 Hz, 1H), 7.18 (d, J = 2Hz, 1H), 7.05 (s, 1H), 7.03 (dd, J_1 = 8 Hz, J_2 = 2 Hz, 1H), 6.77 (d, J = 6 Hz, 2H), 4.25 (t, J = 7 Hz, 2H), 2.35 (t, J = 7 Hz, 2H), 2.18 (s, 6H), 1.05 – 1.98 (m, 2H). MS (ESI) calculated exact mass for $C_{24}H_{26}N_6O$ = 414.22. Found $[M+H]^+$ = 415.2.

Spectrum 3-87: *N*-(1-(3-(dimethylamino)propyl)-6-(pyridin-4-ylamino)-1*H*-benzo[*d*]imidazol-2-yl)benzamide **(24i)** ^{1}H NMR (400 MHz, DMSO)
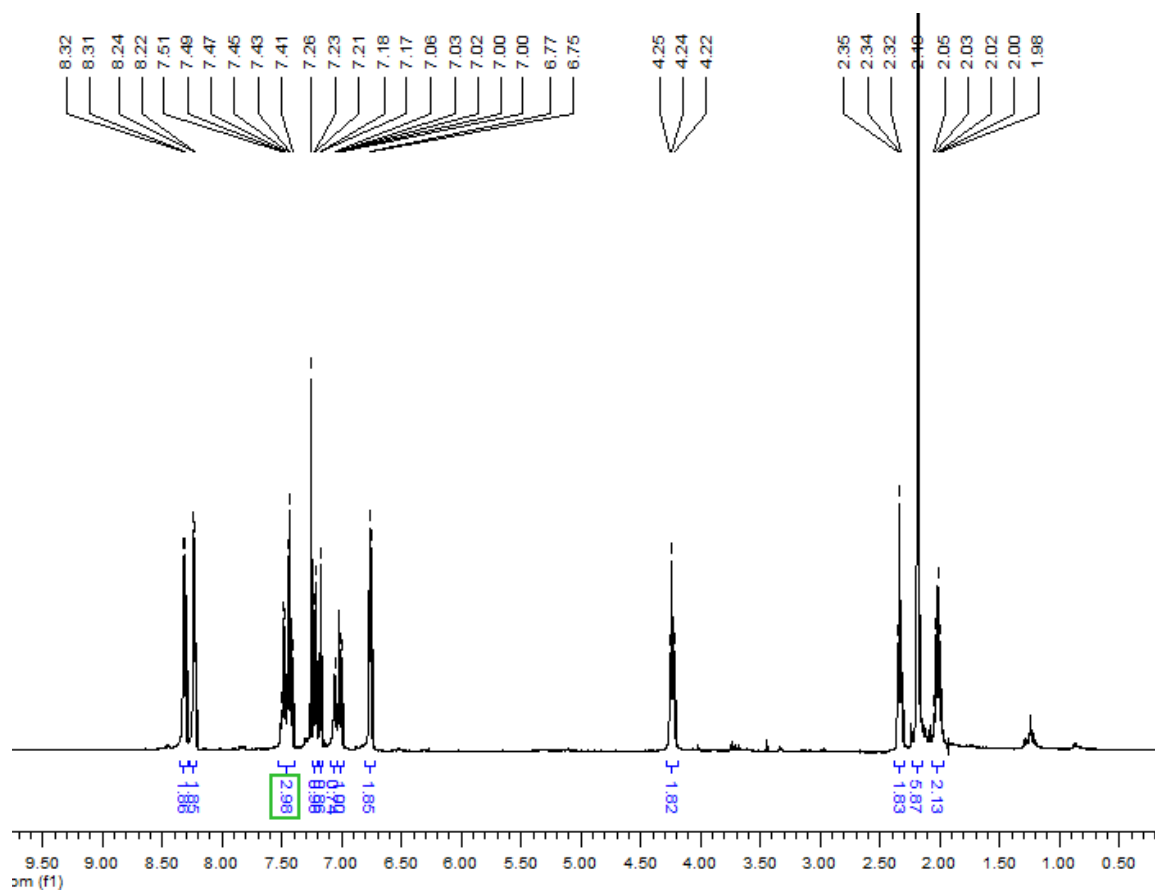
N-(7-(3-(dimethylamino)phenyl)-1-(3-(dimethylamino)propyl)-1H-benzo[d]imidazol-2-yl)benzamide (24j)
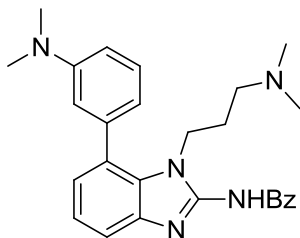
To a 250 ml rb flask was added N^2-(3-(dimethylamino)propyl)-$N^{3'}$,$N^{3'}$-dimethyl-3-nitro-[1,1'-biphenyl]-2,3'-diamine (**23**) (558 mg, 1.63 mmol) and methanol (100 ml). The flask was flushed with Ar gas before Pd/C (60 mg) was added. The reaction was stirred at RT under H_2 atmosphere for 22 hours before filtration and concentration. The oil residue was dissolved in ACN (100ml) and Benzoyl isothiocyanate (240 μl, 1.63 mmol) was added. The reaction was stirred at RT for 27 hours when DIPC (254 μl, 1.63 mmol) and K_2CO_3 (225 mg, 1.63 mmol) were added. The reaction was stirred at RT for 44 hours before it was filtered and concentrated. The crude was purified via flash column chromatography (DCM – MeOH : 90 % - 10 %) to yield slight yellow-gray color oil as the product (280 mg, 39 % yield). ^{1}H NMR (400 MHz, CDCl₃) δ: 8.32 (d, J = 7 Hz, 2H), 7.48 – 7.41 (m, 3H), 7.31 (t, J = 8 Hz, 2H), 7.25-7.21 (m, 2H), 7.12 (d, J = 7 Hz, 1H), 6.82 – 6.68 (m, 3H), 4.01 (m, 2H), 2.99 (s, 6H), 2.12 (s, 6H), 2.00 (m, 2H), 1.62 (m, 2H). MS (ESI) calculated exact mass for $C_{27}H_{31}N_5$ = 441.25. Found [M+H]$^+$ = 442.3.

Spectrum 3-88: *N*-(7-(3-(dimethylamino)phenyl)-1-(3-(dimethylamino)propyl)-1*H*-benzo[*d*]imidazol-2-yl)benzamide (**24j**) ^{1}H NMR (400 MHz, CDCl$_3$)
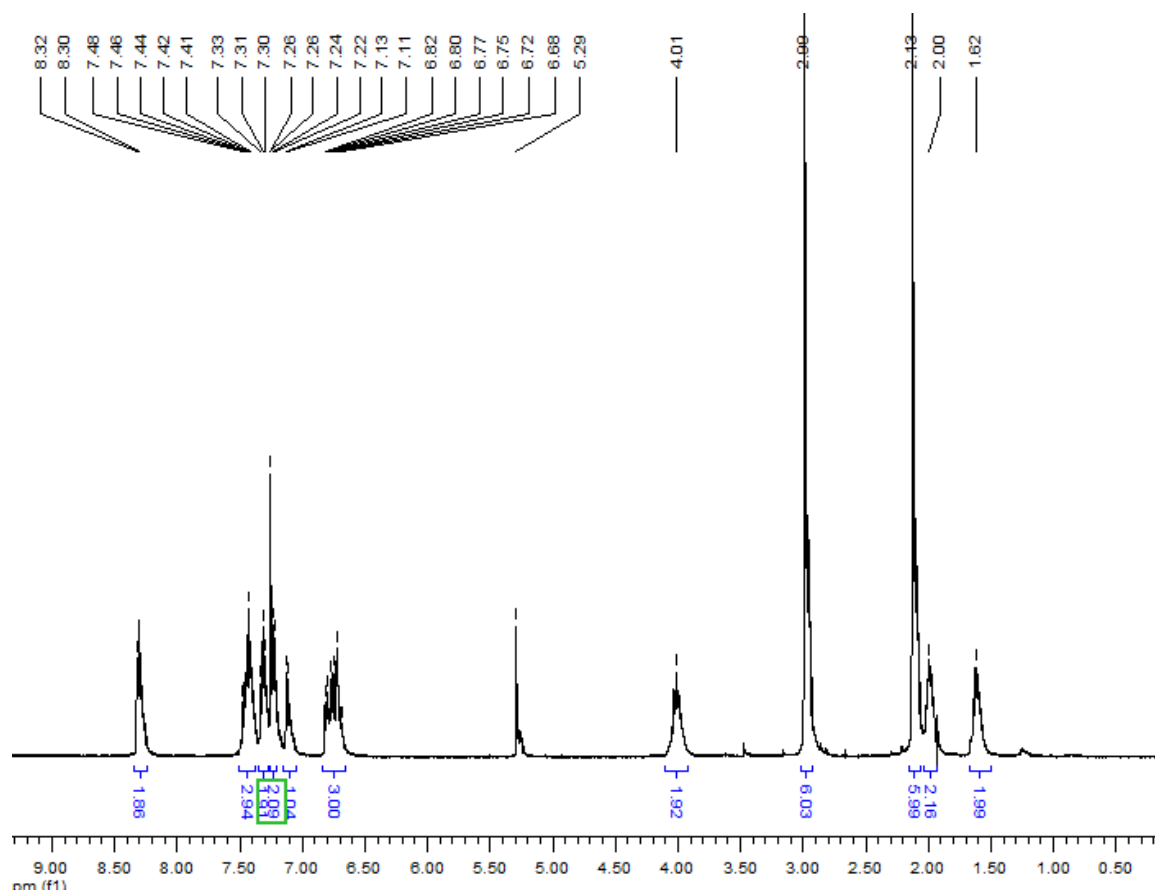
1-(3-(dimethylamino)propyl)-N^6-(pyridin-3-yl)-1H-benzo[d]imidazole-2,6-diamine (6h)
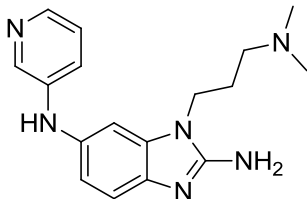
To a 100 ml round bottom flask was added N^3-(3-(dimethylamino)propyl)-4-nitro-N^1-(pyridin-3-yl)benzene-1,3-diamine (**24h**) (403 mg, 1.30 mmol) and 1M HCl aq. (50 ml). The reaction was stirred and heated to reflux for 19 hours before cooling to RT. It was extracted with saturated $NaHCO_3$ aq and $CHCl_3$-EtOH : 2 − 1 (100ml and 2 x 200 ml). The combined organic layers were dried over Na_2SO_4. After filtration and concentration, the crude was purified via flash column chromatography (DCM − MeOH : 80 % - 20 %) to yield dark yellow oil as the product (228 mg, 56 % yield). ^{1}H NMR (400 MHz, CD_3OD) δ: 8.15 (d, J = 3 Hz, 1H), 7.83 (d, J = 5 Hz, 1H), 7.34 − 7.31 (m, 1H), 7.19 (d, J = 8 Hz, 1H), 7.15 (dd, J_1 = 8 Hz, J_2 = 5 Hz, 1H), 6.99 (d, J = 2 Hz, 1H), 6.89 (dd, J_1 = 8 Hz, J_2 = 2 Hz, 1H), 3.98 (t, J = 6 Hz, 2H), 2.27 (t, J = 7 Hz, 2H), 2.19 (s, 6H), 1.93 − 1.86 (m, 2H). ^{13}C NMR (400 MHz, CD_3OD) δ: 155.59, 143.95, 138.06, 137.91, 136.33, 134.65, 134.42, 124.25, 120.87, 115.86, 115.23, 101.61, 55.19, 44.01, 39.40, 26.10. MS (ESI) calculated exact mass for $C_{17}H_{22}N_6$ = 310.19. Found $[M+H]^+$ = 311.3.

Spectrum 3-89: 1-(3-(dimethylamino)propyl)-*N*⁶-(pyridin-3-yl)-1*H*-benzo[*d*]imidazole-2,6-diamine (**6h**) ¹H NMR (400 MHz, CD₃OD)
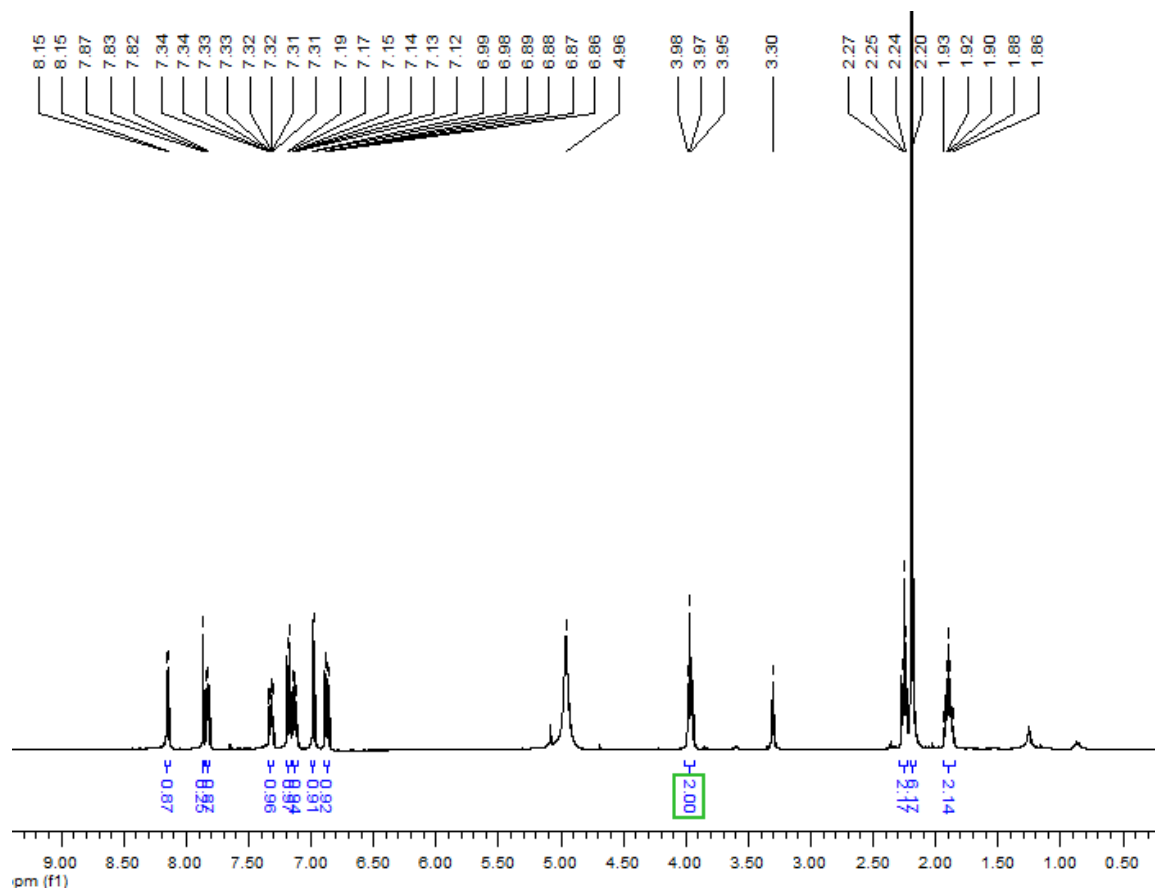
Spectrum 3-90: 1-(3-(dimethylamino)propyl)-N^6-(pyridin-3-yl)-1H-benzo[d]imidazole-2,6-diamine (**6h**) ^{13}C NMR (400 MHz, CD$_3$OD)
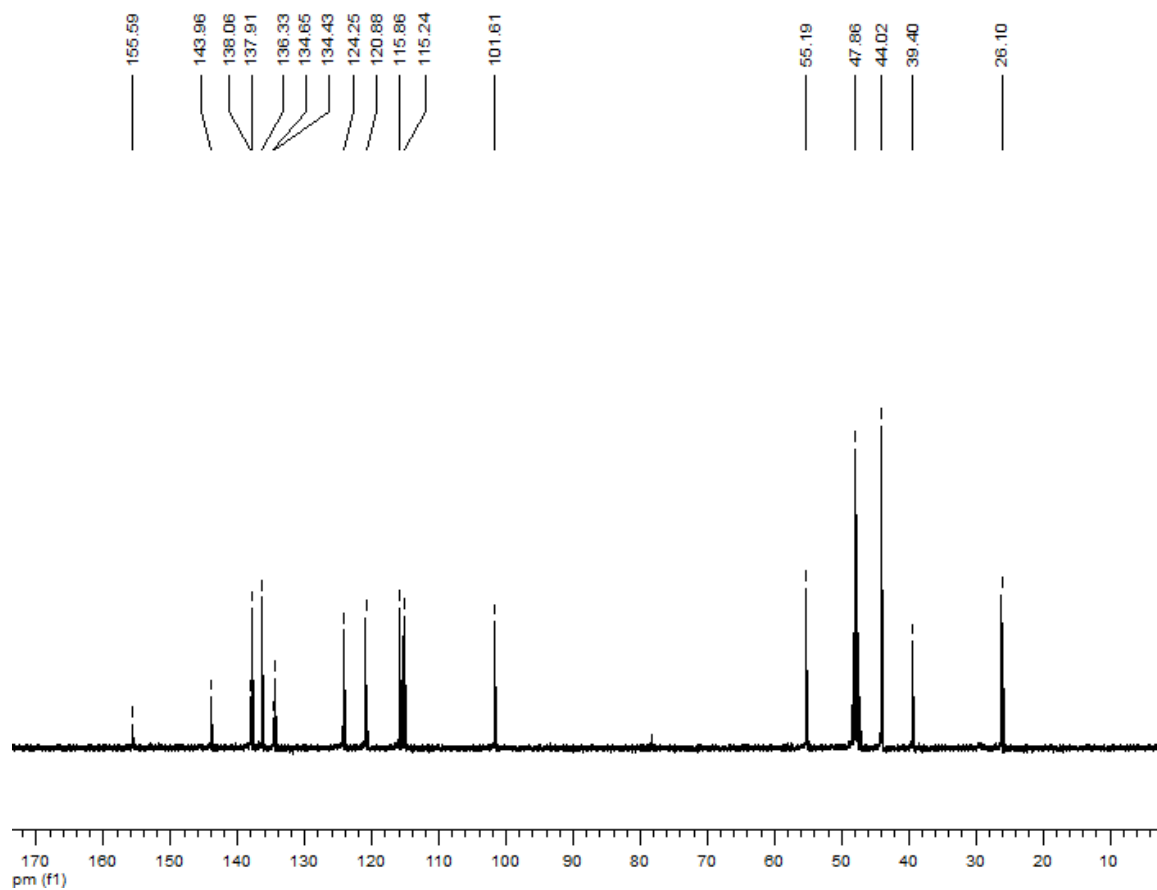
1-(3-(dimethylamino)propyl)-N^6-(pyridin-4-yl)-1H-benzo[d]imidazole-2,6-diamine (6i)
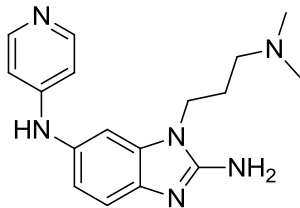
To a 100 ml round bottom flask was added N^3-(3-(dimethylamino)propyl)-4-nitro-N^1-(pyridin-4-yl)benzene-1,3-diamine (**24i**) (652 mg, 1.57 mmol) and 1N HCl aq (50 ml). The reaction was stirred and heated to reflux for 21 hours before cooling to RT. It was extracted with saturated NaHCO3 aq and CHCl$_3$-EtOH : 2 – 1 (100ml and 2 x 200 ml). The combined organic layers were dried over Na$_2$SO$_4$. After filtration and concentration, the crude was purified via flash column chromatography (DCM – MeOH : 80 % - 20 %) to yield off white solid as the product (208 mg, 43 % yield). ^{1}H NMR (400 MHz, CD$_3$OD) δ: 8.01 (d, J = 6 Hz, 2H), 7.22 (d, J = 8 Hz, 1H), 7.04 (d, J = 2 Hz, 1H), 6.92 (dd, J_1 = 8 Hz, J_2 = 2 Hz, 1H), 6.76 (d, J = 6 Hz, 2H), 4.01 (t, J = 7 Hz, 2H), 2.29 (t, J = 7 Hz, 2H), 2.20 (s, 6H), 1.95 – 1.88 (m, 2H). ^{13}C NMR (400 MHz, CD$_3$OD) δ: 155.96, 153.86, 148.72, 139.21, 134.56, 132.20, 117.51, 115.12, 108.33, 103.57, 55.22, 44.01, 39.44, 26.13. MS (ESI) calculated exact mass for C$_{17}$H$_{22}$N$_6$ = 310.19. Found [M+H]$^+$ = 311.3.

Spectrum 3-91: 1-(3-(dimethylamino)propyl)-N^6-(pyridin-4-yl)-1H-benzo[d]imidazole-2,6-diamine **(6i)** ^{1}H NMR (400 MHz, CD$_3$OD)
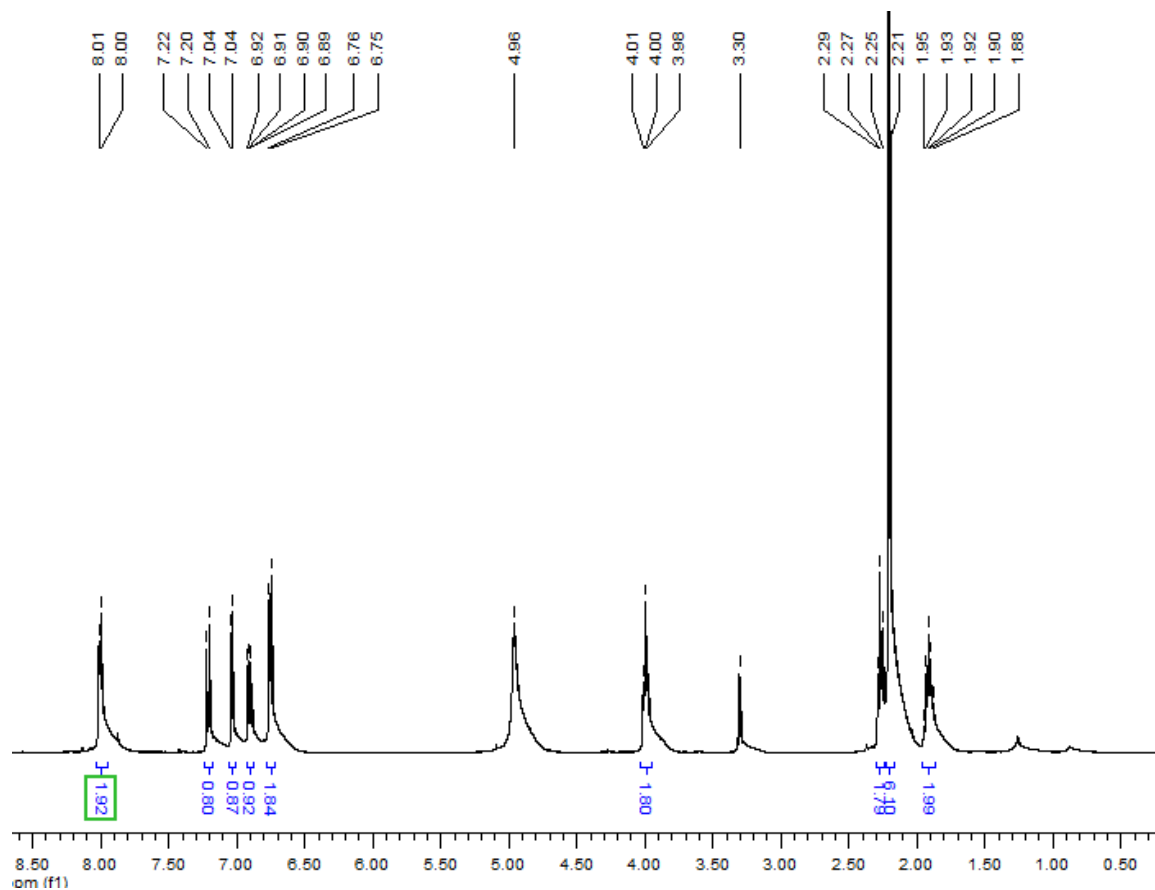
Spectrum 3-92: 1-(3-(dimethylamino)propyl)-N^6-(pyridin-4-yl)-1H-benzo[d]imidazole-2,6-diamine **(6i)** ^{13}C NMR (400 MHz, CD$_3$OD)
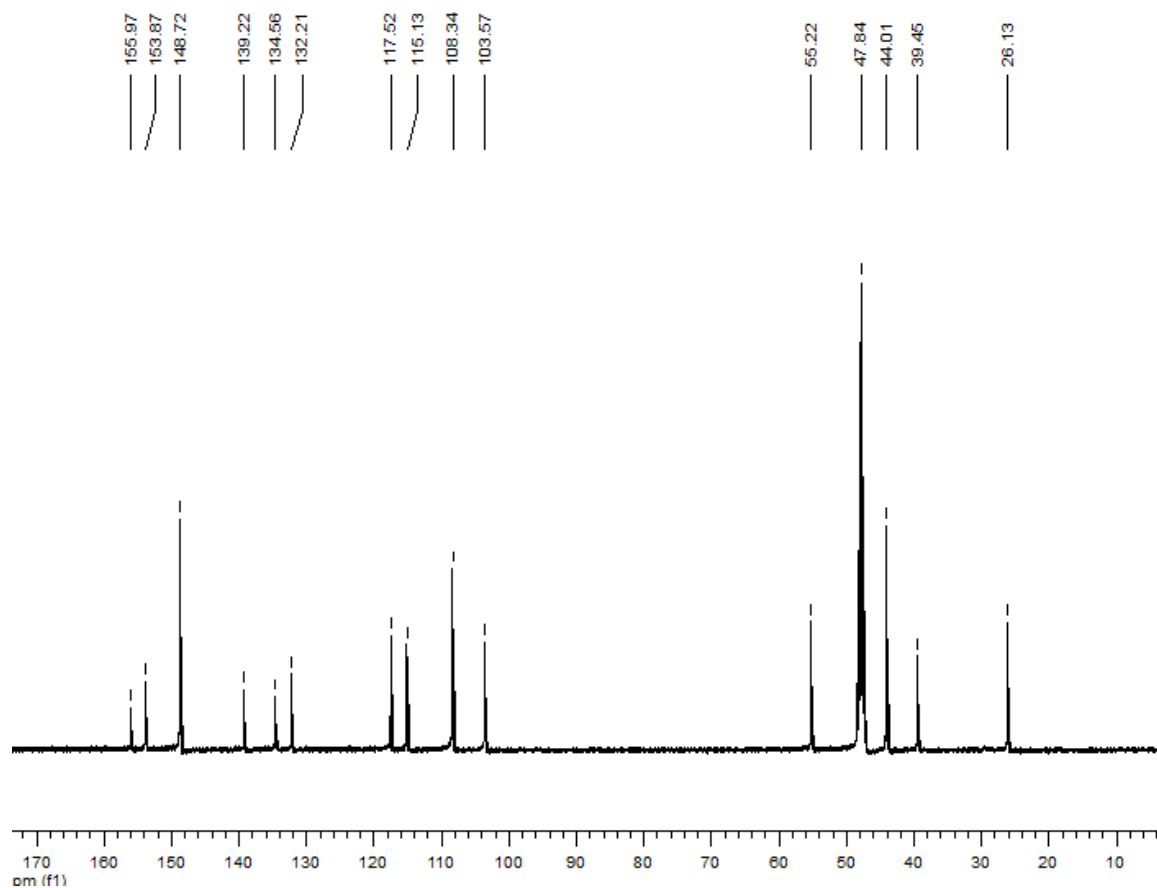
7-(3-(dimethylamino)phenyl)-1-(3-(dimethylamino)propyl)-1*H*-benzo[*d*]imidazol-2-amine (6j)
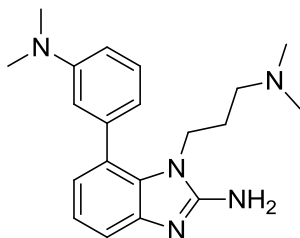
Into a 100 ml round bottom flask was added N-(7-(3-(dimethylamino)phenyl)-1-(3-(dimetylamino)proply)-1H-benzo[d]imidazol-2-yl)benzamide (**24j**) (210 mg, 0.5 mmol) and 1N HCl aq (40 ml). The reaction was stirred and heated to reflux for 17 hours before cooling to RT. It was poured into 200 ml of saturated NaHCO$_3$ and was extracted with chloroform (5 x 100 ml). The combined organic layers were dried over Na$_2$SO$_4$. After filtration and evaporation of solvent, the crude was purified via flash column (DCM − MeOH : 70 % - 30 %) to yield slight yellow oil as the product (73 mg, 46 % yield). ^{1}H NMR (400 MHz, CDCl$_3$) δ:7.40 (d, *J* = 7 Hz, 1H), 7.27 (t, *J* = 7 Hz, 1H), 7.11 (t, *J* = 7 Hz, 1H), 6.87 (d, *J* = 8 Hz, 1H), 6.76 (s, 6H), 6.34 (s, broad, 2H), 3.79 (t, *J* = 6 Hz, 2H, 2.96 (s, 6H), 2.13 (s, 6H), 2.02 (s, 2H), 1.36 (s, 2H). ^{13}C NMR (400 MHz, CDCl$_3$) δ: 156.84, 149.97, 143.37, 140.32, 131.17, 128.54, 126.01, 122.13, 120.61, 118.72, 115.26, 114.64, 111.71, 54.00, 44.59, 40.85, 40.13, 27.04. MS (ESI) calculated exact mass for C$_{20}$H$_{27}$N$_5$ = 337.23. Found [M+H]$^+$ = 338.3.

Spectrum 3-93: 7-(3-(dimethylamino)phenyl)-1-(3-(dimethylamino)propyl)-1*H*-benzo[*d*]imidazol-2-amine **(6j)** ^{1}H NMR (400 MHz, CDCl$_3$)
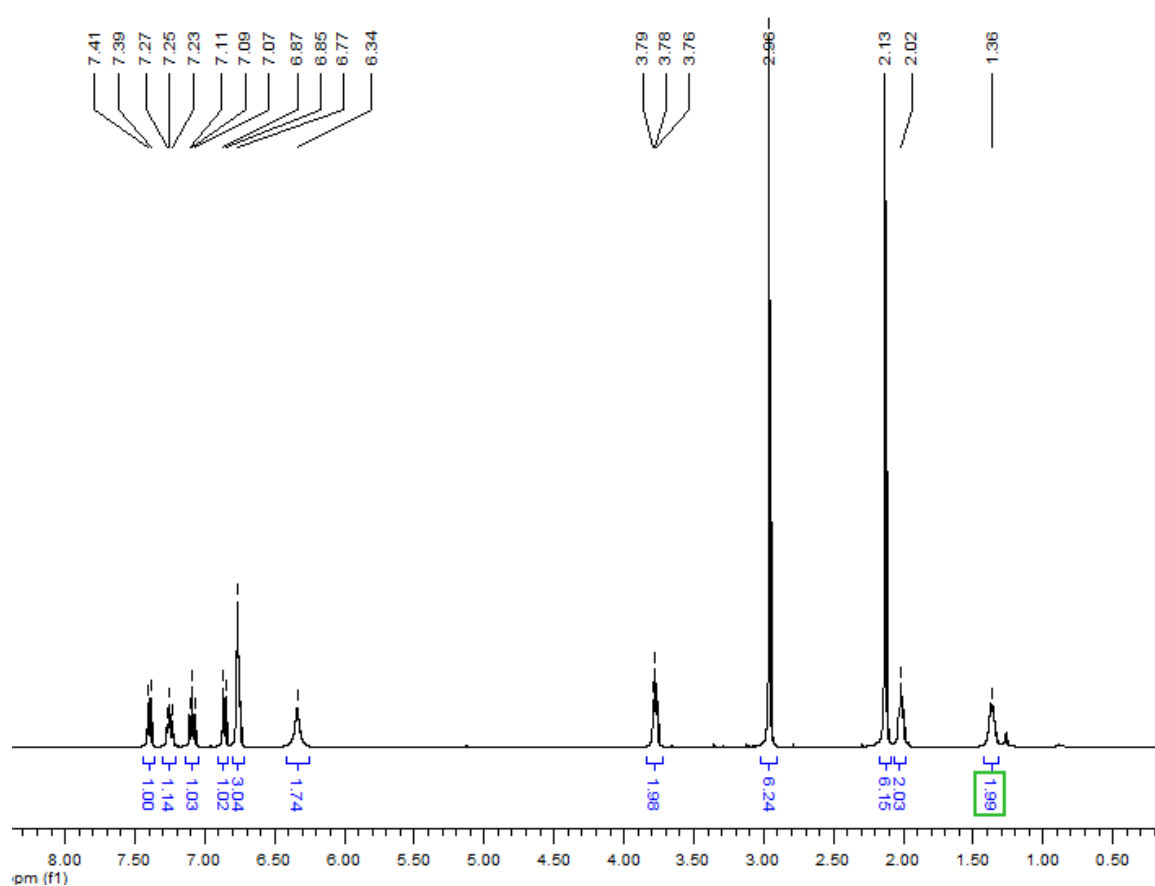
Spectrum 3-94: 7-(3-(dimethylamino)phenyl)-1-(3-(dimethylamino)propyl)-1*H*-benzo[*d*]imidazol-2-amine **(6j)** ^{13}C NMR (400 MHz, CDCl$_3$)
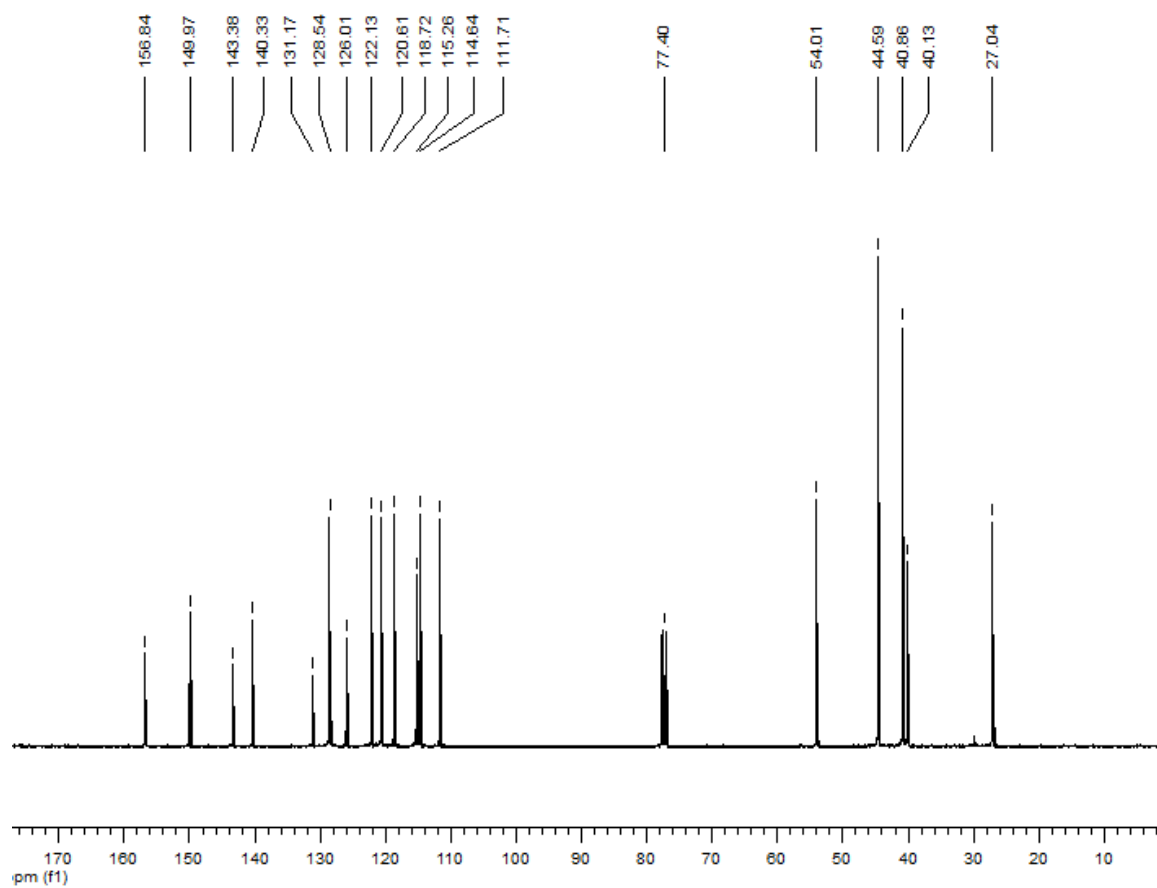
FRET Assay

The compounds were tested in triplicate. The assay solution mix was prepared using PCR tubes with a final volume of 120 μl each. The labeled subdomain IIa RNA (Chapter 2, Figure2-4) was prepared in assay buffer (10 mM HEPES, 2.0 mM $MgCl_2$, pH 7.0). Calculated amount was added to the PCR tube to obtain a final concentration of 100 nM RNA. The compounds were prepared in 50 mM DMSO stocks. They were either added directly or diluted with assay buffer before added to the mix to reach the desired final concentrations. The rest of the volume of the mix was filled using assay buffer. Positive control of the assay was 1 μM benzimidazole **2** (Figure 3-2). Negative control was 100 nM RNA and assay buffer without a compound.

The prepared assay mix was heated to 65 °C for 5 minutes and then cooled to 4 °C. The sample was spun down and 100 μl of the mix was loaded onto a 96 well plate. The plate was read by a plate reader. Excitations and emissions of the Cy3 (520/570 nm) and Cy5 (620/670 nm) labels were read. EC_{50} value was determined from fitting of single-site binding dose response curves to the titration data using Sigma Plot program.

This chapter, in part, has been accepted for publication of the material as it may appear in: Ding, K.; Wang, A.; Boerneke, M.A.; Dibrov, S.M.; Hermann, T. Aryl-substituted aminobenzimidazoles targeting the hepatitis C virus internal ribosome entry site. *Bioorg. Med. Chem. Lett*. 2014, In press. The dissertation author was the primary investigator and author of this material.

References

(1)   Seth, P. P.; Miyaji, A.; Jefferson, E. A.; Sannes-Lowery, K. A.; Osgood, S. A.; Propp, S. S.; Ranken, R.; Massire, C.; Sampath, R.; Ecker, D. J.; Swayze, E. E.; Griffey, R. H. *J Med Chem* **2005**, *48*, 7099.

(2)   Parker, M. A.; Satkiewicz, E.; Hermann, T.; Bergdahl, B. M. *Molecules* **2011**, *16*, 281.

(3)   Berry, K. E.; Peng, B.; Koditek, D.; Beeman, D.; Pagratis, N.; Perry, J. K.; Parrish, J.; Zhong, W.; Doudna, J. A.; Shih, I. H. *J Biomol Screen* **2011**, *16*, 211.

(4)   Walters, W. P.; Stahl, M. T.; Murcko, M. A. *Drug Discovery Today* **1998**, *3*, 160.

(5)   Seifert, M. H.; Kraus, J.; Kramer, B. *Curr Opin Drug Discov Devel* **2007**, *10*, 298.

(6)   Lyne, P. D. *Drug Discovery Today* **2002**, *7*, 1047.

(7)   Jorgensen, W. L. *Science* **2004**, *303*, 1813.

(8)   Bostrom, J.; Berggren, K.; Elebring, T.; Greasley, P. J.; Wilstermann, M. *Bioorgan Med Chem* **2007**, *15*, 4077.

(9)   Oprea, T. I.; Matter, H. *Curr Opin Chem Biol* **2004**, *8*, 349.

(10)   Jain, A. N. *Current Opinion in Drug Discovery & Development* **2004**, *7*, 396.

(11)   McInnes, C. *Curr Opin Chem Biol* **2007**, *11*, 494.

(12)   Lavecchia, A.; Di Giovanni, C. *Curr Med Chem* **2013**, *20*, 2839.

(13)   Gillet, V. J. *Wires Comput Mol Sci* **2011**, *1*, 580.

(14)   Mestres, J. *Biochem Soc T* **2002**, *30*, 797.

(15)   Lang, P. T.; Brozell, S. R.; Mukherjee, S.; Pettersen, E. F.; Meng, E. C.; Thomas, V.; Rizzo, R. C.; Case, D. A.; James, T. L.; Kuntz, I. D. *RNA* **2009**, *15*, 1219.

(16)   Martin, Y. C.; Kofron, J. L.; Traphagen, L. M. *J Med Chem* **2002**, *45*, 4350.

(17)   Eckert, H.; Bajorath, J. *Drug Discov Today* **2007**, *12*, 225.

(18)   Muchmore, S. W.; Edmunds, J. J.; Stewart, K. D.; Hajduk, P. J. *J Med Chem* **2010**, *53*, 4830.

(19)   Sauer, W. H. B.; Schwarz, M. K. *J Chem Inf Comp Sci* **2003**, *43*, 987.

(20)   Nicholls, A.; McGaughey, G. B.; Sheridan, R. P.; Good, A. C.; Warren, G.; Mathieu, M.; Muchmore, S. W.; Brown, S. P.; Grant, J. A.; Haigh, J. A.; Nevins, N.; Jain, A. N.; Kelley, B. *Journal of Medicinal Chemistry* **2010**, *53*, 3862.

(21)   Moffat, K.; Gillet, V. J.; Whittle, M.; Bravi, G.; Leach, A. R. *Journal of Chemical Information and Modeling* **2008**, *48*, 719.

(22)   McGaughey, G. B.; Sheridan, R. P.; Bayly, C. I.; Culberson, J. C.; Kreatsoulas, C.; Lindsley, S.; Maiorov, V.; Truchon, J. F.; Cornell, W. D. *J Chem Inf Model* **2007**, *47*, 1504.

(23)   Pandit, D.; So, S. S.; Sun, H. M. *Journal of Chemical Information and Modeling* **2006**, *46*, 1236.

(24)   Ballester, P. J.; Richards, W. G. *J Comput Chem* **2007**, *28*, 1711.

(25)   Bologa, C. G.; Revankar, C. M.; Young, S. M.; Edwards, B. S.; Arterburn, J. B.; Kiselyov, A. S.; Parker, M. A.; Tkachenko, S. E.; Savchuck, N. P.; Sklar, L. A.; Oprea, T. I.; Prossnitz, E. R. *Nat Chem Biol* **2006**, *2*, 207.

(26)   Rush, T. S., 3rd; Grant, J. A.; Mosyak, L.; Nicholls, A. *J Med Chem* **2005**, *48*, 1489.

(27)   Kirchmair, J.; Distinto, S.; Markt, P.; Schuster, D.; Spitzer, G. M.; Liedl, K. R.; Wolber, G. *J Chem Inf Model* **2009**, *49*, 678.

(28)   Paulsen, R. B.; Seth, P. P.; Swayze, E. E.; Griffey, R. H.; Skalicky, J. J.; Cheatham, T. E., 3rd; Davis, D. R. *Proc Natl Acad Sci U S A* **2010**, *107*, 7263.

(29)   Dibrov, S. M.; Ding, K.; Brunn, N. D.; Parker, M. A.; Bergdahl, B. M.; Wyles, D. L.; Hermann, T. *Proc Natl Acad Sci U S A* **2012**, *109*, 5223.

(30)   Irwin, J. J.; Shoichet, B. K. *J Chem Inf Model* **2005**, *45*, 177.

(31)   Irwin, J. J.; Sterling, T.; Mysinger, M. M.; Bolstad, E. S.; Coleman, R. G. *J Chem Inf Model* **2012**, *52*, 1757.

(32)   Lipinski, C. A.; Lombardo, F.; Dominy, B. W.; Feeney, P. J. *Adv Drug Deliv Rev* **2001**, *46*, 3.

(33)   Lipinski, C. A. *J Pharmacol Toxicol Methods* **2000**, *44*, 235.

(34)   Tietze, M.; Iglesias, A.; Merisor, E.; Conrad, J.; Klaiber, I.; Beifuss, U. *Organic Letters* **2005**, *7*, 1549.

Chapter 4. Design and Synthetic Development of 2-Aminoquinazolin-4-one and 2-Amino-*lin*-benzoguanine Analogs Targeting HCV IRES Subdomain IIa RNA

Ligand-Bound HCV IRES Subdomain IIa RNA X-Ray Crystal Structure

The high resolution X-ray crystal structure of HCV IRES subdomain IIa in complex with benzimidazole inhibitor **2** was solved in 2012 [1], which revealed key interactions that further guided the design and data analysis of aryl-substituted benzimidazoles (Chapter 3). As seen in the crystal complex, the subdomain IIa of the HCV IRES refolds at its internal loop region and forms a well defined and tightly fitting binding pocket that surrounds the bound benzimidazole inhibitor (**Figure 4-1**), causing the extension of the original bent conformation of domain IIa in the absence of a bound ligand to an overall linear structure (**Figure 4-1.a**). This is in agreement with the findings from the FRET study [2].

The binding of the ligand to the domain IIa internal loop is mediated mainly through hydrogen bonding and stacking interactions. The nitrogen atoms of the 2-aminoimidazole moiety of **2** form two hydrogen bonds with the guanine Hoogsteen edge in the C58-G110 base pair (**Figure 4-1.c**). A third hydrogen bond occurs between the protonated dimethylamino-proply side chain of the ligand and the phosphate group

of A109. The benzimidazole also forms stacking interactions between A53 above and the

G52-C111 pair below (**Figure 4-1.b**).
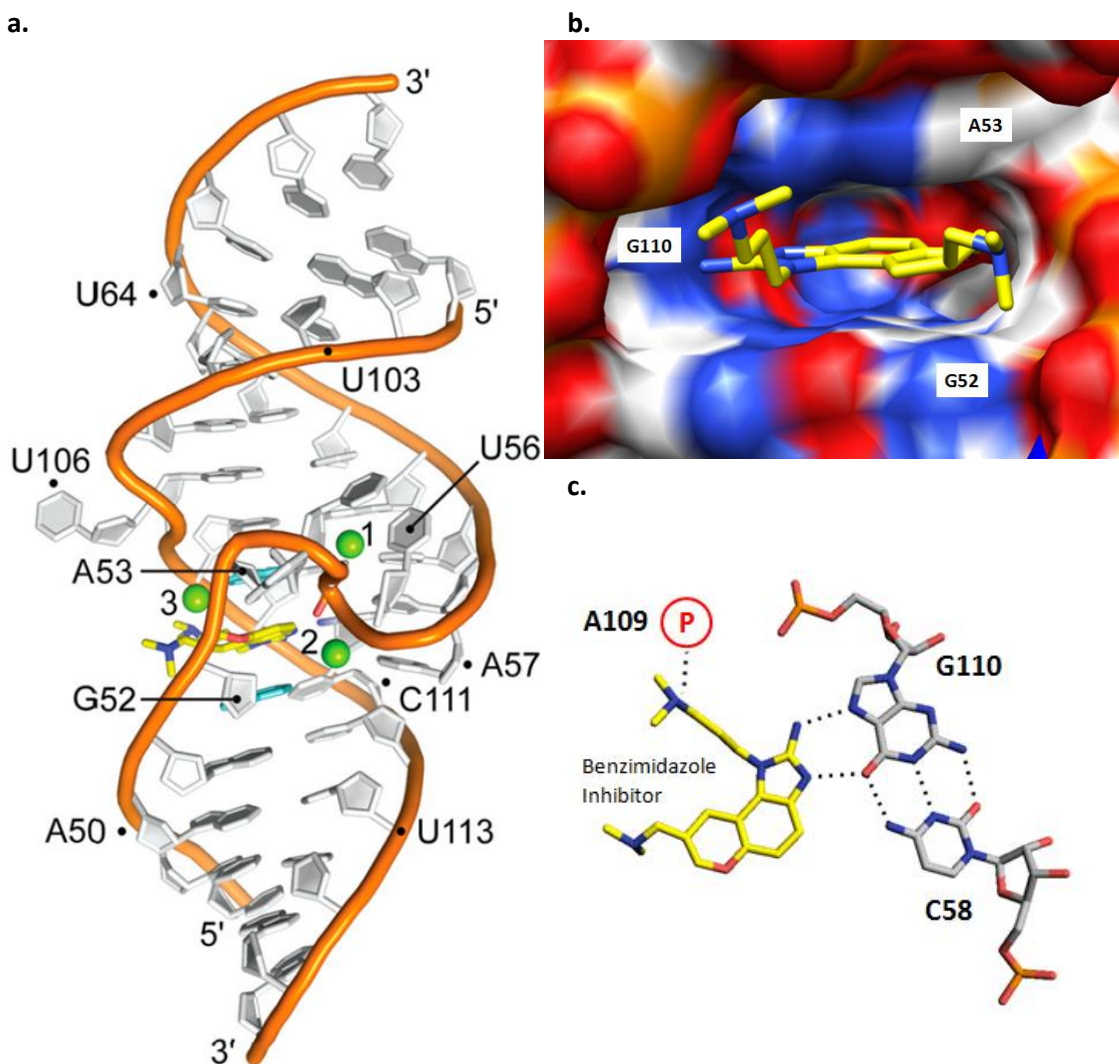
Figure 4-1: Crystal structure of the HCV subdomain IIa RNA bound with benzimidazole inhibitor **2** [1] (PDB ID: 3TZR). **a**. The overall linear architecture of the ligand bound RNA structure. **b**. Ligand docked inside the binding pocket that is shown in surface representation. **c**. The benzimidazole inhibitor forms two hydrogen bonds with the guanine Hoogsteen edge in the C58-G110 base pair, and one additional hydrogen bond with the phosphate group of A109.

Structural Similarity with Self-Splicing Group I Intron Base Triple

The RNA self-splicing group I intron, first found in *Tetrahymena* [3], catalyzes the splicing of an intron from the preribosomal RNA transcripts with the concomitant union of two exons [4]. This intricate reaction occurs in the absence of any protein thereby demonstrates the first enzymatic activity found outside the protein family [5]. In order to achieve this highly selective function, the terminal guanosine residue at the 3' splice site of the intron must interact with the intron's internal guide sequence.

As seen in the high resolution X-ray crystal structures [6], the 3' terminal guanosine (G414) interacts with a G264-C311 base pair at the binding site to form a planar base triple structure (**Figure 4-2**). The guanosine pairs at the binding site guanosine (G264) Hoogsteen edge through two hydrogen bonds, one with its imidazole ring nitrogen and the other with the carbonyl oxygen respectively. Meanwhile, the cytosine exocyclic amine of the guanosine (G414) interacts with the cytosine (C311) exocyclic amine via its carbonyl oxygen.
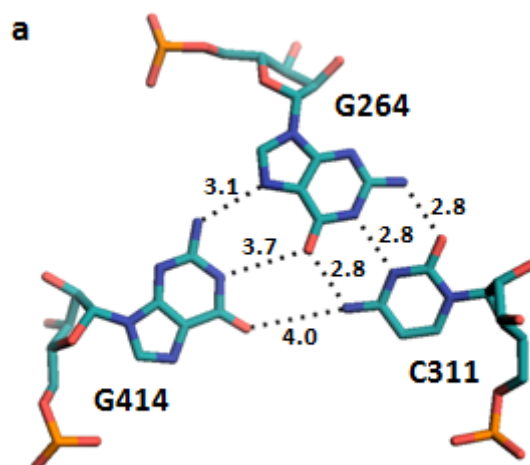
Figure 4-2: Structures of planar base triples found in *Tetrahymena* self-splicing group I intron RNA. Residue numberings are from the original publication. Hydrogen bonds are indicated in dash lines and distances are labeled. Base triple seen in a 3.8 Å resolution crystal structure of the intron in the absence of its RNA substrate [7] (PDB: 1X8W).

The interactions within group I intron base triple resemble that between the benzimidazole **2** and the HCV IRES subdomain IIa (**Figure 4-1.c**), where the small molecule pairs with the Hoogsteen edge of G110 through two hydrogen bonds. The difference, however, is that the smaller imidazole ring and the absence of a carbonyl group that prevent further interaction with the C58.

2-Amino-quinazolin-4-one and 2-Amino-*lin*-benzoguanine

Based on the X-ray crystal structures, it was hypothesized that expending the imidazole ring of a benzimidazole to a six-member amino-pyrimidone ring such as the one in 2-aminoquinazolin-4-one **26** (**Figure 4-3**) would provide additional H-bond interaction between the ligand and the C58 of HCV subdomain IIa RNA and improve the

binding affinity of the ligand. Alternatively, both the amino-imidazole ring and amino-pyrimidone ring can be incorporated into one scaffold of the 2-amino-*lin*-benzoguanine **27** (2,6-diamino-3*H*-imidazo[4,5-*g*]quinazolin-8(7*H*)-one) (**Figure 4-3**), where the amino-pyrimidone side of the molecule form H-bond interaction with the binding site G-C base pairs while the amino-imidazole can form additional H-bonds with the IIa RNA to provide further stabilization of the binding.

2-aminoquinazolin-4-one
26

2-amino-*lin*-benzoguanine **27**
(2,6-diamino-3*H*-imidazo[4,5-*g*]quinazolin-8(7*H*)-one)
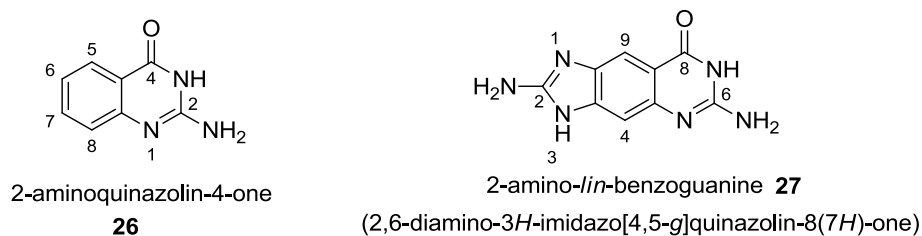
Figure 4-3: Structures of the 2-aminoquinazolin-4-one **26** (left) and 2-amino-lin-benzoguanine **27** (2,6-diamino-3*H*-imidazo[4,5-*g*]quinazolin-8(7*H*)-one (2-amino-*lin*-benzoguanine) (right).

Structural Comparison of Guanine, 2-Aminoquinazolin-4-one, 2-Amino-*lin*-benzoguanine and their Binding to the G-C Base Pair

Guanine's unique structure allows it to form H-bond interactions with the G-C base pair seen in the group I intron RNA. The structure of guanine is a fused pyrimidone-imidazole ring system with conjugated double bonds (**Figure 4-4**). The biological activity of guanine is primarily based upon its hydrogen bond forming capability with cytosine in the DNA and RNA. In a Watson-Crick guanosine-cytidine (G-C) base pair (**Figure 4-4**), guanine forms three hydrogen bonds through its amino-pyrimidone ring that contributes one hydrogen bond acceptor via carbonyl oxygen and two hydrogen bond donors via two NH's.
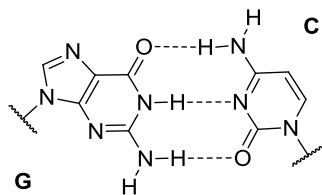
Figure 4-4: Structure of Watson-Crick Guanosine (**G**) – Cytidine (**C**) base pair that has three intermolecular hydrogen bonds.

The structure of 2-aminoquinazolin-4-one is similar to the guanine nucleobase structure, where the imidazole ring of guanine is replaced by a benzene and the amino-pyrimidone ring through which the H-bond forming capability is maintained (**Figure 4-5**). There are three main benefits to include a benzene ring of the 2-aminoquinazolin-4-one compared to a imidazole moiety. First, it maintains the capability of 2-aminoquinazolin-4-one molecule to stack with base pairs above and below the binding plane. Second, it greatly reduces the polarity and basicity of the scaffold by the carbonyl electron withdrawing group so that the scaffold is more drug-like. Third, the imidazole ring of guanine, when not protected, have two tautomeric forms that will give rise to a mixture of regio-isomers upon protection or substitution that need to be separated. By comparison, a benzene ring is relatively easier to synthesize and functionalize. Selective substitutions at different positions of the ring can facilitate future structure-activity-relationship studies.
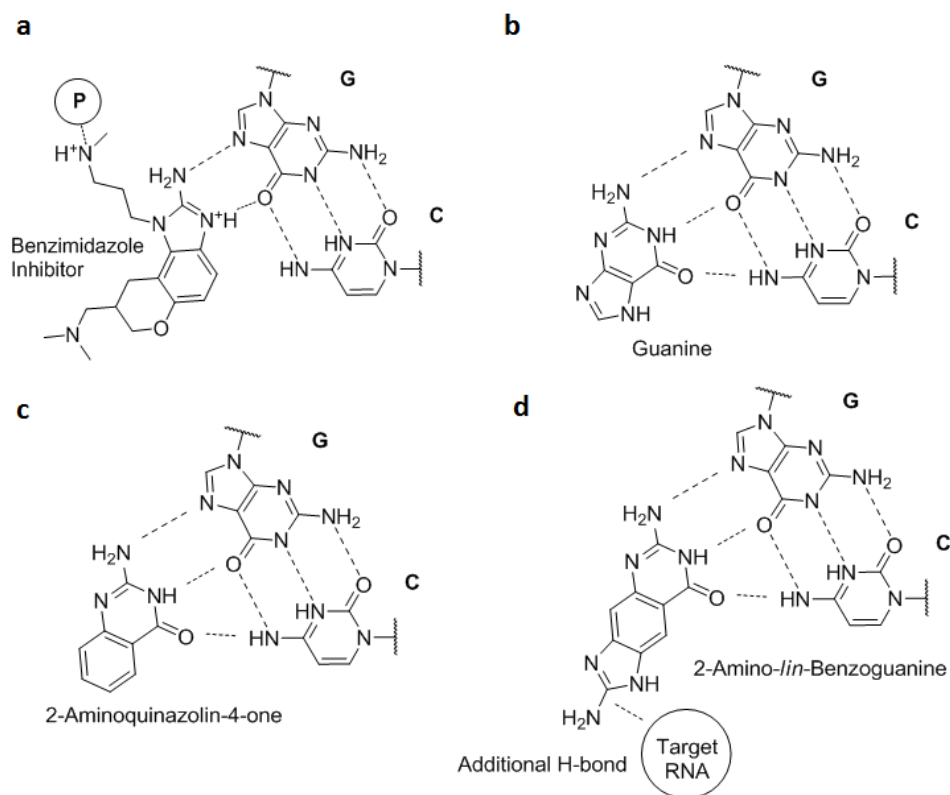
Figure 4-5: Schematic structures and interactions of benzimidazole, guanine, 2-amino-quinazolin-4-one, 2-amino-*lin*-benzoguanine and G-C base pair. **a**. Observed interactions between benzimidazole and G-C base pair at the binding site in subdomain IIa cocrystal structure [1] ; **b**. Structure of guanine and its H-bond interactions with the G-C base pair as seen in the group I intron base triple crystal structure [6]; **c**. Structure of 2-aminoquinazolin-4-one and its predicted H-bond interaction with the binding site G-C base pair of the HCV IRES subdomain IIa RNA. **d**. Structure of 2-amino-*lin*-benzoguanine and its predicted H-bond interactions with the binding site G-C base pair of the HCV IRES subdomain IIa RNA.

The 2-amino-*lin*-benzoguanine scaffold can be seen as either a guanine with benzene insertion or as an integration of 2-aminoquinazolin-4-one and benzimidazole. It has both the imidazole and the amino-pyrimidone rings that can theoretically provide additional stacking interaction as well as more hydrogen bonds with the target RNA (**Figure 4-5**). It is also a longer molecule than the 2-aminoquinazolin-4-one scaffold so

that it docks tightly in the binding site (**Figure 4-6**). The amino-imidazole ring nitrogen atoms are in close proximity to the dimethyl-amino side chain of the benzimidazole **2** that can potentially stabilize the binding by forming H-bond interaction with the RNA.

It is possible that the 2-amino-*lin*-benzoguanine have two binding modes with the RNA. Either the amino-pyrimidone or the amino-imidazole can bind to the binding site G-C base pair. Although the amino-pyrimidone ring can form three hydrogen bonds with the G-C base pair, the amino-imidazole ring, on the other hand, is more basic than the amino-pyrimidone. It is therefore difficult to predict which binding mode is favored.

The potential that the flat molecule may interact non-specifically can be overcome by inclusion of substitutions at various positions. For example, modifications can be made at either or both of the two nitrogens (N3 and N5) and/or the benzene carbon (C4) located on the side of the molecule that is predicted to point away from the binding site.
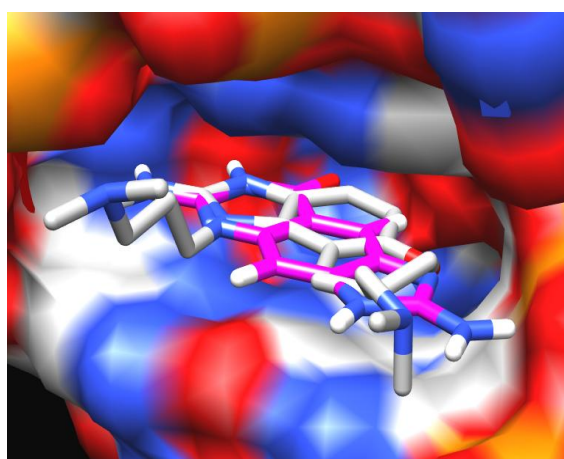
Figure 4-6: 2-Amino-*lin*-benzoguanine (pink) is docked more tightly at the ligand binding site. The co-crystal structure of benzimidazole inhibitor **2** is shown in white and HCV IRES subdomain IIa RNA is shown in surface presentation.

Preliminary FRET Assay Testing of Guanine and 2-Aminoquinazolin-4-one

Inspired by the finding in the interactions as seen in the group I intron base triple, guanine and 2-aminoquinazolin-4-one molecules that are commercially available were tested using FRET assay that has been described before [8,9]. As shown in the titration curves (**Figure 4-7**), the FRET signals decrease as the concentrations of molecules increase, indicating the binding of the molecules to the binding site and the widening of the interhelical angle of the RNA. The binding affinities of both molecules were very weak and accurate EC_{50} values could not be calculated based on the data available. However, the binding of both compounds to the subdomain IIa RNA called for further development of the 2-aminoquinazolin-4-one and 2-amino-*lin*-benzoguanine molecules targeting the HCV IRES subdomain IIa RNA.
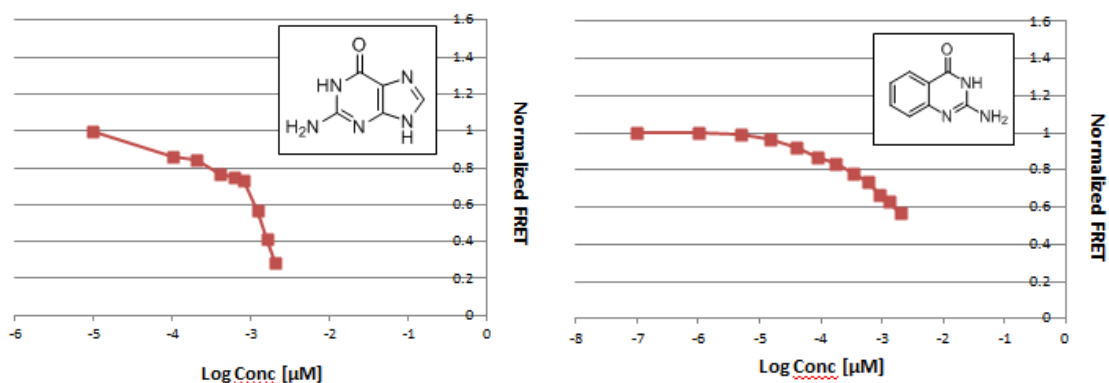
Figure 4-7: Titration of guanine (left) and 2-amino-quinazolin-4-one (right) in the FRET assay using labeled subdomain IIa RNA construct (Chapter 2). The binding affinities of both molecules were very weak and accurate EC_{50} values could not be calculated based on the data available.

The Design of 2-Aminoquinazolin-4-one and 2-Amino-*lin*-benzoguanine Molecules Targeting HCV IRES Subdomain IIa RNA

Based on the structure analysis of the two scaffolds and their predicted binding modes to the binding site G-C base pair, the preferred substitution sites of the two scaffolds will be positions N1 and C7 for 2-aminoquinazolin-4-one and positions N3 and N5 for 10-amino-*lin*-benzoguanine. These positions were preferred because they all locate at the opposite side from the binding pocket of the RNA. They also do not participate in key binding interactions with the target RNA (**Figure 4-5**). And there is space available near these positions for the addition of substitutions based on the docking study (**Figure 4-6**).

C8 of 2-aminoquinazolin-4-one and C4 of 2-amino-*lin*-benzoguanine could also be used as substitution sites. They are less favorable because they locate farther away from the left and right ends of the molecules where interactions with the RNA were observed based on the co-crystal structure. Longer linkers maybe required to allow terminal functional groups to interact with the RNA. The substitutions at the N1 and/or C7 position of 2-aminoquinazolin-4-one and N1 and/or N9 position of 10-amino-*lin*-benzoguanine are the most suitable (**Figure 4-8**).
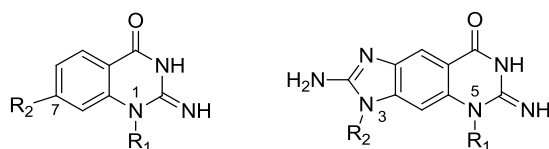
Figure 4-8: The preferred substitution positions of the 2-aminoquinazolin-4-one scaffold (left) and 2-amino-*lin*-benzoguanine scaffold (Right).

Prior Synthesis of 2-Amino-*lin*-benzoguanine

Being the more complex of the two, 2-amino-*lin*-benzoguanine synthesis was

studied first with the hope that its synthetic development would greatly simplify the

synthesis of 2-aminoquinazolin-4-one. The SciFinder search of the 2-amino-*lin*-

benzoguanine resulted in a single article that described the synthesis of the *lin*-

benzoguanine and its related analogues and their use as tRNA-guanine transglycosylase

inhibitors [10]. The synthesis of 2-amino-*lin*-benzoguanine was also included in this article.

According to the article, the synthesis of *lin*-benzoguanine commences from

benzimidazole-carboxylic acid **27**, which after conversion to methyl-ester **28** was

nitrated to install the nitro group *ortho* to the ester (**Scheme 4-1**). Catalytic reduction of

the nitro group of **29** followed by cyclization reaction using chloroformamidinium

chloride **32** then gave *lin*-benzoguanine **31.**
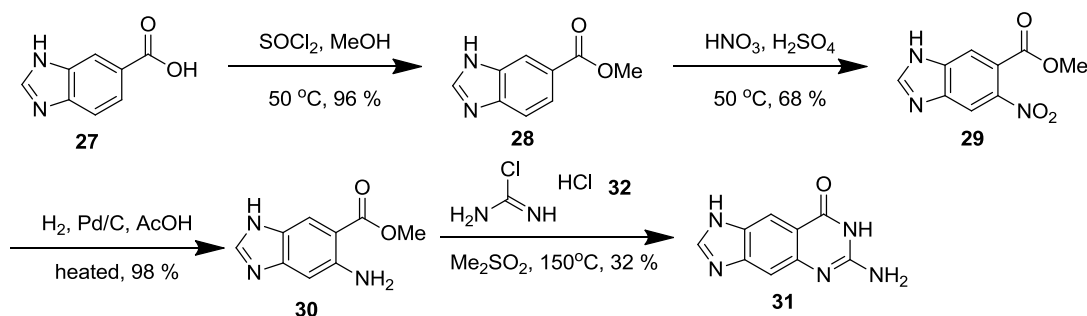
Scheme 4-1: Synthesis of lin-benzoguanine from 1*H*-benzimidazole-6-carboxylic acid [10].

Functionalization of the C2 position of imidazole ring was achieved by treating

the protected benzimidazole **34** with LiN(TMS)$_2$ and CBr$_4$ (**Scheme 4-2**). The brominated

product **35** then reacted with 4-(aminomethyl)-pyridine **36** to afford the 2-aminomethyl-

pyridine-substituted benzimidazole **37**. Reduction of the nitro group with Zn provided

the amine that was further reacted with chloroformamidinium chloride **32** to give crude

39. The dimethylamino-sulfonyl protecting group was removed during this reaction. The

HPLC purification of **39** using water (3% TFA) and acetonitrile (ACN) resulted yielded 2-

amino-*lin*-benzoguanie **27**.
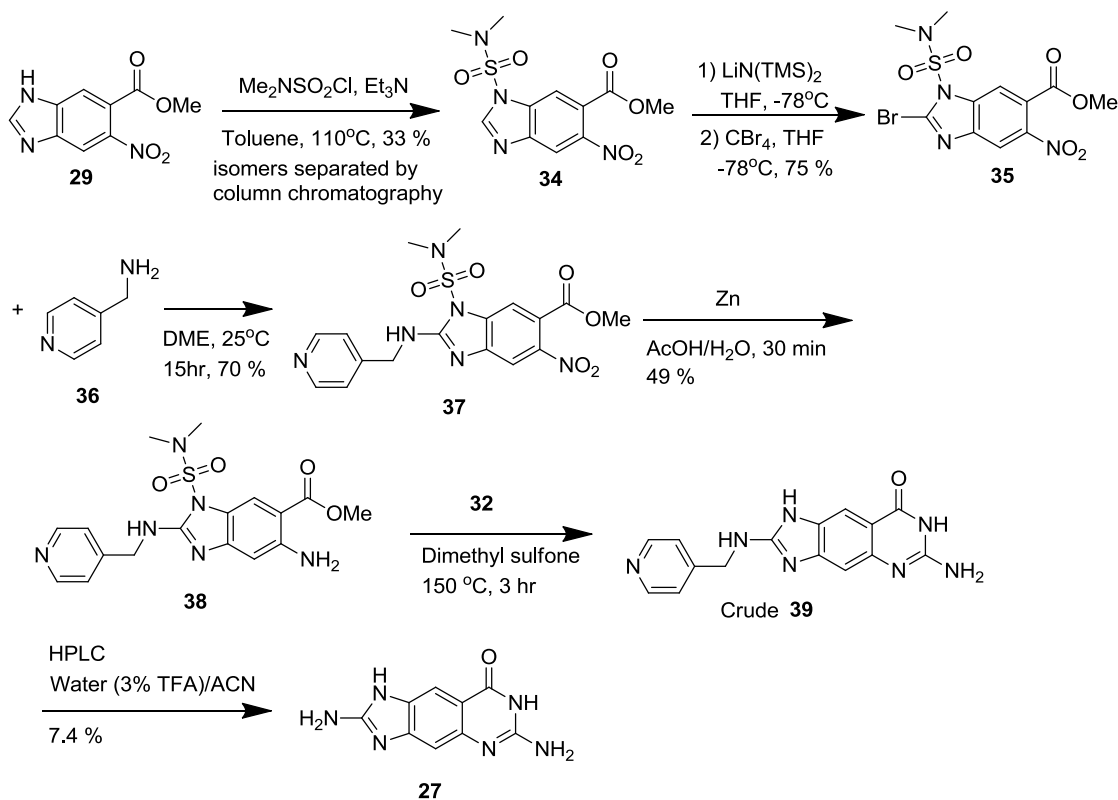
Scheme 4-2: Synthesis of 2-amino-lin-benzoguanine **27** from benzimidazole **29**.

There are a few drawbacks of this reported synthesis. First of all, It was not

intended specifically for the 2-amino-lin-benzoguanine molecule. Instead **27** was

purified as a byproduct from the ring-closing reaction. It was not clear whether the

methyl-pyridine group was removed during the ring-closing reaction or during the HPLC

purification of crude **39**. The yield of **27** from **38** was low.

There were two reactions from the described synthesis that gave mixtures of products. First, a mixture of products were synthesized in the nitration reaction. The directing effect of the precursor of the nitration reaction had limited the yield of the reaction because it didn't favor either one of the two regioisomers that were synthesized, although the reported yield slightly favored the desired product. Second, the protection of the imidazole N-H by dimethyl-sulfonyl group also yielded a mixture of products, resulting from the two tautomers of the benzimidazole **33**. Although only one final product would be obtained after deprotection, this mixture of compounds complicated the synthesis, purification and identification of intermediate molecules.

The amino-pyrimidone ring closing reaction was carried out using harsh reaction conditions at 150 °C and a non-conventional solvent dimethyl sulfone that is a crystalline solid at room temperature. Dimethyl sulfone melted at 109 °C before it could serve as the solvent for the reaction. It is predicted that dimethylsulfone can be difficult to remove.

In addition, at elevated temperature, the dimethyl-sulfonyl protecting group was lost. The deprotected imidazole ring nitrogen of **39** could be reactive towards the chloroform amidinium chloride **32** and therefore compete with the amine that was *ortho* to the methyl-ester of **38** to give rise to undesired byproducts. This might be partially responsible for the low yield of the ring-closing reaction.

In summary, the reported synthesis of the 2-amino-*lin*-benzoguanine does not provide a straight forward and high-yielding pathway to the molecule. A new synthetic

strategy needs to be developed to suit our molecular design as well as improved chemical efficiency.

Retro-synthetic Analysis of 2-Amino-*lin*-benzoguanine

The synthetic challenge of the 2-amino-*lin*-benzoguanine arises mainly from 1) the two ring-closing reactions for the amino-imidazole ring and the amino-pyrimidone ring, 2) the nitration reaction, and 3) the functionalization of the scaffold.

The sequence of the ring-closing can have significant impact of the synthesis. If the amino-imidazole ring is closed first as similar to what has been described by Hortner et al [10], the synthesis of 2-amino-lin-benzoguanine **27** can begin with 4-chloro-3-nitrobenzoic acid **43** (**Scheme 4-3**). After protection of the benzoic acid functional group, the chlorine of **42** can be substituted easily by an amine since this position is activated by both the *ortho* nitro and the *para* carbonyl electron withdrawing groups. After reduction of the nitro group, the 2-amino-benzimidazole **41** can be synthesized using reagents like cyanogene bromide or isothiocyanate that have been described in the previous chapter. Nitration of **41** will likely give a mixture of two products that need to be purified. Once the compound **40** is obtained, its nitro group is reduced and the resulting aniline can react with a ring closing reagent to give the final product **27**.
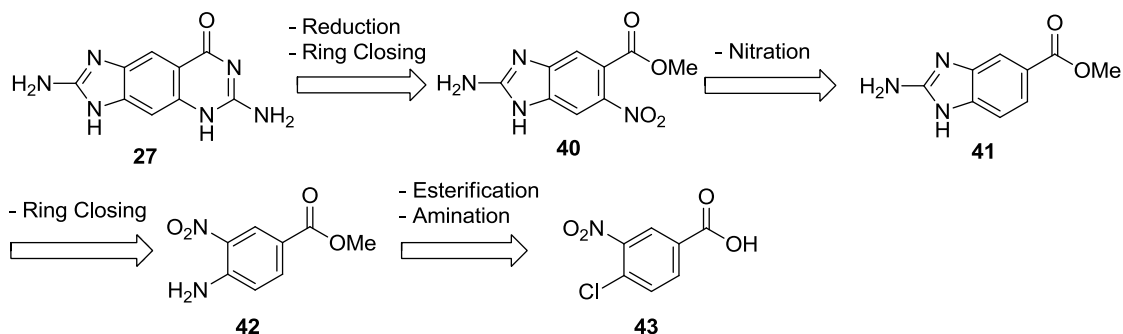
Scheme 4-3: Retro-synthesis of 2-amino-*lin*-benzoguanine scaffold using 4-chloro-3-nitrobenzoic acid as the starting material.

Alternatively, the sequence of the ring-closing reactions can be switched [11], that is the amino-imidazole ring is to be closed after the amino-pyrimidone ring. Using this strategy, 2-amino-*lin*-benzoguanine **27** can be synthesized from either of the two readily available starting materials, 2,4-dichlorobenzoic acid **47** or 4-chloro-2-nitrobenzoic acid **48** (**Scheme 4-4**). The final ring closing of the amino-imidazole ring in **27** requires the presence of *ortho* diamine. This can be achieved by reduction of the nitro functional group in **44**. The nitro group in turn can be installed by nitration reaction of **45**. The analysis of the directing effect of functional groups in **45** indicated that the **44** can be synthesized as the more favored product because of less steric hindrance. **45** can be synthesized by the ring-closing reaction from **46**, which can be made by esterification and amination or reduction from **47** and **48** respectively.
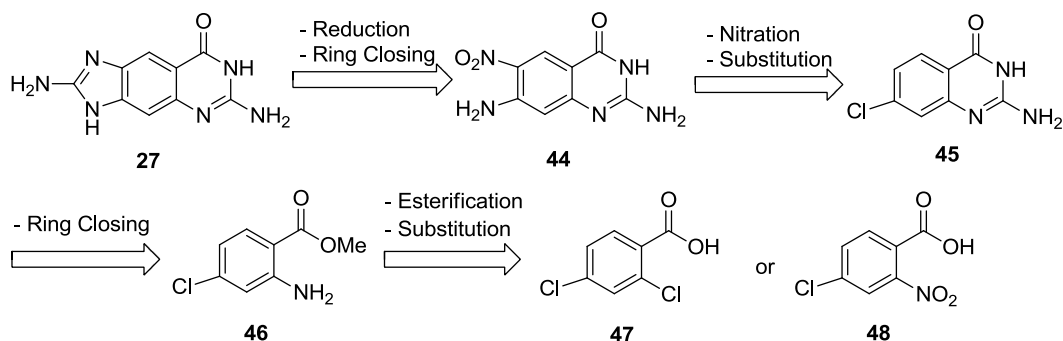
Scheme 4-4: Retro-synthesis of 2-amino-*lin*-benzoguanine scaffold using 2,4-dichlorobenzoic acid **47** or 4-chloro-2-nitrobenzoic acid **48** as the starting material.

One advantage of the retro-synthesis illustrated in **Scheme 4-4** is that once **46** is synthesized, it can either be modified at the *para*- chloro position or directly undergo ring-closing reaction to give 2-aminoquinazolin-4-one molecules **45** and **49** (**Scheme 4-5**). The disadvantage of this strategy is that the carboxylic functional group is a relatively weak electron-withdrawing group. The substitutions at both *ortho*- and *para*-chloro positions can be difficult under non-catalyzed nucleophilic aromatic substitution (S$_N$Ar) reaction.
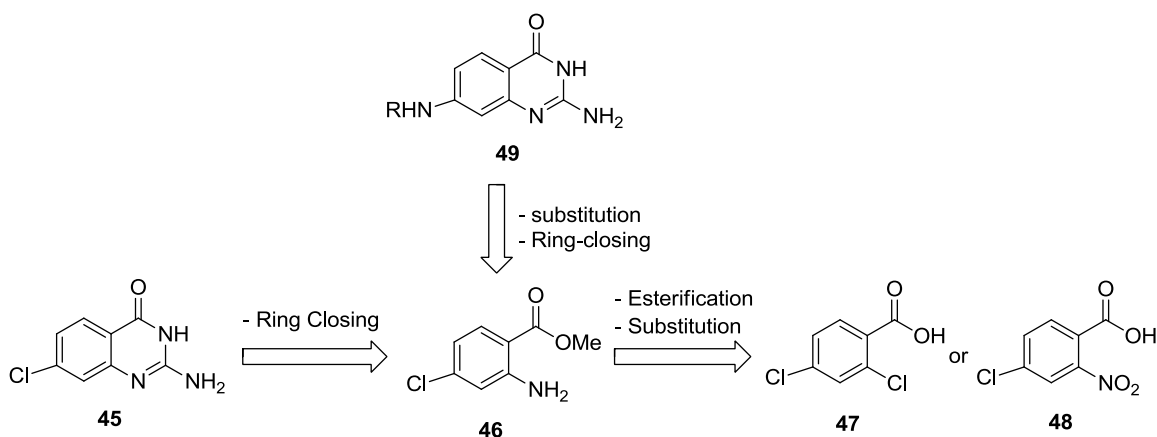
Scheme 4-5: Retro-synthesis of 2-aminoquinazolin-4-one scaffold using 2,4-dichlorobenzoic acid **47** or 4-chloro-2-nitrobenzoic acid **48** as the starting material.

Although the nitration of **45** should favor **44** based on the initial analysis, it is still expected that some byproduct is generated in that step that could be difficult to isolate afterward. So, in order to avoid loss of material during the later synthesis, another retro-synthesis scheme is developed where the nitration reaction is moved forward (**Scheme 4-6**). In this scheme, the 2,4-dichlorobenzoic acid **47** is first protected as methyl ester. It is then nitrated to afford **51** as the more favored product. **51** is a compound that has two electron withdrawing groups on it, and thus it is predicted to be able to undergo two sequential amination reactions under non-catalyzed nucleophilic aromatic substitution (S$_N$Ar) reaction conditions. Once the amines are installed, nitro group in **50** is reduced and the amino-imidazole ring is closed first using the benzoylisothiocyanate reagent so that the exocyclic amine is protected at the same time. Without a protecting group, this amine can affect the next ring-closing reaction. **50** can then undergo a second ring-closing reaction to afford the amino-pyrimidone ring, followed by the deprotection reaction to give the final product **27**.

The advantage of this synthetic scheme is that 1) the nitration product is isolated early on where the molecules are non-polar and easy to purify. When more nitrogen atoms are added, the purification of two very similar compounds can be difficult and time-consuming; 2) the sequential amination reactions are non-catalyzed and regio-selective. The first amination reaction is predicted to occur at the chlorine atom that is *ortho-* to the nitro group because nitro group is a better electron withdrawing group than the ester. The second amination reaction will then occur at the chlorine atom *para-* to the nitro group. The disadvantage of this synthetic scheme is the need to use a

protecting group for the amino-imidazole ring nitrogen atom, which needs to be removed later. It is also not clear whether the remaining one NH of the imidazole ring will affect the ring-closing reaction of the amino-pyrimidone ring. As described by Hortner et al (**Scheme 4-2**) [10], the dimethylamino sulfonyl protecting group of **38** was removed during the final ring closing reaction. And it might have affected the yield of the reaction through side reactions of the NH.
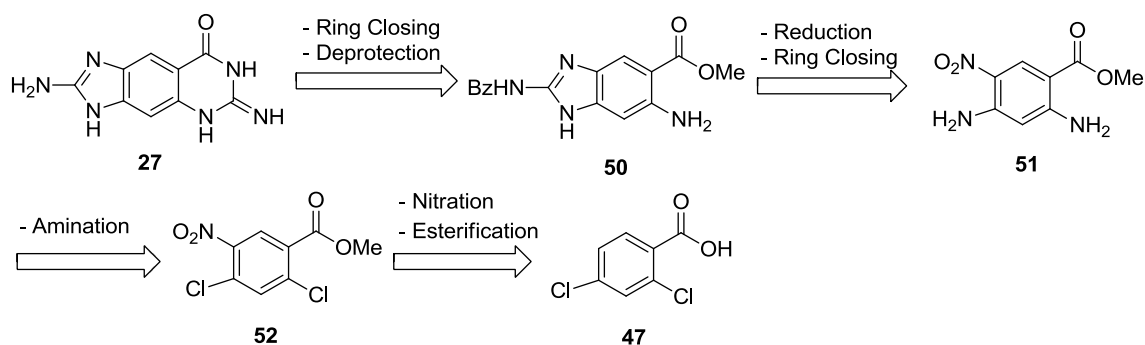
Scheme 4-6: Retro-synthesis of 2-amino-*lin*-benzoguanine scaffold using 2,4-dichloro-benzoic acid **47** as the starting material.

Methods for Amino-pyrimidone Ring Formation

Chloroformamidinium chloride **32** was used by Hortner et al [10] in the synthesis of 2-amino-*lin*-benzoguanine **27**. Slightly different chemistry was also used by Keyser et al [11] in the synthesis of *lin*-benzoguanine (**Scheme 4-7**), where the cyanamide and hydrochloric acid was added to the reaction to generate chlroformamidinium chloride *in situ*.

One limitation of this approach is that it requires harsh reaction conditions at very high temperature and the use of non-conventional solvent such as dimethyl sulfone. At such reaction condition, less stable molecules can decompose or react to form undesired byproducts. This is evidenced by the removal of dimethyl-sulfonyl protecting group of **39** [10]. It is therefore necessary to examine other ring formation methods that can proceed under milder reaction conditions and still give good yield of the product.
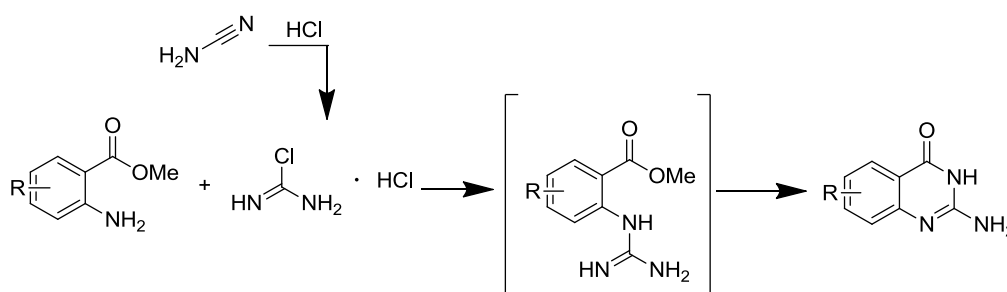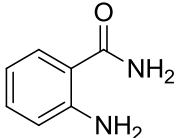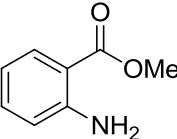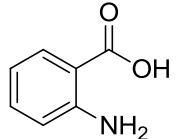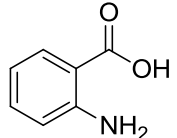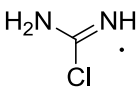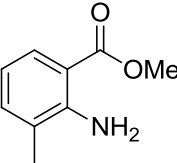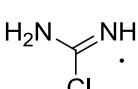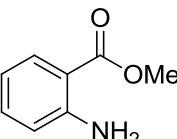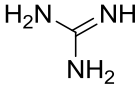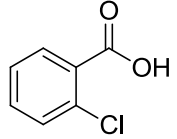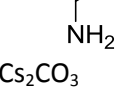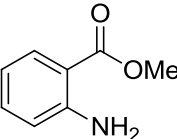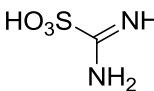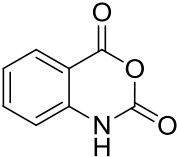
Scheme 4-7: Six-member amino-pyrimidone ring closing reaction using cyanamide and hydrochloric acid [11].

Literature search for examples for the synthesis of amino-pyrimidone ring using Scifinder gave nine different reactions (**Table 4-1**). The reactants used in these reactions are mainly methyl anthranilate (Entry 2, 5, 6, 8), anthranilic acid (Entry 3, 4), 2-aminobenzamide (Entry 1), 2-chlorobenzoic acid (Entry 7) and isatoic anhydride (Entry 9). Reagents used include cyanogene bromide (Entry 1), cyanamide and HCl (Entry 2, 3), chloroform amidinium chloride (Entry 4, 5), isothiocyanate (Entry 6), guanidinium chloride and CuI (Entry 7), and formamidinesulfonic acid (Entry 8), among which

cyanamide and HCl are used to generate chloroform amidinium chloride *in situ* so are considered the same method as the later.

Table 4-1: Literature examples for the synthesis of amino-pyrimidone ring.

Entry	Reactant	Reagent	Solvent	Condition	Yield
1 [12]	2-amino-benzamide	N≡C−Br	N/A	N/A	N/A
2 [11]	methyl 2-aminobenzoate	N≡C−NH₂ HCl	H₂O EtOH	6 h relux	86 %
3 [13]	2-aminobenzoic acid	N≡C−NH₂ HCl	H₂O Me₂SO₂ Sulfolane	1h 165 °C	N/A
4 [13]	2-aminobenzoic acid	H₂N−C(=NH)Cl · HCl	Me₂SO₂	1h 165 °C	N/A
5 [14]	methyl 3-methyl-2-aminobenzoate	H₂N−C(=NH)Cl · HCl	Me₂SO₂	1 h 150 °C	98 %
6 [15]	methyl 2-aminobenzoate	1) EtO−C(=O)−NCS EtN=C=N(CH₂)₃NMe₂ 2) NaOH	1) ACN 2) H₂O, MeOH	1) 4h, RT 2) 2h, reflux	45 % overall
7 [16]	2-chlorobenzoic acid	H₂N−C(=NH)−NH₂ · HCl Cs₂CO₃ CuI	DMF	40h, 110 °C	53%
8 [17]	methyl 2-aminobenzoate	HO₃S−C(=NH)−NH₂	AcOH glacial	48 h, 105 °C	39%
9 [18]	isatoic anhydride	N≡C−NH₂ tBuOK	DMF	3h, 155 °C	55%

Some of the ring-closing reaction conditions were tested. First the methyl

anthranilate **46** and chloroformamidinium chloride **32** were mixed with dimethylsulfone

and heated to 160 °C for 2 hours to give **45** with 49 % yield (**Scheme 4-8**). The product

was purified using flash column chromatography. Methyl anthranilate **46** was

synthesized from 4-chloro-2-nitrobenzoic acid **48** that is commercially available (**Scheme

4-9**).
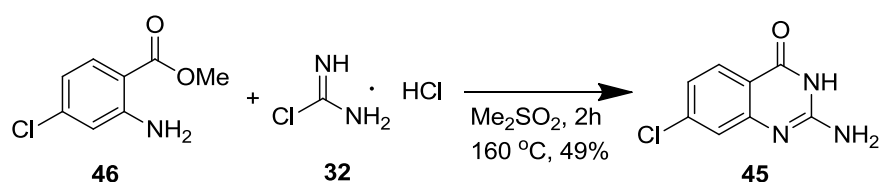
Scheme 4-8: Synthesis of 2-amino-7-chloroquinazolin-4(3*H*)-one **45** using methyl
anthranilate **46** and chloroformamidinium chloride **32**.
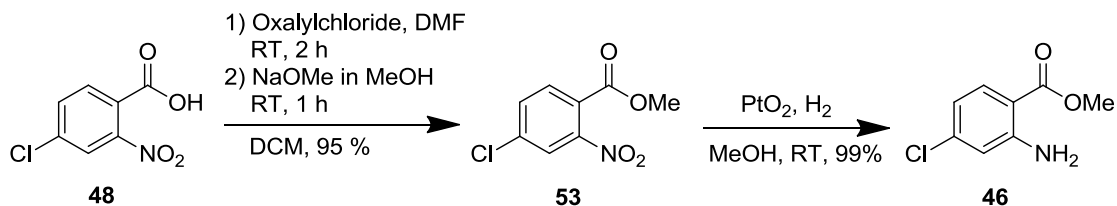
Scheme 4-9: Synthesis of methyl anthranilate **46** from 4-chloro-2-nitrobenzoic acid **48**.

Next, the synthesis of 2-aminoquinazolin-4(3*H*)-one **55** was attempted using 2-

aminobenzamide **54** and cyanogene bromide (**Scheme 4-10**). The reaction was heated

to reflux in acetonitrile (ACN) for 48 hours but most of the starting material remained

unreacted. The mass spectrometry of the crude product did not show a product peak.

The 2-aminobenzamide **54** was synthesized either from methyl 4-chloro-2-

nitrobenzamide **58** or 2-nitrobenzamide **57** using Pd/C catalyzed hydrogenation

reaction. **58** and **57** were synthesized from commercially available 2-nitrobenzoic acid

56 and 4-chloro-2-nitrobenzoic acid **48** respectively (**Scheme 4-11**). The chlorine of **58**

was eliminated under Pd/C catalyzed hydrogenation condition.
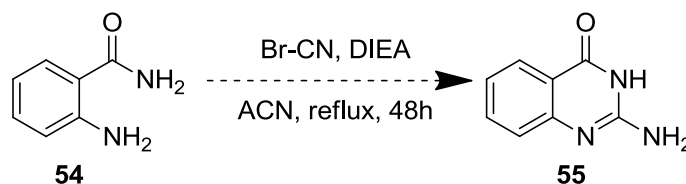
Scheme 4-10: Synthesis of 2-aminoquinazolin-4(3*H*)-one **55** using 2-aminobenzamide **54** and cyanogene bromide.
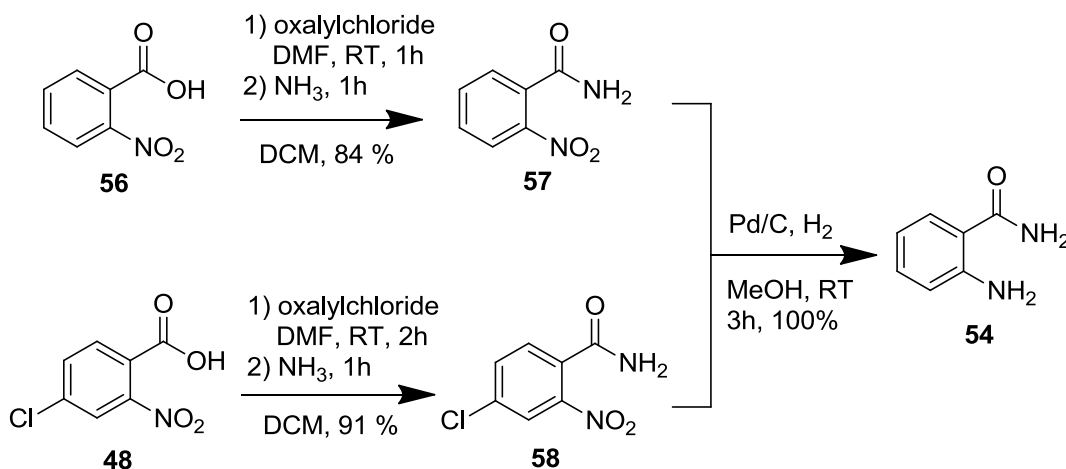
Scheme 4-11: Synthesis of 2-aminobenzamide **54** from 2-nitrobenzoic acid **56** and 4-chloro-2-nitrobenzoic acid **48**.

In a separate reaction, 2-aminobenzamide **54** was reacted with benzoyl

isothiocyanate **59** to afford the *N*-(2-mercapto-4-oxo-1,2,3,4-tetrahydroquinazolin-2-

yl)benzamide **60**, which was further reacted with coupling reagent diisopropyl

carbodiimide (DIPC) to elminate the mercapto group and finally give compound **61**.

Probably due to the flatness of the **61**, it was of poor solubility and its purification was complicated. After several rounds of column chromatography, it was still not pure (**Spectrum 4-12**).
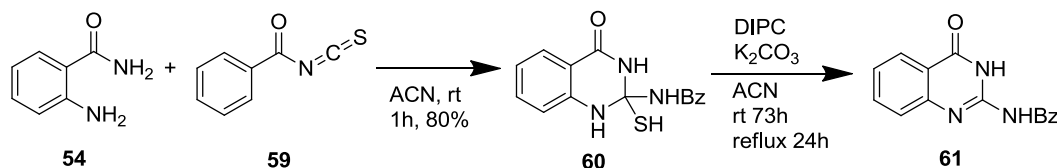
Scheme 4-12: Synthesis of N-(4-oxo-3,4-dihydroquinazolin-2-yl)benzamide **61** from 2-aminobenzamide **54** using isothiocyanate ring-closing reagent.

Next the reaction condition from **Table 4-1 Entry 7** [16] was tested using 2,4-dichlrobenzoic acid **47** to make **45** (**Scheme 4-13**). Under the CuI catalyzed reaction condition, the guanidinium chloride presumably reacts and substitutes the *ortho-* chloro first. The installed guanidine then attacks the acid to form the final product. However, when the reaction was monitored by TLC after it was heated overnight, it showed a series of closely spaced spots together with large amount of remaining starting material. The reaction was not continued.

Based on the CuI catalyzed reaction mechanism, a different approach was attempted where the 2,4-dichlorobenzoyl chloride **62** was reacted with the guanidine under basic condition. Under this reaction condition, the guanidine reacts with the acid chloride first to form the acylguanidine intermediate, which then attacks the *ortho*-chloro position to form the 2-amino-7-chloroquinazolin-4(3*H*)-one **45**. After the reaction was refluxed in THF for 72 hours, TLC showed large amount of the remaining starting

material as well as a few very small new spots. Mass spectroscopy confirmed formation

of the product. The reaction was not purified due to the very low conversion of the

reaction.
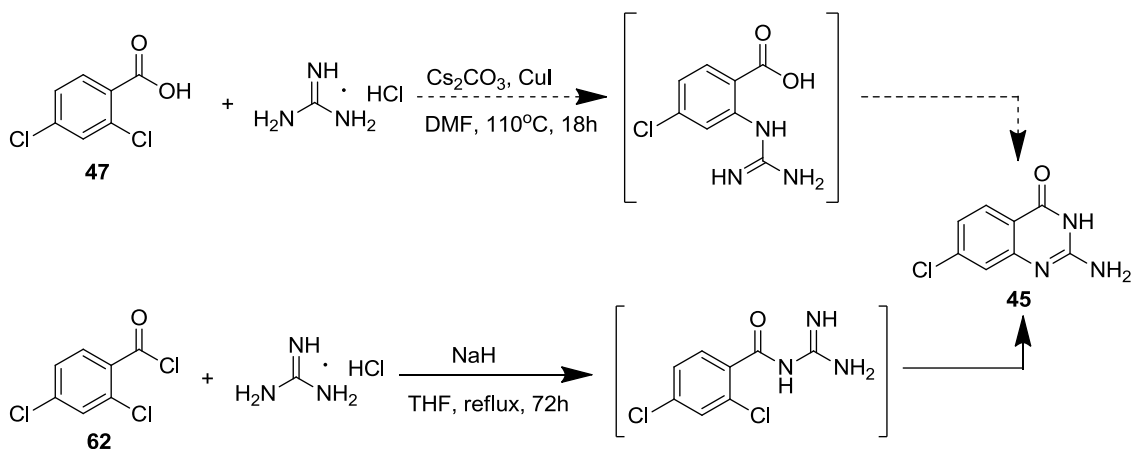
Scheme 4-13: Synthesis of **45** under two different reaction conditions that utilize
different reaction mechanisms.

The formation of acylguanine was probably the rate limiting step of the

transformation of **62** to **45** because of the presence of starting material but not the

intermediate in the reaction. So in another reaction, 2-nitrobenzamide **57** was reacted

with chloroformamidinium chloride to try to form the acylguanine **63** to see if a faster

reaction rate could be achieved under this condition (**Scheme 4-14**). But no formation of

product was detected. The starting material remained unreacted. Using N-substituted

benzamide **64** and similar reaction condition also resulted in no product formation

(**Scheme 4-15**). The starting material remained unreacted. *N*-benzyl-2,4-

dichlorobenzamide **64** was synthesized from 2,4-dichlrobenzoic acid using oxalylchloride

and then benzyl amine with 80 % yield.
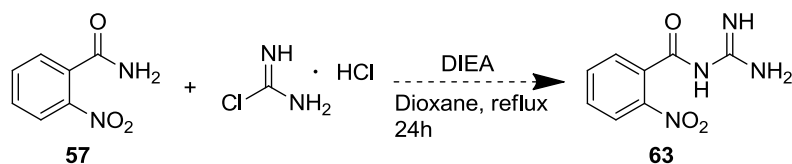
Scheme 4-14: Reaction of 2-nitrobenzamide **57** with chlorformamidinium chloride.
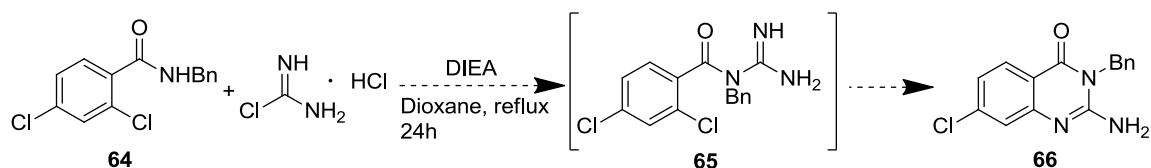
Scheme 4-15: Reaction of N-benzyl-2,4-dichlorobenzamide **64** with chloroform-amidinium chloride.

Among the methods that were tested for the synthesis of the amino-pyrimidone ring, the chloroformamidinium chloride reagent worked the best even though the reaction takes place at very high temperature and gives only moderate yield. Benzoyl isothiocyanate gave good yield under very mild reaction conditions for the formation of **60**. However, the subsequent elimination reaction was slow and the final product **61** was very difficult to purify. Reaction utilizing cyanogene bromide gave no product at all. And reactions using guanidinium chloride were very slow and low yielding.

Attempted Synthesis of 2-Amino-*lin*-benzoguanine from 2,4-Dichlorobenzoic Acid

The synthesis of 2-amino-*lin*-benzoguanine was attempted using strategy shown in **Scheme 4-6**. Commercially available 2,4-dichlorobenzoic acid **47** was used as the starting material (**Scheme 4-16**). Nitration of **47** using concentrated sulfuric acid and nitric acid gave a 6:1 mixture of **67** and **68** (The ratio was calculated based on the amounts of the purified products from the following esterification reaction). After working up the reaction, the crude was used without further purification in the Fisher esterification reaction to convert the acid functional group to methyl ester **52**, which was then purified by column chromatography. The purified yield of **52** was 67 % over two steps. Due to the two electron-withdrawing groups, **52** could readily undergo two consecutive amination reactions with benzyl amine without the need of a catalyst to install the required nitrogen atoms, first at the position *ortho-* to the nitro group and then at the position *para-* to the nitro group. The two amination could also be done in one pot to give **70**. After **70** was reduced by Zn, the crude *ortho*-diamine was subjected to the ring closing reaction by benzoyl isothiocyanate (Bz-NCS). The 2-mercapto intermediate **71** was purified by flash column chromatography to give 75 % over two steps. The elimination of the 2-mercapto group of **71** was done using diisopropyl-carbodiimide (DIPC) and DIEA. The reaction took 9 days to go to completion and 40 % yield was achieved after purification of the product **72**. The amino-pyrimidone ring-closing reaction of **72** was carried out using chloroformamidinium chloride under heat. However, the reaction occurred at the amino-imidazole ring nitrogen to give **73** with 43% yield. The exact substitution site could not be determined by NMR. The imidazole

ring nitrogen was thought to be more nucleophilic and sterically accessible. But the

reaction could also occur at the amide nitrogen atom.
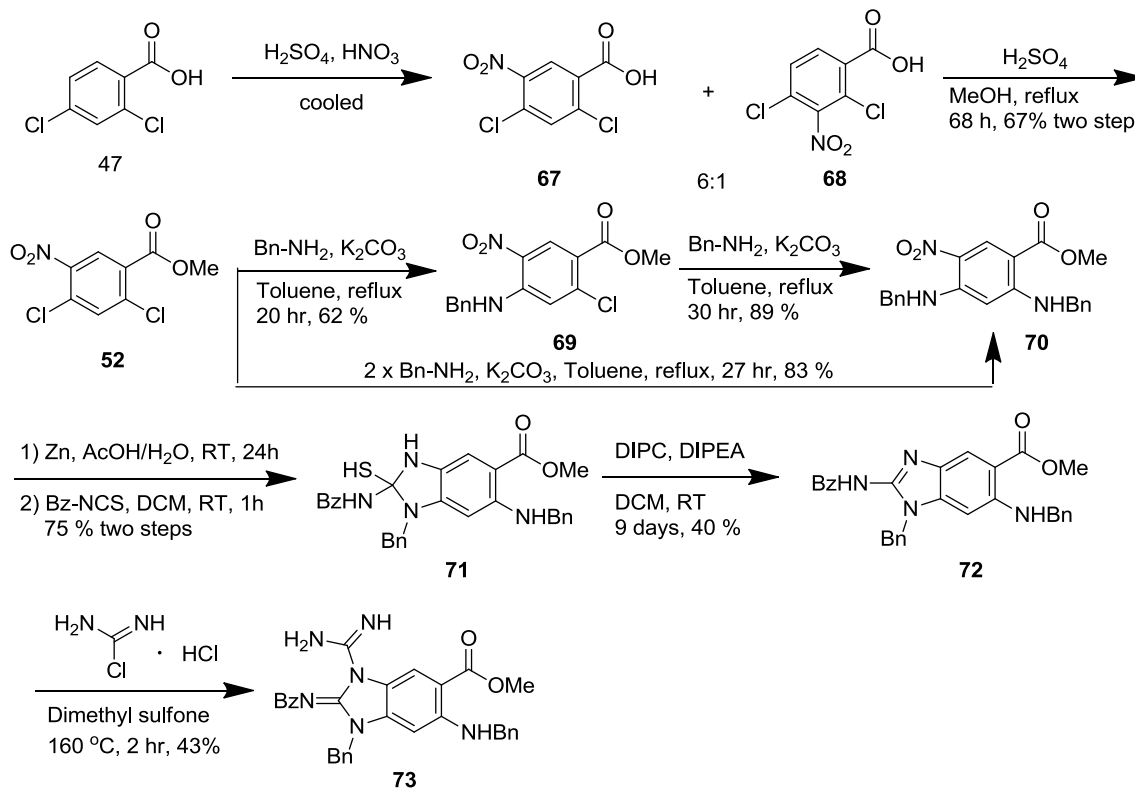
Scheme 4-16: Attempted synthesis of 2-amino-*lin*-benzoguanine using retro-synthetic strategy shown in scheme 4-9.

In a later reaction where ammonia was used in the second amination reaction of

69 instead of the benzyl amine to make the nitrogen at the 2-position more freely

accessible, the reaction did not proceed (**Scheme 4-17**). And when methyl 2,4-dichloro-

5-nitrobenzoate **52** was reacted with excess of ammonia under heat, only

monoaminated product **75** was obtained (**Scheme 4-18**).
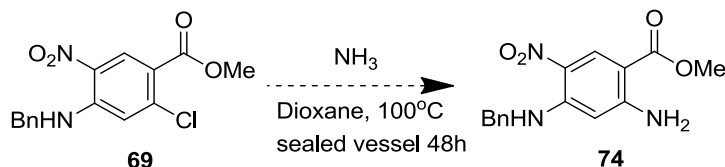
Scheme 4-17: Attempted synthesis of methyl 2-amino-4-(benzylamino)-5-nitrobenzoate **74** from methyl 4-(benzylamino)-2-5-nitrobenzoate **69**.
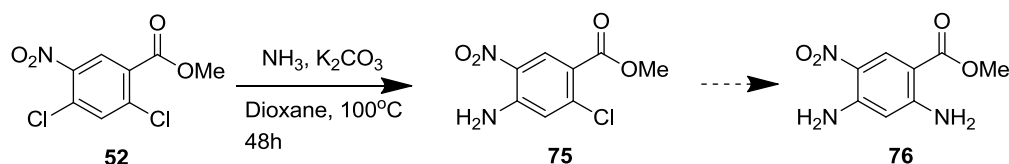
Scheme 4-18: Amination of methyl 2,4-dichloro-5-nitrobenzoate **52** only gave mono-aminated product 75. Di-aminated product **76** could not be detected.

The attempted synthesis of 2-amino-*lin*-benzoguanine revealed that the reactivity of the nitrogen atom *ortho*- to the methyl ester was lower than the nitrogens of the amino-imidazole even when they were protected. Thus, closing the amino-pyrimidone ring after the amino-imidazole ring gave rise to the formation of the undesired product **73**. The future synthesis of the 2-amino-*lin*-benzoguanine should follow the retro-synthesis shown in **Scheme 4-4**. This retro-synthetic strategy also shares a common intermediate of the 2-amino-quinazolin-4-one pathway.
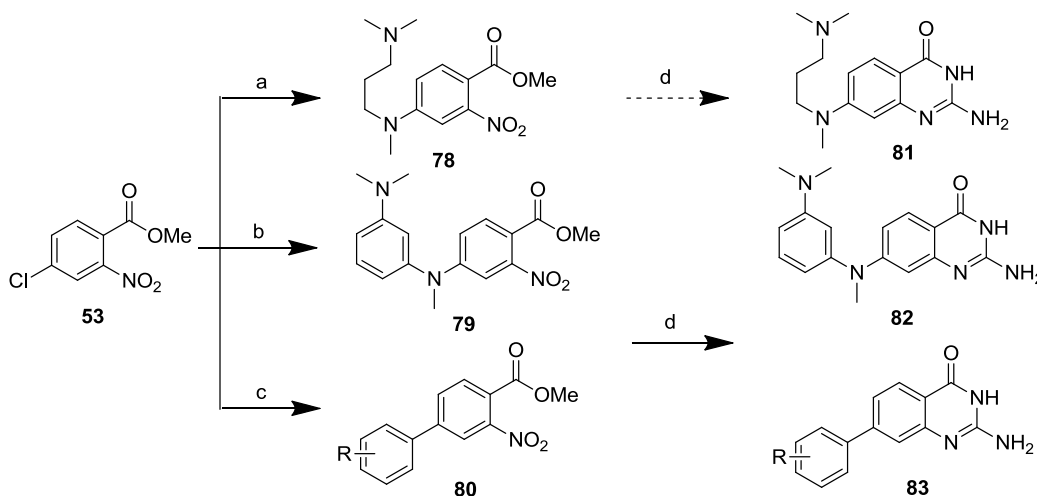
Synthesis of 7-Substituted 2-Aminoquinazolin-4-one Molecules

Since the ring-closing reaction using chloroformamidinium chloride was successful, the main challenges of the synthetic development of 2-aminoquinazolin-4-one is the functionalization of the molecule at its 2- and 4- positions. The core of the 2-aminoquinazolin-4-one has been synthesized using this method (**Scheme 4-8**). The 4-chloro substituent of **45** can be eliminated using Pd/C catalyzed hydrogenation reaction (**Scheme 4-11**).

The functionalization of the 7-position was achieved when using 4-chloro-2-nitrobenzoic acid **48** as the starting material. After protecting the acid **48** as the methyl ester **53** (**scheme 4-9**), **53** could be substituted at the 7-position using alkyl amines without a catalyst, or using anilines and aryl-boronic acids with palladium catalyzed Buchwald-Hartwig reaction or Suzuki reaction (**Scheme 4-19**). For compound **81** and **82** where the 7-substitutions are either alkylamine or aniline, it was found necessary to methylate the amino groups of **78** and **79** because they were found to otherwise affect the ring-closing reactions of the amino-pyrimidone ring. The nitro groups were reduced using Pd/C catalyzed hydrogenation reactions. The final amino-pyrimidone ring was closed by chloroformamidinium chloride under heat.

The dimethylaminopropyl amino-substituted compound **78**, after reacting with chloroformamidinium chloride at 160 °C for 2 hours, gave a mixture of many spots by TLC (DCM – MeOH : 90%-10%). Purification of the crude using flash column chromatography could not yield any desired product **81**. The dimethylaminopropyl

amino substitution was probably not stable enough to undertake the high temperature

of the ring-closing reaction.

Scheme 4-19: Synthesis of 7-substituted 2-aminoquinazolin-4-one molecules. **a.** 1) *N,N*-Dimethylaminopropylamine, K_2CO_3, Dioxane, reflux, 45h, 2) Iodomethane, K_2CO_3, Dioxane, resluc, 21h, 84%; **b.** 1) 3-dimethylaminoaniline, $Pd_2(dba)_3$, *rac*-BINAP, Cs_2CO_3, Dioxane, reflux, 28h, 46%, 2) Iodomethane, K_2CO_3, ACN, reflux, 46h, 83%; **c.** aryl-boronic acid, $Pd_2(dba)_3$, *rac*-BINAP, Cs_2CO_3, Dioxane, reflux, 19-30h, 42-66%;   **d.** 1) H_2, Pd/C, MeOH, RT, 1-24 h, 2) chlroformamidinium chloride, dimethyl sulfone, 160 °C, 2h, 5-13 %.

FRET Assay Testing of 7-Substituted 2-Aminoquinazolin-4-one Molecules

The synthesized 7-substituted 2-aminoquinazolin-4-one molecules were tested

using FRET assay that was also used to test the aryl-substituted benzimidazole

molecules previously (**Chapter 3**). The 2-amino-7-chloroquinazolin-4-one **45** core gave

slight decrease of the FRET signal as the compound concentration increased (**Table 4-2**),

suggesting very weak binding to the target HCV IRES subdomain IIa RNA. By contrast, 7-

aryl-substited compound **83a**, **83b**, **83c** did not show typical dose-response titration curves in the FRET assay (**Table 4-2**). Instead, the fluorescent signal of both Cy3 and Cy5 decreased to zero (or nearly zero), suggesting non-specific interaction between the molecule and the RNA that caused precipitation of the RNA out of the solution. If the molecule was only quenching one of the two dyes, the other dye would still give its fluorescence. However, in the curves shown below (**Table 4-2**), both Cy3 and Cy5 signals decreased simultaneously.

The FRET titration curve for compound **82** was different from all others because in the titration curve the Cy3 signal first went down to zero at ~ 200 µM but then increased steadily. In the meantime, the Cy5 and the FRET signal remained at zero. Precipitation of the compound and RNA mixture was visually observed at 200 µM or higher concentration of the compound, confirming that the compound 82 and RNA were probably precipitated out. So as a result, the increase in fluorescence was probably from the compound **82**. When **82** alone was dissolved in 10 mM HEPES buffer (2.0 mM MgCl$_2$, pH 7.0) and its fluorescence was read at the wave lengths near the Cy3 excitation (520 nm) and emission (570 nm) region, it was found that **82** gave the strongest emission at 570 nm when excited at 520 nm, which is the same as the optimal Cy3 excitation and emission wavelengths. The optical property of **82** makes it a potential Cy3 replacement fluorescent molecule. However, more study is required to characterize the fluorescent property of the molecule.

Table 4-2: Structure and FRET titration curves of the 7-substituted 2-aminoquinazolin-4-one molecules and a 7-aryl-substituted benzimidazole molecule.
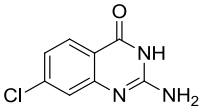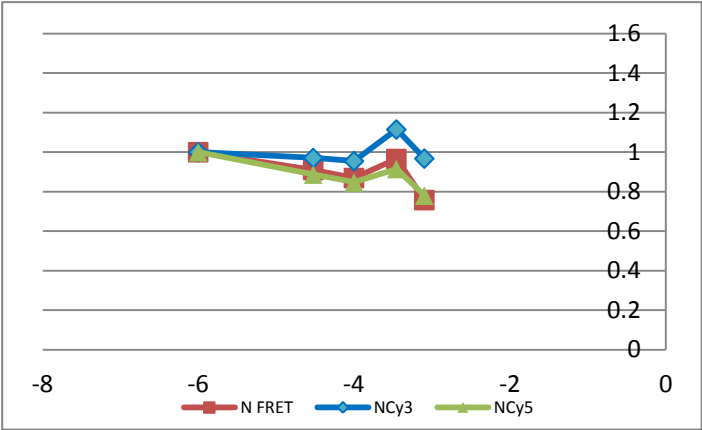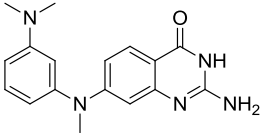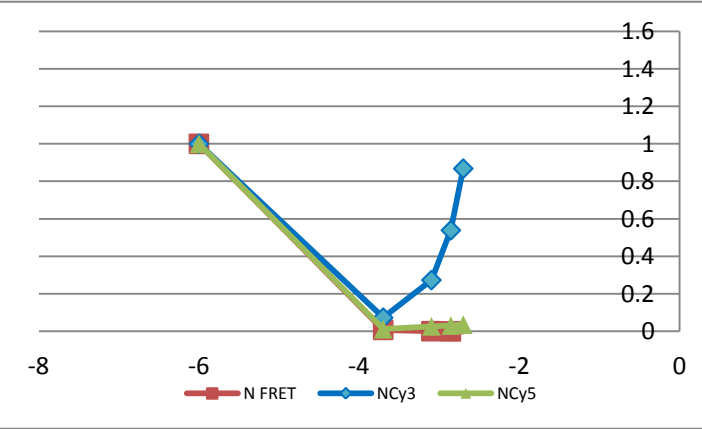
ID	Structure	FRET Titration Curve
45		
82		
83a		

Table 4-2: Continued.

ID	Structure	FRET Titration Curve
83b		
83c		
84		

In order to answer the question whether the diaryl-substitution at the 7-position caused the compounds and RNA to precipitate, 7-aryl-substituted benzimidazole **84** was synthesized using method that has been described in **Chapter 3**. Compound **84** has the N^1-dimethylaminopropyl substitution that is the same as the benzimidazole **2** molecule in the cocrystal structure study (**Figure 4-1**). And it also has the 3-dimethylamino aryl-substitution at the 7 position that is the same as compound **83c**. Therefore, **84** was incorporated the structural features that were known to bind to the HCV IRES subdomain IIa bulge, as well as the 7-aryl substitution that was hypothesized to have caused precipitation of the RNA. **84** was synthesized from N^1-(5-chloro-2-nitrophenyl)-N^3,N^3-dimethylpropane-1,3-diamine (**20h**) (**Chapter 3**) using Suzuki coupling followed by reduction and ring-closing reaction using cyanogene bromide (**Scheme 4-20**). When **84** was tested in the FRET assay, it behaved similarly to that of **83**. The fluorescent signals simultaneously decreased as the concentration of the compound increased, suggesting that the aryl-substitution at the 7 position was very likely to have caused non-specific binding of the molecule to the RNA and consequently caused the RNA to precipitate. Aryl-substitution at the 7 position of both scaffolds, 2-aminoquinazolin-4-one and 2-aminobenzimidazole, should be avoided in the future.
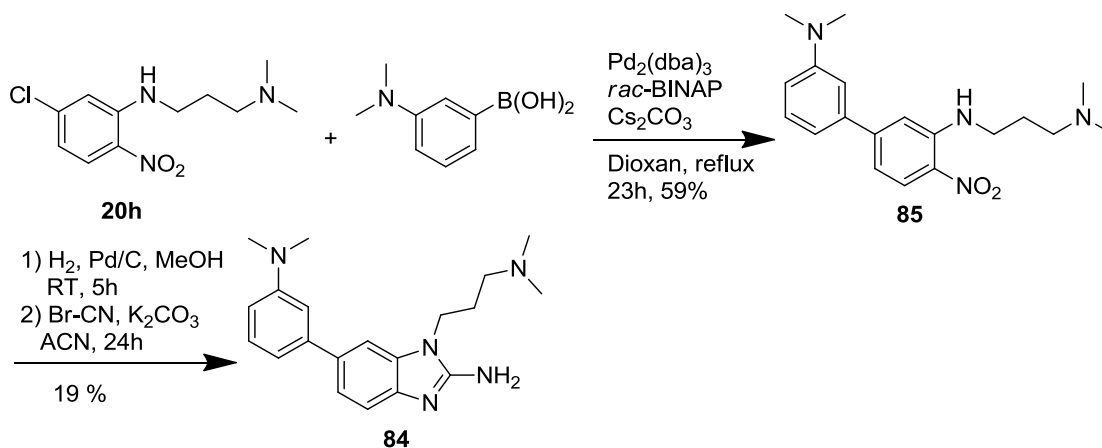
Scheme 4-20: Synthesis of 6-(3-(dimethylamino)phenyl)-1-(3-(dimethylamino)propyl)-1H-benzo[d]imidazol-2-amine **84** from N^1-(5-chloro-2-nitrophenyl)-N^3,N^3-dimethylpropane-1,3-diamine **20h**.

Functionalization of the N1 Position of 2-Aminoquinazolin-4-one Scaffold

There are in general two ways to functionalize the N1 position of the 2-aminoquinazolin-4-one scaffold. One is to use the methyl 4-chloro-2-nitrobenzoate (**53**) as the starting material and react it with an amine through either a nucleophilic aromatic substitution (S_NAr) or a metal catalyzed amination reaction (**Scheme 4-21**). The other way is to use methyl 2-amino-4-chlorobenzoate **89** or methyl 2-aminobenzoate **90** and react with a halide either in a non-catalyzed or catalyzed reaction.
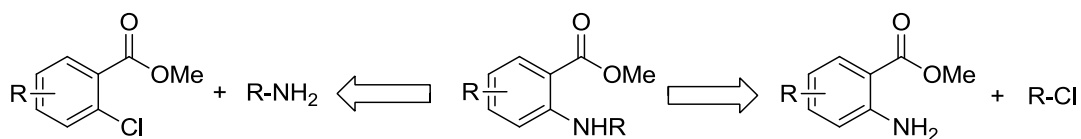
Scheme 4-21: General strategy for functionalization of N1 position of 2-aminoquinazolin-4-one scaffold.

Both strategies were tested using both alkyl amine and aniline reactants under non-catalyzed and catalyzed conditions (**Scheme 4-22**). When methyl 4-chloro-2-nitrobenzoate (**53**) and benzyl amine were refluxed in toluene for 25 hours, no formation of the product **86** was detected and both starting materials remained unreacted. Copper (I) iodide (6 mol%) was then added and the reaction was heated to reflux. But the reaction did not proceed after 94 hours. In order to eliminate the possibility that benzyl amine was not reacted due to its bulky phenyl ring, **53** was then reacted with dimethylaminopropylamine under similar reaction conditions. But no product formation could be detected either. In another experiment where **53** was reacted with the 3-dimethylamino aniline under Palladium catalyzed Buchwald-Hartwig reaction condition, the product methyl 4-chloro-2-((3-(dimethylamino)phenyl)amino)-benzoate **87** was successfully synthesized. However the yield of the reaction was lower when compared to the similar reactions done in the synthesis of benzimidazole compounds (Chapter 3) that had *ortho*-nitro groups instead of methyl ester. It was hypothesized that the reduced yield maybe due to the steric hindrance of the ester functional group.

When methyl 2-amino-4-chlorobenzoate **89** was reacted with dimethylaminopropyl chloride in toluene under reflux condition for 26 hours, the formation of the product **87** was detected by mass spectrometry (MSI, calculated Exact Mass: 270.11, Found [M+H]$^+$: 271.06) but the conversion was so low that no product was purified using flash column chromatography. Using NaH in THF and allowing longer reaction time did not improve the yield.
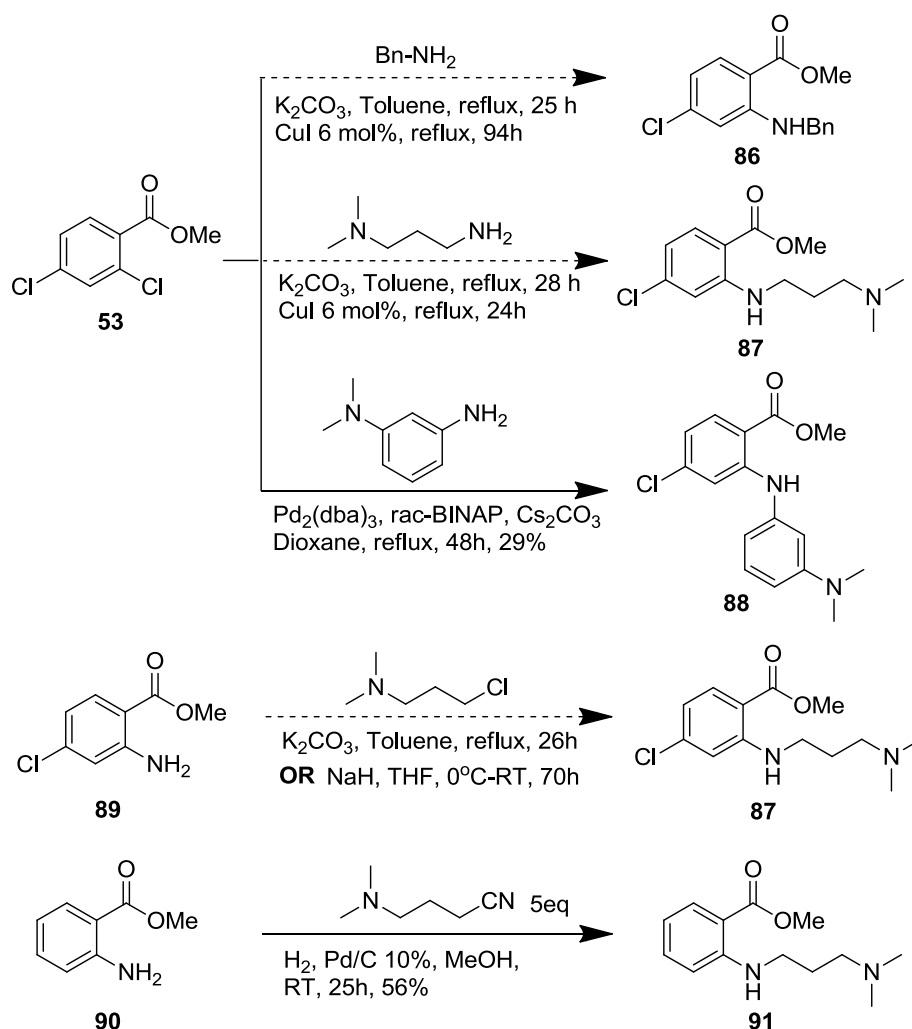
Scheme 4-22: Functionalization of N1 position of 2-aminoquinazolin-4-one scaffold.

In a recent attempt to synthesize **91**, a reductive N-alkylation of the aniline **90** was attempted using 4-(dimethylamino) butanenitrile (5 eq), 10 % Pd/C and H$_2$ atmosphere [19] (**Scheme 4-22**). The methyl 2-((3-(dimethylamino)-propyl)amino)-benzoate **91** was synthesized with 56 % yield using the reported reaction conditions. Based on preliminary study by Sajiki et al [19], This reaction is mediated by the nucleophilic attack of amines on the nitrile carbon that is activated by the coordination

of Pd to form the amidine, followed by then the reduction of the amidine by Pd and

hydrogen gas (**Scheme 4**-23).
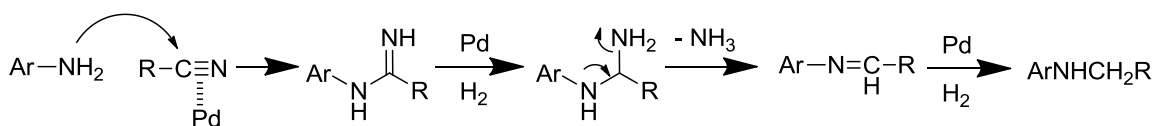
Scheme 4-23: Reaction mechanism of Pd catalyzed reductive monoalkylation of aniline using nitrile as an alkylating reagent [19].

In summary, the functionalization of N1 position of 2-aminoquinazolin-4-one

scaffold can be achieved either using **53** under Palladium catalyzed Huchwald-Hartwig

amination reaction condition with aromatic aniline or using **90** and alkyl-nitrile under

Pd/C and H_2 atmosphere reaction condition.

Materials and Methods

2-Amino-7-chloroquinazolin-4(3*H*)-one (45)
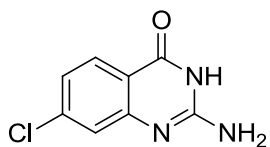
To a 5 ml glass vial was added methyl 2-amino-4-chlorobenzoate **46** (325 mg,

1.25 mmol), chloroformamidinium chloride 32 (402 mg, 2 eq) and dimethylsulfone (400

mg). The reaction was stirred using a small magnetic stir bar while heated to 160 °C for 2

hours. After it was cooled to RT, the solid residue was purified using flash column

chromatography (DCM – MeOH : 90 % - 10 %) to yield white solid as the product (166

mg, 49 %). ^{1}H NMR (400MHz, DMSO-d6) δ: 11.17 (s, 1H), 7.85 (d, *J* = 8 Hz, 1H), 7.18 (d, *J*

= 2 Hz, 1H), 7.09 (dd, J_1 = 8 Hz, J_2 = 2 Hz, 1H), 6.64 (s, 2H). ^{13}C NMR (400MHz, DMSO-d6)

δ: 162.17, 153.34, 152.86, 139.16, 128.40, 123.14, 121.99, 116.36. MS (ESI) calculated

exact mass for $C_8H_6ClN_3O$ = 195.02. Found $[M+H]^+$ = 195.87.

Spectrum 4-1: 2-Amino-7-chloroquinazolin-4(3*H*)-one (**45**) ^{1}H NMR (400MHz, DMSO-d6)
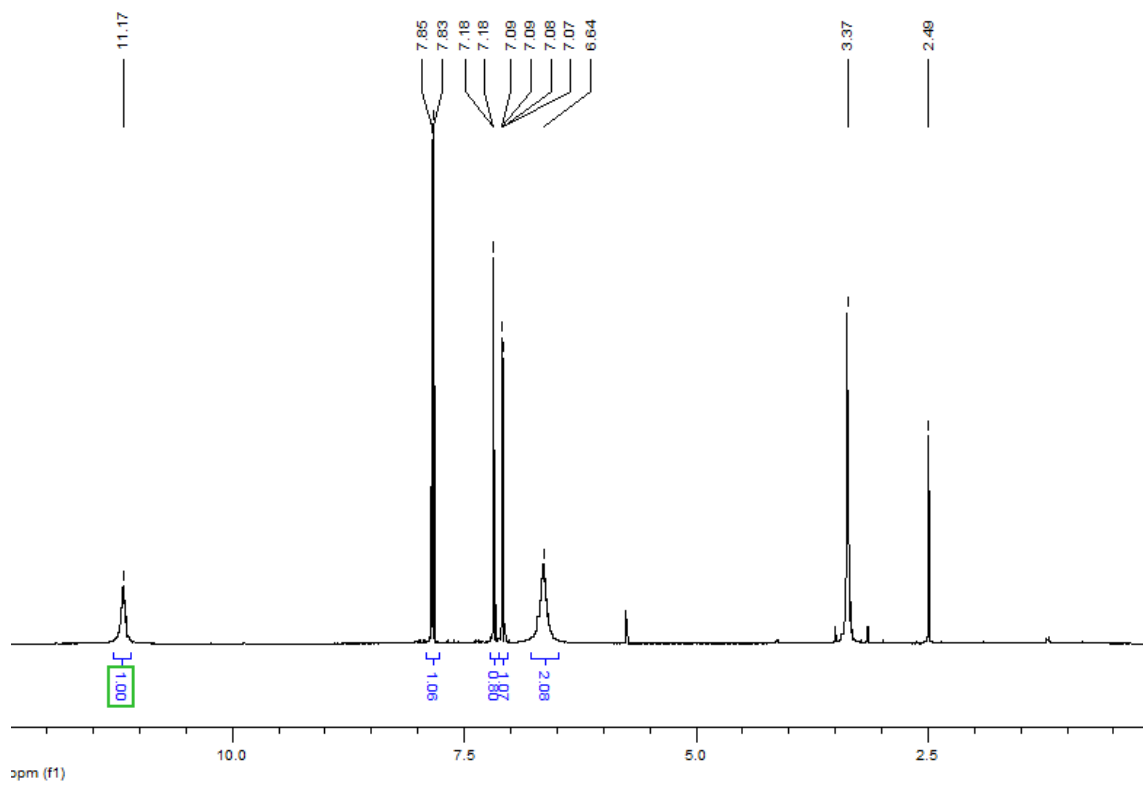
Spectrum 4-2: 2-Amino-7-chloroquinazolin-4(3*H*)-one (**45**) ¹³C NMR (400MHz, DMSO-d6)
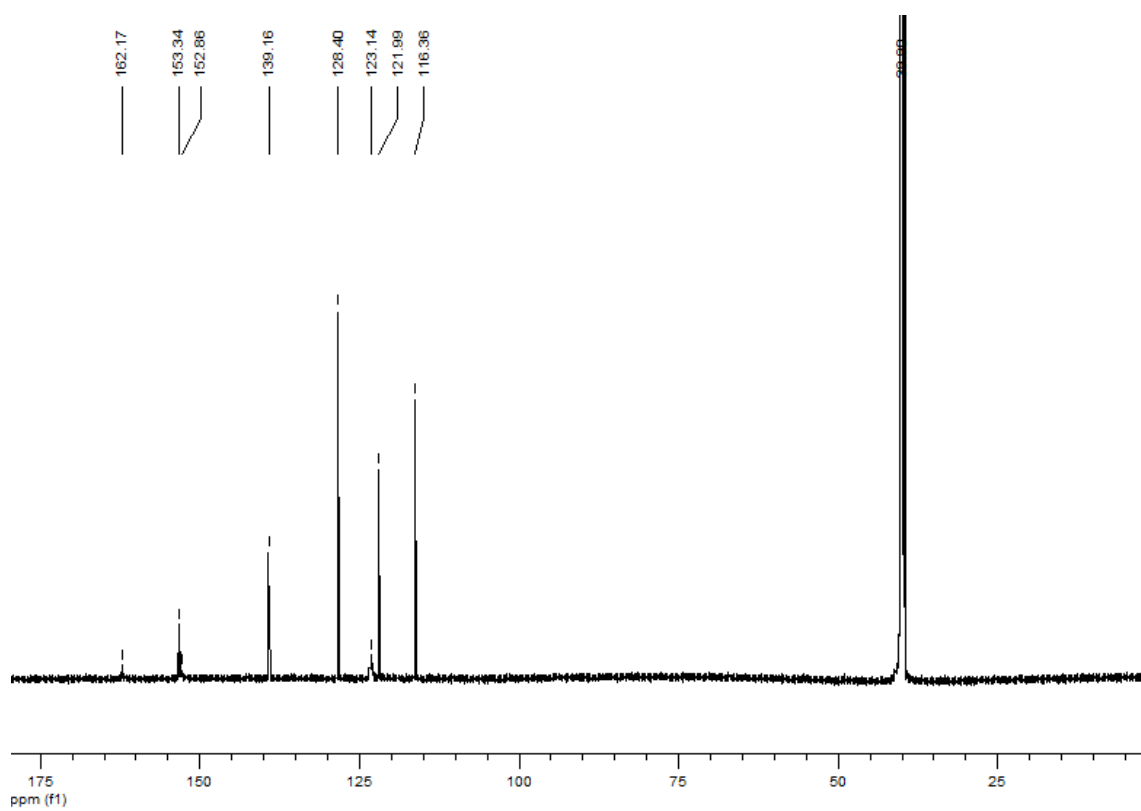
Methyl 4-chloro-2-nitrobenzoate (53)
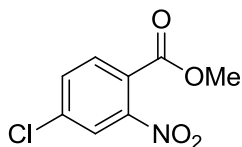
To a 1L round bottom flask was added 4-chloro-3-nitro-benzoic acid **48** (10 g, 49.6 mmol), DCM (400 ml), DMF (10 µl) and oxalylchloride (4.47 ml, 52.08 mmol, 1.05 eq). The reaction was stirred at RT for 2 hours before NaOMe (25 % in MeOH, 25 ml) was added. The reaction was stirred at RT for 1 hour. It was then filtered and concentrated. The crude was passed through a short plug of silica gel, eluting with Hexane – DCM (80 % - 20 %). After removal of solvent, slight yellow oil product was obtained as the product (9.27 g, 88 % yield). ^{1}H NMR (400 MHz, DMSO-d6) δ: 8.23 (s, 1H), 7.91 (m, 2H), 3.83 (s, 3H). ^{13}C NMR (400 MHz, DMSO-d6) δ: 164.69, 149.59, 137.98, 133.94, 132.43, 124.86, 124.79, 54.05.

Spectrum 4-3: Methyl 4-chloro-2-nitrobenzoate (**53**) ^{1}H NMR (400MHz, DMSO-d6)
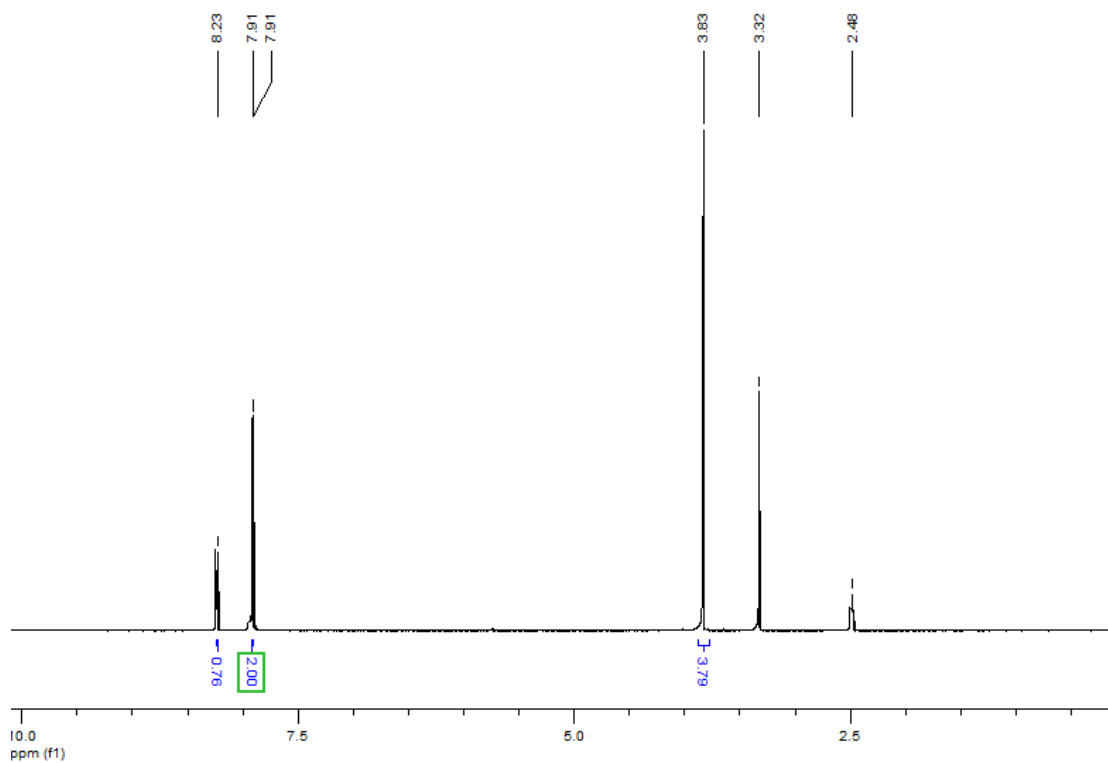
Spectrum 4-4: Methyl 4-chloro-2-nitrobenzoate (**53**) ^{13}C NMR (400MHz, DMSO-d6)
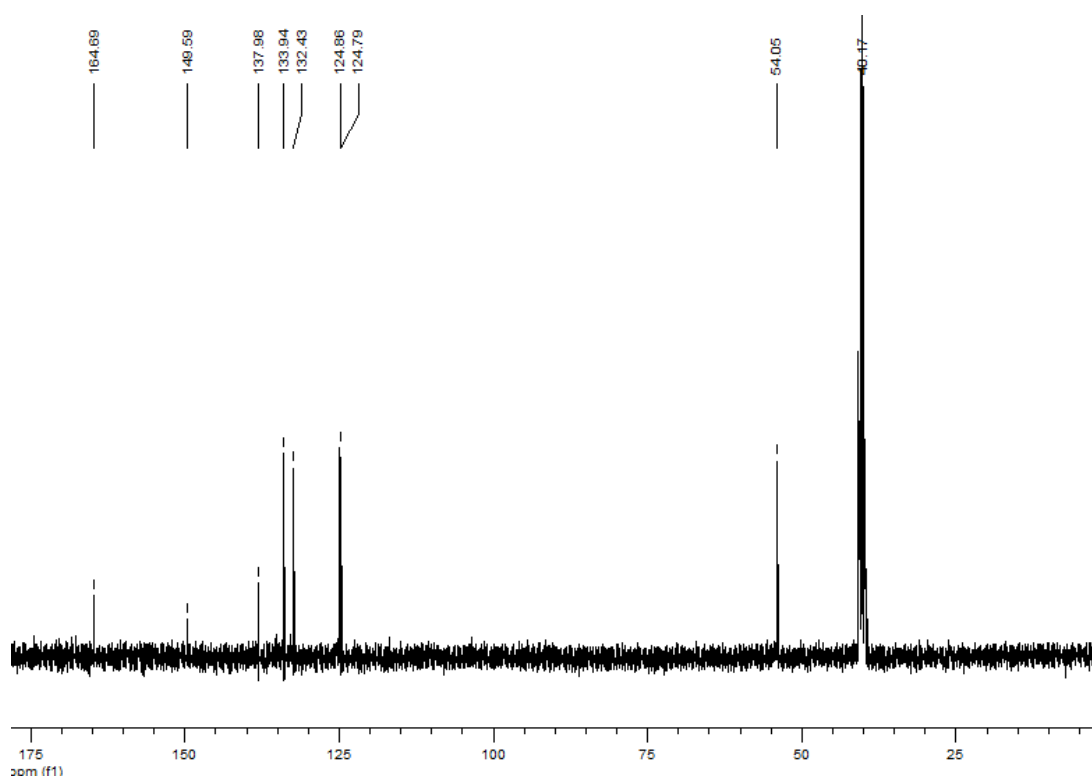
Methyl 2-amino-4-chlorobenzoate (46)
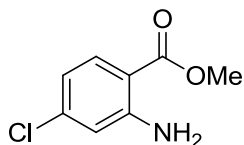
To a 250 ml round bottom flask was added methyl 4-chloro-2-nitrobenzoate (**53**) (500 mg, 2.32 mmol), MeOH (100 ml) and PtO_2 (50 mg, 10 wt %). The reaction was sealed under H_2 atmosphere. It was stirred at RT for 31 hours before filtration and concentration. The crude was purified via flash column to yield white solid as the product (450 mg, 99 % yield). ^{1}H NMR (400 MHz, DMSO-d6) δ: 7.66 (d, J = 9 Hz, 1H), 6.85 (s, 2H), 6.83 (d, J = 2Hz, 1H), 6.51 (dd, J_1 = 8 Hz, J_2 = 2 Hz, 1H), 3.75 (s, 3H). ^{13}C NMR (400 MHz, DMSO-d6) δ: 167.79, 152.87, 139.26, 133.20, 115.93, 115.38, 108.29, 52.19. MS (ESI) calculated exact mass for $C_8H_8ClNO_2$ = 185.02. Found $[M+H]^+$ = 185.88.

Spectrum 4-5: Methyl 2-amino-4-chlorobenzoate (**46**) ¹³C NMR (400MHz, DMSO-d6)
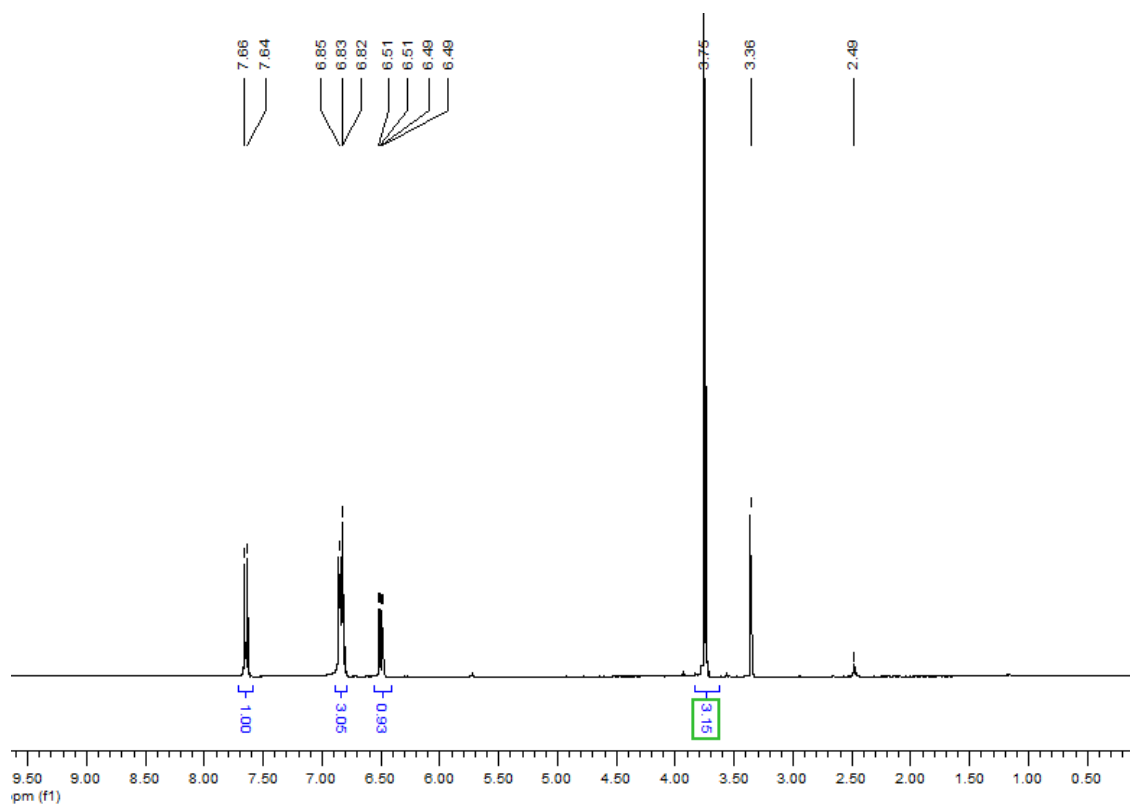
Spectrum 4-6: Methyl 2-amino-4-chlorobenzoate (**46**) ^{1}H NMR (400MHz, DMSO-d6)
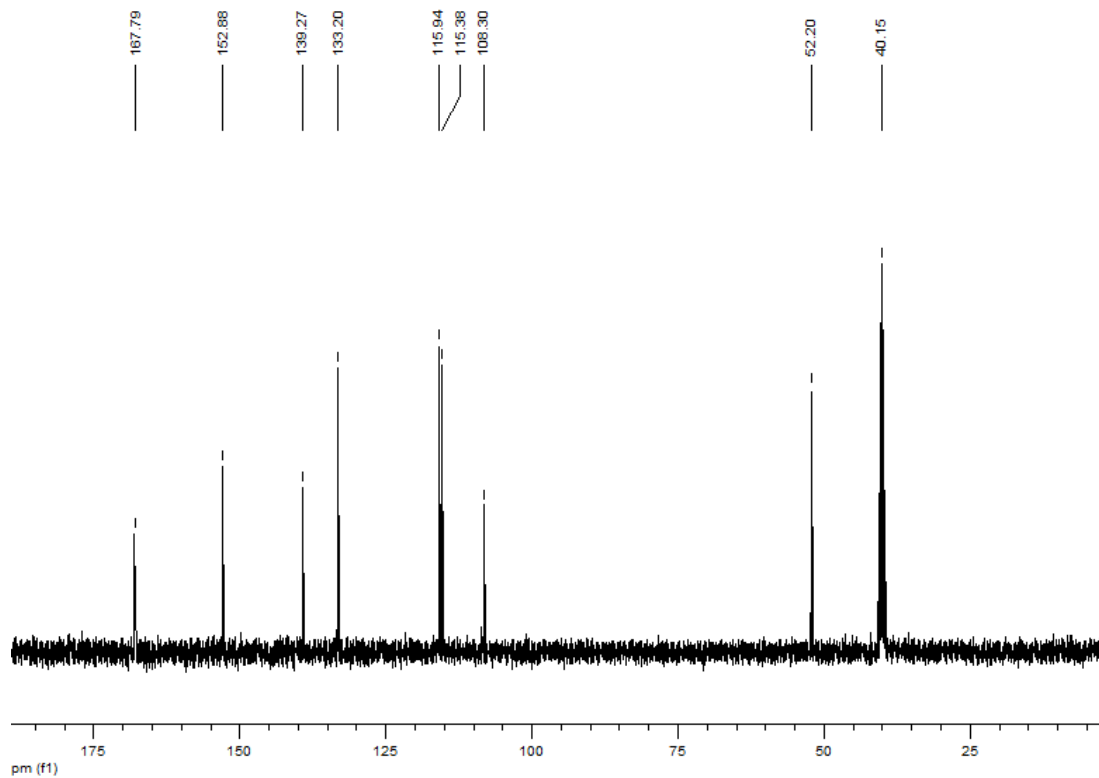
2-Nitrobenzamide (57)
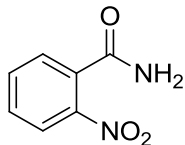
To a 250 ml round bottom flask was added 2-nitro-benzoic acid **56** (2.0 g, 12.0

mmol), DCM (100 ml) and DMF (10 μl). The solution was stirred when oxalyl chloride

(1.14 ml, 13.2 mmol) was added drop-wise. The reaction was stirred at RT for 1 hour

before NH_3 gas was bubbled into the reaction. The reaction was stirred at RT for 1 hour.

After concentration, the crude was purified via flash column (DCM - MeOH: 90 % - 10 %)

to yield white solid as the product (1.7 g, 84 % yield). ^{1}H NMR (400 MHz, DMSO-d6): δ

8.14 (s, broad, 1H), 7.99 (dd, J_1 = 8 Hz, J_2 = 1 Hz, 1H), 7.77 (td, J_1 = 8Hz, J_2 = 1Hz, 1H), 7.69

(s, broad, 1H), 7.67 (td, J_1 = 8 Hz, J_2 = 1 Hz, 1H), 7.62 (dd, J_1 = 8 Hz, J_2 = 1 Hz, 1H). ^{13}C

NMR (400 MHz, DMSO-d6): δ 167.83, 147.90, 134.01, 133.24, 131.30, 129.51, 124.62.

MS (ESI) calculated exact mass for $C_7H_6N_2O_3$ = 166.04. Found $[M+Na]^+$ = 355.07.

Spectrum 4-7: 2-nitrobenzamide (**57**) ^{1}H NMR (400MHz, DMSO-d6)
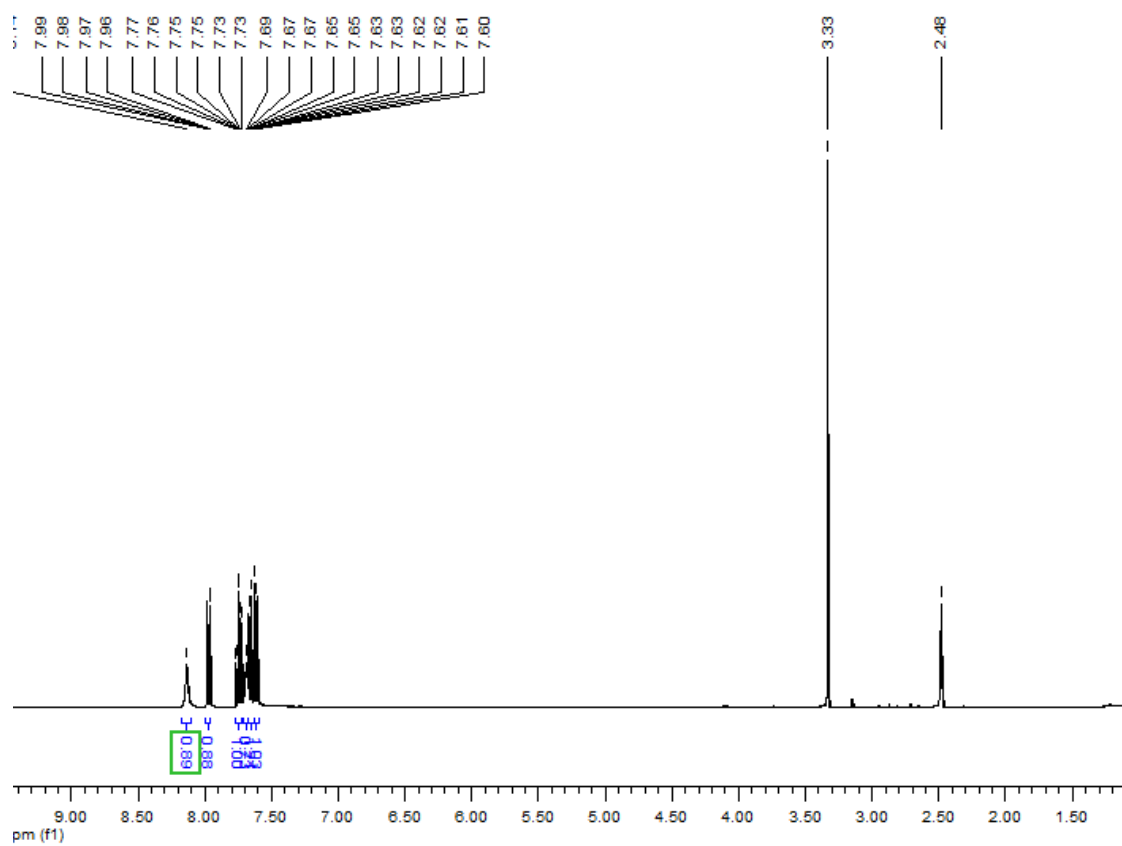
Spectrum 4-8: 2-nitrobenzamide (**57**) ^{13}C NMR (400MHz, DMSO-d6)
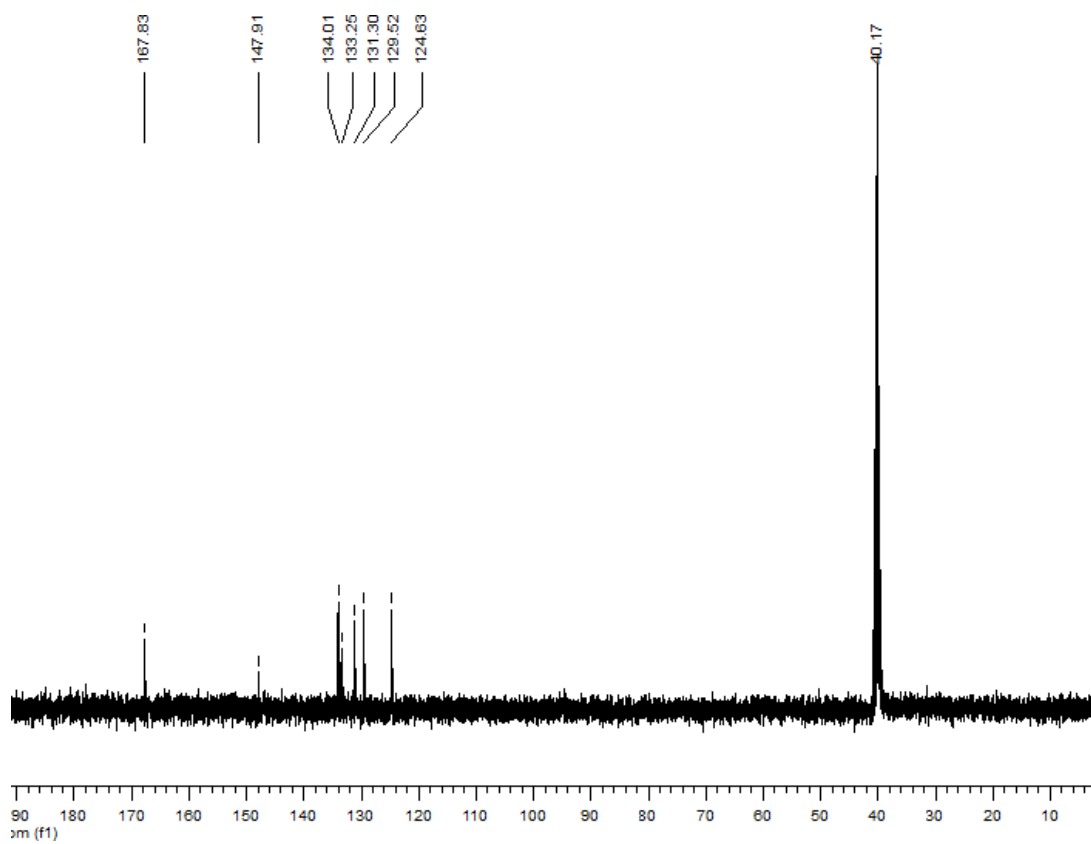
2-Aminobenzamide (54)
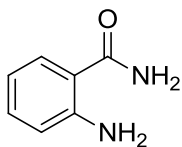
General Procedure: 2-nitrobenzamide **57** or 4-chloro-2-nitrobenzamide **58** was dissolved in methanol. Pd/C (10 wt%) was added. The reaction was stirred at RT for ~3 hours. The reaction progress was monitored by TLC (DCM 100 %). Once completed, the reaction was filtered by celite and concentrated. The white solid product was of very high purity. ^{1}H NMR (400 MHz, DMSO-d6): δ 7.70 (s, 1H), 7.51 (d, J = 7 Hz, 1H), 7.12 (t, J = 7 Hz, 1H), 7.04 (s, 1H), 6.66 (d, J = 8 Hz, 1H), 6.53 (s, 2H), 6.47 (t, J = 7 Hz, 1H). ^{13}C NMR (400 MHz, DMSO-d6): δ 171.95, 150.86, 132.55, 129.41, 117.05, 115.01, 114.30.

Spectrum 4-9: 2-aminobenzamide (**54**) ^{1}H NMR (400MHz, DMSO-d6)
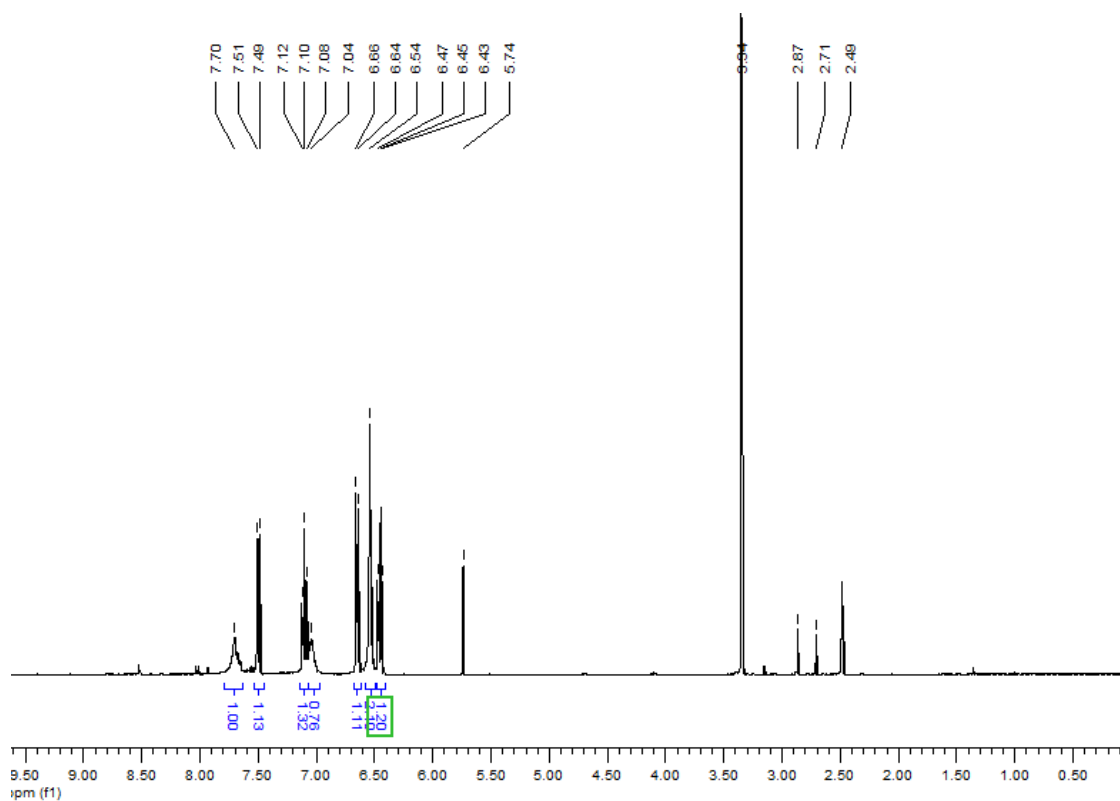
Spectrum 4-10: 2-aminobenzamide (**54**) ^{13}C NMR (400MHz, DMSO-d6)
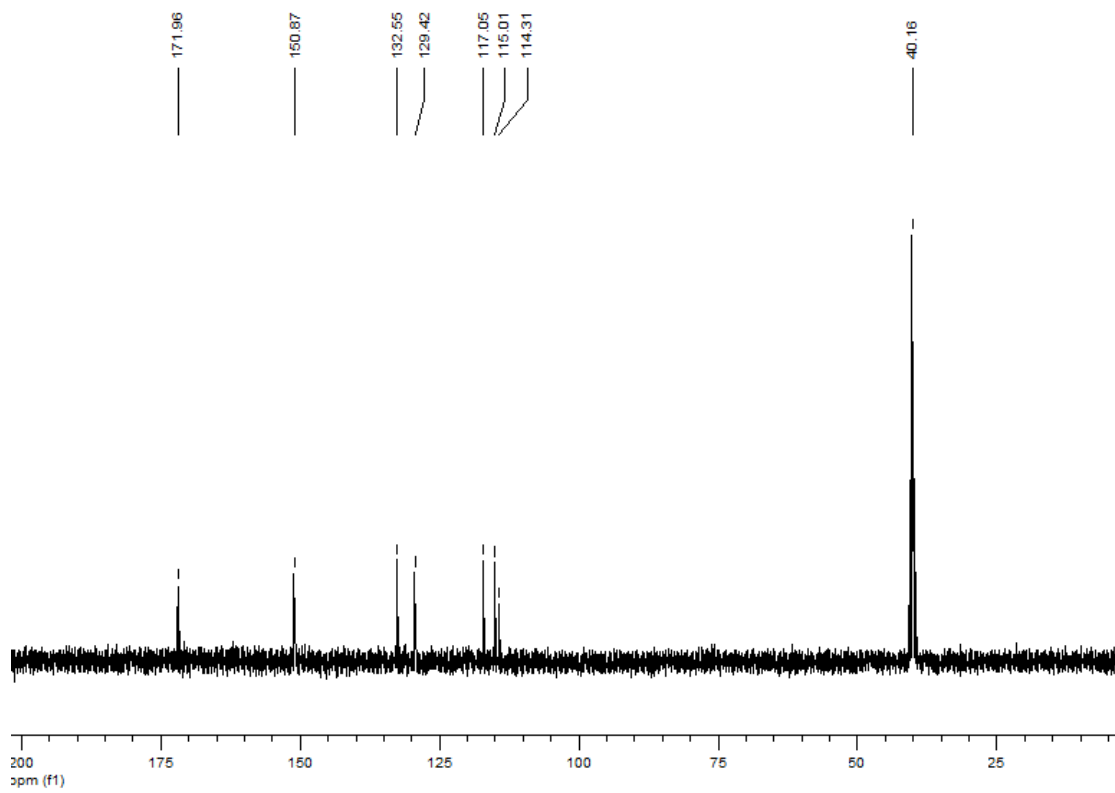
4-Chloro-2-nitrobenzamide (58)
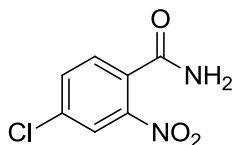


To a 250 round bottom flask was added 4-chloro-2-nitrobenzoic acid **48** (5.0 g,

24.8 mmol), DCM (100 ml), and DMF (10 μl). While stirred, oxalylchloride (2.55 ml, 29.7

mmol, 1.2 eq) was added drop-wise. The reaction was stirred at RT for 2 hours before

NH_3 (in DCM 100 ml, extracted from 50 ml concentrated NH_4OH) was added. The

reaction was stirred at RT for 1 hour before it was filtered and concentrated. The crude

was passed through a short plug of silica gel, eluting with DCM – MeOH (90 % - 10 %).

After removal of solvent, pure white solid was obtained as product (4.53 g, 91 % yield).

^{1}H NMR (400 MHz, DMSO-d6): δ 8.20 (s, 1H), 8.12 (d, J = 2 Hz, 1H), 7.85 (dd, J_1 = 8 Hz, J_2

= 2 Hz, 1H), 7.77 (s, 1H), 7.66 (d, J = 8 Hz, 1H). ^{13}C NMR (400 MHz, DMSO-d6): δ 166.75,

148.80, 135.35, 133.64, 131.55, 131.14, 124.63.

Spectrum 4-11: 4-chloro-2-nitrobenzamide (**58**) ^{1}H NMR (400MHz, DMSO-d6)

Spectrum 4-12: 4-chloro-2-nitrobenzamide (**58**) ^{13}C NMR (400MHz, DMSO-d6)
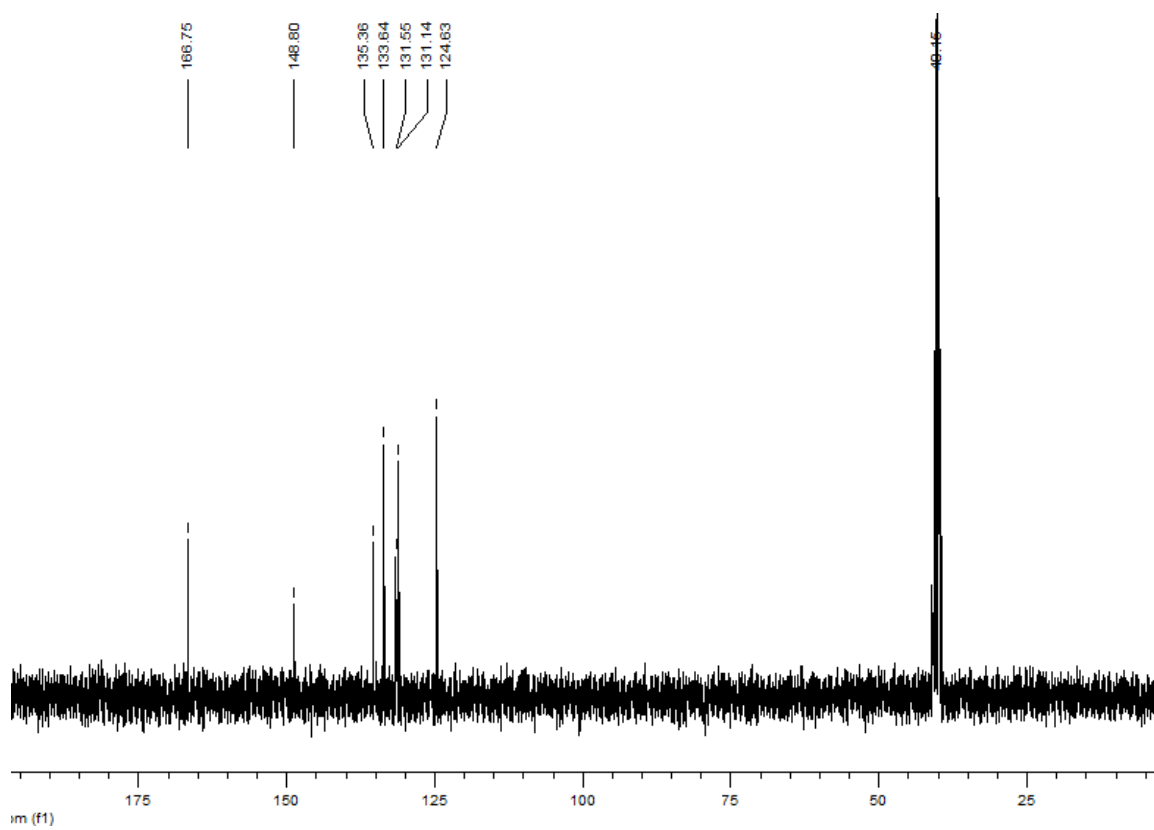
***N*-(2-mercapto-4-oxo-1,2,3,4-tetrahydroquinazolin-2-yl)benzamide (60)**
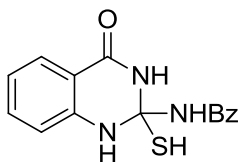
To a 100 ml round bottom flask was added 2-nitrobenzamide (500 mg, 3.0 mmol) and MeOH (40 ml). The flask was flushed with Ar gas before Pd/C (50 mg, 10 wt %) was added. The reaction was then sealed under H_2 atmosphere and stirred at room temperature for 1 hour before filtered and concentrated. ACN (40 ml) was added followed by benzoyl isothiocyanate (406 μl, 3.0 mmol). The reaction was stirred at rt for 1 hour before concentrated and purified via flash column chromatography (DCM – MeOH : 90 % – 10 %) to yield white solid product (720 mg, 80 % yield). ^{1}H NMR (400 MHz, DMSO-d6): δ 11.50 (s, 1H), 8.14 (d, *J* = 8 Hz, 1H), 8.09 (s, 1H), 7.96 (d, *J* = 8Hz, 2H), 7.66 – 7.47 (m, 6H), 7.32 (t, *J* = 7 Hz, 1H). ^{13}C NMR (400 MHz, DMSO-d6): δ 180.08, 169.59, 167.98, 137.10, 133.74, 132.88, 130.50, 130.16, 129.36, 129.12, 128.53, 127.70, 126.50. MS (ESI) calculated exact mass for $C_{15}H_{13}N_3O_2S$ = 299.07. Found [M+Na]$^+$ = 322.02.

Spectrum 4-13: *N*-(2-mercapto-4-oxo-1,2,3,4-tetrahydroquinazolin-2-yl)benzamide **(60)**
^{1}H NMR (400MHz, DMSO-d6)

Spectrum 4-14: *N*-(2-mercapto-4-oxo-1,2,3,4-tetrahydroquinazolin-2-yl)benzamide (**60**)
^{13}C NMR (400MHz, DMSO-d6)
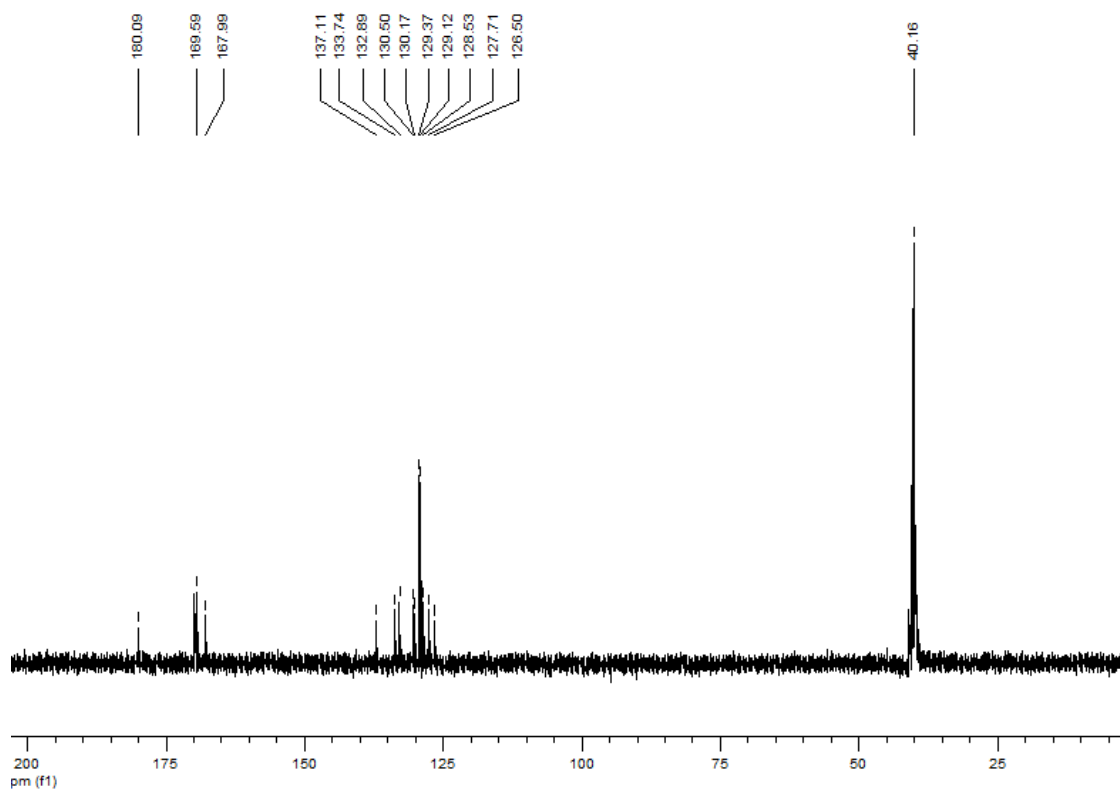
N-(4-oxo-3,4-dihydroquinazolin-2-yl)benzamide (61)
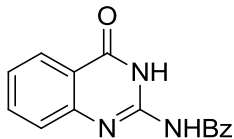
To a 500 ml round bottom flask was added *N*-(2-mercapto-4-oxo-1,2,3,4-tetrahydroquinazolin-2-yl)benzamide **60** (720 mg, 2.4 mmol), ACN (250 ml), DIPC (420 µl, 2.4 mmol), and K2CO= (331 mg, 2.4 mmol). The reaction was stirred at rt for 73 hours, after which the TLC (DCM-MeOH : 90 % - 10 %) still showed presence of starting material. The reaction was then heated to reflux for 24 hours before filtration and concentration. The crude was purified via flash column chromatography (DCM - MeOH : 90 % - 10 %) to yield yellow solid product (78 mg, 12 % yield). The ^{1}H NMR spectrum suggested that the product was not pure.

Spectrum 4-15: *N*-(4-oxo-3,4-dihydroquinazolin-2-yl)benzamide (**61**) ¹H NMR (400MHz, DMSO-d6)
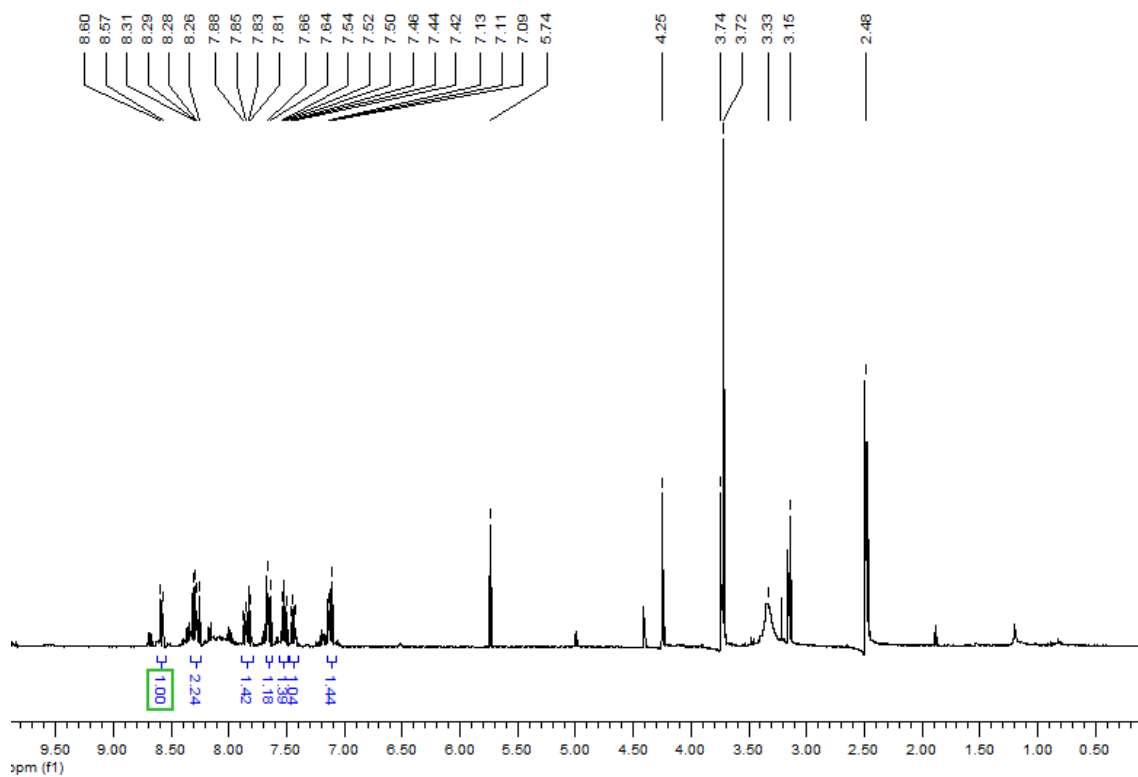
_N_-Benzyl-2,4-dichlorobenzamide (64)
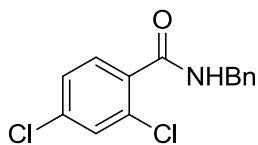
To a 100 ml round-bottom flask was added 2,4-dichlorobenzoic acid (1.0 g, 5.24

mmol), DCM (40 ml), DMF (1 drop), and oxalylchloride (539 μl, 6.29 mmol, 1.2 eq). The

reaction was stirred at RT for 1 hour before it was added drop-wise to a stirred mixture

of K_2CO_3 (1.6 g, 11.53 mmol, 2.2 eq) and benzylamine (832 μl, 6.29 mmol) in DCM (100

ml). The reaction was then stirred at RT for 2.5 hours before it was filtered and

extracted with water (150 ml). The organic layer was collected and dried over Na_2SO_4.

After filtration and concentration, the crude was purified via flash column

chromatography (DCM 100 %) to yield white solid as the product (1.48 g, 98 % yield). [1]H

NMR (400 MHz, DMSO-d6): δ 9.04 (t, _J_ = 6 Hz, 1H), 7.68 (t, _J_ = 1 Hz, 1H), 7.48 (d, _J_ = 1 Hz,

2H), 7.34 – 7.33 (m, 4H), 7.26 – 7.22 (m, 1H), 4.44 (d, _J_ = 6 Hz, 2H).   ^{13}C NMR (400 MHz,

DMSO-d6): δ 163.60, 146.27, 137.74, 134.45, 130.32, 130.01, 128.92, 53.86. MS (ESI)

calculated exact mass for $C_{14}H_{11}Cl_2NO$ = 279.02. Found [M+H][+] = 279.92.

Spectrum 4-16: *N*-Benzyl-2,4-dichlorobenzamide (**64**) ^{1}H NMR(400MHz, DMSO-d6)
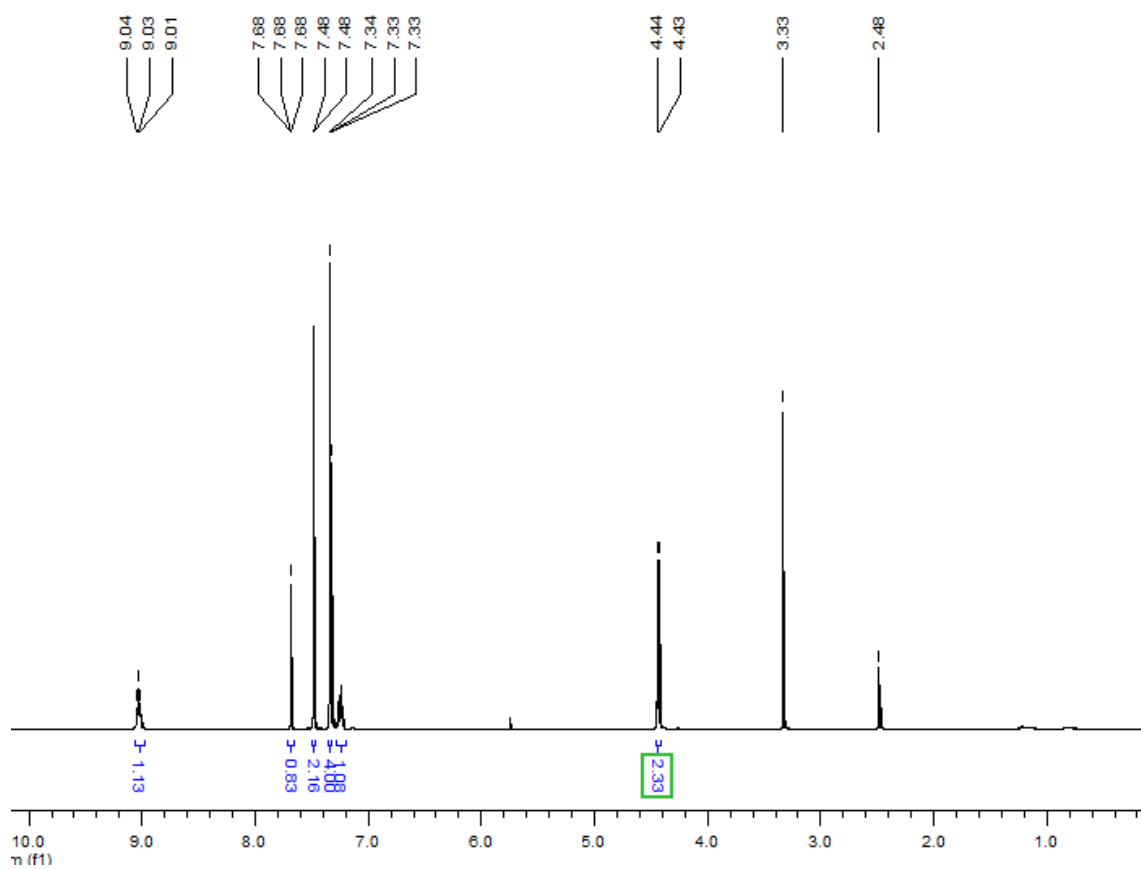
Spectrum 4-17: *N*-Benzyl-2,4-dichlorobenzamide (**64**) ^{13}C NMR(400MHz, DMSO-d6)
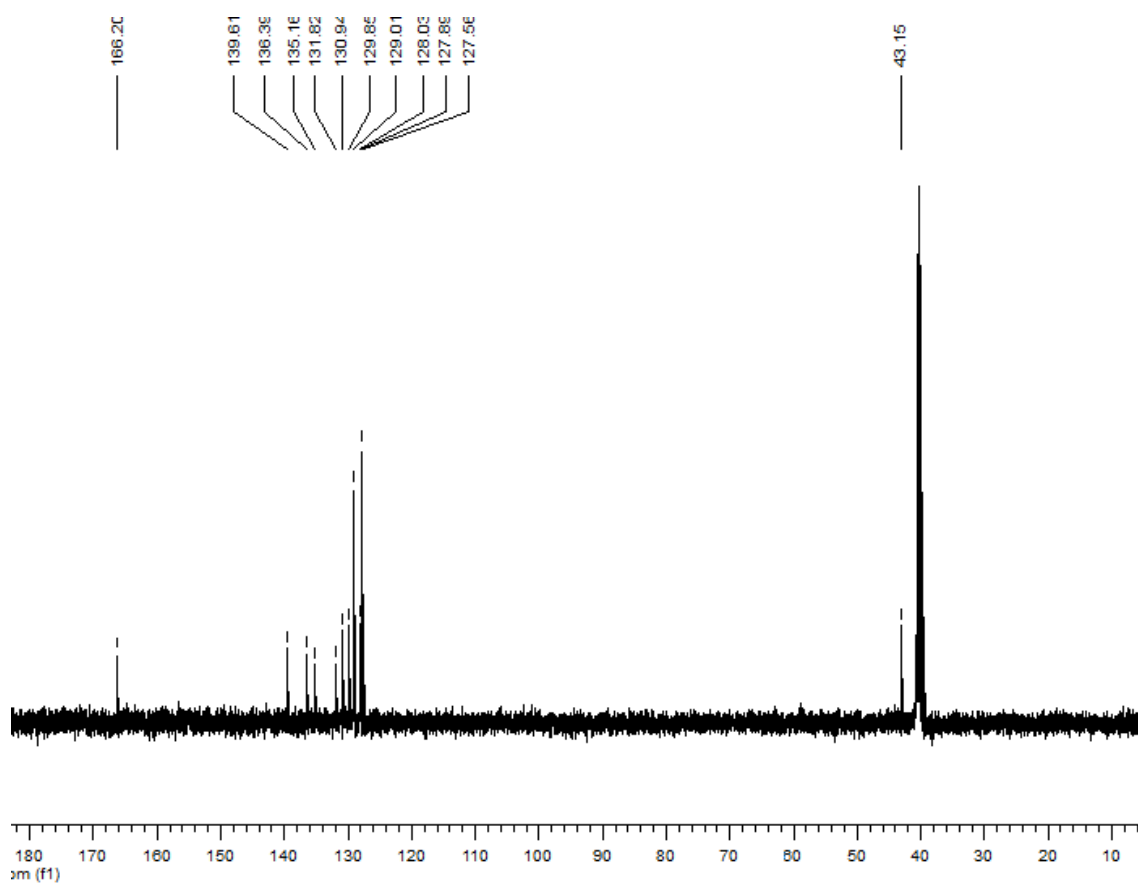
2,4-dichloro-5-nitrobenzoic acid (67)
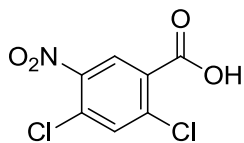
To a 25 ml round bottom flask containing 2,4-dichlorobenzoic acid **47** (5.0 g, 26.2 mmol) was added concentrated sulfuric acid (15 ml) drop-wise while stirred at 0 °C. A mixture of concentrated sulfuric acid (1 ml) and concentrated nitric acid (1 ml) was then added drop-wise. The reaction was stirred at 0 °C for 5 minutes before warming up to RT. It was stirred RT for 1.5 hr before it was poured into an ice-water mixture (250 ml) and extracted with EtOAc (2 x 200 ml). The organic layers were combined and washed with water (2 x 200 ml), brine (150 ml) and dried over Na_2SO_4. The drying agent was filtered out and the solvent was removed *in vacuuo* to yield a white solid as the crude product (5.02 g) that was used without further purification. MS (ESI) calculated exact mass for $C_7H_3Cl_2NO_4$ = 234.94. Found $[M-H]^+$ = 233.93.

Methyl 2,4-dichloro-5-nitrobenzoate (52)
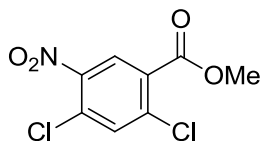
To a 250 ml round bottom flask was added crude 2,4-dichloro-5-nitrobenzoic acid **67** (5.02 g, 21.3 mmol), methanol (100 ml) and concentrated sulfuric acid (1 ml). The mixture was stirred and heated to reflux for 68 hr before it was cooled to RT and concentrated. The yellow residue was dissolved in EtOAc (200 ml) and extracted with water (3 x 100 ml). The organic layers were collected and combined. It was washed with brine (100 ml) and dried over Na_2SO_4. After filtration and concentration, the yellow oil crude was purified via flash column chromatography (Hexane – EtOAc : 90 % - 10 %) to yield a slight yellow solid as the product (3.55 g, 66.7 % yield over two steps). ^{1}H NMR (400 MHz, DMSO-d6): δ 8.49 (s, 1 H), 8.14 (s, 1 H), 3.88 (s, 3 H). ^{13}C NMR (400 MHz, DMSO-d6): δ 163.60, 146.27, 137.74, 134.45, 130.32, 130.01, 128.92, 53.86. MS (ESI) calculated exact mass for $C_8H_5Cl_2NO_4$ = 248.96. Found $[M+MeOH+H]^+$ = 282.33.

Spectrum 4-18: Methyl 2,4-dichloro-5-nitrobenzoate (**52**) ^{1}H NMR (400MHz, DMSO-d6)
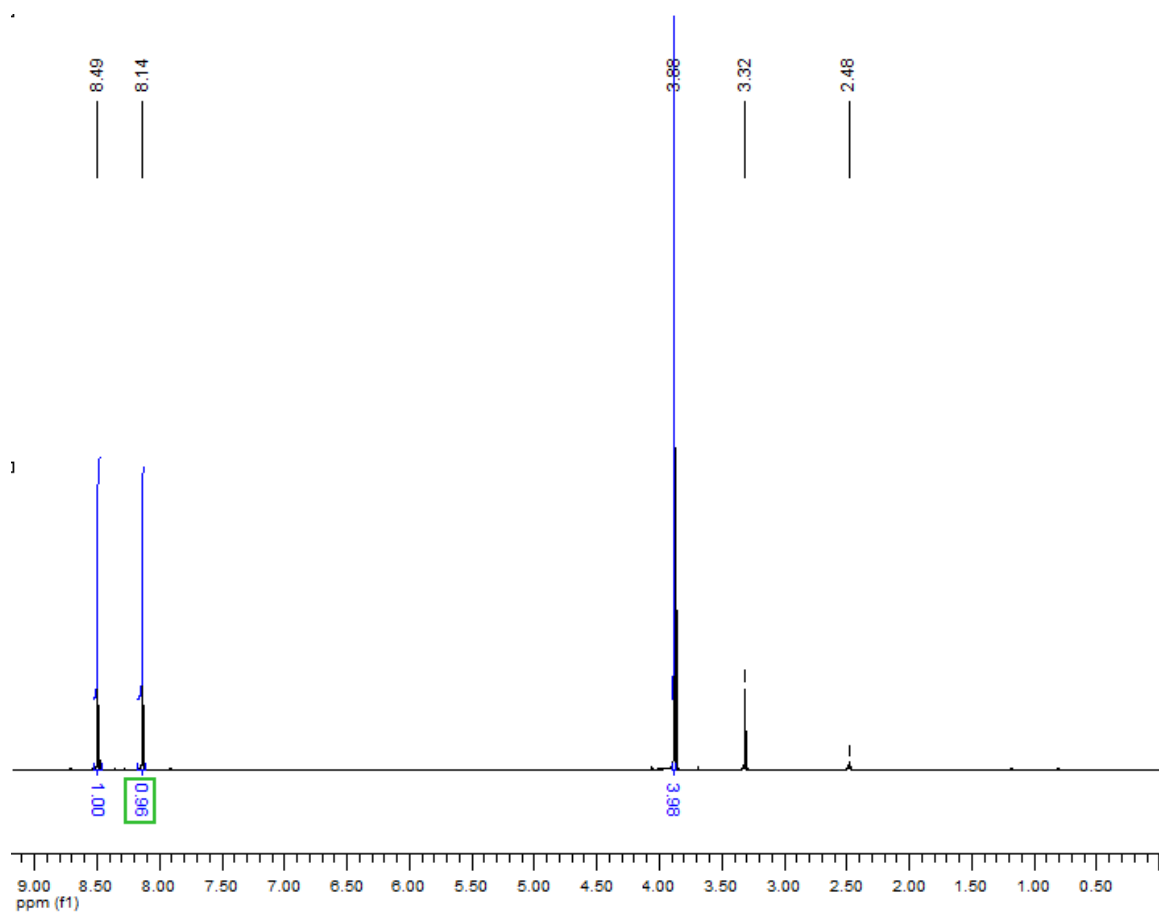
Spectrum 4-19: Methyl 2,4-dichloro-5-nitrobenzoate (**52**) ^{13}C NMR (400MHz, DMSO-d6)
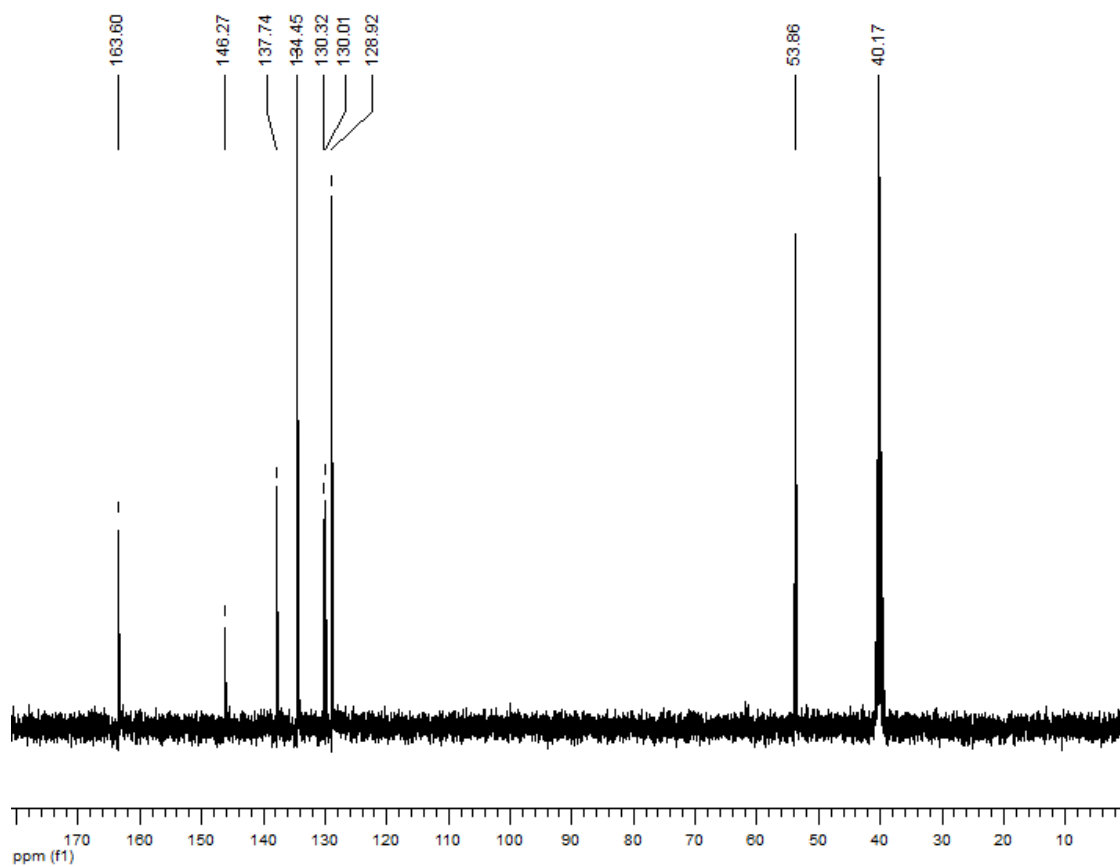
Methyl 4-(benzylamino)-2-chloro-5-nitrobenzoate (69)
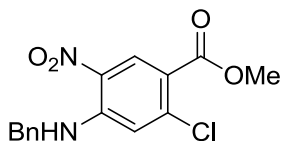
To a 100 ml round bottom flask was added methyl 2,4-dichloro-5-nitrobenzoate

52 (3.55 g, 14.2 mmol), toluene (40 ml), benzyl amine (1.55 ml, 14.2 mmol) and

potassium carbonate (1.96 g, 14.2 mmol). The reaction was heated to reflux while

stirred under Ar for 20 hrs before cooling to RT. It was filtered into 100 ml of water and

extracted. The organic layer was collected. The water layer was extracted with

additional 60 ml of toluene. The combined organic layers was washed with brine (100

ml) and dried over Na_2SO_4. After filtration and concentration, the crude was purified via

flash column chromatography (Hexane – EtOAc : 60 % - 40 %) to yield yellow solid as the

product (2.84 g, 62 % yield). ^{1}H NMR (400 MHz, DMSO-d6): δ 9.06 (t, *J* = 6 Hz, 1H), 8.63

(s, 1H), 7.36 (m, 3H), 7.34 (s, 1H), 7.31-7.39 (m, 2H), 7.00 (s, 1H), 4.69 (d, *J* = 6 Hz, 2H),

3.78 (s, 3H).   ^{13}C NMR (400 MHz, DMSO-d6): δ 163.85, 147.01, 140.80, 138.23, 131.86,

130.37, 129.37, 127.97, 127.61, 117.22, 114.96, 52.95, 46.41. MS (ESI) calculated exact

mass for $C_8H_5Cl_2NO_4$ = 320.06. Found [M+H]$^+$ = 321.08.

Spectrum 4-20: Methyl 4-(benzylamino)-2-chloro-5-nitrobenzoate (**69**) ^{1}H NMR (400MHz, DMSO-d6)
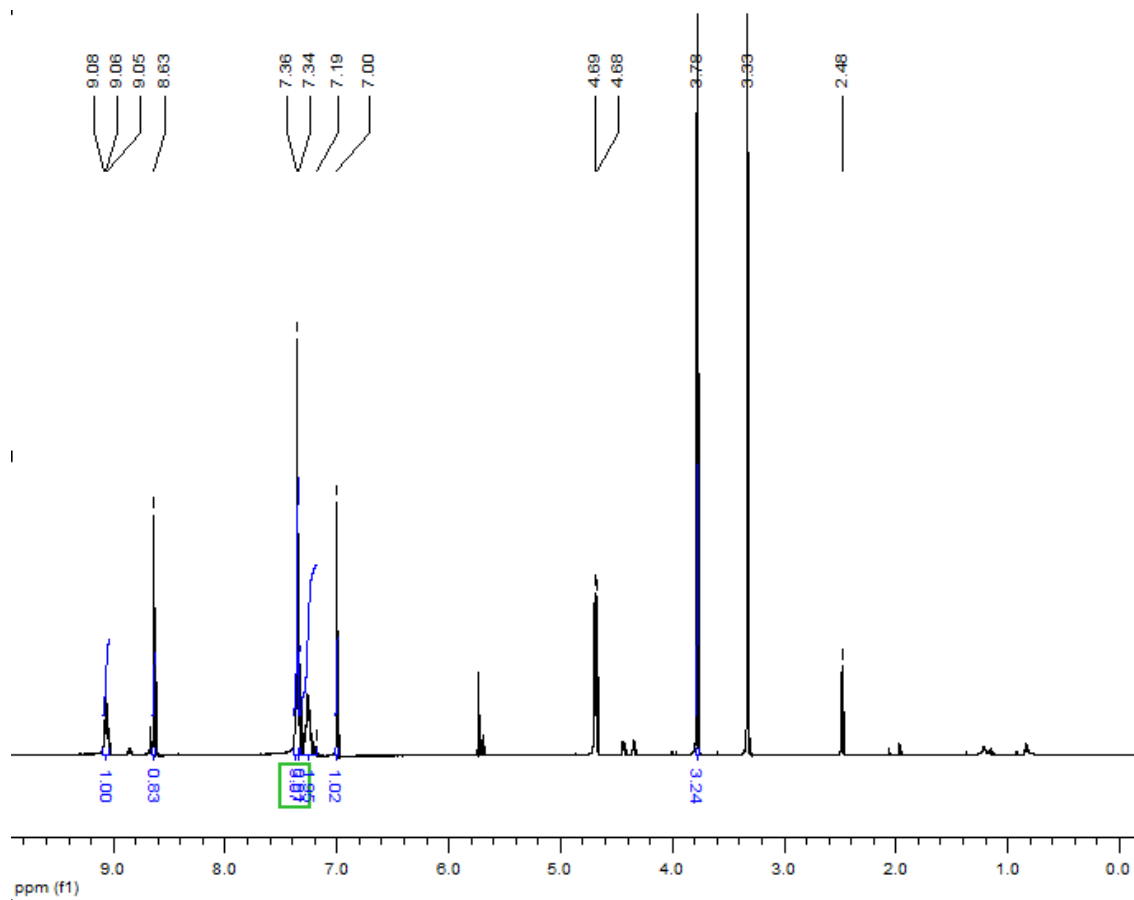
Spectrum 4-21: Methyl 4-(benzylamino)-2-chloro-5-nitrobenzoate (**69**) ^{13}C NMR (400MHz, DMSO-d6)
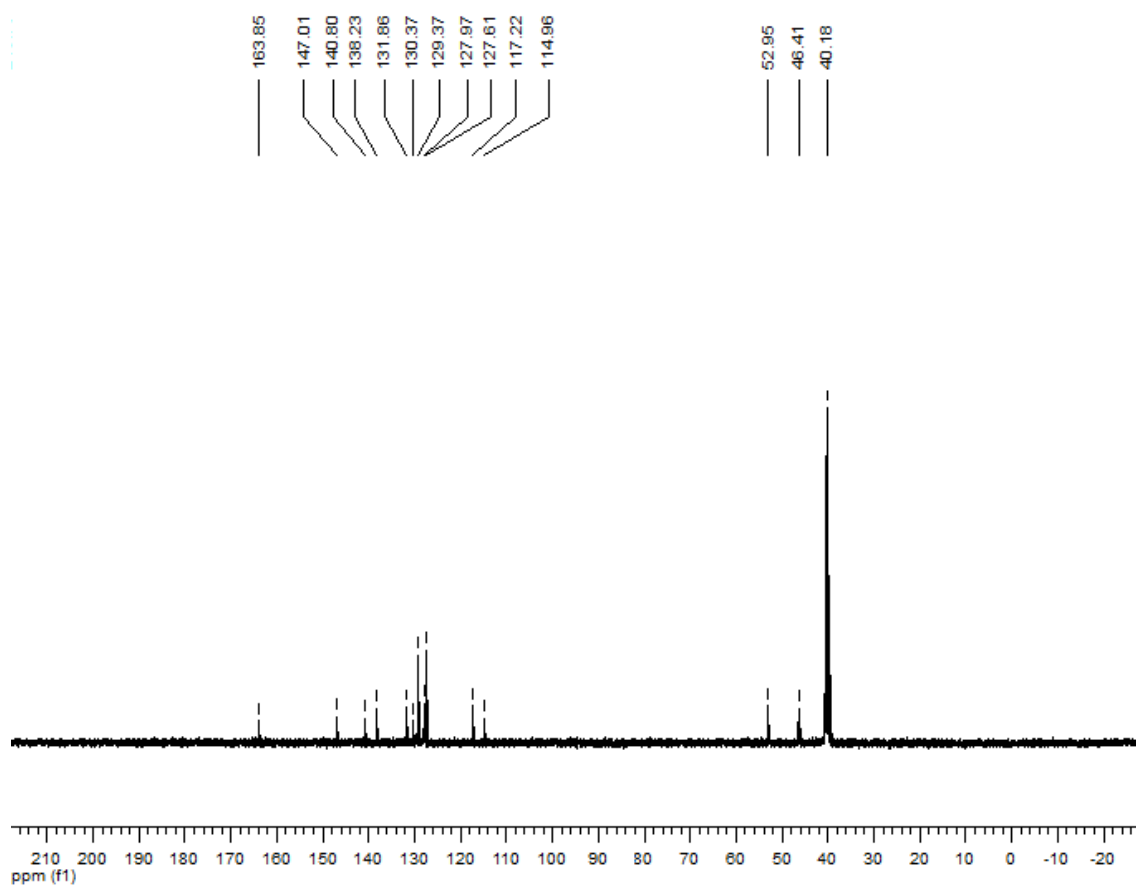
Methyl 2,4-bis(benzylamino)-5-nitrobenzoate (70)
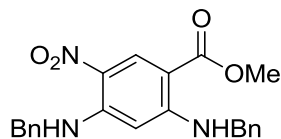
To a 100 ml round-bottom flask was added methyl 4-(benzylamino)-2-chloro-5-nitrobenzoate **69** (1.0 g, 3.1 mmol), toluene (40 ml), benzyl amine (340 µl, 3.1 mmol) and K_2CO_3 (430 mg, 3.1 mmol). The reaction was stirred and heated to reflux under Ar for 30 hr. After cooling to RT, it was filtered and concentrated. The crude was purified via flash column chromatography (DCM – Hexane : 60 % - 40 %) to yield yellow solid as the product (1.08 g, 89 % yield). ^{1}H NMR (400 MHz, DMSO-d6): δ 8.85 (t, *J* = 6 Hz, 1H), 8.68 (s, 1H), 8.62 (t, *J* = 6 Hz, 1H), 7.30-7.19 (m, 10H), 5.69 (s, 1H), 4.44 (d, *J* = 6 Hz, 2H), 4.35 (d, *J* = 6 Hz, 2H), 3.76 (s, 3H).   ^{13}C NMR (400 MHz, DMSO-d6): δ 167.28, 154.10, 148.75, 138.45, 138.37, 133.35, 129.29, 129.25, 127.89, 127.81, 127.77, 123.62, 102.31, 91.82, 52.49, 46.70, 46.58.

Spectrum 4-22: Methyl 2,4-bis(benzylamino)-5-nitrobenzoate (**70**) ^{1}H NMR (400MHz, DMSO-d6)
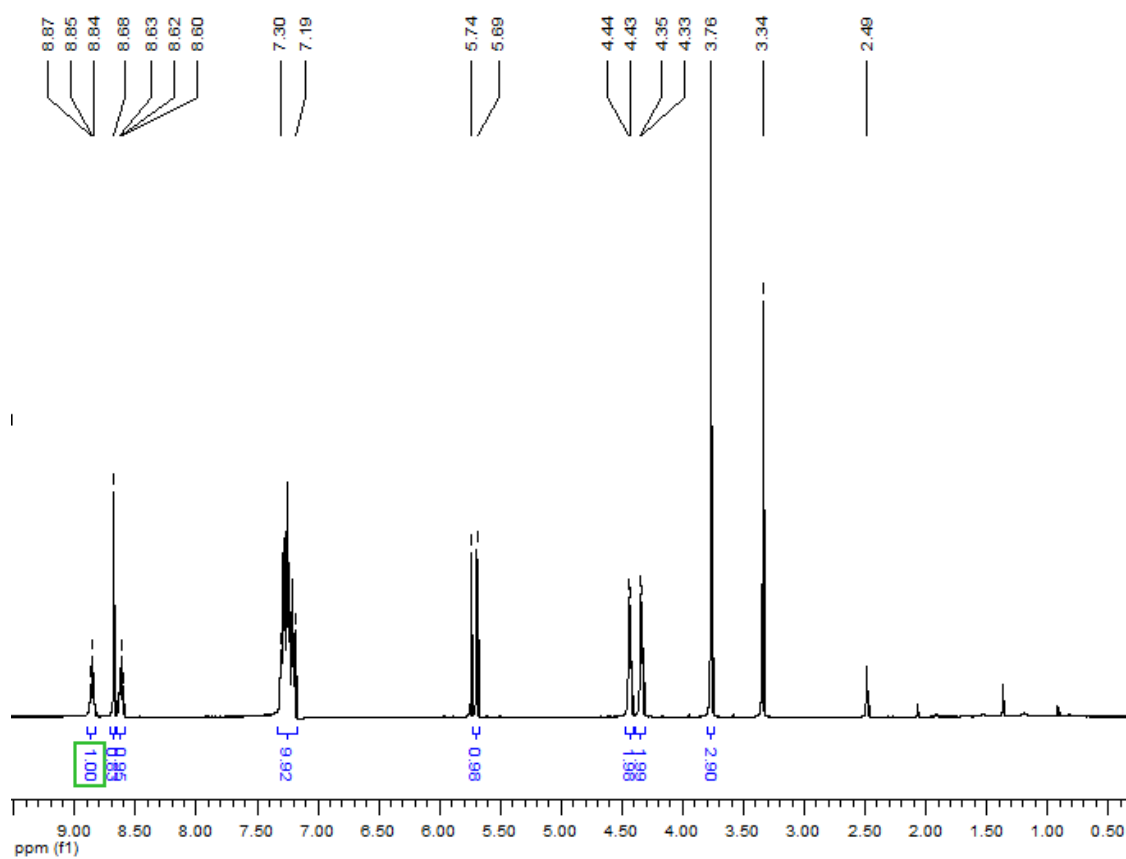
Spectrum 4-23: Methyl 2,4-bis(benzylamino)-5-nitrobenzoate (**70**) ^{13}C NMR (400MHz, DMSO-d6)
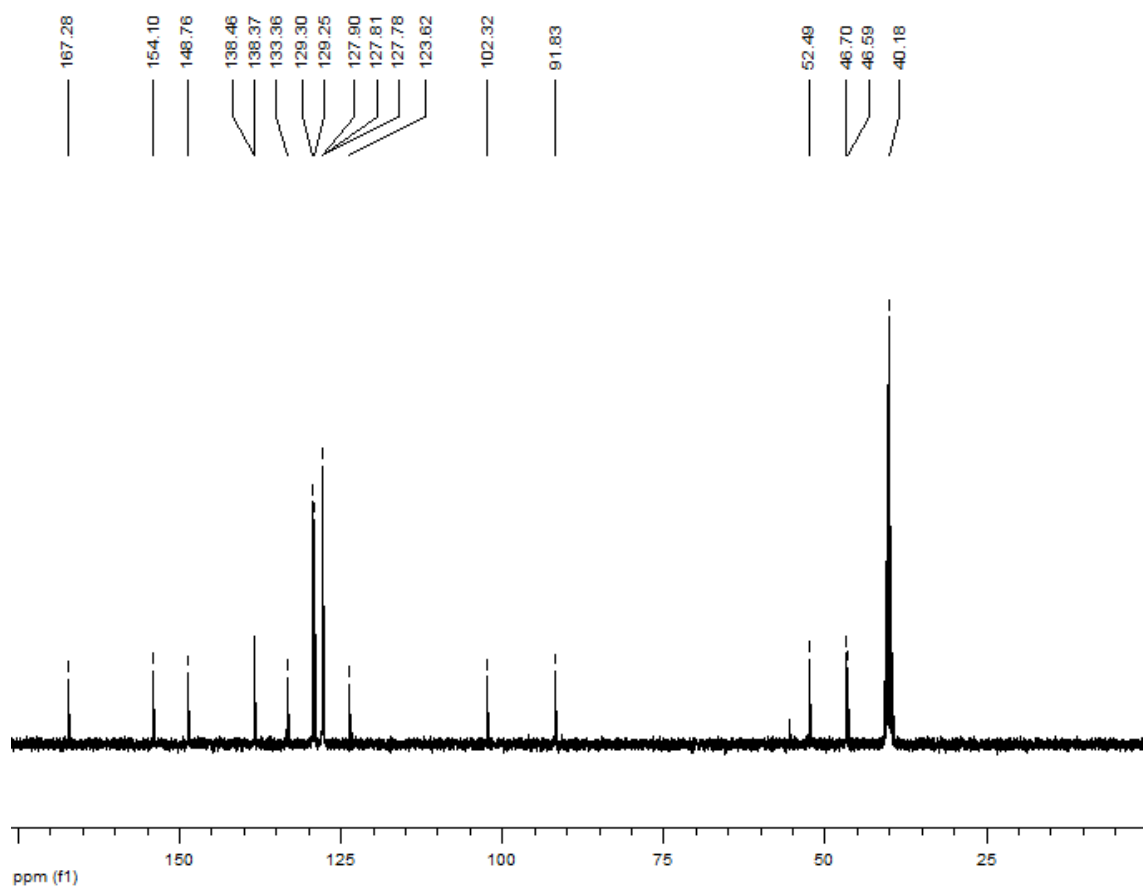
Methyl 2-benzamido-1-benzyl-6-(benzylamino)-2-mercapto-2,3-dihydro-1*H*-benzo[d]imidazole-5-carboxylate (71)
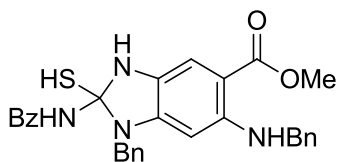
To a 100 ml round-bottom flask was added methyl 2,4-bis(benzylamino)-5-nitrobenzoate **70** (770 mg, 2.0 mmol) and glacial acetic acid-water (40 ml, 5:1). The solution was stirred while Zn powder (1.3 g, 20 mmol, 10 eq) was added portion-wise. The reaction was stirred at RT for 24 hours before filtered into 200 ml of 10 % NH_4OH aq and extracted with DCM (2 x 150 ml). The combined organic layers was washed with water (100 ml), brine (100 ml) and dried over Na_2SO_4. After filtration and concentration, the crude was passed through a short plug of silica gel using DCM – MeOH (90 % - 10 %). The solvent was evaporated and the oil residue was dissolved in DCM (40 ml). Benzoyl isothiocyanate (261 µl, 2.0 mmol) was added dropwise. The reaction was stirred at RT for 1 hour before it was filtered and concentrated. It was purified via flash column (DCM – EtOAc : 90 % - 10 %) to yield relatively pure product that was further recrystalized using DCM-Hexane (80 % - 20%) to obtain a yellow solid as the product (775 mg, 75 % yield over two steps). ^{1}H NMR (400 MHz, DMSO-d6): δ 11.68 (s, 1H), 11.56 (s, 1H), 8.13 (t, *J* = 6 Hz, 1H), 8.00 (d, *J* = 8 Hz, 2H), 7.66 (t, *J* = 7 Hz, 1H), 7.54-7.50 (m, 3H), 7.29 – 7.17 (m, 10H), 6.76 (t, *J* = 6 Hz, 1H), 5.62 (s, 1H), 4.26 (d, *J* = 6 Hz, 2H), 4.19 (d, *J* = 6 Hz, 2H), 3.67 (s, 3H). ^{13}C NMR (400 MHz, DMSO-d6): δ 183.31, 168.73, 168.24, 152.00, 149.38, 139.86, 139.78, 133.66, 133.11, 131.86, 129.35, 129.16, 129.09, 128.90, 127.84, 127.60,

127.52, 127.32, 113.92, 98.10, 92.25, 51.54, 46.80, 46.19. MS (ESI) calculated exact mass

for $C_{30}H_{28}N_4O_3S$ = 524.19. Found $[M+H]^+$ = 525.22

Spectrum 4-24: Methyl 2-benzamido-1-benzyl-6-(benzylamino)-2-mercapto-2,3-dihydro-1*H*-benzo[d]imidazole-5-carboxylate (**71**) ^{1}H NMR (400MHz, DMSO-d6)
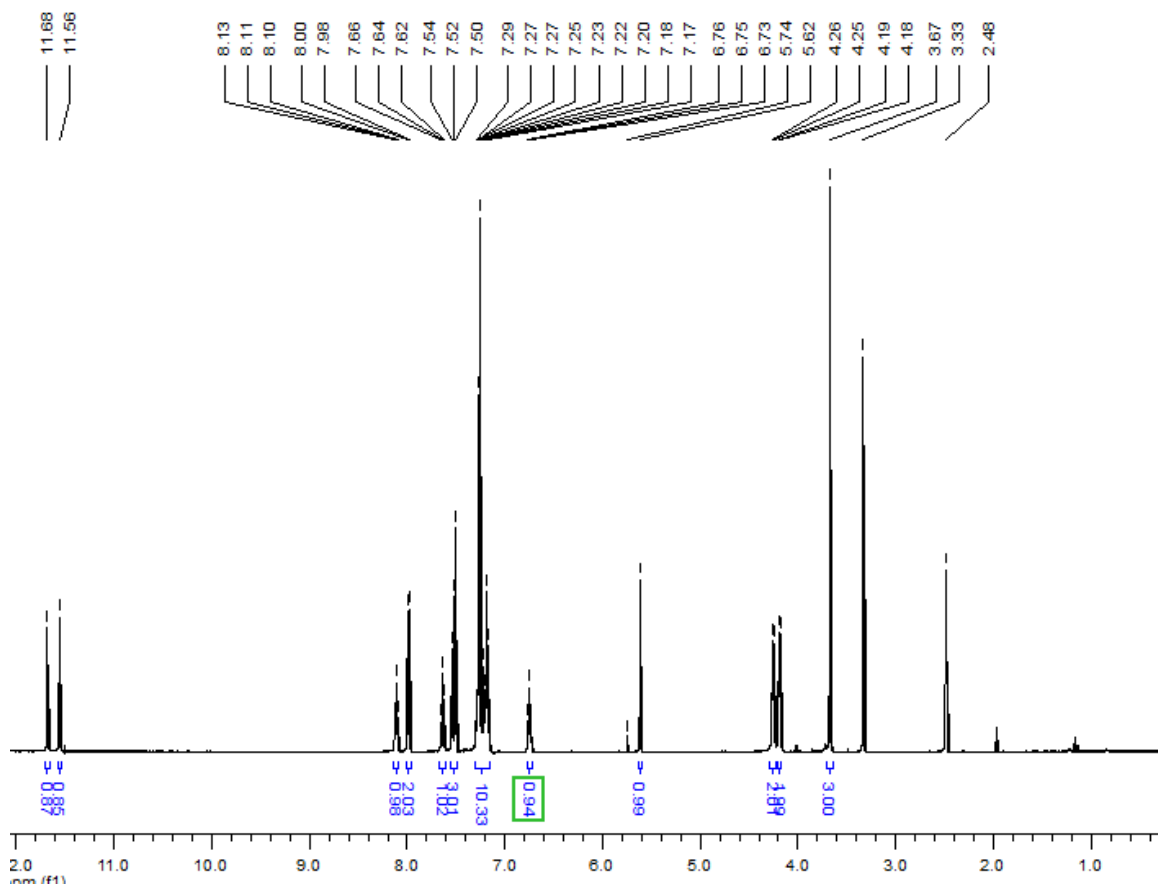
Spectrum 4-25: Methyl 2-benzamido-1-benzyl-6-(benzylamino)-2-mercapto-2,3-dihydro-1*H*-benzo[d]imidazole-5-carboxylate (**71**) ^{13}C NMR (400MHz, DMSO-d6)

Methyl 2-benzamido-1-benzyl-6-(benzylamino)-1*H*-benzo[*d*]imidazole-5-carboxylate (72)

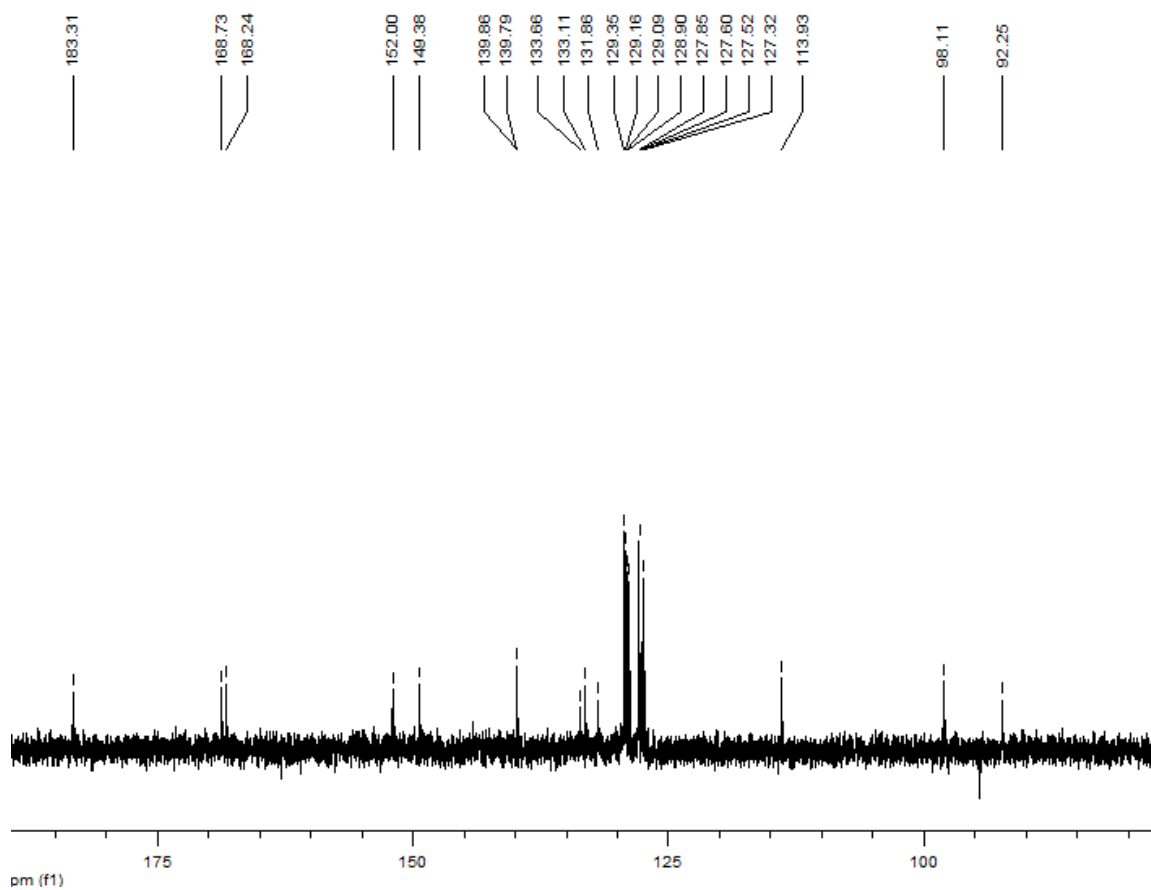To a 250 ml round bottom flask was added methyl 2-benzamido-1-benzyl-6-(benzylamino)-2-mercapto-2,3-dihydro -1*H*-benzo[*d*]imidazole-5-carboxylate **71** (775 mg, 1.5 mmol), DCM (100 ml), DIPEA (237 µl, 1.5 mmol) and DIPC (261 µl, 1.5 mmol). The reaction was stirred at RT for 9 days before it was concentrated and purified via flash column (DCM – EtOAc : 100 % - 0 % to 80 % - 20 %) to yield yellow-green solid as the product (294 mg, 40 % yield). ^{1}H NMR (400 MHz, DMSO-d6): δ 8.25 – 8.21 (m, 3H), 7.95 (s, 1H), 7.51 – 7.43 (m, 3H), 7.34 – 7.22 (m, 12 H), 6.69 (s, 1H), 5.35 (s, 2H), 4.47 (d, *J* = 6 Hz, 2H), 3.80 (s, 3H). ^{13}C NMR (400 MHz, DMSO-d6): δ 174.24, 168.76, 153.92, 148.93, 139.72, 138.62, 137.12, 135.73, 131.83, 129.47, 129.30, 129.22, 128.71, 128.63, 128.31, 127.94, 127.67, 120.08, 114.93, 105.63, 92.36, 52.35, 47.10, 45.35. MS (ESI) calculated exact mass for $C_{30}H_{26}N_4O_3$ = 490.20. Found [M+H]$^+$ = 491.20.

Spectrum 4-26: Methyl 2-benzamido-1-benzyl-6-(benzylamino)-1*H*-benzo[*d*]imidazole-5-carboxylate (**72**) ^{1}H NMR (400MHz, DMSO-d6)
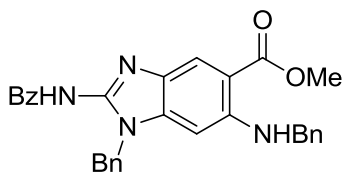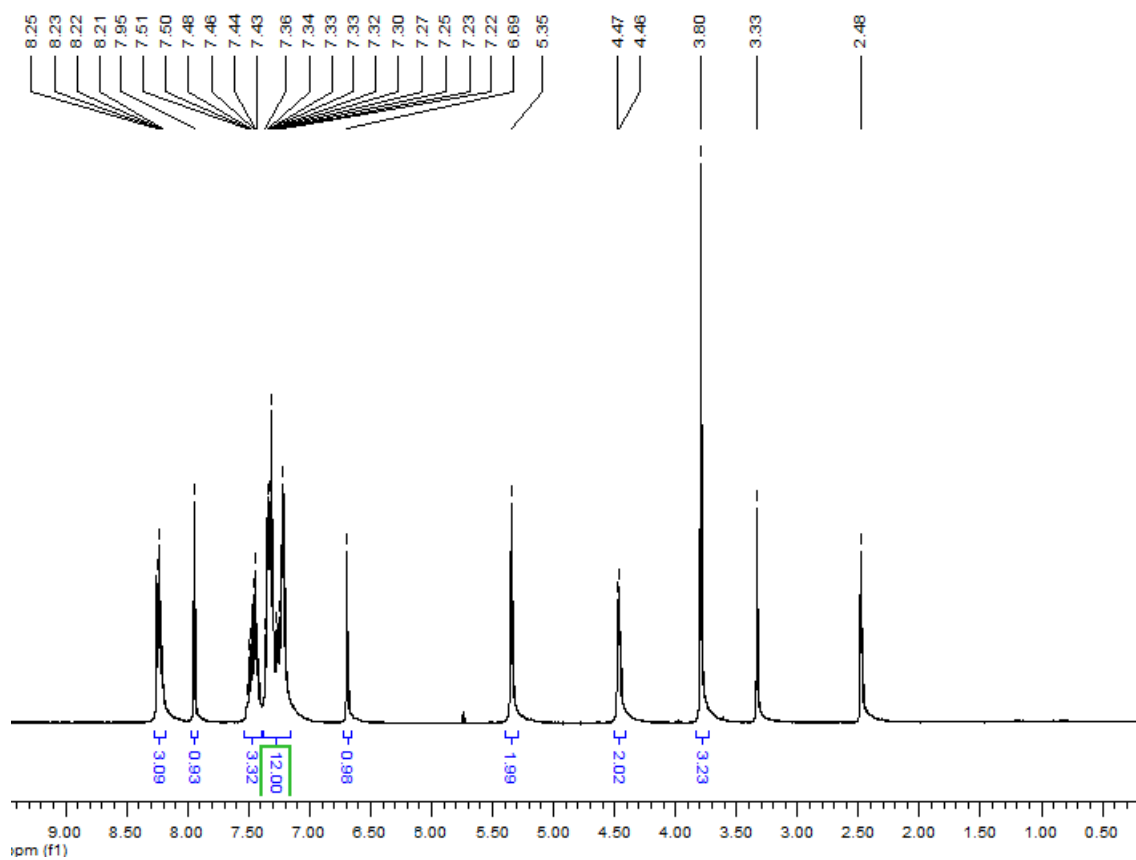
Spectrum 4-27: Methyl 2-benzamido-1-benzyl-6-(benzylamino)-1*H*-benzo[*d*]imidazole-5-carboxylate (**72**) ^{13}C NMR (400MHz, DMSO-d6)

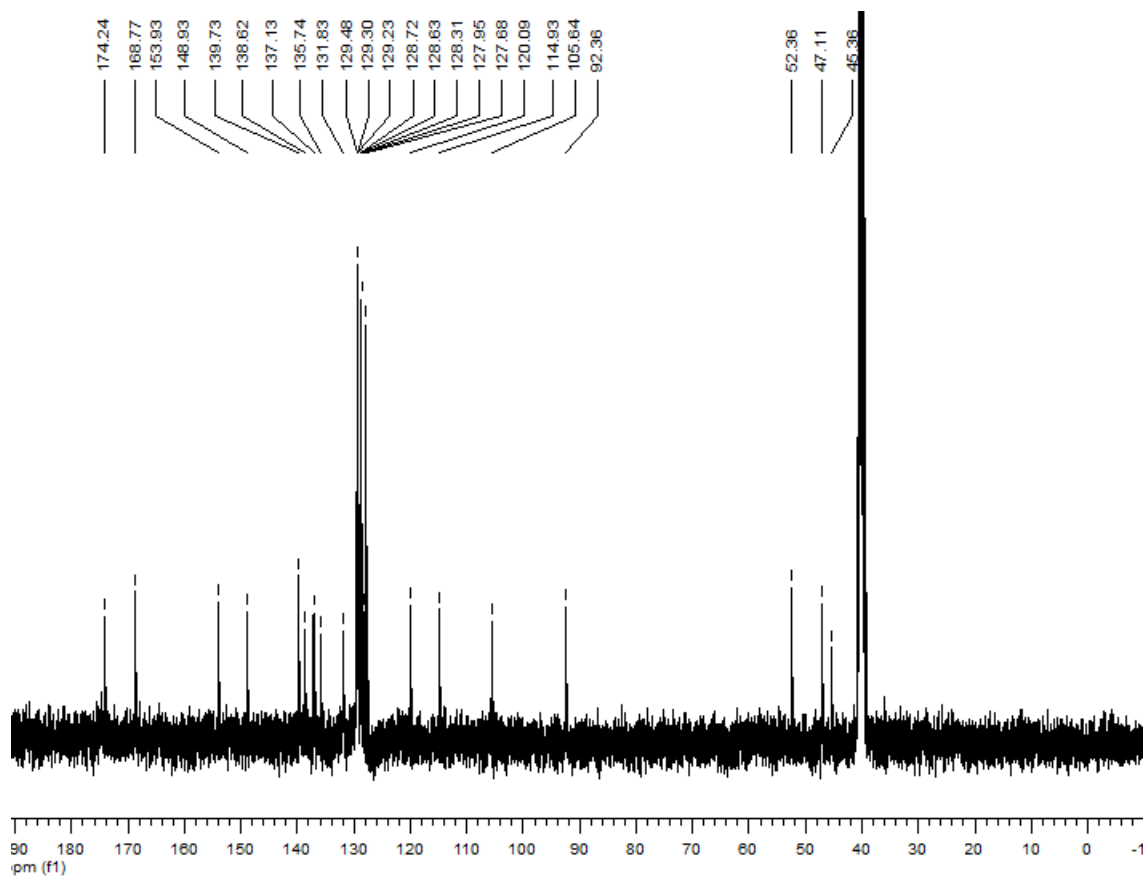**Methyl 2-(benzoylimino)-1-benzyl-6-(benzylamino)-3-carbamimidoyl-2,3-dihydro-1*H*-benzo[*d*]imidazole-5-carboxylate (73)**
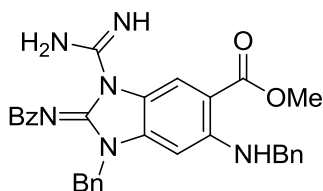
To a 25 ml round bottom flask was added Methyl 2-benzamido-1-benzyl-6-(benzylamino)-1*H*-benzo[*d*]imidazole-5-carboxylate (**72**) (116 mg, 0.3 mmol), chloroformamidinium chloride (51 mg, 0.45 mmol, 1.5 eq) and dimethylsulfone (100 mg). The reaction was stirred and heated to 160 °C for 2 hours before it was cooled to RT. The solid residue was purified via flash column chromatography (DCM – MeOH : 95% - 5%) to yiled slight yellow solid as product (65 mg, 43%). ^{1}H NMR (400MHz, DMSO-d6) δ: 9.00 (s, 1H), 8.61 (t, *J* = 6 Hz, 1H), 8.47 (d, *J* = 7 Hz, 2H), 8.34 (m, 3H), 7.69 (t, *J* = 7 Hz, 1H), 7.62 (t, *J* = 7 Hz, 2H), 7.39-7.27 (m, 10 H), 7.02 (s, 1H), 5.62 (s, 2H), 4.58 (d, *J* = 5 Hz, 2H), 3.88 (s, 3H).

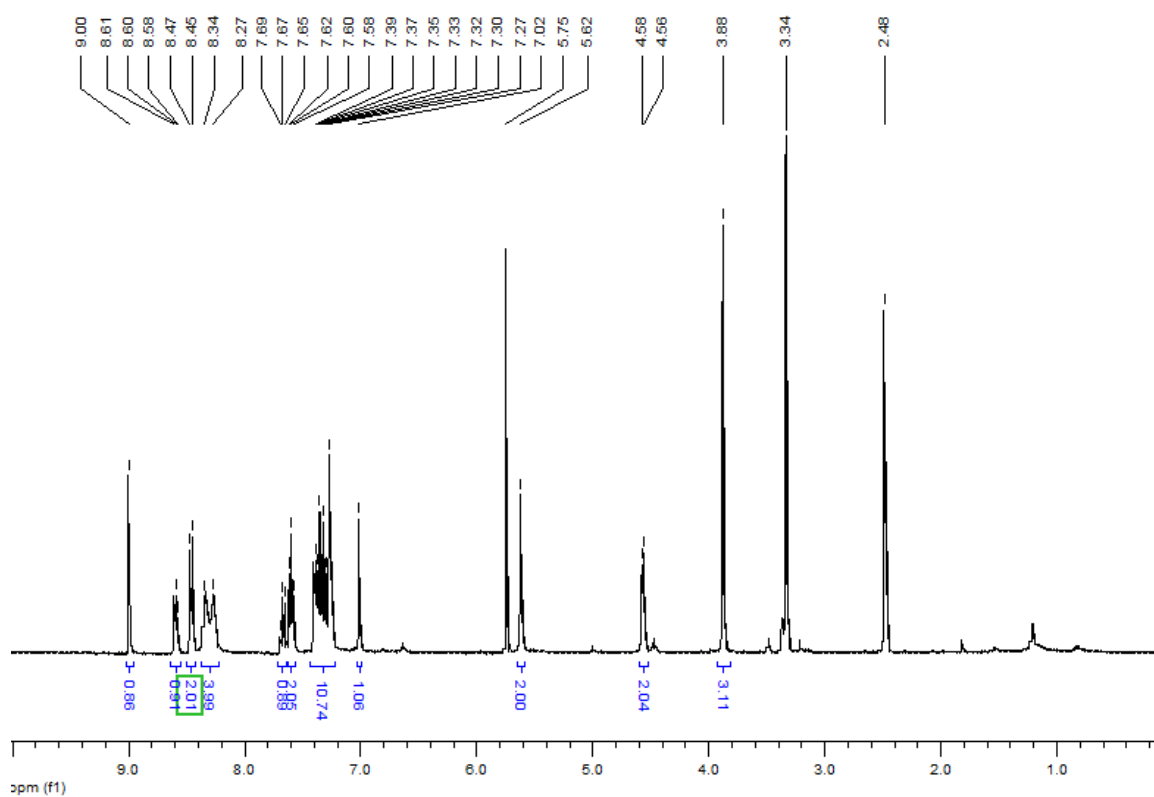**Spectrum 4-28**: Methyl 2-(benzoylimino)-1-benzyl-6-(benzylamino)-3-carbamimidoyl-2,3-dihydro-1*H*-benzo[*d*]imidazole-5-carboxylate (**73**) 1H NMR (400MHz, DMSO-d6)

Methyl 4-amino-2-chloro-5-nitrobenzoate (75)
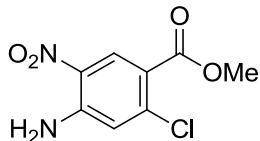
To a 25 ml pressure vessel was added methyl 2,4-dichloro-5-nitrobenzoate 52 (500 mg, 2.0 mmol), NH_3 (0.5M in Dioxane, 15 ml, 7.5 mmol), and K_2CO_3 (552 mg, 4.0 mmol). The reaction was sealed and heated to 130 °C while stirred for 42 hours before it was cooled to RT. After filtration and concentration, the crude was purified by flash column chromatography (DCM 100%) to yield yellow powder as the product (355 mg, 77 %). ^{1}H NMR (400MHz, DMSO-d6) δ: 8.50 (s, 1H), 7.94 (s, 2H), 7.08 (s, 1H), 3.77 (s, 3H). ^{13}C NMR (400MHz, DMSO-d6) δ: 163.76, 148.58, 139.75, 131.59, 129.11, 120.84, 114.78, 52.77. MS (ESI) calculated exact mass for $C_8H_7ClN_2O_4$ = 230.01. Found $[M+H]^+$ = 230.92.

Spectrum 4-29: Methyl 4-amino-2-chloro-5-nitrobenzoate (**75**) ^{1}H NMR (400MHz DMSO-d6)
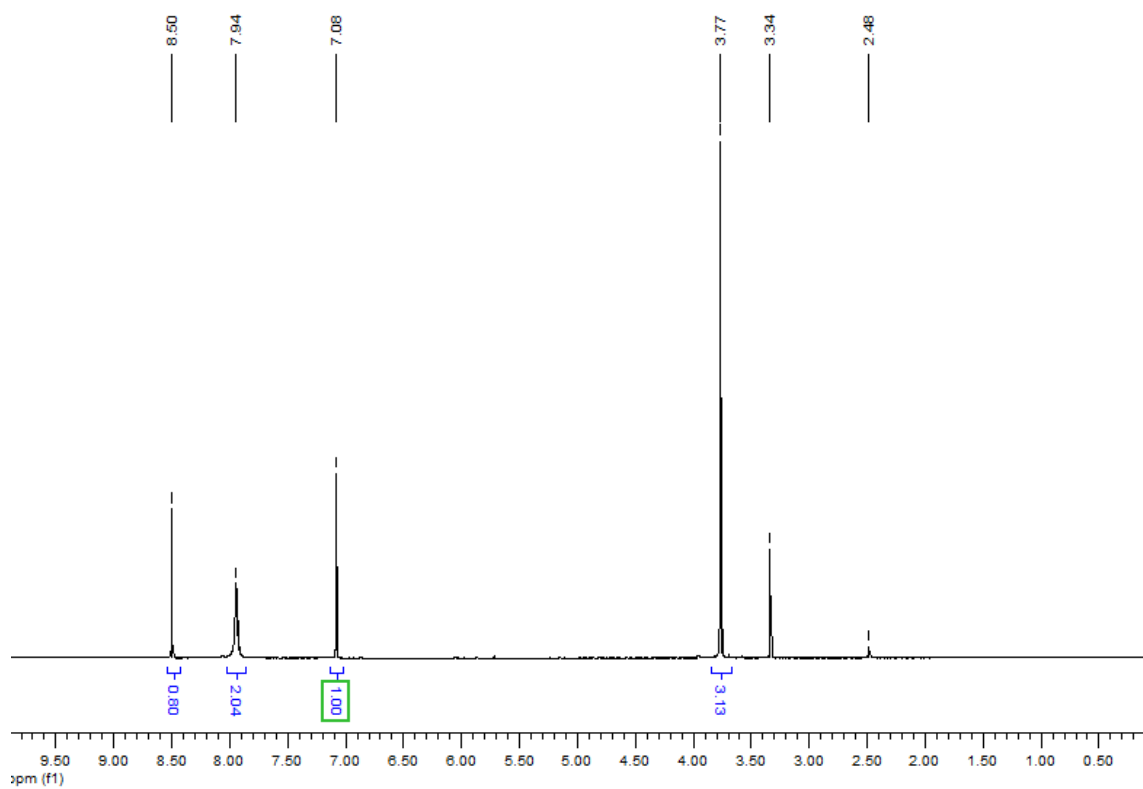
Spectrum 4-30: Methyl 4-amino-2-chloro-5-nitrobenzoate (**75**) ^{13}C NMR (400MHz DMSO-d6)
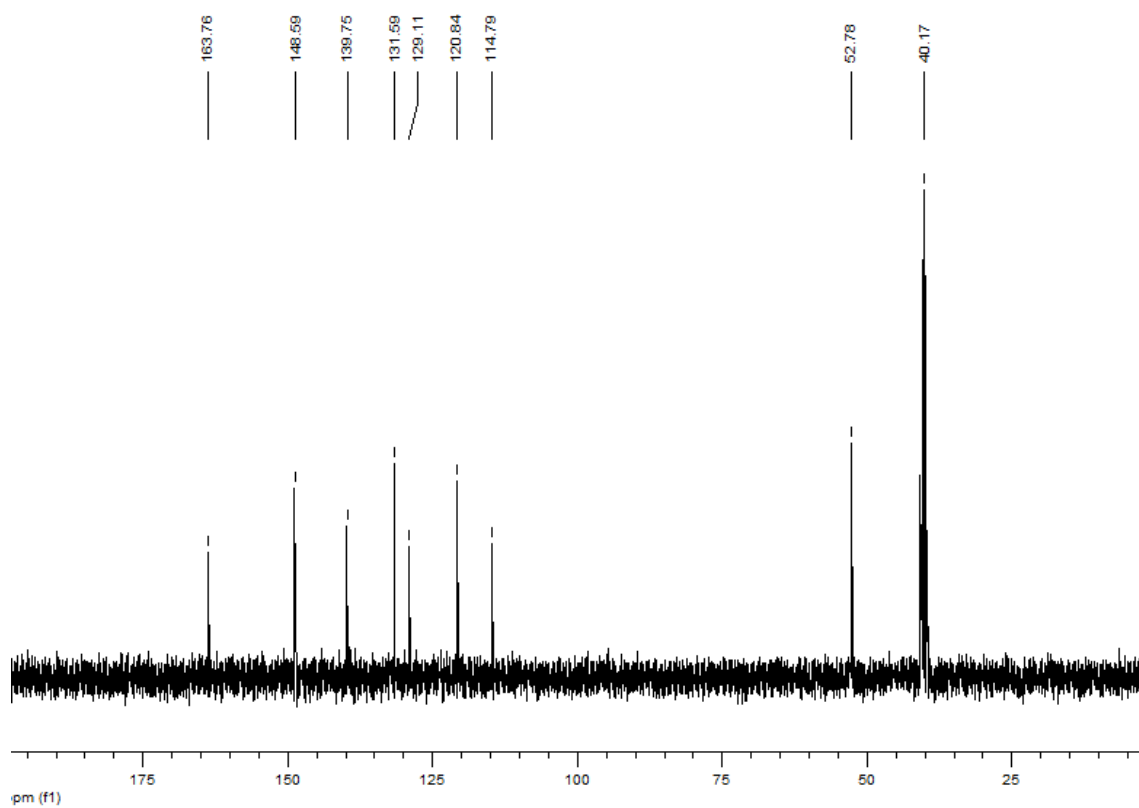
Methyl 4-((3-(dimethylamino)propyl)(methyl)amino)-2-nitrobenzoate (78)
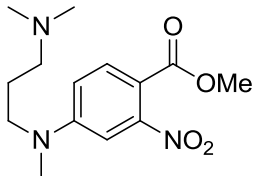
To a 100 ml round bottom flask was added methyl 4-chloro-2-nitrobenzoate (53) (500 mg, 2.32 mmol), dioxane (40ml), N,N-dimethylaminopropyl amine (350 µl, 2.78 mmol, 1.2 eq), and K_2CO_3 (384 mg, 2.78 mmol, 1.2 eq). The reaction was stirred and heated to reflux under Ar for 45 hours. After cooling to RT, the reaction was filtered and concentrated. Dioxane (40 ml), Iodomethan (173 µl, 2.78 mmol, 1.2 eq), and K_2CO_3 (384 mg, 2.78 mmol, 1.2 eq) were added. The reaction was stirred and heated to reflux under Ar for 21 hours, after which it was cooled to RT, filtered and concentrated. The crude was purified via flash column chromatography (DCM – MeOH : 90 % - 10 %) to yield slight yellow oil as the product (574 mg, 84 % yield). ^{1}H NMR (400MHz, DMSO-d6) δ: 7.52 (d, J = 8 Hz, 1H), 7.08 (d, J = 2 Hz, 1H), 6.91 (dd, J_1 = 8 Hz, J_2 = 2 Hz, 1H), 3.80 (s, 3H), 3.29 (m, 2H), 3.05 (m, 8H), 2.75 (s, 3H), 1.95 (m, 2H). ^{13}C NMR (400 MHz, DMSO-d6) δ: 168.20, 152.67, 137.54, 133.16, 120.76, 119.48, 118.68, 63.87, 53.03, 52.11, 49.26, 40.87, 21.11.

Spectrum 4-31: Methyl 4-((3-(dimethylamino)propyl)(methyl)amino)-2-nitrobenzoate (**78**) ^{1}H NMR (400MHz, DMSO-d6)
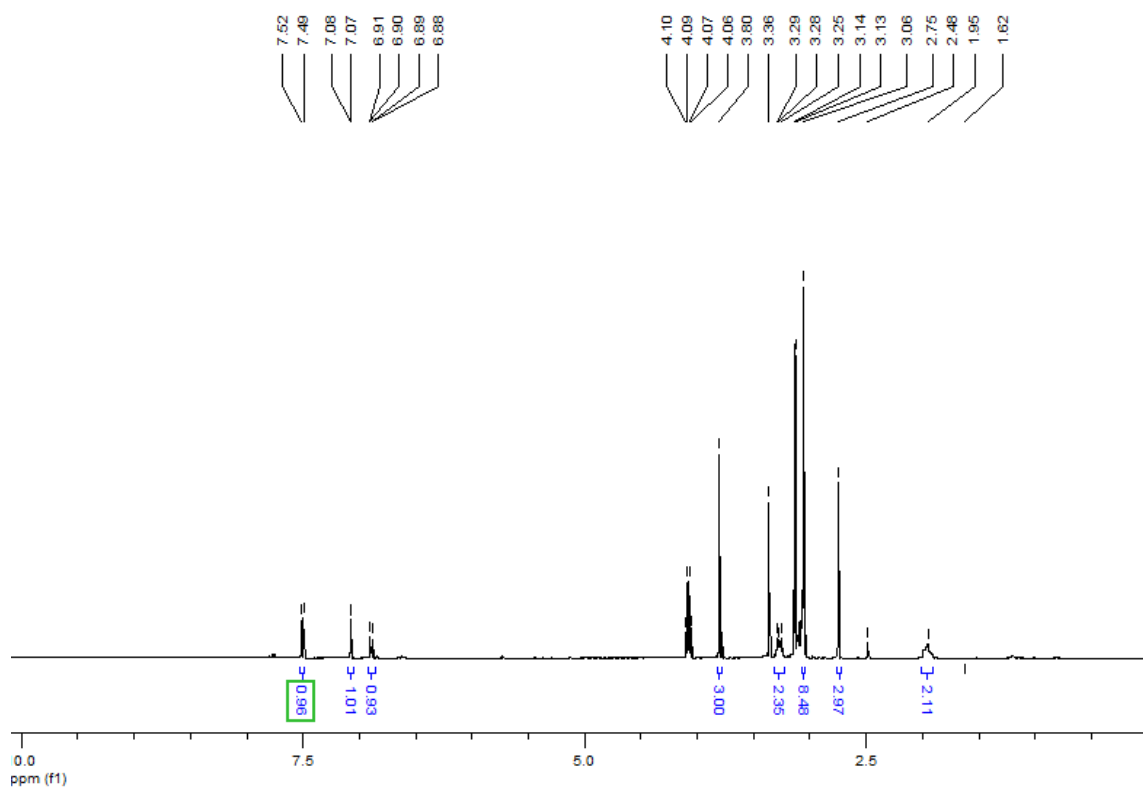
Spectrum 4-32: Methyl 4-((3-(dimethylamino)propyl)(methyl)amino)-2-nitrobenzoate
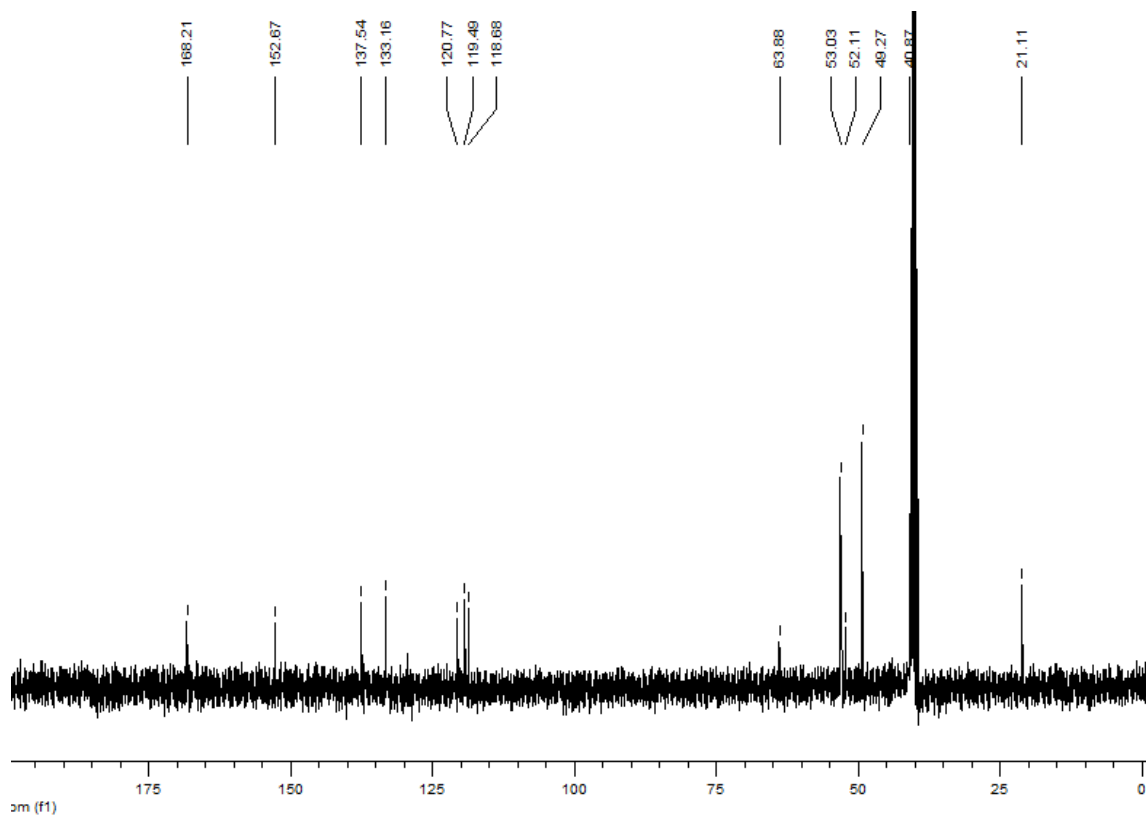(**78**) ^{13}C NMR (400MHz, DMSO-d6)

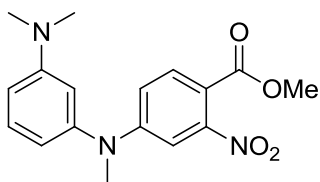## Methyl 4-((3-(dimethylamino)phenyl)(methyl)amino)-2-nitrobenzoate (79)

To a 250 ml round bottom flask was added methyl 4-chloro-2-nitrobenzoate (**53**) (973 mg, 5.86 mmol), 3-dimethylaminoaniline (5.86 mmol, 1.2 eq), $Pd_2(dba)_3$ (223 mg, 0.24 mmol, 5 mol%), *rac*-BINAP (228 mg, 0.37 mmol, 7.5 mol%), and Cs_2CO_3 (2.1 g, 5.86 mmol, 1.2 eq). The reaction was stirred and heated to reflux for 28 hours before it was cooled to RT. After filtration and concentration, the crude was purified via flash column chromatography (DCM – MeOH : 80 % - 20 %) to yield red oil as the intermediate (707 mg, 46 % yield). ^{1}H NMR (400 MHz, DMSO-d6) δ: 9.09 (s, 1H), 8.30 (s, 1H), 7.73 (d, *J* = 9 Hz, 1H), 7.22 (d, *J* = 2 Hz, 1H), 7.16-7.13 (m, 2H), 6.51-6.46 (m, 3H), 3.74 (s, 3H), 2.87 (s, 6H). ^{13}C NMR (400 MHz, DMSO-d6) δ: 164.59, 152.08, 149.97, 141.17, 138.41, 133.02, 130.54, 116.30, 111.86, 109.16, 108.79, 105.30, 79.85, 53.06, 40.70.

The purified methyl 4-((3-(dimethylamino)phenyl)amino)-2-nitrobenzoate was transferred to a 250 ml round bottom flask, followed by ACN (100 ml), iodomethan (173 µl, 2.78 mmol, 1.2 eq), and K_2CO_3 (384 mg, 2.78 mmol, 1.2 eq). The reaction was heated to reflux under Ar while being stirred for 46 hours. After cooling to RT, it was filtered and concentrated. The crude was purified via flash column chromatography (DCM – MeOH : 90 % - 10 %) to yield orange oil as the product (637 mg, 83 % yield). ^{1}H NMR (400MHz, CDCl₃) δ: 7.69 (d, *J* = 9 Hz, 1H), 7.28 (t, *J* = 8 Hz, 1H), 6.84 (d, *J* = 2 Hz, 1H), 6.79 (dd, J_1 = 8 Hz, J_2 = 2 Hz, 1H), 6.65 (dd, J_1 = 7 Hz, J_2 = 2 Hz, 1H), 6.51 (m, 2H), 3.80 (s, 3H),

3.34 (s, 3H), 2.94 (s, 6H). 13C NMR (400MHz, CDCl3) δ: 164.93, 152.63, 152.30, 152.18, 147.07, 132.24, 130.97, 114.63, 114.08, 111.19, 110.23, 107.46, 52.58, 40.63, 40.56. MS (ESI) calculated exact mass for $C_{17}H_{19}N_3O_4$ = 329.14. Found [M+H]$^+$ = 330.06.

Spectrum 4-33: Methyl 4-((3-(dimethylamino)phenyl)amino)-2-nitrobenzoate ^{1}H NMR (400MHz, DMSO-d6)

Spectrum 4-34: Methyl 4-((3-(dimethylamino)phenyl)amino)-2-nitrobenzoate ^{13}C NMR (400MHz, DMSO-d6)

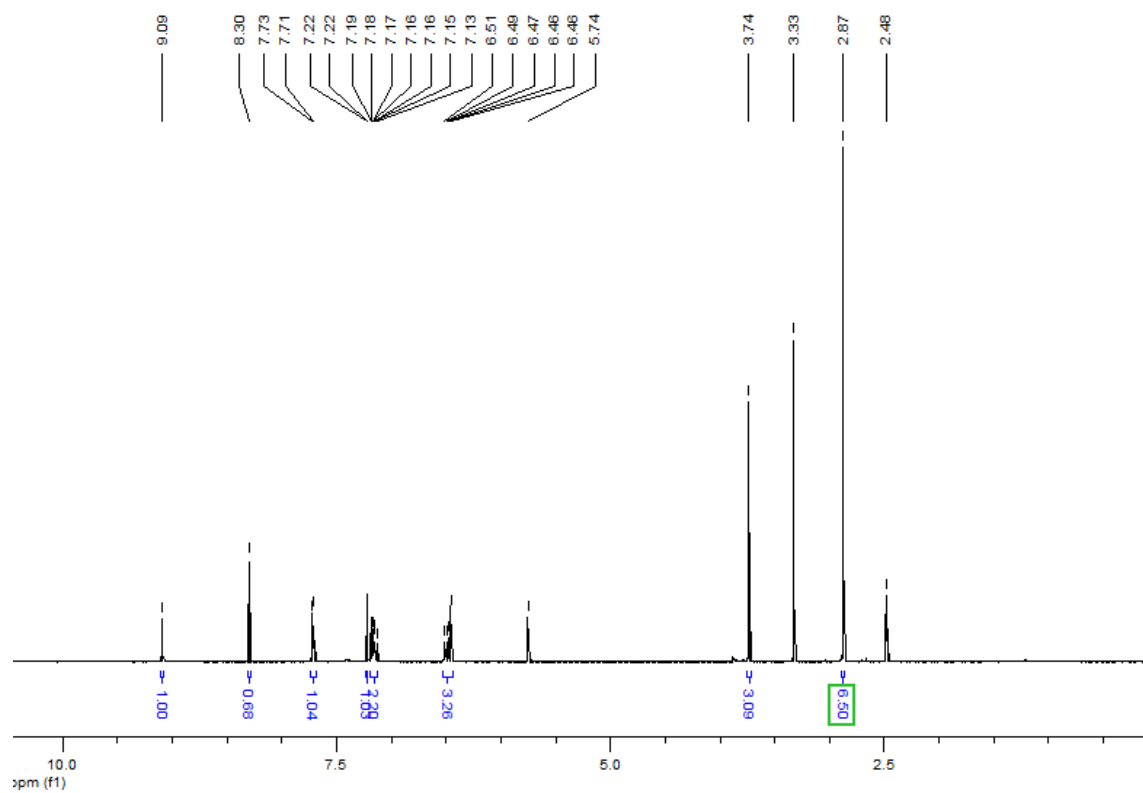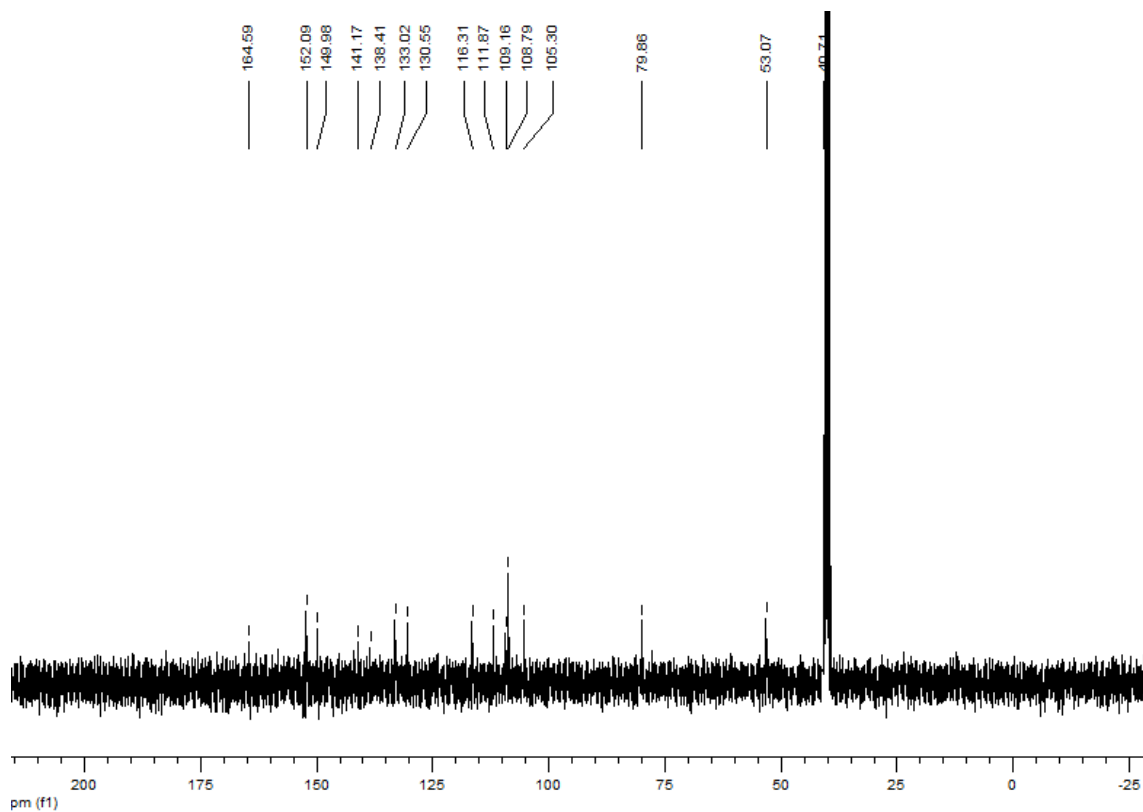**Spectrum 4-35**: Methyl 4-((3-(dimethylamino)phenyl)(methyl)amino)-2-nitrobenzoate (**79**) ^{1}H NMR (400 MHz, CDCl$_3$)
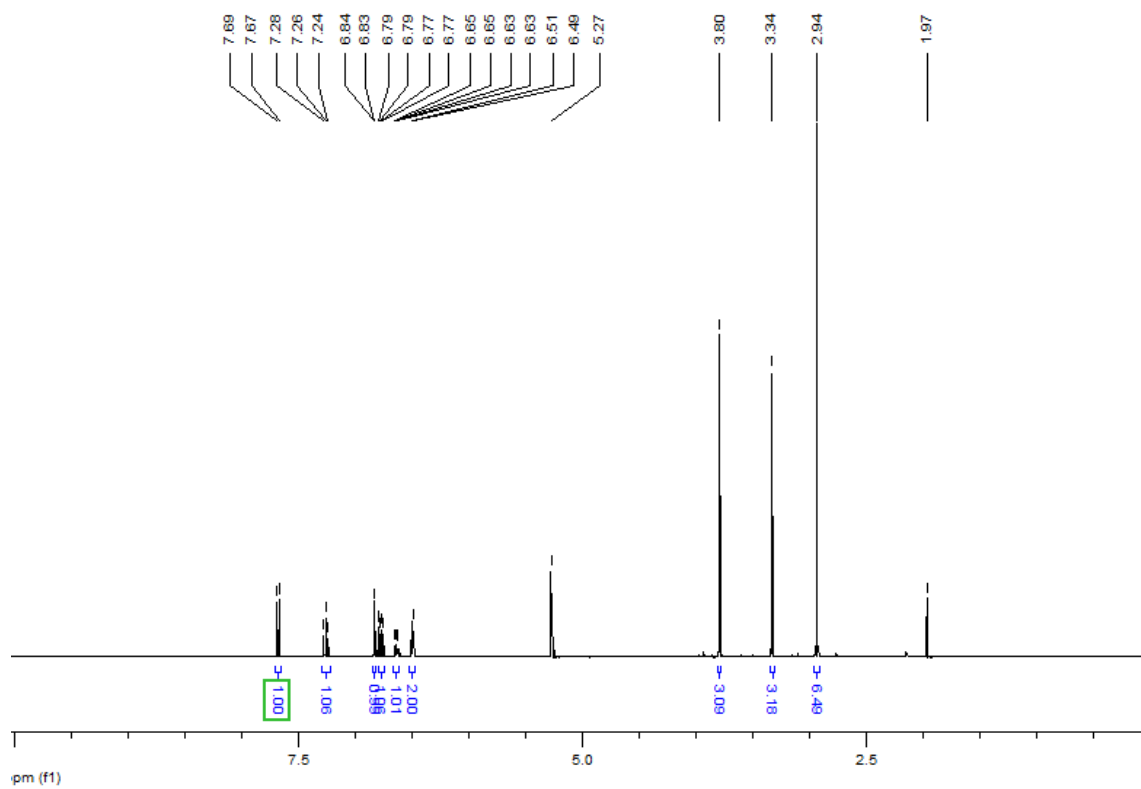
Spectrum 4-36: Methyl 4-((3-(dimethylamino)phenyl)(methyl)amino)-2-nitrobenzoate
(**79**) ^{13}C NMR (400 MHz, CDCl$_3$)
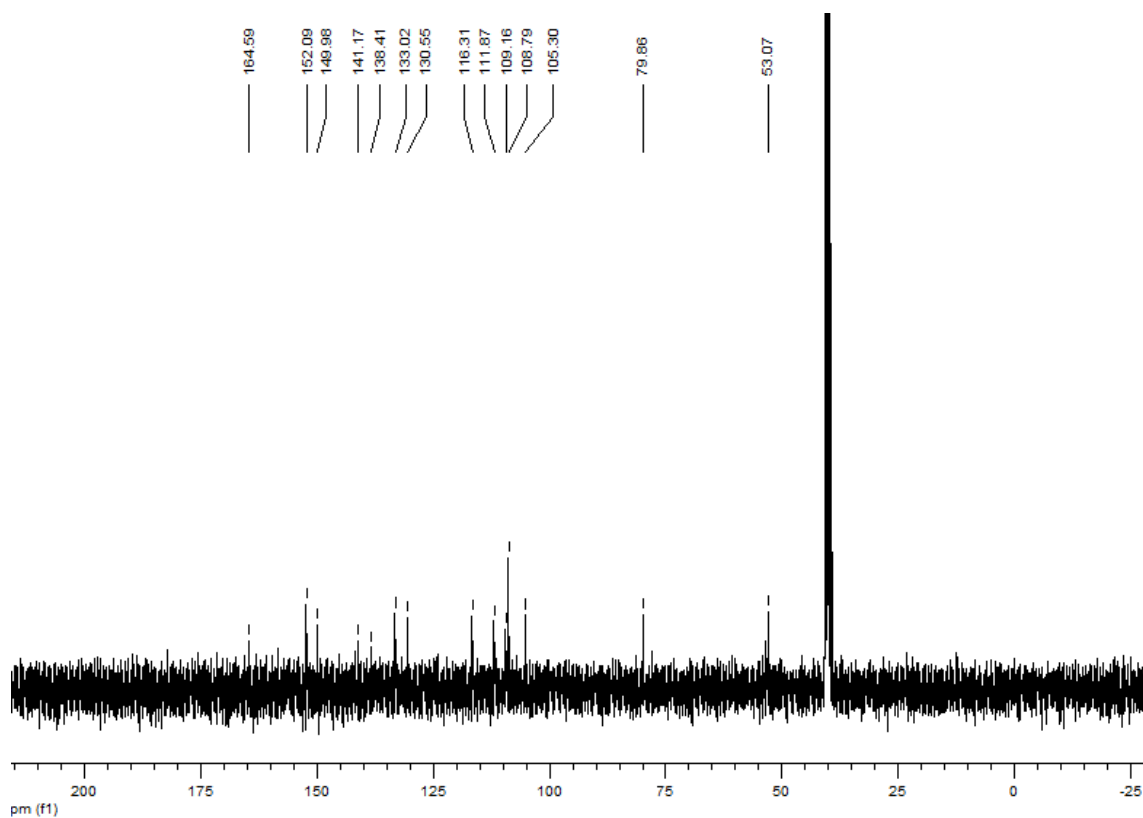
2-amino-7-((3-(dimethylamino)phenyl)(methyl)amino)quinazolin-4(3H)-one (82)
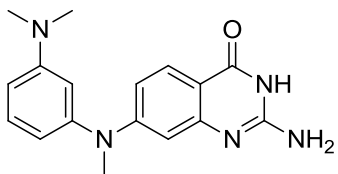
To a 250 ml round bottom flask was added Methyl 4-((3-(dimethylamino)phenyl)(methyl)amino)-2-nitrobenzoate (79) (637 mg, 1.94 mmol) and MeOH (100 ml). The flask was flushed with Ar before Pd/C (63 mg, 10 wt%) was added. The reaction was then stirred at RT for 21 hours before it was filtered and concentrated. The residue was transferred into a 5 ml glass vial and chloroformamidinium chloride (445 mg, 3.87 mmol, 2 eq) was added, followed by dimethylsulfone (300 mg). The reaction was stirred and heated to 160 °C for 2 hours. It was then cooled and the solid residue was purified via flash column (DCM – MeOH : 90 % - 10 %) to yield off white solid as the product (54 mg, 9 % yield). ^{1}H NMR (400MHz, DMSO-d6) δ: 8.3 (s, 1H), 7.61 (d, J = 9 Hz, 1H), 7.23 (t, J = 8 Hz, 1H), 6.60 (dd, J_1 = 8 Hz, J_2 = 2 Hz, 1H), 6.53 (t, J = 2 Hz, 1H), 6.50-6.47 (m, 3H), 6.37 (d, J = 2 Hz, 1H), 2.86 (s, 6H). ^{13}C NMR (400MHz, DMSO-d6) δ: 162.88, 154.19, 152.80, 152.39, 148.60, 130.72, 127.47, 114.32, 111.20, 110.59, 110.50, 107.98, 94.55, 74.98, 55.61, 40.76.MS (ESI) calculated exact mass for $C_{17}H_{19}N_5O$ = 309.16. Found [M+H]$^+$ = 310.04.

Spectrum 4-37: 2-amino-7-((3-(dimethylamino)phenyl)(methyl)amino)quinazolin-4(3H)-one (**82**) ^{1}H NMR (400MHz, DMSO-d6)

Spectrum 4-38: 2-amino-7-((3-(dimethylamino)phenyl)(methyl)amino)quinazolin-4(3H)-one (**82**) ^{13}C NMR (400MHz, DMSO-d6)
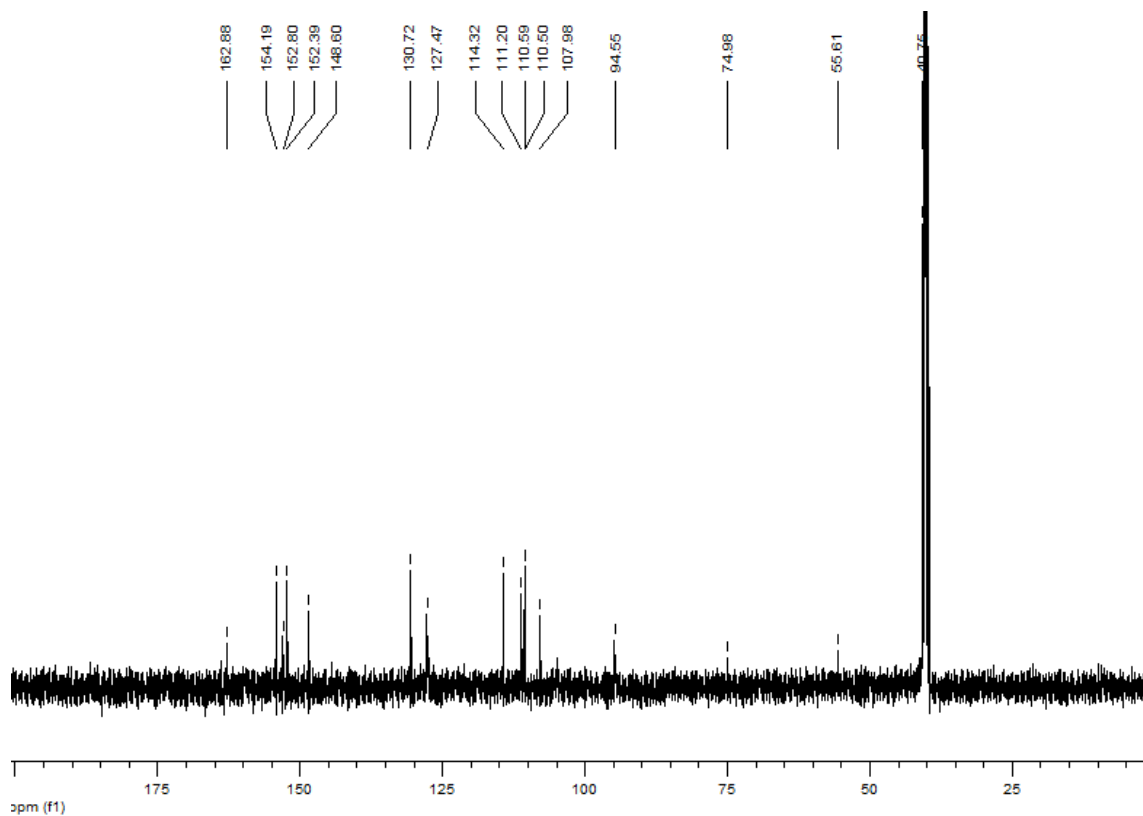
Methyl 3-nitro-[1,1'-biphenyl]-4-carboxylate (80a)
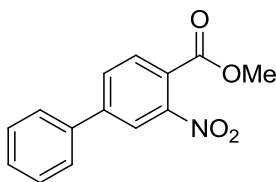
To a 250 ml round bottom flask was added methyl 4-chloro-2-nitrobenzoate (**53**)

(1.3 g, 6.17 mmol), phenyl boronic acid propandiol ester (1.0 g, 6.17 mmol), Dioxane

(100 ml), $Pd_2(dba)_3$ (282 mg, 0.31 mmol), *rac*-BINAP (288 mg, 0.46 mmol), and Cs_2CO_3

(2.2 g, 6.17 mmol). The reaction was stirred and heated to reflux under Ar for 23 hours

before it was cooled to RT. The reaction was then filtered and concentrated. The crude

was purified via flash column chromatography (DCM – Hexane : 60 % - 40 %) to yield a

white solid as the product (1.04 g, 66% yiled). ^{1}H NMR (400MHz, $CDCl_3$) δ: 8.07 (s, 1H),

7.88 (d, *J* = 8 Hz, 1H), 7.85 (d, *J* = 8 Hz, 1H), 7.62 (d, *J* = 7 Hz, 2H), 7.53-7.46 (m, 3H), 3.94

(s, 3H). ^{13}C NMR (400MHz, $CDCl_3$) δ: 165.83, 145.67, 143.14, 137.82, 131.05, 130.81,

129.54, 129.45, 127.43, 125.58, 122.49, 53.51. MS (ESI) calculated exact mass for

$C_{14}H_{11}NO_4$ = 257.07. Found $[M+H]^+$ = 257.62.

Spectrum 3-39: Methyl 3-nitro-[1,1'-biphenyl]-4-carboxylate (**80a**) ^{1}H (400MHz, CDCl$_3$)
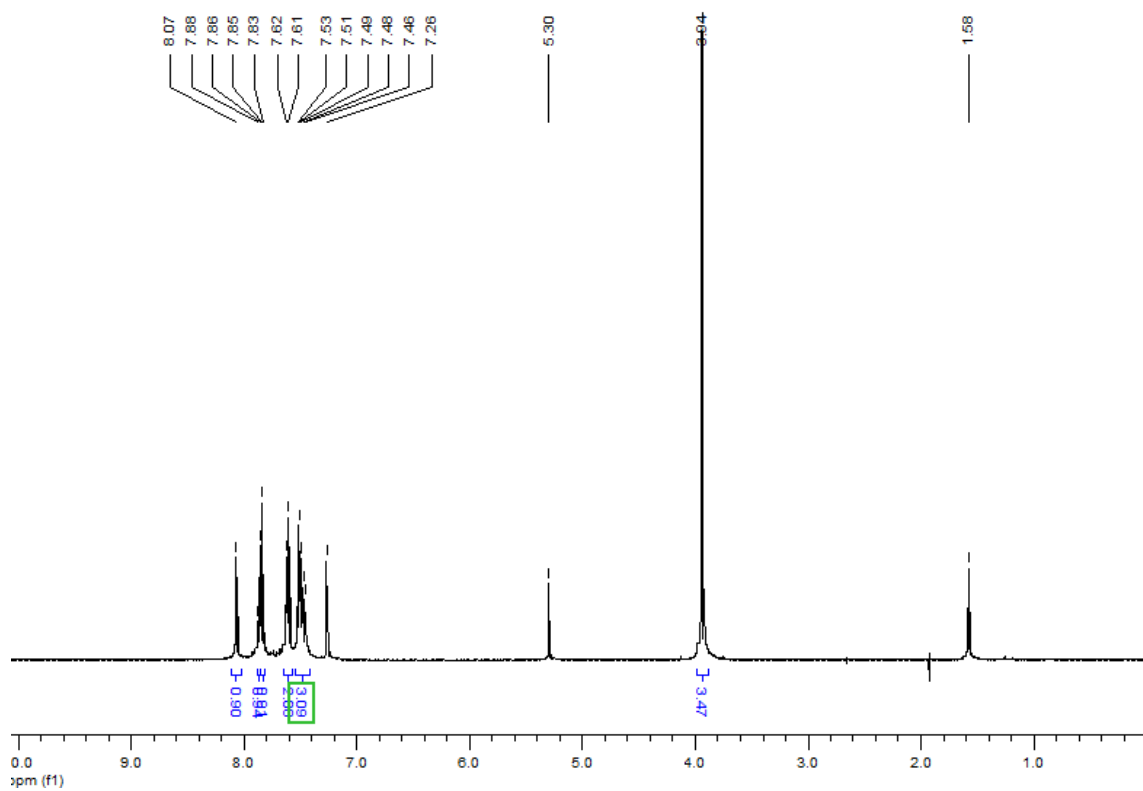
Spectrum 3-40: Methyl 3-nitro-[1,1'-biphenyl]-4-carboxylate (**80a**) [13]C (400MHz, CDCl$_3$)

165.83 146.67 143.14 137.82 131.05 130.81 129.55 129.45 127.43 125.59 122.49 77.25 53.51

175 150 125 100 75 50 25 0

ɔm (f1)

2-amino-7-phenylquinazolin-4(3H)-one (83a)

To a 250 ml round bottom flask was added methyl 3-nitro-[1,1'-biphenyl]-4-carboxylate (**80a**) (1.0 g, 3.89 mmol) and MeOH (100 ml). The reaction was flushed with Ar before Pd/C (100 mg, 10wt%) was added. The reaction was stirred at RT for 25 hours before it was filtered and concentrated. To the oil residue was added chloroformamidinium chloride (895 mg, 7.78 mmol, 2 eq) and dimethyl sulfone (400 mg). The reaction was stirred and heated to 160 °C for 2 hours before it was cooled to RT. The solid residue was purified via flash column chromatography (DCM − MeOH : 90 % - 10 %) to yield white solid as the product (27 mg, 4.5 % yield). ^{1}H NMR (500MHz, DMSO-d6) δ: 7.95 (d, J = 8 Hz, 1H), 7.88 (d, J = 8 Hz, 1H), 7.72 (d, J = 8 Hz, 2H), 7.66 (t, J = 8 Hz, 1H), 7.51 (t, J = 8 Hz, 2H), 7.43 (m, 3H), 7.19 (d, J = 8 Hz, 1H), 7.10 (t, J = 7 Hz, 1H). ^{13}C NMR (500MHz, DMSO-d6) δ: 146.17, 139.93, 134.49, 129.49, 128.67, 127.44, 127.11, 126.37, 121.97, 120.82, 117.63, 116.64. MS (ESI) calculated exact mass for $C_{14}H_{11}N_3O$ = 237.09. Found $[M+H]^+$ = 237.97.

Spectrum 4-41: 2-amino-7-phenylquinazolin-4(3H)-one (**83a**), ^{1}H NMR (500MHz, DMSO-d6)

Spectrum 4-42: 2-amino-7-phenylquinazolin-4(3H)-one (**83a**), ^{13}C NMR (500MHz, DMSO-d6)
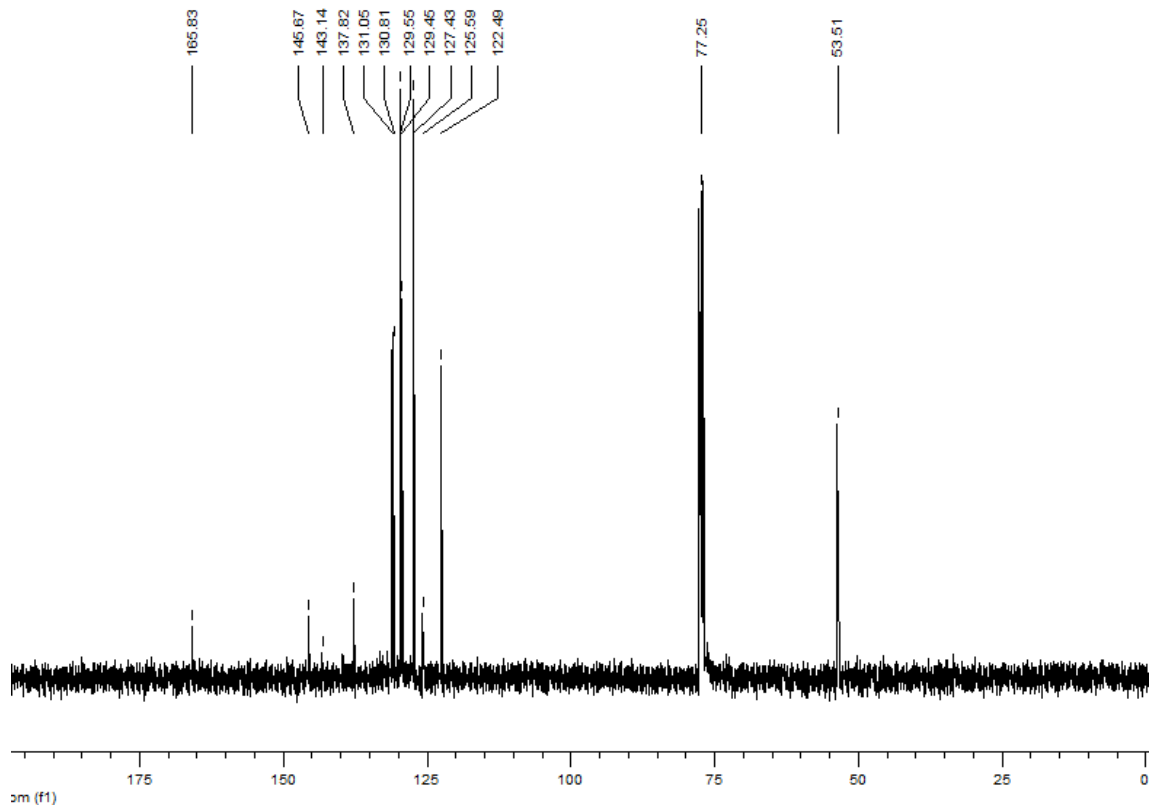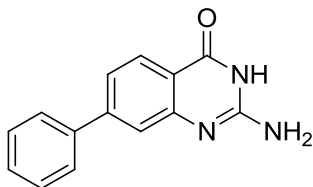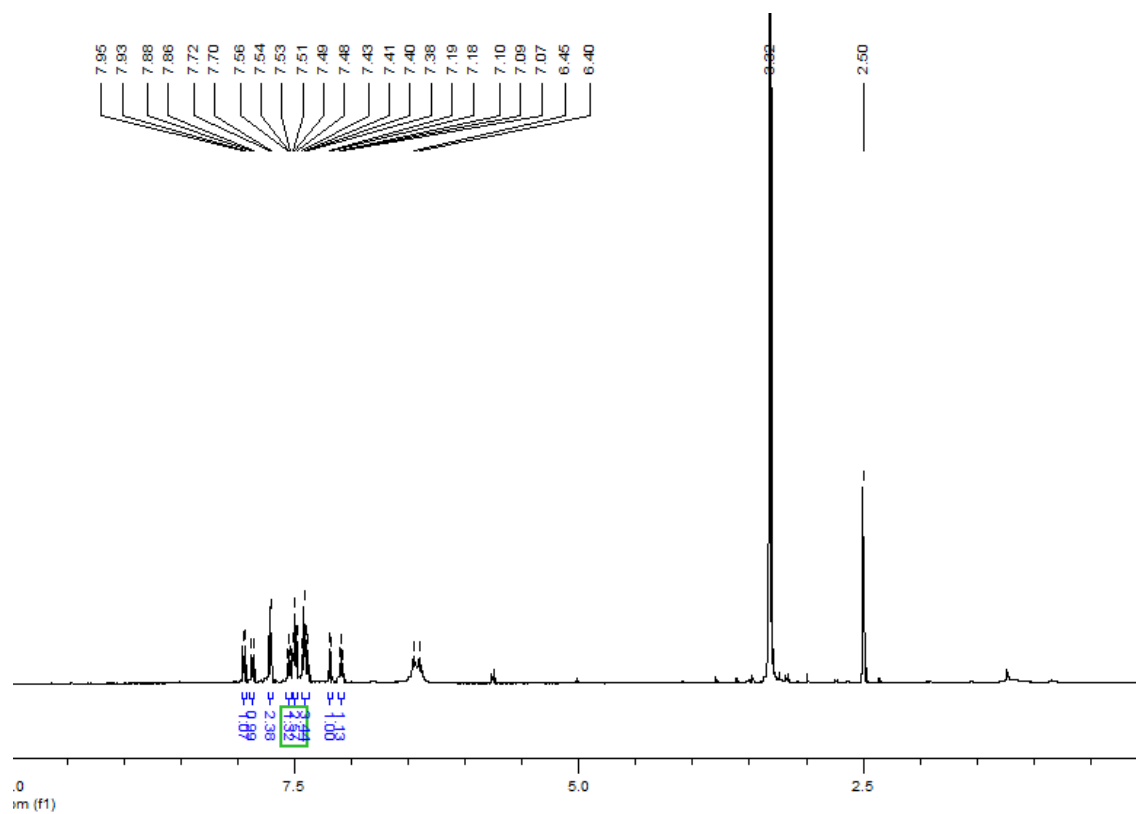
Methyl 3'-methoxy-3-nitro-[1,1'-biphenyl]-4-carboxylate (80b)
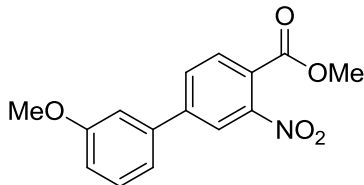
To a 250 ml round bottom flask was added methyl 4-chloro-2-nitrobenzoate (**53**) (1.48 g, 7.23 mmol), dioxane (100 ml), 3-methoxyphenylboronic acid (1.0 g, 6.58 mmol), Pd2(dba)3 (301 mg, 0.3 mmol), rac-BINAP (307 mg, 0.5 mmol), and Cs2CO3 (2.6 g, 7.23 mmol). The reaction was stirred and heated to reflux under Ar for 30 hours before it was cooled to RT. After filtration and concentration, the crude was purified via flash column (DCM – Hexane : 60 % - 40 %) to yield slight yellow oil as the product (792 g, 42 % yield). ^{1}H NMR (400MHz, DMSO-d6) δ: 8.32 (d, J = 2 Hz, 1H), 8.14 (dd, J_1 = 8 Hz, J_2 = 2 Hz, 1H), 7.95 (d, J = 8 Hz, 1H), 7.45 (t, J = 8 Hz, 1H), 7.37 – 7.34 (m, 2H), 7.05 (dd, J_1 = 8 Hz, J_2 = 2 Hz, 1H), 3.84 (s, 3H), 3.82 (s, 3H). ^{13}C NMR (400MHz, DMSO-d6) δ: 165.28, 160.59, 149.88, 145.19, 138.81, 131.59, 131.40, 131.05, 124.55, 122.61, 120.14, 115.86, 113.14, 56.00, 53.89. MS (ESI) calculated exact mass for $C_{15}H_{13}NO_5$ = 287.08. Found [M+H]$^+$ = 287.96.

Spectrum 4-43: methyl 3'-methoxy-3-nitro-[1,1'-biphenyl]-4-carboxylate (**80b**) ^{1}H NMR (400MHz, DMSO-d6)
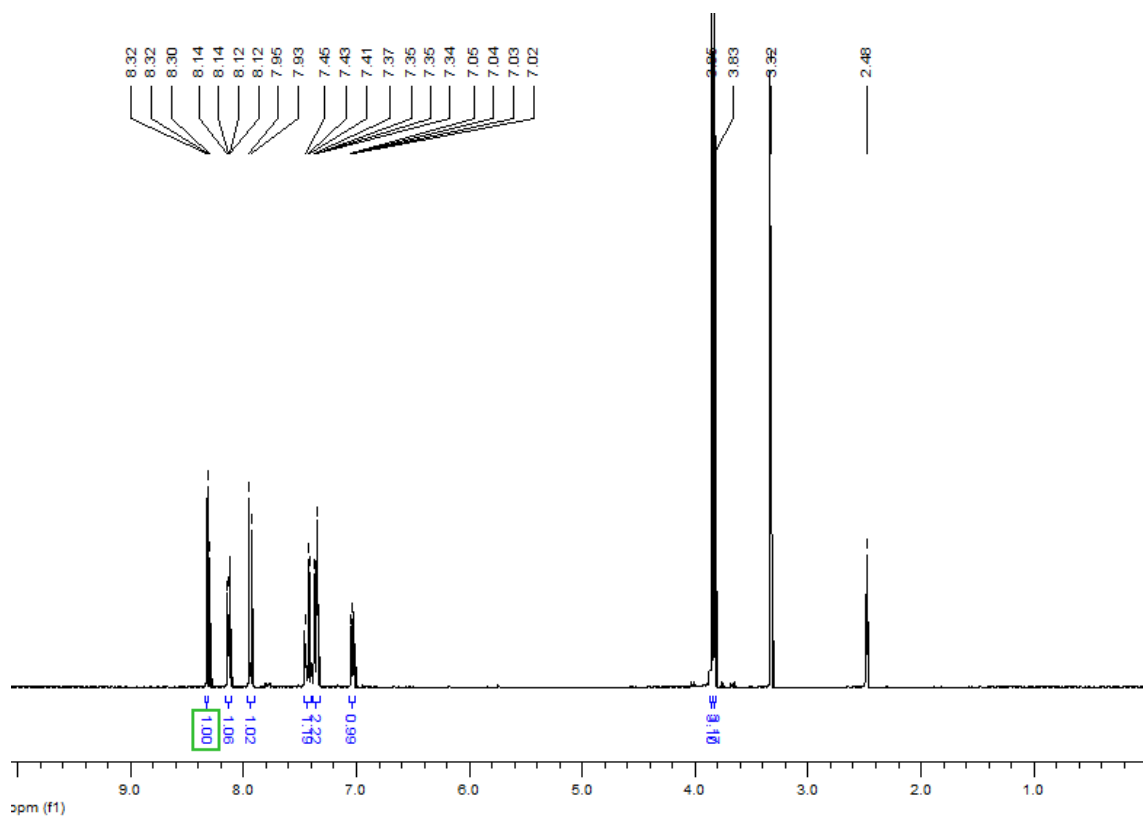
Spectrum 4-44: methyl 3'-methoxy-3-nitro-[1,1'-biphenyl]-4-carboxylate (**80b**) ^{13}C NMR (400MHz, DMSO-d6)
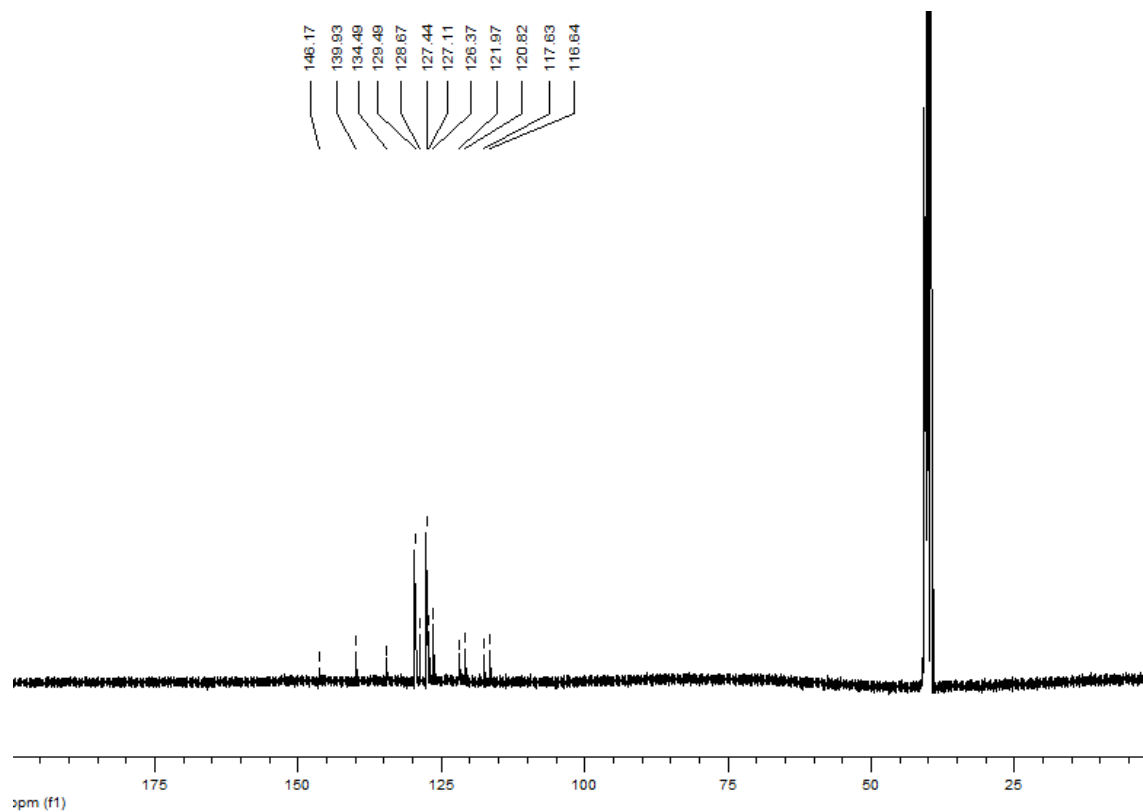
2-amino-7-(3-methoxyphenyl)quinazolin-4(3H)-one (83b)

To a 250 ml round bottom flask was added methyl 3'-methoxy-3-nitro-[1,1'-biphenyl]-4-carboxylate (**80b**) (780 mg, 2.72 mmol) and methanol (100 ml). The flask was flushed with Ar gas before Pd/C (78 mg, 10 wt %) was added. The reaction was sealed under H_2 atmosphere and stirred at RT for 18 hours before it was filtered and concentrated. It was then transferred to a 5 ml glass vial. Chloroformamidinium chloride (624 mg, 5.43 mmol, 2eq) and dimethylsulfone (400 mg) were added. The reaction was stirred and heated to 160 °C for 2 hours. After cooling down to RT, the solid residue was purified via flash column chromatography (DCM – MeOH : 90 % - 10 %) to yield white solid (77 mg, 11 %). 1H NMR (400MHz, DMSO-d6) δ: 11.13 (s, 1H), 7.93 (d, J = 8 Hz, 1H), 7.40-7.35 (m, 3H), 7.25 (d, J = 8 Hz, 1H), 7.21 (t, J = 2 Hz, 1H), 6.97 (dd, J_1 = 8 Hz, J_2 = 2 Hz, 1H), 3.81 (s, 3H). 13C NMR (400MHz, DMSO-d6) δ: 160.39, 150.64, 146.31, 141.66, 130.76, 127.28, 121.20, 119.97, 116.90, 114.56, 113.03, 101.04, 95.54, 55.82. MS (ESI) calculated exact mass for $C_{15}H_{13}N_3O_2$ = 267.10. Found $[M+H]^+$ = 268.05.

Spectrum 4-45: 2-amino-7-(3-methoxyphenyl)quinazolin-4(3H)-one (**83b**) ^{1}H NMR (400MHz, DMSO-d6)
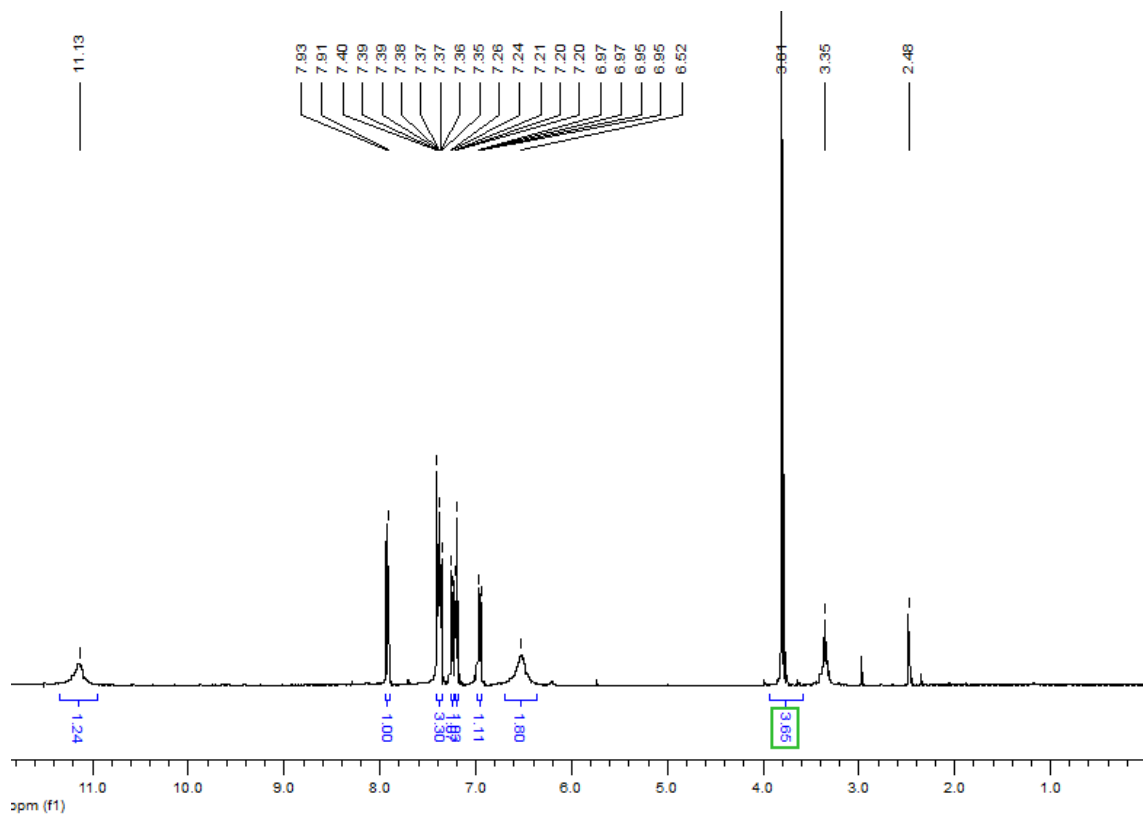
Spectrum 4-46: 2-amino-7-(3-methoxyphenyl)quinazolin-4(3H)-one (**83b**) ^{13}C NMR (400MHz, DMSO-d6)
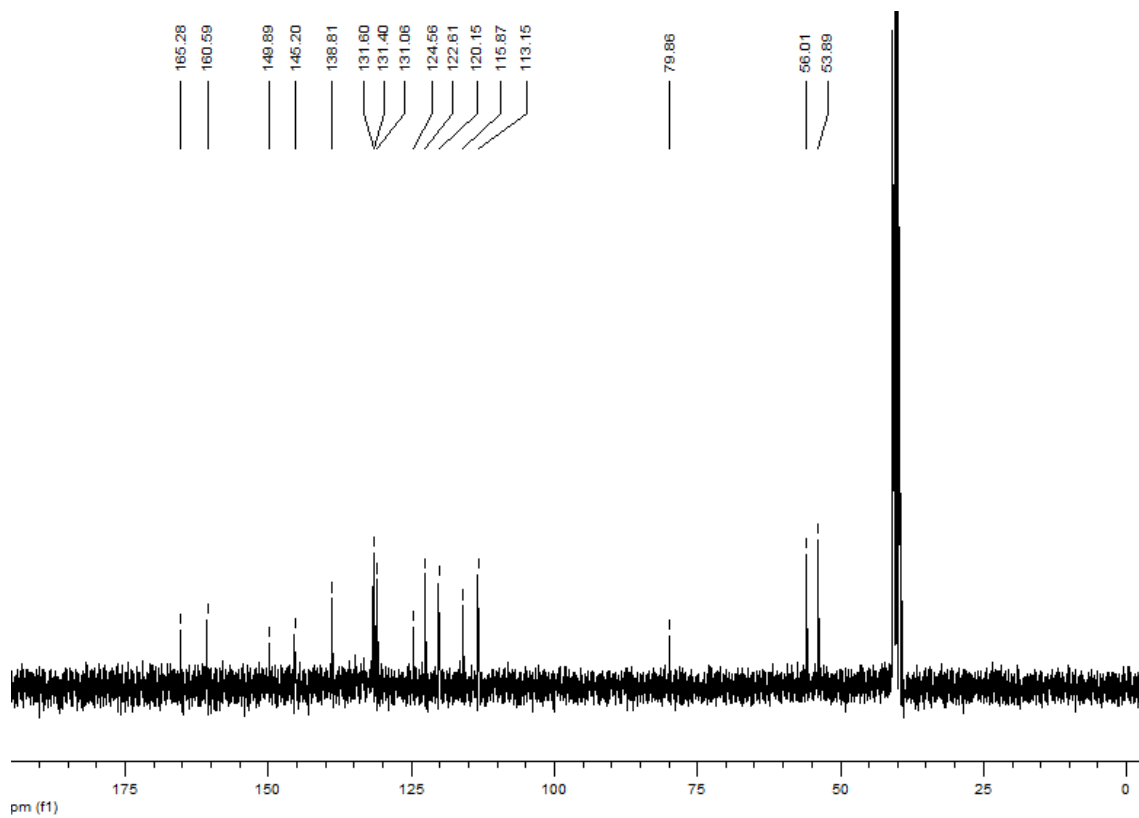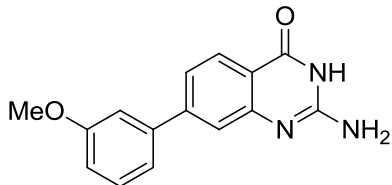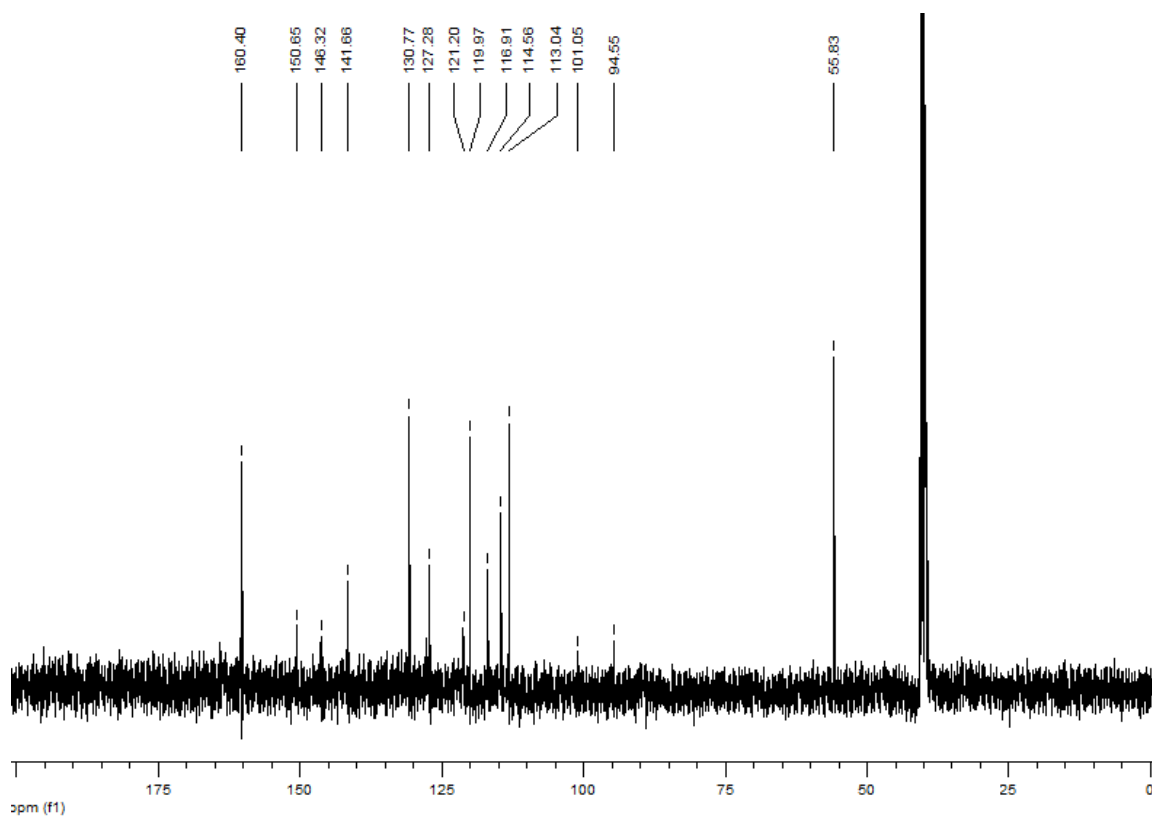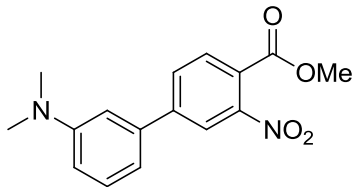
Methyl 3'-(dimethylamino)-3-nitro-[1,1'-biphenyl]-4-carboxylate (80c)

To a 100 ml round bottom flask was added methyl 4-chloro-2-nitrobenzoate (**53**) (500 mg, 2.32 mmol), 3-dimethylaminophenyl bornic acid (421 mg, 2.55 mmol), dioxane (40 ml), Pd$_2$(dba)$_3$ (106 mg, 0.1 mmol), *rac*-BINAP (108 mg, 0.2 mmol), and Cs$_2$CO$_3$ (837 mg, 2.32 mmol). The reaction was stirred and heated to reflux for 19 hours before it was cooled to RT. After filtration and concentration, the crude was purified via flash column chromatography (DCM 100 %) to yield orange oil as the product (415 mg, 60 %). 1H NMR (400MHz, DMSO-d6) δ: 8.27 (d, *J* = 2 Hz, 1H), 8.10 (dd, J$_1$ = 8 Hz, *J*$_2$ = 2 Hz, 1H), 7.93 (d, *J* = 8 Hz, 1H), 7.32 (t, *J* = 8 Hz, 1H), 7.03 (m, 2H), 6.82 (dd, *J*$_1$ = 8 Hz, *J*$_2$ = 2 Hz, 1H), 3.84 (s, 3H), 2.95 (s, 6H). 13C NMR (400MHz, DMSO-d6) δ: 165.31, 151.65, 149.93, 146.42, 138.16, 131.46, 131.30, 130.48, 124.12, 122.49, 115.54, 113.85, 111.39, 55.60, 40.83. MS (ESI) calculated exact mass for C$_{16}$H$_{16}$N$_2$O$_4$ = 300.31. Found [M+H]$^+$ = 301.06.

Spectrum 4-47: methyl 3'-(dimethylamino)-3-nitro-[1,1'-biphenyl]-4-carboxylate (**80c**) ^{1}H NMR (400MHz, DMSO-d6)
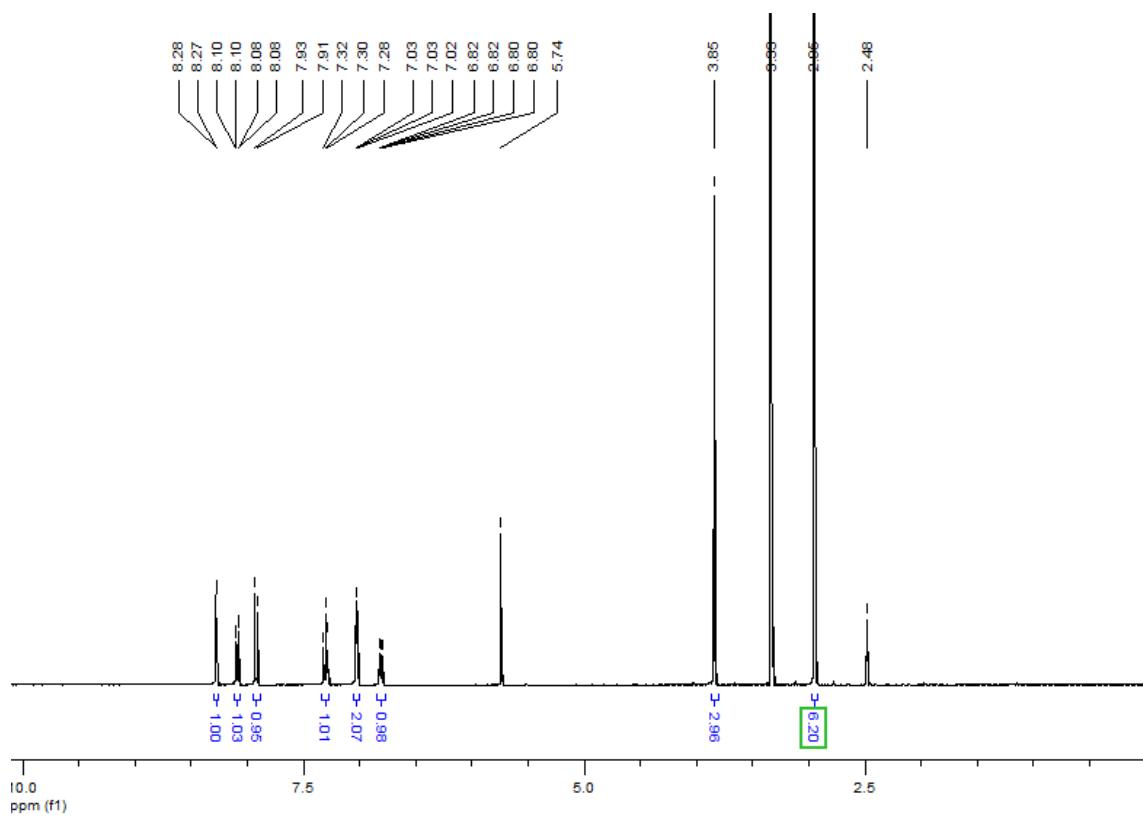
Spectrum 4-48: methyl 3'-(dimethylamino)-3-nitro-[1,1'-biphenyl]-4-carboxylate (**80c**)
^{13}C NMR (400MHz, DMSO-d6)
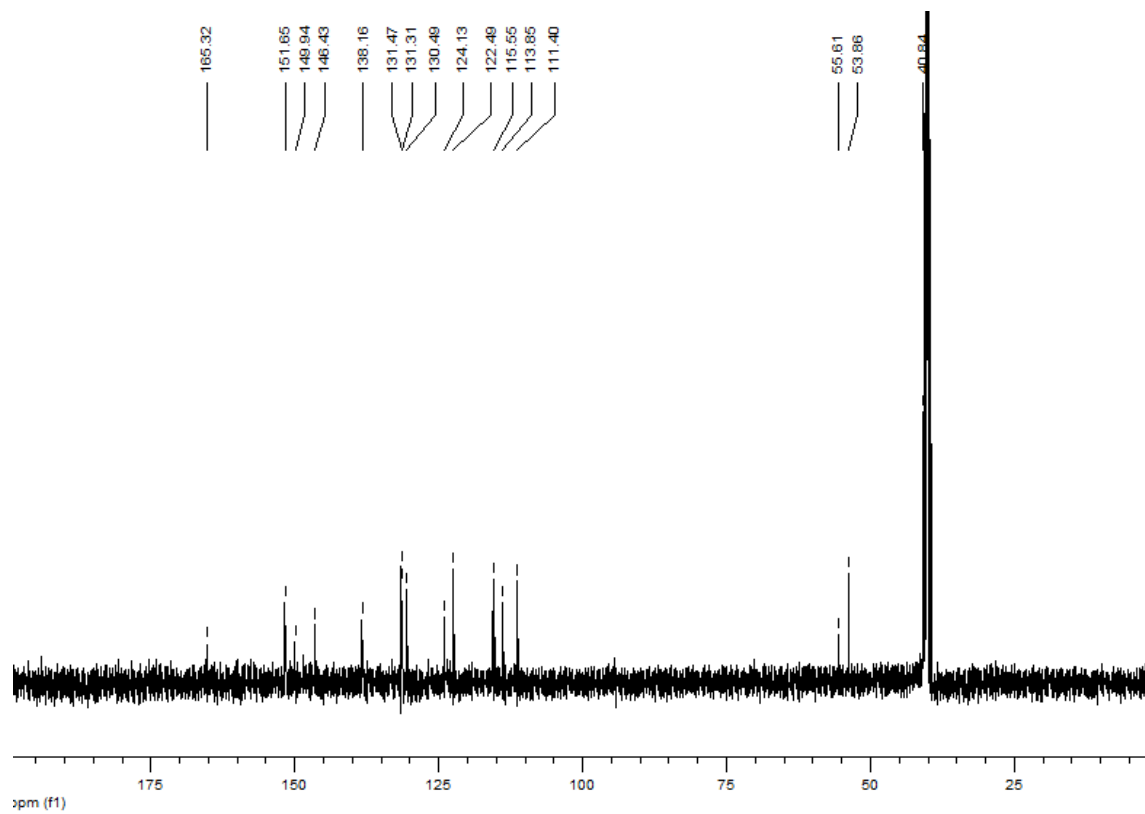
2-amino-7-(3-(dimethylamino)phenyl)quinazolin-4(3H)-one (83c)
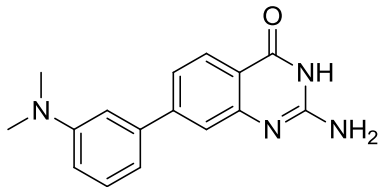
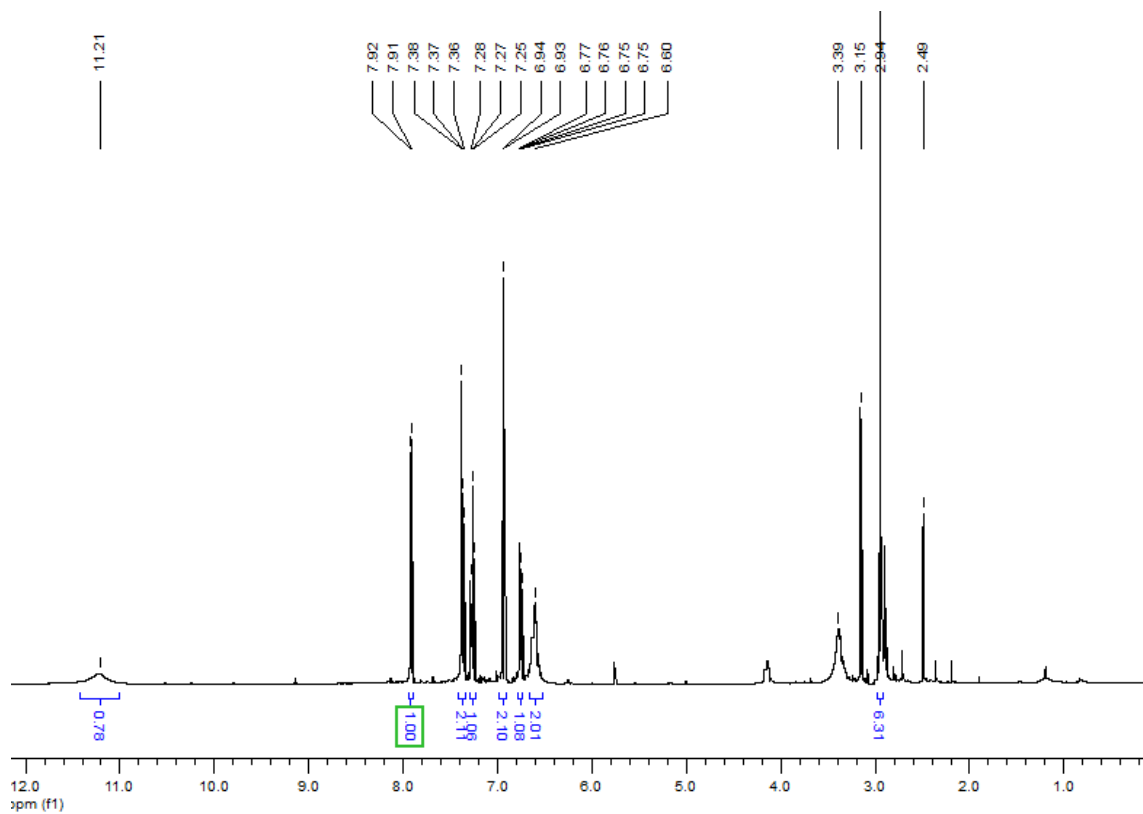To a 100 ml round bottom flask was added methyl 3'-(dimethylamino)-3-nitro-[1,1'-biphenyl]-4-carboxylate (**80c**) (412 mg, 1.38 mmol) and MeOH (40 ml). The flask was flushed with Ar gas before Pd/C (40 mg, 10 wt %) was added. The flask was then sealed under H_2 atmosphere. It was stirred at RT for 4 hours before it was filtered and concentrated. The residue was transferred to a 5 ml glass vial. And chloroform-amidinium chloride (317 mg, 2.76 mmol, 2 eq) and dimethyl sulfone (500 mg) were added. The reaction was stirred and heated to 160 °C for 2 hours before it was cooled to RT. The solid crude was purified via flash column (DCM – MeOH : 90 % - 10 %) to yield slightly yellow solid as the product (50 mg, 13 %). 1H NMR (400MHz, DMSO-d6) δ: 11.21 (s, 1H), 7.92 (d, *J* = 8 Hz, 1H), 7.38 (s, 1H), 7.37 (d, *J* = 8 Hz, 1H), 7.28 (t, *J* = 8 Hz, 1H), 6.94 (m, 2H), 6.77 (m, 1H), 6.60 (s, 2H), 2.94 (s, 6H). 13C NMR (400MHz, DMSO-d6) δ: 163.14, 152.90, 151.24, 147.31, 140.75, 129.96, 126.92, 121.10, 116.41, 115.36, 112.71, 111.16, 49.04, 40.63. MS (ESI) calculated exact mass for $C_{16}H_{16}N_4O$ = 280.13. Found $[M+H]^+$ = 281.05.

Spectrum 4-49: 2-amino-7-(3-(dimethylamino)phenyl)quinazolin-4(3H)-one (**83c**) ^{1}H NMR (400MHz, DMSO-d6)

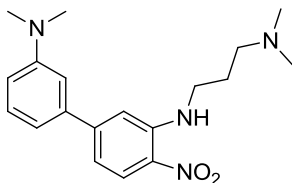**Spectrum 4-50**: 2-amino-7-(3-(dimethylamino)phenyl)quinazolin-4(3H)-one (**83c**) ^{13}C NMR (400MHz, DMSO-d6)

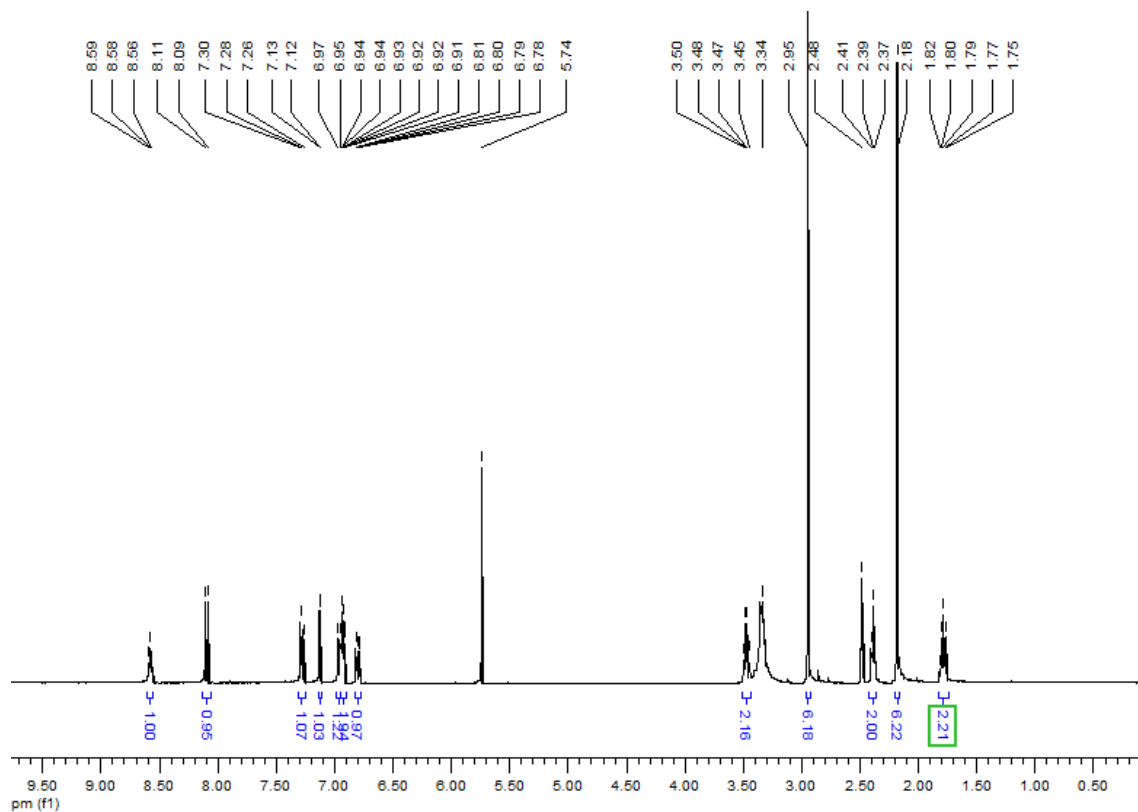ppm (f1)
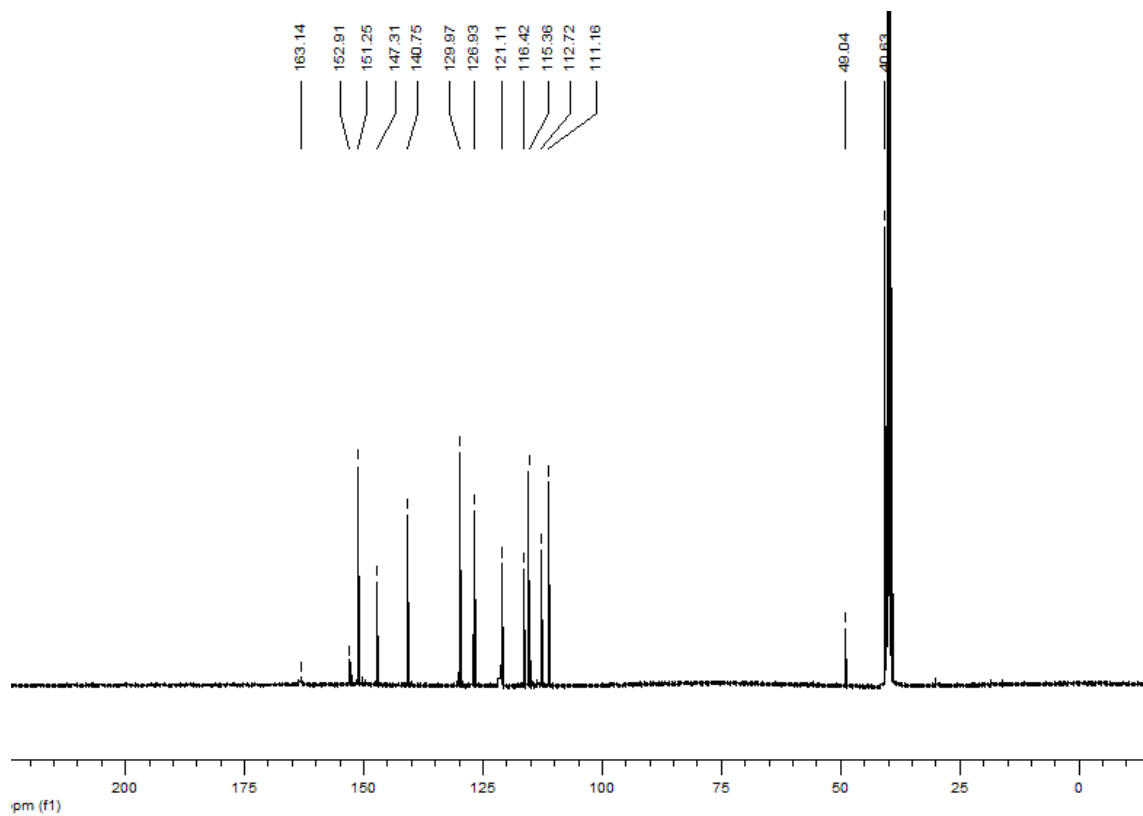
N*³-(3-(dimethylamino)propyl)-*N*^{3'},*N*^{3'}-dimethyl-4-nitro-[1,1'-biphenyl]-3,3'-diamine (85)

To a 100 ml round bottom flask was added *N*¹-(5-chloro-2-nitrophenyl)-*N*³,*N*³-dimethylpropane-1,3-diamine (**20h**) (500 mg, 1.94 mmol), 3-dimethylaminophenyl boronic acid (352 mg, 2.13 mmol, 1.1 eq), $Pd_2(dba)_3$ (89 mg, 5 mol %), *rac*-BINAP (91 mg, 7.5 mol %), and Cs_2CO_3 (769 gm, 2.13 mmol). The reaction was stirred and heated to reflux under Ar for 23 hours before it was cooled to RT. After filtration and concentration, the crude was purified via flash column chromatography (DCM − MeOH : 90 % - 10 %) to yield orange oil as the product (394 mg, 59 %). ^{1}H NMR (400MHz, DMSO-d6) δ: 8.59 (t, *J* = 5 Hz, 1H), 8.11 (d, *J* = 9 Hz, 1H), 7.30 (t, *J* = 8 Hz, 1H), 7.13 (d, *J* = 2 Hz, 1H), 6.97 (d, *J* = 8 Hz, 1H), 6.94 (m, 2H), 6.81 (dd, *J*$_1$ = 8 Hz, *J*$_2$ = 2 Hz, 1H), 3.50 (q, *J* = 8 Hz, 2H), 2.94 (s, 6H), 2.41 (t, *J* = 7 Hz, 2H), 2.18 (s, 6H), 1.82 (m, 2H). 13C NMR (400MHz, DMSO-d6) δ: 151.46, 149.88, 146.11, 140.21, 130.56, 130.20, 127.55, 115.75, 114.97, 113.65, 112.37, 111.48, 57.53, 55.61, 45.68, 40.85, 26.32. MS (ESI) calculated exact mass for $C_{19}H_{26}N_4O_2$ = 342.21. Found $[M+H]^+$ = 343.20.

Spectrum 4-51: N^3-(3-(dimethylamino)propyl)-$N^{3'}$,$N^{3'}$-dimethyl-4-nitro-[1,1'-biphenyl]-3,3'-diamine (**85**) ^{1}H NMR (400MHz, DMSO-d6)

Spectrum 4-52: N^3-(3-(dimethylamino)propyl)-$N^{3'}$,$N^{3'}$-dimethyl-4-nitro-[1,1'-biphenyl]-3,3'-diamine (**85**) ^{13}C NMR (400MHz, DMSO-d6)
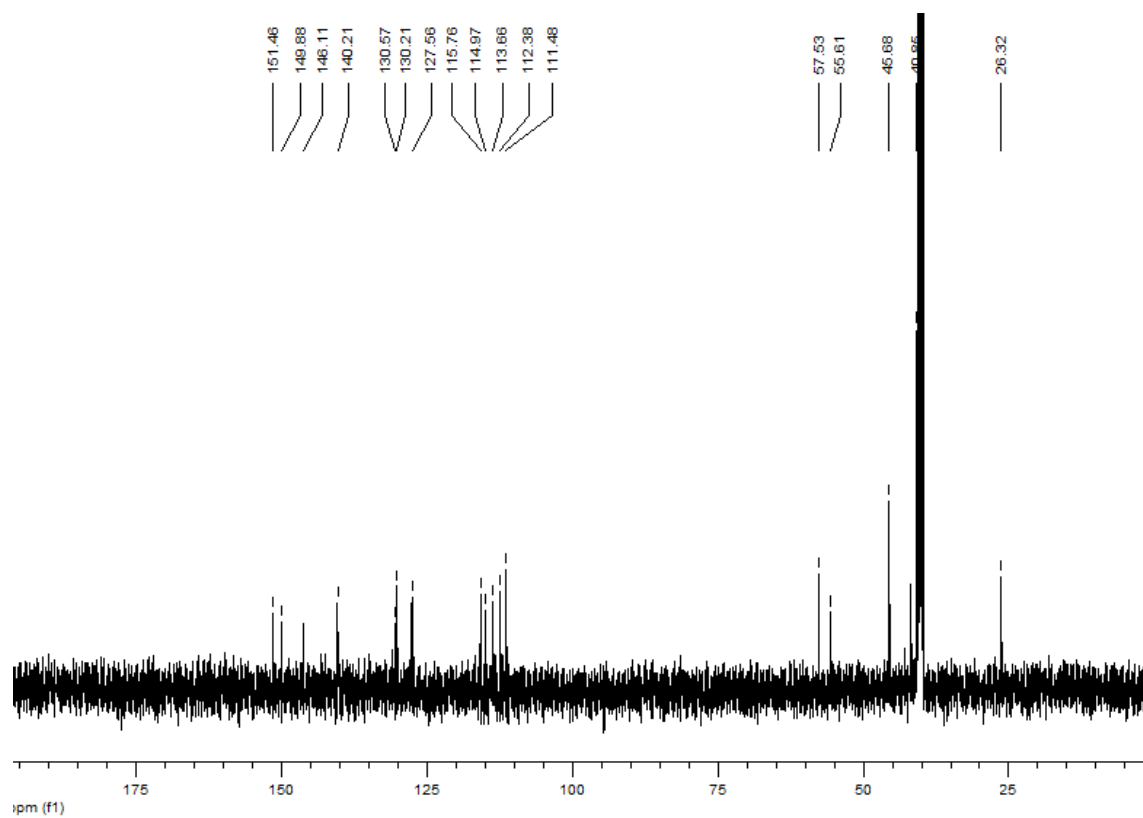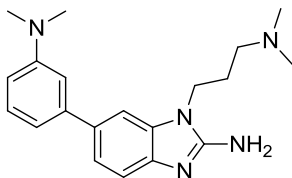
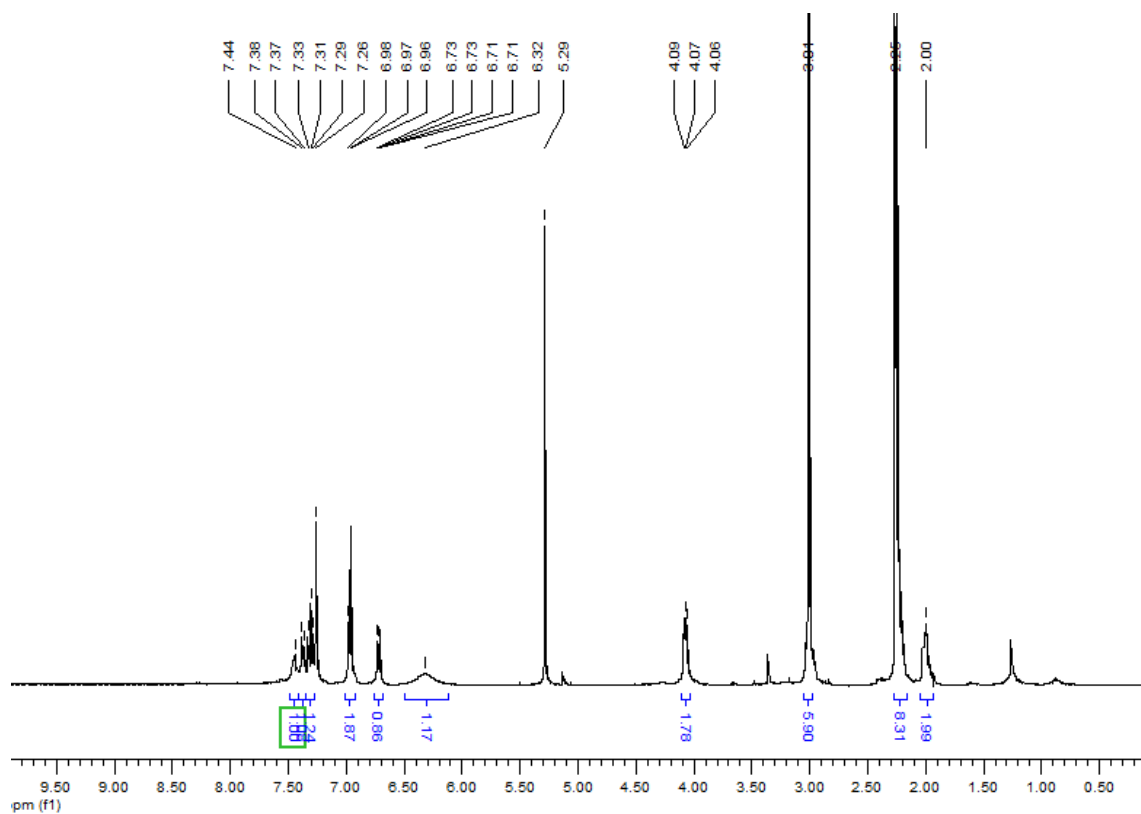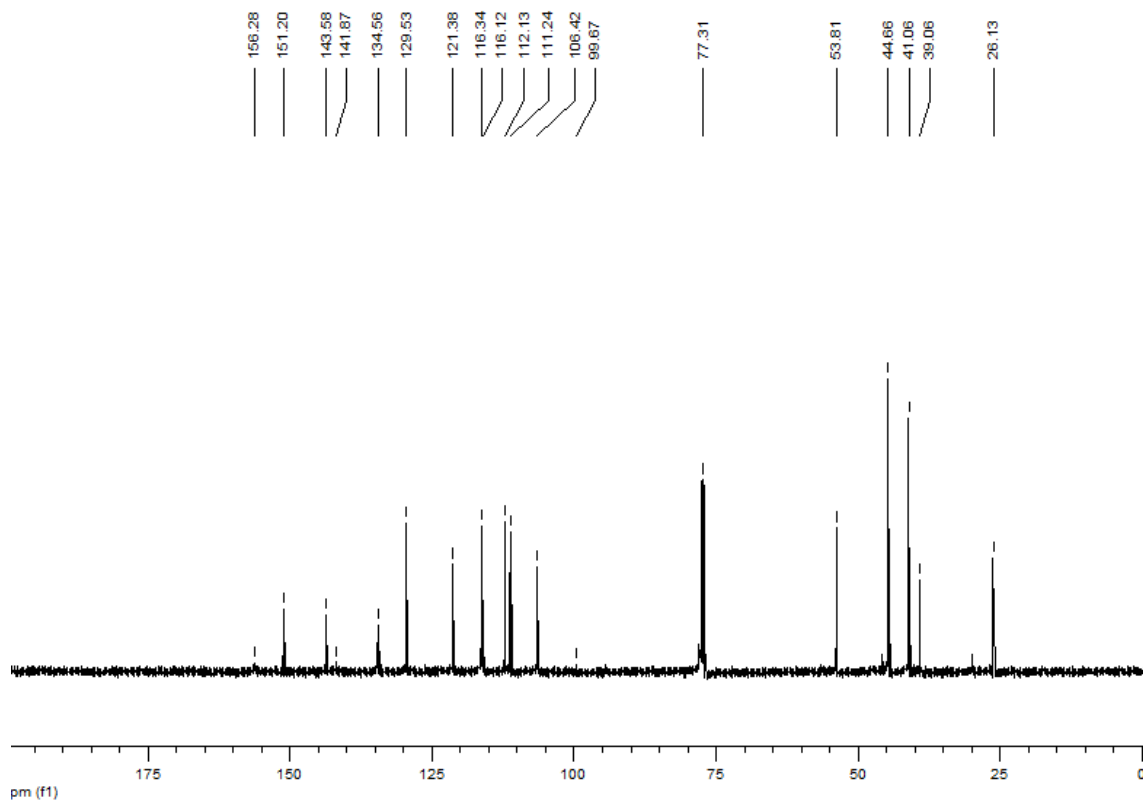**6-(3-(dimethylamino)phenyl)-1-(3-(dimethylamino)propyl)-1*H*-benzo[*d*]imidazol-2-amine (84)**

N[3]-(3-(dimethylamino)propyl)-*N*[3'],*N*[3']-dimethyl-4-nitro-[1,1'-biphenyl]-3,3'-diamine (**85**) (394 mg, 1.15mmol) and methanol (100 ml). The flask was flushed with Ar gas before Pd/C (40 mg, 10 wt %) was added. The reaction was then sealed under H_2 atmosphere and stirred at RT for 5 hours before it was filtered and concentrated. ACN (100 ml) was then added. While stirred at RT, cyanogene bromide (146 mg, 1.38 mmol, 1.2 eq) was added, followed by K_2CO_3 (190 mg, 1.38 mmol, 1.2 eq). The reaction was stirred at RT for 24 hours. It was then filtered and concentrated. The crude was purified via flash column chromatography (DCM – MeOH : 80 % - 20 %) to yield white solid as the product (75 mg, 19 % yield). ^{1}H NMR (400MHz, CDCl₃) δ: 7.44 (m, 1H), 7.38 (d, *J* = 8 Hz, 1H), 7.33 (t, *J* = 8 Hz, 1H), 6.98 (m, 2H), 6.73 (dd, *J*₁ = 7 Hz, *J*₂ = 2 Hz, 1H), 6.32 (s, 1H), 4.09 (t, *J* = 5 Hz, 2H), 3.01 (s, 6H), 2.26 (s, 8H), 2.00 (m, 2H). ^{13}C NMR (400MHz, CDCl₃) δ: 156.27, 151.20, 143.58, 141.87, 134.55, 129.53, 121.38, 116.34, 116.11, 112.13, 111.24, 106.42, 99.66, 53.80, 44.66, 41.06, 39.05, 26.13. MS (ESI) calculated exact mass for $C_{20}H_{27}N_5$ = 337.23. Found $[M+H]^+$ = 338.17.

Spectrum 4-53: 6-(3-(dimethylamino)phenyl)-1-(3-(dimethylamino)propyl)-1*H*-benzo[*d*]imidazol-2-amine (**84**) ^{1}H NMR (400MHz, CDCl₃)
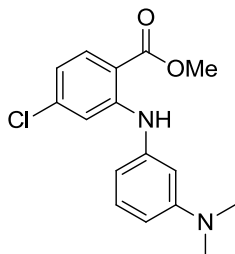
Spectrum 4-54: 6-(3-(dimethylamino)phenyl)-1-(3-(dimethylamino)propyl)-1*H*-benzo[*d*]imidazol-2-amine (**84**) ^{13}C NMR (400MHz, CDCl$_3$)

Methyl 4-chloro-2-((3-(dimethylamino)phenyl)amino)benzoate (88)

To a 100 ml round bottom flask was added methyl 4-chloro-2-nitrobenzoate (**53**) (500 mg, 2.44 mmol), dioxane (40 ml), 3-dimethylaminoanilne (2.44 mmol), Pd2(dba)3 (112 mg, 0.1 mmol), rac-BINAP (114 mg, 0.2 mmol), and Cs2CO3 (881 mg, 2.44 mmol). The reaction was stirred and heated to reflux under Ar for 48 hours before it was cooled to RT and filtered. After concentration, the crude was purified via flash column chromatography (DCM - Hexane : 80 % - 20 %) to yield yellow oil as the product (119 mg, 16 % yield). ^{1}H NMR (400MHz, CDCl$_3$) δ: 9.50 (s, 1H), 7.88 (d, J = 8 Hz, 1H), 7.25 (m, 2H), 6.66 (dd, J_1 = 8 Hz, J_2 = 2 Hz, 2H), 6.57 (s, 2H), 3.90 (s, 3H), 2.97 (s, 6H). ^{13}C NMR (400MHz, CDCl$_3$) δ: 166.65, 151.85, 149.65, 140.70, 133.05, 130.19, 117.02, 113.83, 111.86, 109.31, 107.90, 52.09, 40.86. MS (ESI) calculated exact mass for C$_{16}$H$_{17}$ClN$_2$O$_2$ = 304.10. Found [M+H]$^+$ = 305.24.

Spectrum 4-55: methyl 4-chloro-2-((3-(dimethylamino)phenyl)amino)benzoate (**88**) ^{1}H NMR (400MHz, CDCl$_3$)

Spectrum 4-56: methyl 4-chloro-2-((3-(dimethylamino)phenyl)amino)benzoate (**88**) ^{13}C NMR (400MHz, CDCl$_3$)
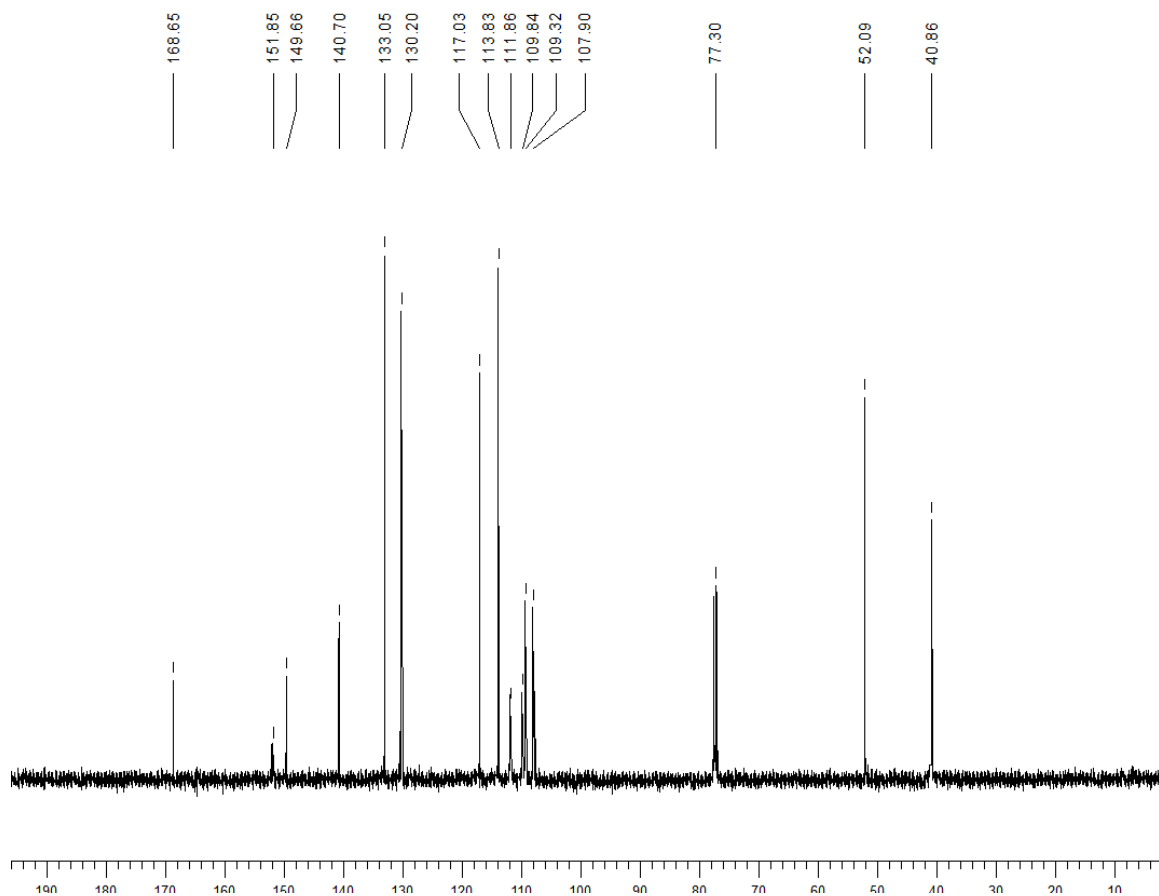
Methyl 2-((3-(dimethylamino)propyl)amino)benzoate (91)
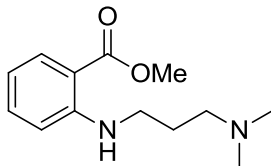
To a 250 ml round bottom flask was added methyl 2-aminobenzoate (90) (1g,

5.25 mmol), methanol (100 ml), and 3-dimethylaminopropionitrile (3 ml, 27.6 mmol).

The reaction was flushed with Ar gas before Pd/C (1 g, 10 wt%, final 10% Pd) was added.

The reaction was then sealed under H2 atmosphere. It was stirred at RT for 25 hours

before it was filtered and concentrated. The crude was purified via flash column

chromatography (DCM - MeOH : 70 % - 30 %) to yield an oil as the product (729 mg, 56

% yield). ^{1}H NMR (400MHz, DMSO-d6) δ: 7.78 (dd, J_1 = 8 Hz, J_2 = 2 Hz, 1H), 7.64 (t, J = 5

Hz, 1H), 7.39 (m, 1H), 6.79 (d, J = 8 Hz, 1H), 6.58 (td, J_1 = 7 Hz, J_2 = 1 Hz, 1H), 3.77 (s, 3H),

3.28 (q, J = 6 Hz, 2H), 2.87 (t, 7 Hz, 2H), 2.53 (s, 6H), 1.94 (m, 7 Hz, 2H). ^{13}C NMR

(400MHz, DMSO-d6) δ: 151.08, 140.68, 135.54, 131.85, 115.16, 112.16, 109.85, 55.57,

52.25, 43.40, 36.07, 24.97. MS (ESI) calculated exact mass for $C_{13}H_{20}N_2O_2$ = 236.15.

Found [M+H]$^+$ = 237.01.

Spectrum 4-57: methyl 2-((3-(dimethylamino)propyl)amino)benzoate (**91**) ^{1}H NMR (400MHz, DMSO-d6)
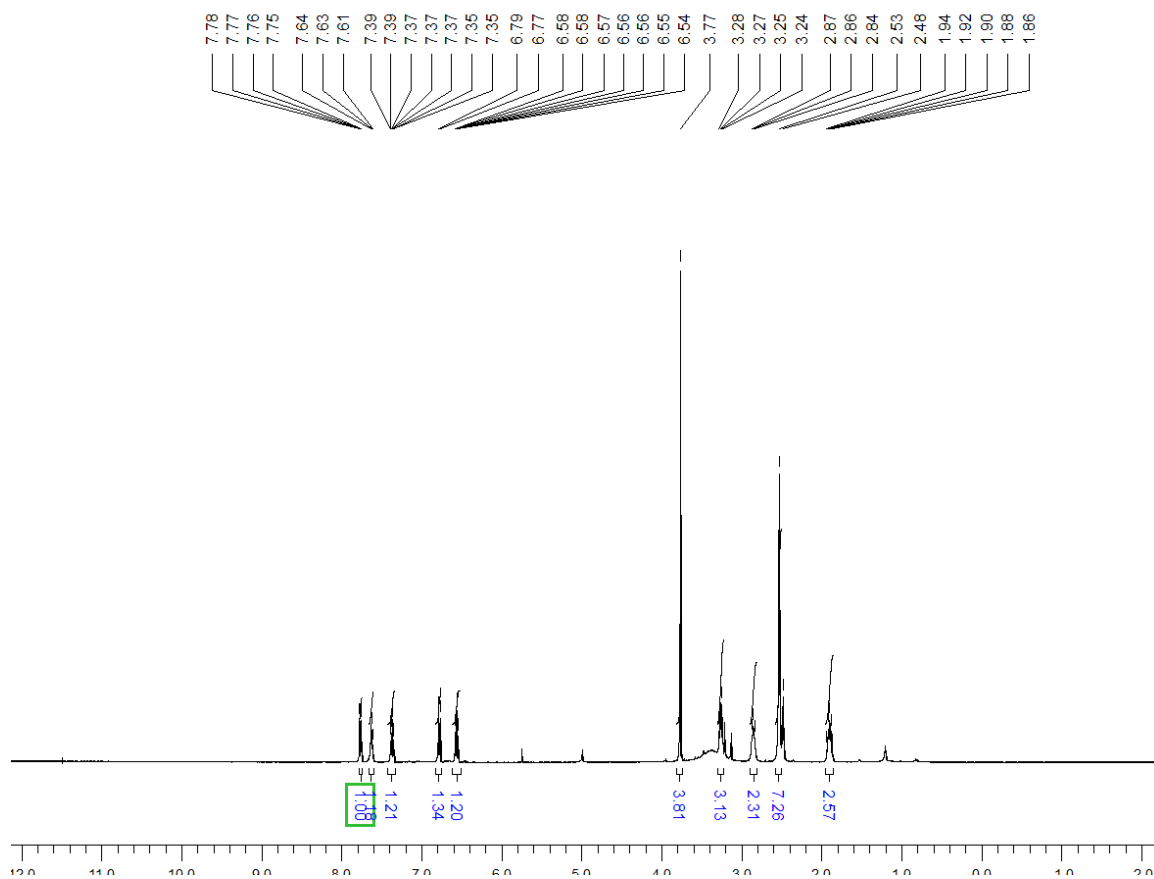
Spectrum 4-58: methyl 2-((3-(dimethylamino)propyl)amino)benzoate (**91**) ^{13}C NMR (400MHz, DMSO-d6)
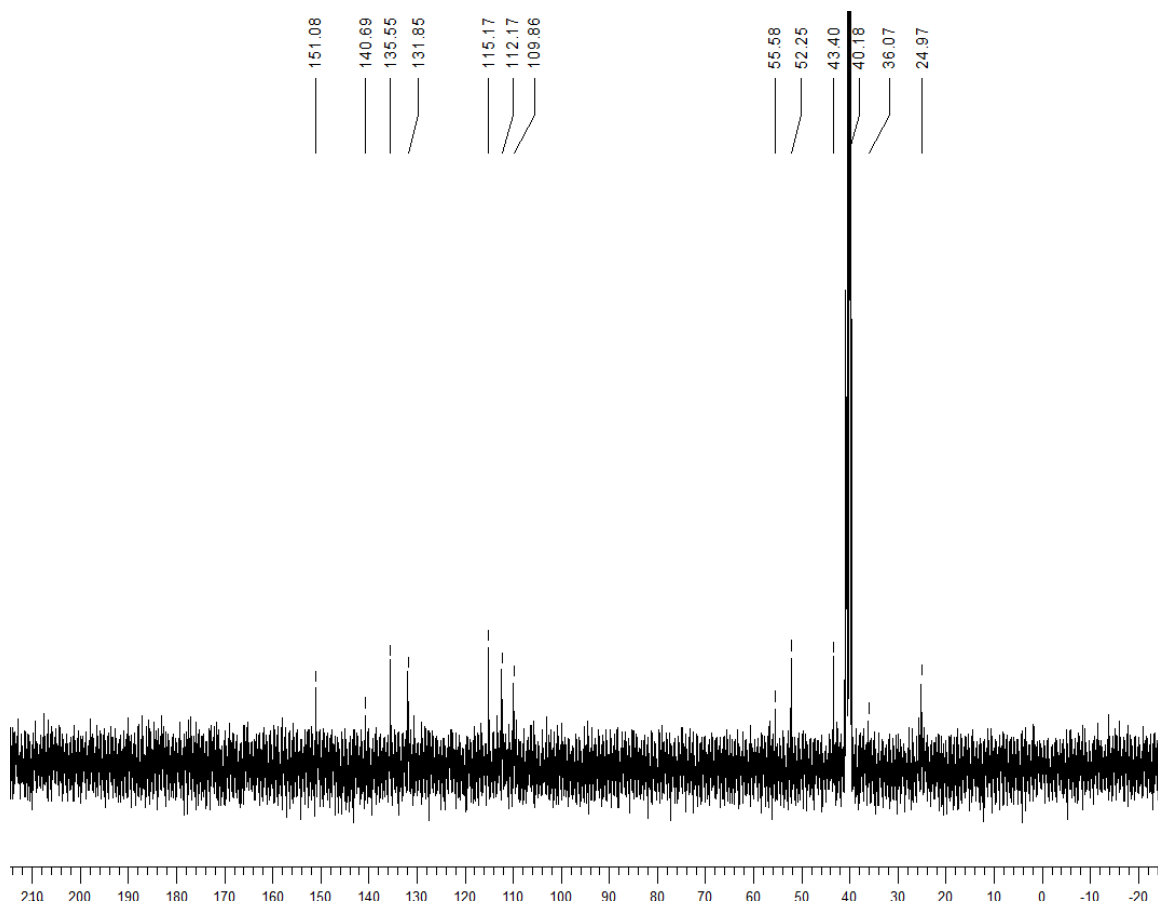
References:

(1)   Dibrov, S. M.; Ding, K.; Brunn, N. D.; Parker, M. A.; Bergdahl, B. M.; Wyles, D. L.; Hermann, T. *Proc Natl Acad Sci U S A* **2012**, *109*, 5223.

(2)   Parsons, J.; Castaldi, M. P.; Dutta, S.; Dibrov, S. M.; Wyles, D. L.; Hermann, T. *Nat Chem Biol* **2009**, *5*, 823.

(3)   Cech, T. R.; Zaug, A. J.; Grabowski, P. J. *Cell* **1981**, *27*, 487.

(4)   Cech, T. R. *Cell* **1986**, *44*, 207.

(5)   Kruger, K.; Grabowski, P. J.; Zaug, A. J.; Sands, J.; Gottschling, D. E.; Cech, T. R. *Cell* **1982**, *31*, 147.

(6)   Adams, P. L.; Stahley, M. R.; Kosek, A. B.; Wang, J.; Strobel, S. A. *Nature* **2004**, *430*, 45.

(7)   Guo, F.; Gooding, A. R.; Cech, T. R. *Mol Cell* **2004**, *16*, 351.

(8)   Parsons, J.; Castaldi, M. P.; Dutta, S.; Dibrov, S. M.; Wyles, D. L.; Hermann, T. *Nat Chem Biol* **2009**, *5*, 823.

(9)   Zhou, S.; Rynearson, K. D.; Ding, K.; Brunn, N. D.; Hermann, T. *Bioorg Med Chem* **2013**, *21*, 6139.

(10)   Hortner, S. R.; Ritschel, T.; Stengl, B.; Kramer, C.; Schweizer, W. B.; Wagner, B.; Kansy, M.; Klebe, G.; Diederich, F. *Angew Chem Int Edit* **2007**, *46*, 8266.

(11)   Keyser, G. E.; Leonard, N. J. *Journal of Organic Chemistry* **1976**, *41*, 3529.

(12)   Bischoff, C.; Schröder, E. *Journal für Praktische Chemie* **1983**, *325*, 88.

(13)   Smits, R. A.; De, E. I. J. P.; Leurs, R.; Google Patents: 2010.

(14)   Meyer, E. A.; Brenk, R.; Castellano, R. K.; Furler, M.; Klebe, G.; Diederich, F. *Chembiochem* **2002**, *3*, 250.

(15)   Lecoutey, C.; Fossey, C.; Rault, S.; Fabis, F. *European Journal of Organic Chemistry* **2011**, *2011*, 2785.

(16)   Huang, X. H.; Yang, H. J.; Fu, H.; Qiao, R. Z.; Zhao, Y. F. *Synthesis-Stuttgart* **2009**, 2679.

(17)   Prashad, M.; Chen, L. J.; Repic, O.; Blacklock, T. J. *Synthetic Commun* **1998**, *28*, 2125.

(18)   Leonard, N. J.; Kazmierczak, F.; Rykowski, A. Z. *The Journal of Organic Chemistry* **1987**, *52*, 2933.

(19)   Sajiki, H.; Ikawa, T.; Hirota, K. *Organic Letters* **2004**, *6*, 4977.